Interleukin-17 Orchestrates Neutrophil Dynamics to Amplify Neuroinflammation in a Murine Model of Multiple Sclerosis

---

Dissertation
Zur Erlangung des Grades
Doktor der Naturwissenschaften

Am Fachbereich Biologie
Der Johannes Gutenberg-Universität in Mainz

Vorgelegt von
Katlynn Carter
Geboren am 01. Juni 1993 in Indianapolis, USA

Mainz, 2025

Dekan: Prof. Dr. Eckhard Thines

1. Berichtserstatter: Dr. rer. nat. Tommy Regen
2. Berichtserstatter: Prof. Dr. Miguel Andrade

Tag der mündlichen Prüfung:

To the women who came before me, real and fictional, who inspired in me a world to believe in. A world not as it is, but as it can be.

Table of Contents

Figure Index

List of Abbreviations

APC	Antigen presenting cell
AT-EAE	Adoptive transfer EAE
AUC	Area under the curve
BBB	Blood-brain barrier
C/EBP	CCAAT/enhancer-binding protein
CFA	Complete Freund's Adjuvant
CMP	Common myeloid progenitor
CNS	Central nervous system
CSF	Cerebrospinal fluid
DC	Dendritic cell
DMT	Disease modifying therapy
DPI	Day post-immunization
DPT	Day post-transfer
EAE	Experimental autoimmune encephalomyelitis
EBV	Epstein-Barr virus
ECM	Extracellular matrix
EDSS	Expanded Disability Status Scale
ENS	Enteric nervous system
FMT	Fecal microbiome transplantation
GM-CSF	Granulocyte-macrophage colony-stimulating factor
G-MDSC	Granulocyte myeloid-derived suppressor cell
GMP	Granulocyte-monocyte progenitor
GWAS	Genome-wide association studies
HLA	Human leukocyte antigen
HSC	Hematopoietic stem cell
IBD	Inflammatory bowel disease
ICAM	Intercellular adhesion molecule
IFN	Interferon
IL	Interleukin

LN	Lymph node
LT	Lymphotoxin
MDP	Monocyte-macrophage/dendritic cell precursor
M-MDSC	Monocyte myeloid-derived suppressor cell
MDSC	Myeloid-derived suppressor cell
MHC	Major histocompatibility complex
MOG	Myelin oligodendrocyte glycoprotein
MPO	Myeloperoxidase
MS	Multiple sclerosis
NET	Neutrophil extracellular trap
NF-κB	Nuclear factor kappa-light-chain-enhancer of activated B cells
NOS	Nitric oxygen species
OPC	Oligodendrocyte precursor cell
OR	Odds ratio
PCR	Polymerase chain reaction
PDGF	Platelet derived growth factor
PD-L1	Programmed death ligand 1
PPMS	Primary progressive multiple sclerosis
PRMS	Progressive relapsing MS
PTx	Pertussis toxin
PvC	Perivascular cell
ROS	Reactive oxygen species
RRMS	Relapsing-remitting multiple sclerosis
RT-PCR	Reverse transcriptase PCR
S1P	Sphingosine-1-phosphate
SAS	Subarachnoid space
SEM	Standard error of the mean
SFB	Segmented filamentous bacteria
SLO	Secondary lymphoid organ
SPMS	Secondary progressive MS
TCR	T cell receptor
Th	T helper

TNF	Tumor necrosis factor
TRAF	TNF receptor associated factor
Treg	Regulatory T cell
TSNE	T-distributed stochastic neighbor embedding
UMAP	Uniform manifold approximation projection
VCAM	Vascular cell adhesion molecule
VLA	Very late antigen
ZO	Zona occludens

1 Introduction

1. Multiple Sclerosis

1.1. Clinical Pathology and Disease Course

Multiple sclerosis (MS) is a chronic demyelinating disease characterized by cycles of relapsing and remitting inflammation, followed in its later stages by progressive neurodegeneration. The burden that MS places on society is stark: it is the most prevalent inflammatory disease of the central nervous system (CNS) and affects approximately 2.9 million people worldwide, with the highest rates occurring the western world.[1] The average age of diagnosis is only 30 years young, with approximately 50% of patients requiring permanent use of a wheelchair 25 years after diagnosis.[2]

MS symptoms present as sensory and visual impairments, motor system malfunctioning, fatigue, pain, and in later stages, as worsening cognitive deficits, presented as increased scores on the commonly used Expanded Disability Status Scale (EDSS) for quantifying disability in MS. The pathological hallmarks of the disease are confluent demyelinated lesions within the gray and white matter of the CNS.[3,4] These lesions are the result of the breakdown of the blood-brain barrier (BBB) and infiltration of innate and adaptive immune cells that promote and sustain the processes of demyelination and degeneration of neuronal axons, gliosis, and inflammation which collectively result in worsening disturbances in neuronal signaling throughout the body.[5] As a result, patients experience continual decrease in brain volume from cortical and gray matter atrophy.[6]

Four clinical subtypes of MS were defined by the US National Multiple Sclerosis Society (NMSS) Advisory Committee in 1996 and have been the standard classification for various disease courses ever since.[7] These four disease courses were defined as relapsing remitting (RRMS), secondary progressive (SPMS), primary progressive (PPMS), and progressive relapsing (PRMS). The two core phenotypes of these disease courses relate to an either relapsing or progressive form of disease. Relapsing forms of disease, where patients experience periods of neurological

dysfunction followed by remission, is the most common form of disease. About two thirds of patients transition to the progressive stage of disease within 10-15 years of diagnosis.[8] Only 10% of patients are diagnosed from the onset with progressive forms of disease, where neurological symptoms persist from the start and increase in their severity. Progressive forms of disease are more difficult to treat and have a poor prognosis.

1.2. Disease Etiology and Risk Factors

Multiple sclerosis is considered to be an environmentally triggered disease that occurs among individuals with genetic susceptibility. Genome-wide association studies (GWAS) have identified over 200 risk variants to date and place the genetic component of disease at around 30%.[9,10] The greatest genetic risk for MS is linked to polymorphisms in human leukocyte antigen (HLA) class I and II genes, the human equivalent of the mouse major histocompatibility complex (MHC) genes. In particular, the class II variant HLA-DRB1*15:01 has significant disease association (odds ratio (OR) ~ 3) and remains the most dominant genetic risk factor identified thus far.[11] Conversely, the class I variant HLA-A*02 provides significant protection against disease.[12] Given the strong involvement of both class II primed $CD4^+$ and class I primed $CD8^+$ T lymphocytes in disease pathogenesis, it is likely that variations in the HLA genes may promote either protective or pathogenic T cell responses that contribute to disease initiation.

The remaining 70% of non-genetic disease-driving factors are classified as environmental. These non-genetic risk factors can be further divided into two categories: those that compound with an already present genetic risk and those occurring independently. Environmental risk factors observed to compound with already existing genetic risk factors are previous Epstein-Barr Virus (EBV) infection, smoking, and adolescent obesity. Compelling evidence suggests that these three risk factors work by activating auto-reactive T cells, eventually leading to their CNS-targeted effects.

The most significant nongenetic risk factor for MS is previous infection with Epstein-Barr Virus (EBV), particularly when it results in symptomatic infectious mononucleosis, typically occurring during adolescence or early adulthood.[13] Nearly all MS patients have antibody titers against EBV nuclear antigen 1 (EBNA1). While this might not seem surprising—over 90% of the population have antibody titers against EBV—a clear linear relationship has been documented

between higher serum titers of anti-EBNA1 IgG antibodies and the increased risk of MS development.[14] In a study of over 10 million members of the US military, risk of MS development increased 32-fold in young adults after EBV infection. Only one of the 801 MS cases occurred in an EBV-negative individual.[15,16] Research into potential mechanisms provides evidence for molecular mimicry mediated via cross-recognition of T and B lymphocytes. EBNA1-specific T cells were shown to frequently recognize myelin antigens and produced inflammatory cytokines, including interferon-γ (IFNγ) and interleukin (IL)-2, as a response, but not in response to other autoantigens.[17] More recently, it was observed that B cell autoantibodies recognizing EBNA1 have a similarly high affinity for CNS antigen GlialCAM.[18] These insights underscore the complex interplay between viral infection and adaptive immune responses in the development of MS.

Environmental risk factors influencing MS susceptibility independently of genetic risk—such as vitamin D status, gender, and diet—are more challenging to study, largely due to the intersectionality of these risk factors with other inseparable societal factors, such as wealth disparities, access to resources, and many more. Proposed biological explanations include hormone effects on T cell functioning and the myriad impacts of modern-day stress, though these theories require much more scientific validation.[19–21] Overall, MS is a complex disease likely driven by multiple, interacting genetic and non-genetic factors.

1.3. Immunopathology and Cellular Involvement

Theories on the triggers of MS diverge into two schools of thought known as the "inside-out" versus the "outside-in" hypotheses.[22] The "inside-out" hypothesis of MS development points to CNS-intrinsic "cytodegeneration", or cellular damage within the CNS, that leads to antigen drainage through the cerebrospinal fluid (CSF) to initiate autoimmune responses.[23] In contrast, the "outside-in" hypothesis proposes that the CNS-extrinsic activation of autoreactive T cells responsible for later disease development occurs starting in the periphery.[24] The heterogeneity of MS hints towards a likelihood of both hypotheses occurring simultaneously and to a different degree between patients.

Cellular drivers of MS include a multitude of immune cell subsets of both lymphocyte and myeloid origin. T lymphocytes play a crucial role in MS as the adaptive immune cells which

recruit myeloid cells that promote destruction of the myelin sheaths of neuronal axons. Among $CD4^+$ T lymphocytes, research suggests MS patients have both fewer suppressive and more pathogenic effector helper T (Th) cells. Suppressive $CD25^+$ regulatory T cells (Tregs) of MS patients are reduced in number, have lower suppressive capacity *in vitro* and produce less IL-10 upon restimulation.[25–27] The major pathogenic effector T cell subsets described to promote MS development are T helper type 1 (Th1) and T helper 17 (Th17) cells. In MS patients, both effector Th1 and Th17 cells are documented to express higher levels of pro-inflammatory cytokines IFNγ and IL-17, respectively.[28] While MS has traditionally been studied as a $CD4^+$ T cell-mediated disease due to the genetic associations with MHC class II alleles, MHC class I-associated $CD8^+$ T cells are found at equal or greater numbers than $CD4^+$ T cells in plaques of MS patients, suggesting a central role.[29] Activated $CD8^+$ T cells secrete the inflammatory cytokines IFNγ, tumor necrosis factor (TNF), and IL-2, as well as lytic enzymes, such as perforin and granzymes, which are shown to be particularly cytotoxic to neurons.[30]

Interest into the role of B lymphocyte involvement during MS has also piqued after the discovery of the success of B cell depletion therapies with anti-CD20 monoclonal antibodies.[31] These therapies sustainably reduce relapse rates without altering the levels of circulating antibodies, suggesting that B cells contribute to disease pathogenesis though antibody-independent mechanisms, such as antigen presentation or by promoting lymphogenesis.[32] Memory B cells have been shown to stimulate the proliferation of self-reactive $CD4^+$ T cells via HLA-DR15, the main genetic risk factor for MS.[33] Additional studies indicate that B cells in MS patients have a higher activation status, and increased lymphotoxin (LT), TNF, and granulocyte-macrophage colony-stimulating factor (GM-CSF) production that may support effector $CD4^+$ and $CD8^+$ T cell responses.[34–36] Additionally, B cell-related chemokines, including CXCL10/13, LTα, IL-6, and IL-10 are elevated in the CSF of MS patients and may support the formation of tertiary lymphoid structures that support chronic inflammation in the leptomeninges.[37]

Research on innate immune involvement in MS has expanded in the last decade but remains highly underdeveloped. Both CNS-intrinsic and extrinsic myeloid cells play a pivotal role in driving and sustaining inflammation in MS lesions. Microglia, the CNS-intrinsic myeloid cells, are long-lived resident cells that become activated in the heavily myelinated white matter of MS patients and promote demyelination through phagocytosis.[38] CNS-extrinsic circulating

myeloid cells, predominantly neutrophils and monocytes, are recruited to the CNS by chemokines and cytokines, such as CXCL1, CXCL2, CXCL8, and G-CSF, released by activated glia and T cells.[39] In the CNS parenchyma, myeloid cells contribute to axonal demyelination and BBB breakdown through phagocytosis and the secretion of pro-inflammatory mediators, such as reactive oxygen species (ROS), IL-1β, IL-6, and myeloperoxidase (MPO).[40] Ultimately, MS is an immune-mediated disease involving a complex interplay of both CNS-intrinsic and extrinsic cell types that initiate and perpetuate chronic cycles of demyelination throughout the CNS.

1.4. Treatment Options and Future Clinical Approaches

The progression of MS can be characterized into early, middle, and late stages (Fig. 1).[10] The early, preclinical stage of MS is just as its name states: the signs of disease are below the clinical threshold for diagnosis. No symptoms exist at this stage, though the disease may be incidentally identified via MRI.[41] Once symptoms begin to show, patients enter the relapsing-remitting stage of disease, characterized by episodes of neurological dysfunction followed by stages of remission.[42] Treatment at this stage seeks to prevent relapses and myelin degradation, which can cumulatively lead to permanent neuronal loss. Over time, episodes increase in frequency and severity, until remission phases cease entirely, marking the transition to the progressive stage. At this late stage, CNS damage from chronic demyelination and neuronal death are permanent and irreversible, and only few therapies are available to patients.

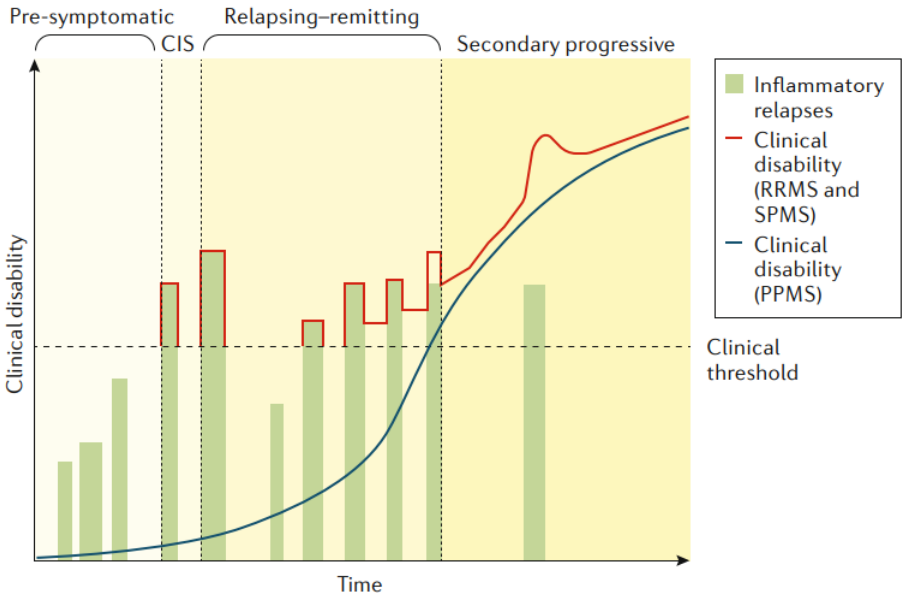

Figure 1: Clinical course of MS progression. *From Filippi et al. 2018.*[10]

The widest range of disease-modifying therapies (DMT) exist for treatment of patients in the relapsing-remitting stage of MS.[43] Though often pleiotropic in nature, drug action of these RRMS-DMTs can be categorized into three main mechanisms of action: 1) lymphocyte depletion, 2) increasing the suppressive to pathogenic T cell ratio, or 3) inhibition of migration and CNS entry. Lymphocyte depletion using anti-CD52 monoclonal antibodies, (alemtuzumab and cladribine), or anti-CD20 monoclonal antibodies (ocrelizumab and rituximab) are effective in reducing lesion volume, decreasing relapse rate, and slowing disease progression.[31,44] While these therapies are efficacious in reducing relapses, they carry risks, with many clinical trials documenting adverse effects, such as the observance of secondary autoimmune disease in 30-40% of patients.[45]

Several DMTs exist to alter T cell dynamics, either by altering the Th1/Th17-Treg axis or interfering with T cell migration. Treatment with the endogenous cytokine interferon-β (IFNβ) is shown to down-regulate MHCII expression, interfere with T cell homeostasis, and protect the BBB by the inhibition of adhesion molecules.[46] Glatiramer acetate, a synthetic mixture of random peptides that mimic myelin proteins, promotes tolerance to these epitopes and increases the number of Tregs.[47] RRMS-DMTs that inhibit migration of lymphocytes target two key events. Sphingosine-1-phosphate (S1P) receptor modulators, such as the S1P agonist fingolimod, sequesters T cells in the periphery by inhibiting their egress out of the lymph nodes.[48,49] Conversely, the α4β1 integrin-targeting antibody, natalizumab, impairs integrin-driven CNS migration by blocking lymphocyte VLA4 binding to VCAM1 on endothelial cells.

Few treatments are effective in the progressive stage of MS, largely due to the irreversible damage to neurons from chronic inflammation. However, current research into oligodendrocytes, the cells that carry the potential to remyelinate neuronal axons, proves promising.[50] Oligodendrocyte precursor cells (OPCs) migrate to sites of inflammation to mature into myelinating oligodendrocytes. Future therapies aim to enhance OPC migration to sites of inflammation and to promote their maturation through the inhibition of inhibitory and pro-inflammatory molecules.[43] Drugs such as miconazole and clobetasol have proved effective in differentiating OPCs *in vitro*, yet so clinical studies are underway for their efficacy in MS patients.[51]

2. Experimental Autoimmune Encephalomyelitis (EAE)

Studying the human CNS during active disease is limited by the invasive nature of tissue analysis. Animal models provide a viable alternative to study the cellular and molecular mechanisms promoting disease development and persistence. Experimental autoimmune encephalomyelitis (EAE) is the most widely used model that mimics key features of the human disease. First described by Rivers and colleagues in 1933, researchers observed that monkeys immunized with rabbit brain extracts developed CNS perivascular infiltrates and demyelination resembling human multiple sclerosis.[52] Since then, several adaptations of the EAE model have been developed that place selective focus on mechanisms underlying processes such as neuroinflammation, immune system activation, or demyelination.[53] Spontaneous models of EAE utilize animals with genetically modified T cell and B cell receptors against CNS antigen.[54,55] In contrast, active EAE involves an artificial induction of the adaptive immune response via injection with CNS antigen in an adjuvant emulsion, with antigens like myelin oligodendrocyte glycoprotein $(MOG)_{35-55}$ inducing a chronic disease course, while proteolipid protein $(PLP)_{139-151}$ induces a relapsing-remitting course.[56] The adoptive transfer model of EAE (AT-EAE), induced by transfer of *in vitro* polarized encephalitogenic T cells from antigen-immunized donor mice, places a focus on T cell mediated disease mechanisms that is largely independent of peripheral organs.[57] Finally, the "inside-out" hypothesis of MS described previously is well-modeled by the cuprizone model of EAE, which administers the copper chelating agent cuprizone to induce damage to oligodendrocytes, placing focus on the de-and remyelination processes occurring during EAE.[58]

2.1. Immunopathology of the MOG_{35-55} EAE model

The MOG_{35-55} EAE model has significantly contributed to research on neuroautoimmune mechanisms due to its chronicity and involvement of both central and peripheral immune processes. Key immune processes, such as peripheral T cell priming and clonal expansion, along with CNS processes like T cell reactivation, myeloid recruitment, and demyelination, are easily-observable and time-dependent (Fig. 2). This model has been used to make great strides in the understanding of MS and in the development of treatments and therapies that limit disease onset or progression.[59] The MOG_{35-55} EAE model is not without its limitations, however. Unlike

in MS, B cells do not appear to play a crucial role, as B-cell deficient mice remain susceptible to MOG_{35-55}-induced EAE.[60] In contrast, other leukocytes, especially T cell and myeloid driven disease pathology, are critical at various stages and well-represented in the MOG_{35-55} EAE model. Dendritic cells are essential for antigenic priming and reactivation, for example, while $CD4^+$ T cells drive the adaptive immune response which recruits myeloid cells that promote demyelination and CNS inflammation.

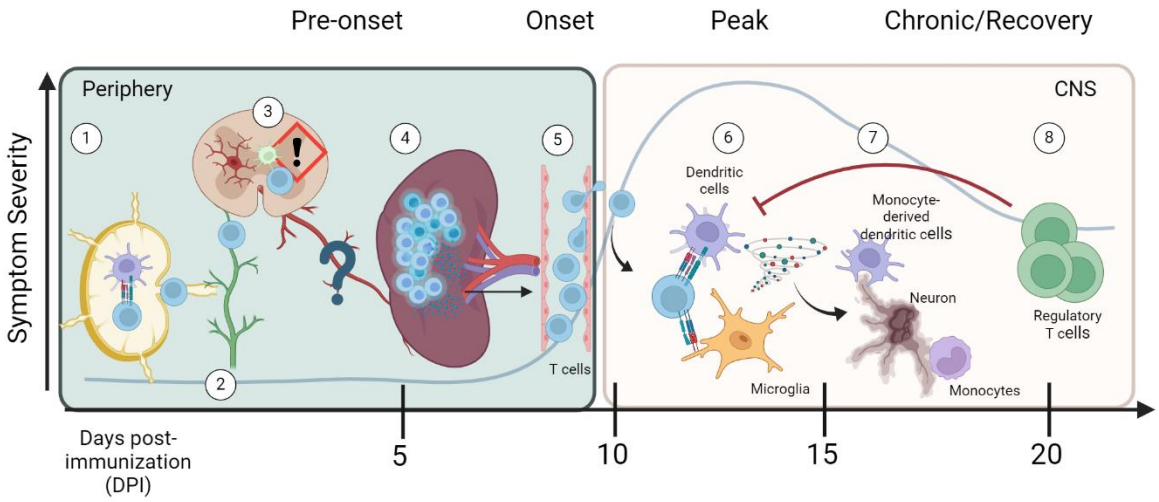

Figure 2: Multi-step pathogenesis of active EAE. *(**1**) T cells encounter cognate antigen in the lymph nodes presented on MHCII complexes of dendritic cells and macrophages. (**2**) Early activated T cells leave the lymph nodes in a so-called "first-wave" to become (**3**) reactivated at the CNS leptomeninges. (**4**) T lymphocytes clonally expand in the spleen before (**5**) migrating with APCs through the blood stream towards the CNS. Once inside the CNS parenchyma, a circular process of T cell reactivation (**6**), myeloid cell recruitment, and release of demyelinating factors (**7**) will continue until inflammation is inhibited by (**8**) CNS-invading regulatory T cells.*

2.1.1. Antigenic T cell priming in the draining lymph nodes

$CD4^+$ T cell priming by antigen presenting cells (APCs) is the initiating step of the adaptive immune response that occurs in both MS and EAE. This process requires two signals given to T cells by APCs: antigen presentation and costimulatory receptor engagement. In the lymph nodes receiving immune cells surrounding the site of immunization, termed the draining lymph nodes (dLNs), professional APCs, such as dendritic cells and macrophages, capture antigens through phagocytosis or endocytosis. These antigens are processed into peptide fragments within lysosomes, then loaded onto MHCII molecules which are transported to the extracellular surface of APCs for presentation to antigen-specific T cell receptors (TCRs).[61]

Alongside TCR-engagement with MHCII, costimulatory ligands on the surface of APCs transmit either activation or inhibitory signals to T cells. Several costimulatory molecules are involved in priming autoreactive T cells during MS and EAE, including activating ligands such as CD28 and CD40, and inhibitory molecules such as CTLA-4 and PD-1.[62] The CD40-CD40L costimulatory dyad seems to be particularly important for T cell priming in the periphery and reactivation in the CNS during MS and EAE.[63,64] Both the MHCII and costimulatory systems have evolved as mediators of central tolerance to self-antigens and activate the adaptive immune response to foreign antigens. In EAE, $CD4^+$ cells only survive and further differentiate into specialized effector subsets after engagement with these two activating signals. Thereafter, the environmental cytokine milieu dictates the differentiation trajectory of effector T cells.

2.1.2. Reactivation of peripherally activated T cells in the subarachnoid space (SAS)

The CNS is composed of three barriers that receive T cells: the arachnoid membrane underneath the skull, the blood-CSF barrier, and the blood-brain barrier (BBB) within the CNS parenchyma (Fig. 3).[59] The arachnoid epithelial membrane acts as a barrier between the dura mater, containing arteries, veins, and lymphatics, and the underlying subarachnoid space (SAS) containing CSF.[65] The choroid plexus epithelium comprises the blood-CSF barrier, where leukocytes and small molecules of the ventricular CSF may pass further into the epithelial basement membrane.[66] Lastly, the BBB of the CNS parenchyma is formed by tightly connected endothelial cells of capillaries and post-capillary venules throughout CNS tissue that separates the vasculature from the underlying basement membrane and glial limitans.[67] Under healthy conditions, the CNS epithelial barriers remain tightly connected by endothelial junctions and maintain a tightly regulated exchange of metabolites and small molecules.[68] During neuroinflammation, disruption of the physical endothelial barriers as well as activation of leukocytes and the endothelium by upregulation of adhesion molecules promotes leukocyte recruitment to the CNS and increases permeability of the BBB.[69] Infiltration of immune cells can occur at the leptomeningeal blood-CSF barrier, the choroid plexus blood-CSF barrier, or through the BBB at post-capillary venules.[23]

T cell migration to the CNS occurs in two "waves" during EAE. The first wave, known as the reactivation phase, acts as a trigger for the larger second wave of leukocyte infiltration that coincides with symptom onset.[70] During reactivation, the first wave of T cells engages with

perivascular MHCII$^+$ APCs to release proinflammatory mediators that prepare the CNS for the forthcoming immune response.[70] The cytokines released by APCs and T cells locally and distally activate microglia throughout the CNS to recruit immune cells to the CNS. In the latency period preceding symptom onset, CD4$^+$ T cells upregulate chemokine receptors such as CCR6, CXCR3 and CXCR4, that facilitate their migration and interaction with adhesion molecules and ligands presented on perivascular endothelial cells and APCs.[71,72] Perivascular macrophages and dendritic cells are the main MHCII$^+$ APCs that engage with T cells during reactivation.[57,70] Live imaging studies investigating the kinetics of T cell reactivation within the SAS suggest that this occurs at 24-60 hours after adoptive transfer or 9-10 days after active EAE immunization.[73] The strength of T cell reactivation plays a crucial role in disease progression, as strongly reactivated T cells produce higher levels of chemokines, promoting increased leukocyte migration to the CNS.

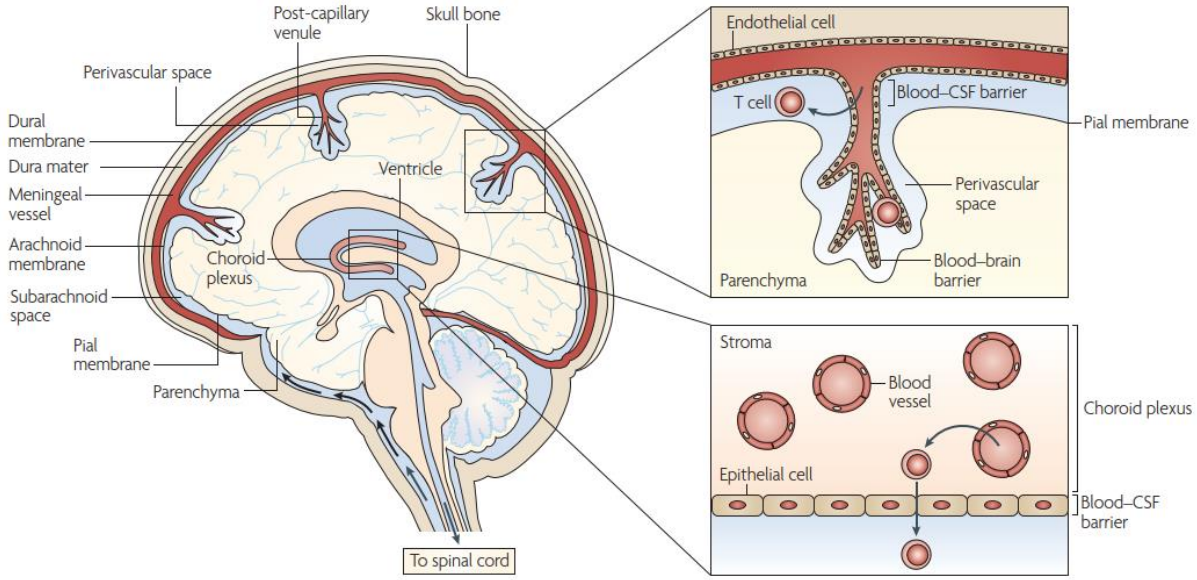

Figure 3: Anatomic organization of the CNS barriers. *From Goverman et al. 2009.*[59]

2.1.3. Clonal expansion and CNS migration of peripherally activated T cells

Upon sensing reactivation signals, CD4$^+$ T cells in peripheral tissues undergo clonal expansion before migrating en masse towards the CNS. While clonal expansion primarily occurs in the spleen, it has been also documented in other peripheral organs ranging from the lungs to the intestine.[74–76] Studies suggest that the location of clonal expansion may impart T cells with specialized effector functions and cytokine profiles upon reaching the CNS.[77,78] The development of various effector T cell subsets are well characterized. The main effector T cell

subsets driving EAE are the Th1 and Th17 cells, matured under the cytokines IL-12 and IL-23, respectively. Th1 cells are characterized by expression of the transcription factor T-bet and secretion of IFNγ, while Th17 cells express the nuclear hormone receptor RORγt and secrete IL-17. In EAE, Th1 and Th17 cells are associated with different disease courses: Th1 cells lead to milder, monocyte-driven neuroinflammation, while Th17 cells cause a more severe, neutrophil-driven neuroinflammation.[79] The cytokine environment of different tissues may influence how EAE is polarized through the development of Th1 versus Th17 cells, although further research is needed in this area.

All clonally expanding $CD4^+$ T cell populations undergo a maturation process towards a more effector, migratory phenotype before entering the bloodstream and circulating towards the CNS. This maturation includes downregulation of activation markers and upregulation of chemokine receptors such as CCR6, CXCR4, and CXCR6, that bind to their respective ligands expressed predominantly in the CNS.[80] Migration of these mature effector $CD4^+$ T cells from peripheral tissues to the CNS is regulated by a myriad of "stay versus go" signals. The signals most relevant in the EAE context include sphingosine-1-phosphate (S1P) signaling and chemokine gradients in the blood.[71]

S1P is a sphingolipid involved in dictating whether T cells remain in or exit secondary lymphoid organs (SLOs).[81] S1P is produced in the plasma by red blood cells, platelets, and endothelial cells to signal to the S1P receptor 1 (S1PR1) on the surface of T cells. Upon binding, S1PR1 is internalized, facilitating T cell trafficking into blood and lymph.[82] In the context of autoimmunity, S1P signaling is highly relevant; the S1P analog fingolimod is a standardized treatment for relapsing forms of MS and works by sequestering T cells in the peripheral SLOs.[83] Studies have also shown that deletion of S1PR1 on Th17 cells confers resistance to disease.[84]

Peripheral autoreactive T cells are recruited to the CNS by the upregulation of integrins and chemokines. Interactions between the T cell expressed chemokine receptor, CCR6, and its ligand CCL20, upregulated on inflamed CNS endothelial cells, appears to be a key feature of the first wave of pathogenic T cells into the CNS during EAE.[85,86] During the second wave, chemokine receptors of both innate and adaptive leukocytes, such as CXCR3/4/6 and CCR2/4/5/6, detect their corresponding ligands (CXCL9/10/11/12/16 and CCL2/20) produced

by astrocytes, glial, and endothelial cells in the CNS.[71,87] Upon reaching the CNS, endothelial integrins ICAM-1 and ICAM2 facilitate leukocyte crawling on endothelial cells of the BBB.[88] At this stage, TNF production appears to be essential for both T cell and myeloid entry into the CNS parenchyma after primary restimulation. Other integrin interactions, such as effector T cell α4β1 integrin binding to VCAM-1 on endothelial cells, promote entry of T cells into the CNS parenchyma.[89,90] Natalizumab, the α4 integrin monoclonal blocking antibody and standard treatment for MS, disrupts these T cell-endothelial cell interactions to inhibit T cell infiltration into the parenchyma and the resulting disease pathogenesis.[91]

2.1.4. Demyelination within the CNS parenchyma

Demyelination of neuronal axons within the CNS, a hallmark pathology of MS and EAE, is driven by infiltrating myeloid cells, mainly monocytes and neutrophils, which are recruited to the CNS by GM-CSF-producing Th17 cells.[92,93] Early in the disease cascade preceding symptoms, reactivation and breakdown of the BBB activate microglia through NF-κB, JNK, and ERK1/2 pathways, leading to microglial TNF secretion.[94,95] Coinciding with weight loss at pre-onset, circulating monocytes invade the CNS parenchyma, polarize, and mature into macrophages at inflammatory sites, sustained in numbers by hyper-myelopoiesis throughout symptomatic disease stages.[96–98] Mononuclear phagocytes engage in myelin degradation through phagocytosis and ROS production[38], while also expressing high mRNA levels of *Nos2*, the matrix metalloproteinases *Mmp12* and *Mmp14*, and inflammatory cytokines such as *Il1b*, that are hypothesized to also contribute to demyelination.[98,99]

Recent studies suggest a potential role of neutrophils in demyelination.[39] Neutrophil-driven EAE associated with Th17 cells results in worsened outcomes than monocyte-driven EAE by Th1 cells.[79] In a cuprizone EAE model, blood circulating $CXCR2^{+}$ neutrophils are essential for demyelination within the CNS, and $CXCR2^{-/-}$ mice are strongly protected against disease.[100] Yet how results from animal models translate to the human disease is still debated. The neutrophil-to-lymphocyte ratio directly correlates with MS disease severity, and while neutrophils are rare in the CNS tissue of MS patients, neutrophil-derived inflammatory mediators—such as elastase, MPO, ROS, and neutrophil extracellular traps (NETs)—are elevated in the blood.[40] Though neutrophil mediators are shown to disrupt the BBB and have high cytotoxic potential, (e.g. in

nerve degeneration in ALS), more research is required to determine whether they directly affect demyelination.[101–103]

While the roles of microglia, monocytes, and neutrophils in MS are not completely elucidated, early depletion in any of these cell types greatly reduces EAE progression and neuroinflammatory processes.[95,104,105] Future therapies targeting these cell types, such as nicotine acetylcholine receptor (nAChR) ligands for the prevention of monocyte and neutrophil infiltration, may prove effective in short-term treatment for MS patients undergoing relapses and work to minimize the demyelination that leads to progressive forms of the disease.[106]

2.1.5. Remyelination and recovery

Resident and circulating myeloid cells in the CNS play a dual role in MS and EAE, contributing both to demyelination, but restorative remyelination processes as well. While phagocytosis of the myelin sheaths contributes to active inflammation, clearance of myelin debris is critical for restoration of the lesion environment to a non-inflamed state. Upon myelin phagocytosis, activated microglia shift towards an anti-inflammatory state, observed by decreased production of the pro-inflammatory cytokines TNF and IL-1β and increased production of anti-inflammatory prostaglandin E2, activin-A, and insulin-like growth factor.[38,107] Infiltrating mononuclear cells promote remyelination. A live *in vivo* imaging study by the Kerschensteiner lab suggests that CNS environmental cues influence infiltrating monocytes towards either a pro-inflammatory or an anti-inflammatory phenotype, as seen in later EAE stages.[98] This shift may involve Ly6C^{lo} non-classical monocytes that repopulate inflammatory macrophages. Non-classical monocytes are shown to patrol the vasculature and can differentiate into anti-inflammatory macrophages to stimulate wound healing and angiogenesis.[38] Anti-inflammatory polarization of microglia and macrophages, characterized by arginase expression, and production of IL-10 and collagen, is observed to lead to enhanced clearance of myelin debris and to promote oligodendrocyte differentiation during remyelination.[108] IFNλ, a cytokine highly involved in EAE, may be key in explaining the temporal and spatial regulation of pro- versus anti-inflammatory signaling at this stage. While IFNλ is known to activate microglia, it alternatively limits peroxidation of myelin lipids to ameliorate EAE.[107,109] Thus, the complex and context-dependent roles of myeloid cells in the CNS underscore a dynamic balance between

pro-inflammatory and anti-inflammatory processes, which is essential for effective tissue repair and recovery during remyelination.

3. Interleukin (IL)-17 signaling pathway in steady state and EAE

The IL-17 cytokine family contains six members, IL-17A through IL-17F, and five receptors, IL-17RA through IL-17RE, which interact in distinct combinations to induce signaling in target cells (Fig. 4).[110,111] Among the cytokines, IL-17A (otherwise known as IL-17 or CXCL8) and IL-17F are the most infamous and well-studied due to their association with pathogenic Th17 cells in autoimmune disease. IL-17A and F share a high sequence homology and form homo- and heterodimers to signal through the same heteromeric IL-17RA/IL-17RC complex. IL-17A is more strongly linked to disease, as IL-17A-deficient mice have strongly decreased EAE, whereas IL-17F-deficient mice exhibit only minimal reductions in disease severity.[112–114] Additionally, complexes formed with homo- or heterodimeric IL-17F have weaker effects on target cells.[110]

Canonical IL-17 signaling begins when IL-17A binds to the IL-17RA/IL-17RC receptor complex on the extracellular membrane of target cells. The cytoplasmic adaptor protein Act1 is recruited to the receptor complex, leading to the polyubiquination of TNF receptor associated factor (TRAF)-6, a direct activator of the pro-inflammatory nuclear factor kappa-light-chain-enhancer of activated B cells (NF-κB) pathway.[115] Other pro-inflammatory pathways, including the mitogen-activated protein kinase (MAPK), and the CCAAT/enhancer-binding protein (C/EBP) transcription factors C/EBPβ and C/EBPδ are also induced by IL-17A.[116] IL-17 often synergizes with other cytokines, such as TNF, LT-β and IL-22, to amplify transcription programs, and induce tissue-specific signaling effects.[117] IL-17 has broad physiological functions across various tissues, likely due to the ubiquitous expression of its receptor IL-17RA, which is the common signaling subunit of four IL-17 ligands.

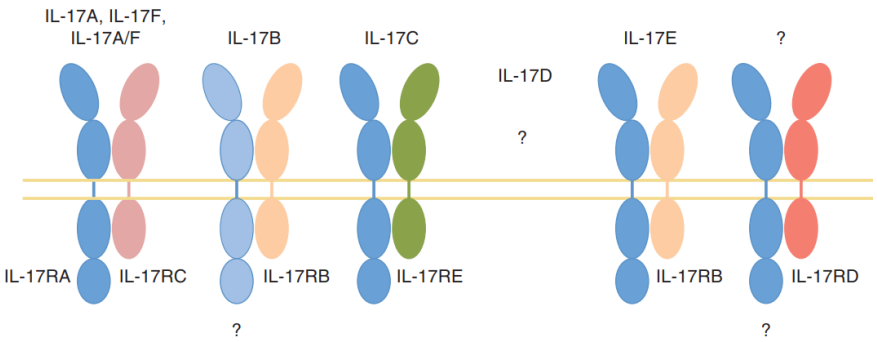

Figure 4: IL-17 family ligand-receptor relationships. *From Monin and Gaffen et al. 2018.*[118]

A critical balance of IL-17 appears essential for its homeostatic or pathogenic functioning, as signaling effects can be helpful in one context and harmful in another.[119] One of IL-17's best documented functions is to support anti-microbial, especially anti-fungal, immune resistance by the chemoattraction of neutrophils.[120–122] This is particularly relevant at the epithelial barriers of the lungs, intestine, and oral mucosa, which encounter trillions of microbial and viral signals daily. Microbial dysbiosis and increased intestinal IL-17 levels, produced by intraepithelial γδ-T cells or lamina propria αβ-T cells, is highly linked to inflammatory bowel disease (IBD).[123,124] In fibrotic tissues, IL-17 stimulates the proliferation and survival of fibroblasts to aid in wound healing, but excess IL-17 can lead to dysregulated tissue remodeling, sclerosis, and fibrosis.[125–127] In the CNS, IL-17 regulates behavior by modulating the neuronal activity of interneurons; in this context, increased IL-17 signaling has also been linked to autistic-like behaviors in mice.[128,129]

3.1. IL-17 during EAE

Both innate and adaptive immune cells produce IL-17 to induce unique signaling effects depending on the tissue environment.[130] Among innate sources, γδ-T cells ($CD3^+CD4^-TCR\gamma\delta^+$) are the largest, best-studied population and play an essential role in IL-17-mediated control of fungal and bacterial infection. *In vitro* culture with IL-1β or IL-23 stimulates rapid secretion of IL-17 from γδ-T cells and some studies suggest these cells are an early source of IL-17 during EAE.[131–133] A lymphoid tissue inducer (LTi)-like subset of ILC3s ($CD3^-CD4^+KIT^+THY1^+$) produces IL-17 to support the formation of lymphoid structures in mucosal and gut-associated lymphoid tissues (MALT/GALT) and in the spleen.[134] IL-17 has been similarly shown to promote tertiary lymphoid structures in the leptomeninges during EAE, although the source of IL-17, whether Th17 or LTi-like cell-produced, is unclear.[135] γδ-T cells, LTi-like cells, invariant NK (iNK) T cells,

and NK cells are abundant at the intestinal intraepithelial layer, where they survey the commensal species and produce cytokines such as IL-17 and IL-22 in response to microbial signals to maintain intestinal homeostasis.

$CD4^+$ Th17 cells are the classical drivers of adaptive IL-17 immunity during EAE, requiring IL-6 and transforming growth factor (TGF)-β for Th17 lineage commitment, and IL-23 for expansion.[136,137] TGFβ, IL-6, and IL-1 activate signal transducer and activation of transcription (STAT)-3 signaling, which induces expression of the lineage-defining transcription factors RORγt and RORα.[138,139] Evidence suggests that Th17 cells are heterogenous and able to adopt pathogenic and non-pathogenic phenotypes dependent on environmental factors.[140] Non-pathogenic Th17 cells are shown to be generated by IL-6 in combination with TGFβ1, while IL-6 in combination with IL-1β, and especially IL-23, are essential for Th17 cell pathogenicity and their production of GM-CSF during autoimmunity.[75,93,141]

Th17 cells differentiate and reside primarily in the immune compartment of the intestine, called the lamina propria (LP), and are influenced in their differentiation by commensal and pathogenic bacteria.[142] Segmented filamentous bacterial (SFB), a commensal, spore-forming gram-positive bacteria that can permeate the small intestinal ileal lining, promotes the expression of epithelium-derived serum amyloid alpha proteins 1 and 2 (SAA1/2) that induces Th17 cell differentiation.[143,144] Additionally, bacterial-derived adenosine 5'-triphosphate (ATP) is shown to drive lamina propria Th17 differentation by $CD11c^+$ cells that secrete IL-6 and TGFβ, while germ-free and antibiotic-fed mice have sharp decreases in Th17 numbers.[145] Indications exist that the state of the microbiome may influence the pathogenic signature of Th17 cells through metabolic reprogramming, as commensal SFB was shown to promote a "quiescent"-like Th17 cell that engages in oxidative phosphorylation and produce large amount of the anti-inflammatory cytokine IL-10, while *Citrobacter rodentium* infection promotes pathogenic Th17 cells which also engage in aerobic glycolysis.[146]

Th17 cells are the most well-published source of IL-17 during MS and EAE in both the CNS and periphery. Within the CNS, the percentage of $IL\text{-}17^+$ $CD4^+$ T cells is the highest at the pre-onset of EAE, suggesting a role in earlier stages of the disease.[76] It has been suggested by several publications that IL-17 may decrease BBB integrity by increasing expression of adhesion

molecules, disrupting the endothelial tight junction proteins occludin and zona-occludens (ZO)-1, and promoting CCR2 and CXCL1 release, allowing for leukocyte infiltration into the CNS.[147–149] However, these *in vitro* studies used 200-2,000 times the physiological level of IL-17 found in mice at the peak of EAE and have not been confirmed *in vivo*. One study suggests that high concentrations of IL-17 during acute EAE can affect synaptic plasticity and cognition in the hippocampus, despite this process typically occurring in later, chronic stages and not in the acute stages of the disease.[150]

No more consensus has been reached regarding IL-17's role within the periphery during EAE. IL-17 from innate γδ-T cells in the lymph nodes has been suggested to recruit IL-1β-producing myeloid cells that promote T cell priming with myelin antigens.[133] Alternatively, IL-17 was shown to activate fibroblastic reticular cells in the spleen for proliferation and survival, although this study found no reduction in EAE severity upon blockade of this signaling.[119] It has further been suggested that IL-17 signaling in the intestine may be relevant to disease development. This is an attractive hypothesis as Th17 cells, the major effector T cells in EAE, develop predominantly in the intestine and could provide a link between the gut and brain in MS. However, studies investigating the role of IL-17 have produced conflicting results, with one study implicating IL-17 signaling as pathogenic, and others suggesting intestinal IL-17 is protective during EAE.[151,152]

Since its discovery as a major effector cytokine of Th17 cells, anti-IL-17 therapies have been of interest for Th17-mediated disease.[153] Since 2015, blockade of IL-17A by treatment with the monoclonal antibody secukinumab is an approved treatment for plaque psoriasis with high efficacy. Treatment for MS patients has proved less promising, however. One study suggests treatment with secukinumab may reduce the presence of new lesions in MS, though cumulative number of active lesions detected by MRI was unchanged.[154] Other antibody treatments targeting the p40 subunit shared between IL-12 and IL-23, which act upstream of IL-17 signaling, showed no significant reductions in any disease parameters measured.[155,156] While one specific role for IL-17 during MS and EAE has not been found, and likely, different cell and tissue-derived IL-17 signals coordinate to modulate neuroautoimmune pathogenesis, greater knowledge of IL-17's pathogenic versus homeostatic functioning may lead to more targeted therapies with better outcomes for MS patients.

4. Gut-Brain Axis in MS and EAE

The gut-brain axis maintains host homeostasis via a complex orchestra of direct and indirect signals involving the enteric nervous system (ENS) and the intestinal microbiome. Direct signaling occurs bidirectionally via afferent and efferent sympathetic and parasympathetic vagal nerve fibers innervating the gut. Efferent signals from the CNS influence immune cells and microbial populations by altering gut motility, epithelial permeability, and secretion of cytokines, neurotransmitters, and neuropeptides.[157,158] Afferent nerve fibers act as sensors of the intestinal environment by expressing receptors for microbial metabolites, cytokines, and neurotransmitters. Additionally, microbes and their circulating metabolic products, such as fatty acids, bile acids, ROS, and polyamines, indirectly regulate the CNS immune system by affecting peripheral and CNS-resident immune cell functions.[159,160] Evidence for the involvement of both direct and indirect gut-brain axis signaling has been demonstrated in both MS and EAE.

4.1. The microbiome in MS

The human microbiome encompasses 100 trillion microbes, encoding about 100 times more genes than the human genome.[161] The microbiome of Western humans is taxonomized into four relatively stable phyla: Firmicutes (~60%), Bacteroidetes (~20%), Actinobacteria (~15%), and Proteobacteria (<5%).[162] Gut dysbiosis, defined as an imbalance in the equilibrium of these phyla and their sub-species, has been consistently observed in MS patients.[163–165] MS patients have increased Actinobacteria, decreased Bacteroidetes and Firmicutes, and an increased Firmicutes/Bacteroidetes ratio.[166] Sub-phyla families and species are variable between regions, making cross-cultural comparisons difficult. However, some studies indicate that MS patients have increases in bacterial species linked to oxidative stress and decreases in anti-inflammatory polyamine- and butyrate-producing bacteria.[167,168]

How intestinal dysbiosis translates into MS pathology is still being elucidated, yet most research in human patients highlights an involvement of T cell reprogramming in the gut. Gut associated lymphoid tissue (GALT) contains many T cells and is a major site for their activation.[159] Several studies suggest that MS-related microbiota exacerbates disease by

increasing the effector to regulatory T cell ratio. Human T cells cultured *in vitro* with bacterial extracts from MS patients tend to preferentially differentiate into effector helper T cells rather than Tregs.[163] Strikingly, these bacterial extracts worsened the severity of EAE when transplanted to germ-free mice. Similarly, a high frequency of intestinal Th17 cells in MS patients was correlated to higher disease activity.[166] One study linked increased *Methanobrevibacter* and *Akkermansia* and reduced *Butyricimonas* in MS patients with differences in gene expression among circulating T cells and monocytes involved in dendritic cell maturation and interferon and NF-κB signaling.[165] *Prevotella*, a commensal species commonly reduced in MS patients, was observed to suppress EAE in humanized mice by promoting tolerogenic dendritic cells that enhance Treg development and suppress effector T cell responses.[166,169] Despite the focus on specific bacterial strains, many competing signals orchestrate the delicate balance between health and disease.

Restoring gut homeostasis through microbiome modulation is a promising therapeutic avenue for several neurological disorders.[170] While many DMTs have adverse side-effects and lose efficacy over time, treatments with fecal microbiome transplantation (FMT) and probiotic supplementation have shown safety, tolerability, and positive outcomes in MS treatment.[171] A 12-week trial found reduced serum levels of CRP, TNF, and IFNγ, and increased $Foxp3^+$ and TGFβ with a twice daily mixed-strain probiotic.[172] Another 16-week trial found lower EDSS scores, reduced depression and anxiety, decreased plasma IL-6 and CRP, and increased IL-10 and nitric oxide (NO).[173] Whether this protection is due to functional changes in immune cells, vagal nerve activity, or both, remains to be determined.

4.2. Role of the microbiome in EAE

Laboratory models of EAE are invaluable for exploring the systemic effects of the microbiome using methods too invasive for human studies. The necessity of the microbiome in EAE is evident, as disease resistance is observed in mice housed under germ-free conditions.[174] Research from the same lab even suggests the microbiome may be the decisive factor in disease development; gut microbiota transplantation from dimorphic twin pairs led to a significantly greater EAE incidence in mice receiving transplants from MS affected twins than healthy twins.[163] Animal models suggest that the microbiome influences neuroinflammation through three mechanisms: 1) modulation of gut-resident T cell populations, 2) indirect effects

on CNS-resident innate immune cells via circulating factors, and 3) direct signaling to enteric neurons.

The microbiome alters T cell distribution, promoting neuroinflammation through Th17 development or suppressing it via Treg induction. Several commensal and pathogenic bacteria, such as SFB, bacterial-derived ATP, and *C. rodentium* increase Th17 prevalence, which is associated with worsening EAE and MS.[143,146,175] Conversely, other bacterial species and metabolites promote intestinal Tregs and limit EAE. For example, polysaccharide A from *Bacteroides fragilis* expands IL-10-producing Tregs at the expense of Th17 cells.[176,177] This may occur by promoting the secretion of retinoic acid, a vitamin A metabolite, by $CD103^+$ dendritic cells, which promotes Tregs and inhibits Th17 cells.[178]

Circulating metabolites also impact the homeostasis and responsiveness of CNS-resident innate immune cells. Presence of the intestinal microbiome is essential for the homeostasis of neuroglia, including microglia and astrocytes.[179] Some studies indicate that microbial metabolites can polarize neuroglia towards type-I immunity to reduce EAE severity. For example, increased LPS-producing lung bacteria polarized microglia towards type-I immune reactivity, effectively weakening their type-II response during EAE.[180] Importantly, altering the lung microbiome with neomycin treatment did not affect the transcriptome of lung T cells, but specifically of microglia. Additionally, dietary tryptophan-derived aryl hydrocarbon receptor (AHR) ligands promoted type-I immunity in astrocytes to suppress inflammation and neurodegeneration in EAE.[181] Bile acid supplementation also prevented inflammatory polarization of astrocytes and microglia and protected oligodendrocytes from cell death during EAE.[182]

Lastly, some research suggests intestinal dysbiosis may alter CNS responses via direct vagal nerve stimulation. In the cuprizone EAE model, vagotomy reduced demyelination and microglial activation, implicating direct neuronal signaling in disease pathogenesis.[183] Interestingly, vagotomy also restored cuprizone-induced intestinal dysbiosis. Conversely, electrical vagal nerve stimulation not only reduced EAE severity and duration, but also decreased demyelination, neutrophil and lymphocyte CNS infiltration, cytokine production, and gliosis by stimulation of the anti-inflammatory cholinergic system.[184] It remains unclear

whether the microbiome itself stimulates the vagal nerve to reduce inflammation or if it modulates acetylcholine-producing T cells that signal to the vagus nerve to inhibit cytokine production.[185]

5. Neutrophils in pathogenesis and immune suppression

The innate immune system is comprised of myeloid cells, such as monocytes, macrophages, granulocytes, and dendritic cells, that rapidly contain pathogens, contribute to the training of the adaptive immune system, and maintain tissue homeostasis. Neutrophils are part of the polymorphonuclear granulocyte system representing the major circulating leukocyte population at around 70% of leukocytes in the blood of humans and 25% in mice.[186] As diverse "first responders" of the innate immune system, neutrophils exhibit potent cytotoxic, antimicrobial, and immunoregulatory functions, and are rapidly produced to mobilize to sites of inflammation to both promote and resolve inflammation through a myriad of stimulus-dependent effector functions.[187,188]

5.1. Origin and development

All circulating leukocytes and erythrocytes originate from hematopoietic stem cells (HSCs) in the bone marrow.[189,190] HSCs differentiate into lineage progenitors with a spectrum of transcriptionally overlapping states (Figure 5). The myeloid lineage is established once HSCs differentiate into common myeloid progenitors (CMPs), which then differentiate into granulocyte-monocyte progenitors (GMPs)—bipotent precursors capable of becoming polymorphonuclear or mononuclear cells.[191–193] Upon GMP-commitment to a neutrophil state, mitosis ceases and neutrophil maturation begins, marked by a transition from rounded to lobed, horseshoe-shaped nuclei. Transcriptomic analysis of bone marrow neutrophils by Evrard et al. 2018 identified a three-stage development trajectory post-GMP stage. The transcription factor C/EBPε drives GMPs into a committed proliferative precursor ("preNeu"), which then differentiates into non-proliferative immature neutrophils before becoming a bonafide mature neutrophil.[191] The maturation process of post-mitotic neutrophils occurs in approximate 5-6 days in humans and 2-3 days in rodents, before which neutrophils are retained in the bone marrow by CXCR4 and released into circulation via CXCR2.[194,195] In circulation, neutrophils have a half-life of a day, but persist up to seven days under inflammatory conditions.[196]

Neutrophils exist in two main "pools": a free-flowing intravascular, recirculating pool and a "marginated" pool held in the bone marrow, spleen, and liver.[197] Studies using radio-labeled granulocytes indicate that the circulating pool represents around 50-70% of total neutrophils in humans and 10-25% in mice[198] Diffusion mapping and RNA velocity analysis of single-cell RNA sequencing data suggest that despite the existence of these two pools, a single maturation continuum occurs across different tissues, with overlaps in maturation between pools.[199] This may vary between context and disease; for example, in a model of *Streptococcus pneumoniae* infection, marginated immature Ly6G^{int} neutrophils underwent emergency granulopoiesis to sustain the circulating, mature Ly6G^{hi} neutrophils needed for bacterial clearance.[200]

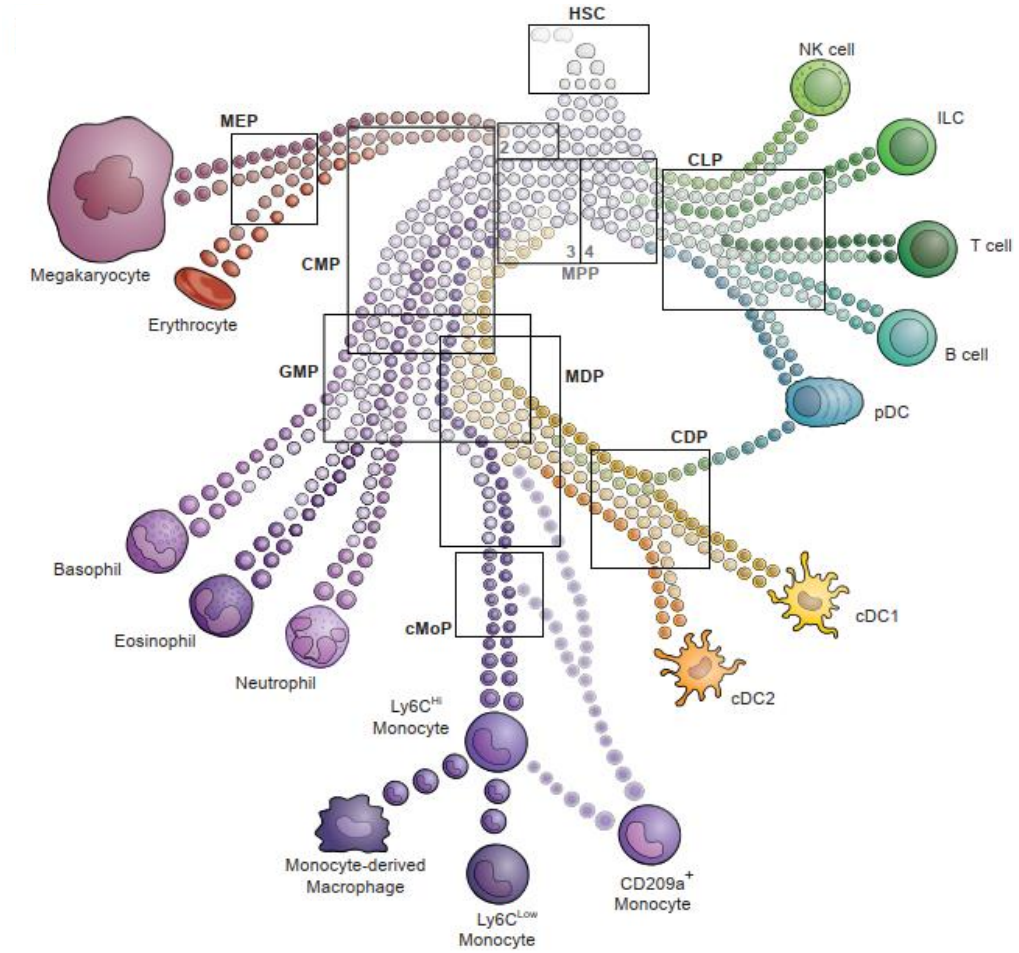

Figure 5: Development of murine leukocytes. *From Guilliams et al. 2018.*[201]

5.2. Effector functions

Neutrophils engage an arsenal of effector functions to contain pathogens and evoke both immunostimulatory and immunosuppressive responses, including: 1) degranulation, 2) release of NETs, 3) production of ROS, and 4) extracellular matrix remodeling.[40] Granulation and NETosis involve the rapid expulsion of clusters of packaged protein and DNA that exert effector functions on surrounding cells.[202] Granules, dense clusters of anti-microbial proteins, fuse with bacterial phagosomal membranes, while NETs are composed of clusters of packed DNA that are expelled to exert immunomodulatory effects on neighboring cells. Neutrophil ROS stimulates their own NET production, where NADPH oxidase-generated ROS activates MPO in the cytoplasm to form a complex with neutrophil elastase (NE). This complex translocates to the nucleus, leading to the proteolytic processing of histones that decondense chromatin for NET formation.[203] Both granules and NETs are highly immunoregulatory to neighboring cells. Granules are potently microbicidal, while NETs can induce apoptosis of epithelial and endothelial cells, activate leukocytes and tumor cells, and contribute to conditions such as thrombosis, atherosclerosis, cancer, and autoimmunity.[204]

Neutrophils possess dynamic cytoskeletal structures and express adhesion molecules and integrins, allowing them to morphologically "treadmill" themselves along the vasculature and extravasate rapidly into tissues.[186] Neutrophils migrate between endothelial cells where they communicate to cells of the basement membrane, such as pericytes, to influence tissue migration of circulating leukocytes. Their release of ECM remodeling signals, including NETs and MMPs, restructures tissue and disrupts tight junctions to alter the permeability of blood-endothelial barriers and influx of circulating leukocytes.[205] NETs have been documented to both promote NF-κB-mediated angiogenesis *in vitro*, while impairing revascularization in models of stroke and wound healing.[206–208]

5.3. Neutrophils during neuroinflammation

As the "first responders" during inflammation, neutrophils are among the earliest cells detected after EAE induction. Within 24 hours of EAE-induction, they appear in the meninges and increase in numbers in the periphery and CNS leading up to the onset of clinical EAE, after which their numbers decrease.[209] Depletion of neutrophils during the pre-onset stage of EAE inhibits disease development, highlighting an early, critical window for their pathogenic

functions.[105,210] Neutrophils play both immunostimulatory and immunosuppressive roles in neuroinflammation.

Their immunostimulatory roles include promoting BBB breakdown, facilitating leukocyte migration, and aiding T cell activation and differentiation. Neutrophils passing over IL-1β-activated endothelial cells release pro-inflammatory mediators like ROS, IL-1β, TNF, and matrix metalloproteinases (MMPs), which disrupt the BBB and recruit and promote the influx of migrating leukocytes.[211] Neutrophils can also phagocytose myelin and induce neuronal death through granule release and NET formation.[40,205]

Neutrophils influence T cell differentiation and activation both directly and indirectly, which can both promote or suppress neuroinflammation. Release of antimicrobial peptides, such as cathelicidin, and acquisition of antigen-presenting function during inflammation promotes pathogenic T cell responses both in the periphery and the CNS.[212] Neutrophils also aid the maturation of CNS APCs, including dendritic cells, macrophages and Ly6C^{lo} monocytes, which reactivate T cells in the perivascular space.[213] Conversely, neutrophils may suppress T cell function directly through their apoptotic bodies, programmed death ligand-1 (PD-L1) and arginase-1 (Arg1) expression and indirectly by promoting Treg differentiation. Neutrophils with these suppressive functions are classified as myeloid-derived suppressor cells (MDSCs) and are increasingly explored as a potential therapy in autoimmune disease.

5.4. Myeloid-derived suppressor cells (MDSCs)

MDSCs were nomered in 2007 upon increasing evidence of "immunosuppressive cells of myeloid origin" with enhanced T cell suppression capabilities.[214] Like other myeloid cells, MDSCs develop from CMPs and are supported by growth factors such as GM-CSF, G-CSF, and M-CSF. The transcription factors C/EBPβ and STAT3 drive the differentiation, expansion, and suppressive functioning of MDSCs, with IFNγ-stimulation further enhancing their suppressive capacity.[215,216] MDSCs are divided into two main subsets: polymorphonuclear/granulocytic (G-MDSCs) or monocytic (M-MDSCs). In humans, G-MDSCs are defined as CD14$^-$ CD15$^+$ and M-MDSCs as CD14$^+$HLA-DR$^-$CD15$^-$. In mice, G-MDSCs are defined as Ly6G$^+$ Ly6C^{lo} and M-MDSCs as Ly6G$^-$ Ly6C^{hi}.[217] Although these surface markers are traditionally used to classify MDSCs, they are a highly plastic and heterogenous population and overlap in surface

phenotype with normal $CD11b^+$ myeloid cells. In mice, MDSCs are solely distinguished from normal myeloid cells by their ability to suppress T cell proliferation and migration and their increased resistance to apoptosis. Compared to their normal counterparts, MDSCs have lower phagocytic capacity, and produce ROS, myeloperoxidase (MPO), arginase-1, prostaglandin E_2, and anti-inflammatory cytokines like IL-10 and TGFβ.[218] MDSCs also generate nitric oxide species (NOS), which can inhibit T cell dynamics through chemokine nitration or directly inducing their apoptosis.[219,220] Due to the highly plastic nature of MDSCs, G-MDSCs and M-MDSCs may utilize any of these suppressive mechanisms organ and context-dependently.

Differences in activation status influence myeloid fate towards "normal" or "suppressive" functioning.[221] While normal myeloid cells arise from strong, acute activation by pathogen-associated or damage-associated molecular patterns (PAMPs and DAMPs), MDSCs arise from persistent, weak activation signals from tumors or other chronic sources of inflammation.[222] Microbial dysbiosis may also influence MDSC development, as MDSCs express receptors for bacterial-derived SCFAs that promote their immunosuppression.[223] During homeostasis, the bone marrow contains the largest pool of MDSCs. During inflammation, rapid myelopoiesis in the bone marrow and egress of immature myeloid cells and progenitors, increases the peripheral pool of MDSCs. To what extent MDSC maturation occurs in the bone marrow or periphery is an open question. One study using single-cell RNA sequencing analysis in a murine breast cancer model showed that G-MDSCs arise in the spleen as a result of an aberrant maturation trajectory of splenic neutrophil progenitors.[224]

Research on MDSCs during neuroinflammation suggests that they play a protective role. As their numbers increase in the spleen, bone marrow, blood, and CNS throughout early and active disease stages, MDSCs globally suppress autoreactive T cells, but are also documented to encourage suppressive lymphocytes and remyelination within the CNS.[188] MDSC depletion worsens EAE, while adoptive transfer mitigates it, reducing T cell infiltration, gliosis, and enhancing myelin repair.[225,226] In the spleen, M-MDSCs and G-MDSCs suppress $CD4^+$ T cell proliferation through arginase-1 and ROS, induce NO-mediated T cell apoptosis, and rely on PD-L1 for their immunosuppressive functions.[227–229] CNS-derived activation signals appear to drive MDSC production during EAE. For example, intrathecal administration of the TLR ligand MIS416 recruits IL-10-producing G-MDSCs with higher suppressive potential than

M-MDSCs.[230] MDSCs may also promote IL-10-secreting regulatory T and B cells that dampen inflammation.[225] At later stages, M-MDSCs were shown to support remyelination by secreting osteopontin to promote OPC survival, proliferation, and differentiation.[231]

Some studies have suggested that MDSCs can exacerbate neuroinflammation by promoting Th17 responses.[232,233] Clinical evidence supporting this comes from the correlation of MDSC presence within lesions with prolonged disease duration in PPMS patients.[234] While MDSCs may inhibit acute inflammation, their role in creating an anti-inflammatory environment could hinder tissue healing processes. It's important to note that most studies investigating MDSCs use traditional surface marker expression (Gr-1, Ly6G, or Ly6C), which overlap significantly with classical monocyte and neutrophil subsets. Identifying MDSC-specific markers is crucial for future research to differentiate the development and functions of MDSCs from their normal myeloid counterparts.

MDSC-mediated immunosuppression shows potential as a novel therapeutic approach for neuroautoimmune diseases. A promising study showed that treating MS patients with the glucocorticosteroid methylprednisolone improved outcomes and increased arginase-1-producing MDSCs.[235] In EAE models, cannabidiol (CBD) attenuated disease by promoting MDSC expansion in the spleen and CNS.[236,237] Additionally, IFNβ, a widely prescribed treatments for RRMS, reduced EAE severity by increasing CNS MDSCs and enhancing their ability to induce T cell apoptosis.[238] Whether these mechanisms apply to IFNβ-treated MS patients has not been elucidated.

6. Rationale of the study

As one of the highest upregulated genes during acute neuroinflammation, IL-17 is strongly associated with disease in MS and EAE.[239,240] Despite this, its precise role and biological targets remain contentious.[119,241,242] Some studies implicate IL-17 in CNS pathology, while others suggest its primary function lies in peripheral tissues during the early stages of EAE.[133,148,243] Beyond its role in autoimmune inflammation, IL-17 is crucial for maintaining microbial homeostasis at epithelial barriers.[117] Recent findings from our laboratory indicate that the IL-17-regulated microbiome may influence peripheral inflammation during EAE. However,

whether this effect is additive to IL-17-mediated inflammation or functions independently remains unresolved.[152] We hypothesize that $CD4^+$ T cell-derived IL-17 contributes to early-stage EAE by acting in the periphery to promote autoimmune neuroinflammation.

The objectives of this project were the following:

1. To define the disease stage at which IL-17 is critical for EAE progression in the periphery.
2. To quantify the influence of the microbiome on EAE outcomes and determine whether this effect is synergistic with or independent of IL-17-mediated inflammation.
3. To identify a cellular target of IL-17 signaling involved in autoimmune neuroinflammation.

2 Materials & Methods

1. Reagents & Equipment

Reagent	Supplier
0.9% NaCl solution for perfusion	Berlin-Chemie, Germany
anti-IFNγ	Bio X Cell, USA
Acetic acid	Sigma-Aldrich, USA
Adjuvant Complete H37Ra (CFA)	BD Biosciences, USA
Agarose (Electrophoresis grade)	Biozym Scientific, Germany
β-Mercaptoethanol	Fluka Chemie GmbH
BD FACS Lysing Solution	BD Biosciences, USA
Bovine Serum Albumin (BSA)	Merck, Germany
Brefeldin A	Merck, Germany
Chloroform	Roth, Germany
Collagenase II	Thermo Fisher Scientific, USA
Dithiothreitol (DTT)	Thermo Fisher Scientific, USA
Dubecco's Modified Eagle Medium (DMEM)	Gibco® Life Technologies™, USA
DNase I	Roche, Switzerland
Dulbecco's modified PBS (DPBS)	Merck, Germany
Ethanol	AppliChem, Germany
Ethylenediaminetetraacetic acid (EDTA)	Merck, Germany
FC Block	BioLegend, USA
Fetal bovine serum (FBS)	Thermo Fisher Scientific, USA
Gene ruler 100 bp DNA ladder	Thermo Fisher Scientific, USA
Gibco® Hank's buffered saline solution (HBSS)	Thermo Fisher Scientific, USA
Gibco® Hank's buffered saline solution (HBSS) with Ca^{2+} and Mg^{2+}	Thermo Fisher Scientific, USA
Gibco® MEM non-essential amino acids (NEAA) 100x	Thermo Fisher Scientific, USA
Gibco® RPMI 1640	Thermo Fisher Scientific, USA
Gibco® Sodium pyruvate	Thermo Fisher Scientific, USA
Glycin	Roth, Germany
GoTaq® qPCR Master Mix	Promega, USA

Hank's Buffered Saline Solution (HBSS)	Sigma-Aldrich, USA
HEPES	Thermo Fisher Scientific, USA
Interleukin (IL)-23	Sino Biological, China
Ionomycin	Merck, Germany
Isopropyl alcohol	AppliChem, Germany
$KHCO_3$	Roth, Germany
L-Glutamine	Thermo Fisher Scientific, USA
Liberase™-TL	Roche, Switzerland
Methanol	Roth, Germany
Midori Green	Nippon Genetics, Germany
Mycobacterium tuberculosis Des. H37Ra	BD Biosciences, USA
Myelin oligodendrocyte glycoprotein (MOG) 35-55	GenScript, USA
NaCl	Roth, Germany
Non-Essential Amino Acids (NEAA)	Gibco® Life Technologies™, USA
Normal goat serum (NGS)	Thermo Fisher Scientific, USA
NH_4Cl	Roth, Germany
Nuclease-free H_2O	Qiagen, Germany
Olive oil	Merck, Germany
Papain	Merck, Germany
Paraformaldehyde (PFA) 4%	Santa Cruz Biotechnology, USA
Penicillin/Streptomycin (P/S)	Thermo Fisher Scientific, USA
Percoll	Merck, Germany
Pertussis toxin from *Bordatella pertussis*	List Labs, USA
Phorbol Myristate Acetate (PMA)	Merck, Germany
Phosphate buffered saline (PBS)	Sigma-Aldrich, USA
Proteinase K	Roche, Switzerland
REDTaq® ReadyMix™	Merck, Germany
Roti Histofix	Roth, Germany
RPMI 1640	Gibco® Life Technologies™, USA
Shandon Immu-Mount	Fisher Scientific, USA
Sodium chloride (NaCl)	Roth, Germany
Sodium dodecylsulfate (SDS)	AppliChem, Germany
Sodium pyruvate	Gibco® Life Technologies™, USA
Sucrose	Merck, Germany

Tamoxifen	Merck, Germany
Tris	Roth, Germany
Triton X-100	Merck, Germany
TRIzol™ Reagent	Thermo Fisher Scientific, USA
Trypan blue	Thermo Fisher Scientific, USA
Tween 20	AppliChem, Germany

Table 1: List of chemicals and reagents

Agilent TapeStation 4150	Agilent, USA
Aspiration system, Vacusafe	Integra Biosciences, Germany
Centrifuge 5417R	Eppendorf, Germany
Centrifuge Megafuge 16R	Thermo Fisher Scientific, USA
CO_2 incubator	SANYO, Japan
Dissection microscope M80	Leica, Germany
FACSCanto II™	BD Biosciences, USA
FACSymphony™ A3	BD Biosciences, USA
Gel-Imager: Gel Doc XR	Biorad, USA
Infinite® M200Pro NanoQuant, Tecan	Tecan, Switzerland
Laminar flow cabinet, Hera Safe	Thermo Fisher Scientific, USA
Microvette Serum Collection Tubes	Sarstedt, Germany
MyCycler™ Thermal cycler	Biorad, USA
Sprout Mini-centrifuge	Technolab GmbH, Germany
StepOnePlus™ Real-Time PCR system	Applied Biosystem, USA
Qubit Flex Fluorometer	Thermo Fisher Scientific, USA

Table 2: Laboratory equipment

2. Buffers, Media, and Kits

Buffer/Medium	Composition
0% media (Made in RPMI 1640 media)	20 mM HEPES 100 U/mL P/S 1 mM Sodium Pyruvate 50 µM β-Mercaptoethanol
3% media (Made in RPMI 1640 media)	3% FBS (v/v) 20 mM HEPES 100 U/mL P/S
10x Ammonium-Chloride-Potassium (ACK) lysis buffer (pH 7.4)	150 mM NH_4Cl 100 mM $KHCO_3$ 10 mM EDTA
50x Tris-acetate-EDTA (TAE) buffer (pH 8.3)	2 M Tris 1 M Acetic acid 50 mM EDTA pH 8.0
FACS buffer	PBS 2% FBS (v/v)
IHC blocking buffer	PBS 2% NGS 0.3% Triton X-100
T cell media (Made in RPMI 1640 media)	10% FBS (v/v) 2 mM L-Glutamine 1% NEAA (v/v) 1 mM Sodium pyruvate 1 mM HEPES 50 µM β-Mercaptoethanol
Tail lysis buffer (TENS)	10 mM Tris 5 mM EDTA 0.2% SDS (v/v) 200 mM NaCl

Table 3: List of buffers and media

Kit	Supplier
anti-CD19 Microbeads	Miltenyi Biotec, Germany
BD cDNA Kit	BD Biosciences, USA
BD Cytofix/Cytoperm Fixation/Permeabilization Solution Kit	BD Biosciences, USA
BD Rhapsody Enhanced Cartridge Reagent Kit	BD Biosciences, USA
BD Single-Cell Multiplexing Kit	BD Biosciences, USA
Calcein, AM Cell Dye	Invitrogen, USA
CD4+ T cell isolation kit	Miltenyi Biotec, Germany
CellTrace™ Violet Cell Proliferation Kit	Thermo Fisher Scientific, USA
Foxp3 / Transcription Factor Staining Kit	eBioscience™, Invitrogen, USA
Mouse IL-17A (homodimer) Uncoated ELISA	Invitrogen, USA
QuantiTect® Reverse Transcription Kit	Qiagen, Germany
StepOnePlus™ Real-Time PCR SYBR Green Kit	Life Technologies, USA

Table 4: List of kits

Antibody	Conjugate	Clone	Host	Dilution	Supplier	Application
CD3	FITC	145-2C11	Armenian Hamster	1:100	Biolegend	FACSymphony
CD3ε	Unconjugated	145-2C11	Armenian Hamster	1:100	Invitrogen	IHC
CD4	Percp	GK-1.5	Rat	1:400	Biolegend	FACS CantoII
CD8a	PE-Cy7	RM4-5	Rat	1:1000	Biolegend	FACS (all)
CD11b	BV510	M1/70	Rat	1:1000	BD Horizon™	FACSymphony
CD11b	PE-Cy7	M1/70	Rat	1:1000	eBioscience	FACS CantoII
CD11c	AlexaFluor700	N418	Arm. Hamster	1:500	BD Pharmingen	FACSymphony
CD19	BYG670-P	6D5	Rat	1:800	Biolegend	FACSymphony
CD43	PE	S7	Mouse	1:1000	BD Pharmingen	FACS (all)
CD44	BV650	IM7	Mouse	1:1000	BD OptiBuild™	FACSymphony
CD44	FITC	IM7	Rat	1:500	eBioscience	FACS CantoII
CD45	BUV805	30-F11	Rat	1:1000	BD Pharmingen	FACSymphony

CD88	APC	20/70	Rat	1:500	Biolegend	FACSymphony
CD90.1	Percp	OX-7	Mouse	1:600	Biolegend	FACS CantoII
CD90.2	APC-eFl780	53-2.1	Rat	1:500	eBioscience	FACS CantoII
CD154 (CD40L)	APC	MR1	Arm. Hamster	1:200	Biolegend	FACS CantoII
CD196 (CCR6)	PE-Cy7	29-2L17	Arm. Hamster	1:800	Biolegend	FACS CantoII
CD274 (PD-L1)	BV605	MIH5	Rat	1:1000	BD OptiBuild™	FACSymphony
CX3CR1	PE-CF594	Z8-50	Rat	1:300	BD Horizon™	FACSymphony
F4/80	BB790	T45-2342	Rat	1:400	BD Pharmingen	FACSymphony
Fixable viability dye	BV450	N/A	N/A	1:1000	eBioscience	FACSymphony
Fixable viability dye	eFluor506	N/A	N/A	1:1000	eBioscience	FACS CantoII
Foxp3	eFluor450	FJK-16S	Rat	1:200	eBioscience	FACS CantoII
GM-CSF	PE	MP1-22E9	Rat	1:200	Biolegend	FACS CantoII
IL-17A	eFluor450	eBio17B7	Rat	1:300	eBioscience	FACS CantoII
IFNγ	PE-Cy7	XMG1.2	Rat	1:500	eBioscience	FACS CantoII
Ly6C	BV570	HK1.4	Rat	1:500	Biolegend	FACSymphony
Ly6G	BV750-P	1A8	Rat	1:500	BD OptiBuild™	FACSymphony
MHCII	BV786	M5/114.15.2	Rat	1:1000	BD OptiBuild™	FACSymphony
NK1.1	APC-Cy7	PK136	Mouse	1:1000	BD Pharmingen	FACSymphony
SiglecF	BV480	E50-2440	Rat	1:500	BD OptiBuild™	FACSymphony
Sirpα	BYG790-P	P84	Rat	1:500	Biolegend	FACSymphony
Secondary Antibodies						
α-Hamster IgG	Alexa488	polyclonal	Goat	1:1200	Sigma Aldrich	IHC

Table 5: List of antibodies

3. Software & Algorithms

Software	Developer/Reference	Source
batchelor	Haghverdi et al. 2018	https://www.bioconductor.org/packages/release/bioc/html/batchelor.html
Cell Ranger	10x Genomics	https://www.10xgenomics.com/support/software/cell-ranger/latest
ClusterExplorer v1.7.6	FlowJo Software	https://flowjo.com/exchange
ClusterProfiler	Xu et al. 2024, *Nature*	https://github.com/YuLab-SMU/clusterProfiler
Downsample v3.3.1	FlowJo Software	https://flowjo.com/exchange
dplyr	Wickham et al. 2023	https://dplyr.tidyverse.org/
edgeR	Robinson et al. 2010	https://bioconductor.org/packages/release/bioc/html/edgeR.html
Enrichr	Chen et al. 2013	https://cran.r-project.org/web/packages/enrichR/vignettes/enrichR.html
fastMNN	Zhang et al. 2019	https://rdrr.io/github/LTLA/batchelor/man/fastMNN.html
FlowJo v10	FlowJo Software	https://www.flowjo.com
FlowSOM v4.1.0	Van Gassen et al. 2015	https://github.com/SofieVG/FlowSOM
GraphPad Prism 10	GraphPad Software	https://www.graphpad.com
magrittr	Wickham et al. 2022	https://magrittr.tidyverse.org/
muscat	Crowell et al. 2024	https://github.com/HelenaLC/muscat
R 4.1.0	The R Foundation	https://www.r-project.org
scater	McCarthy et al. 2017	https://bioconductor.org/packages/release/bioc/html/scater.html
scDblFinder	Germain et al. 2022	https://bioconductor.org/packages/release/bioc/html/scDblFinder.html
scran	Lun et al. 2016	https://bioconductor.org/packages/release/bioc/html/scran.html
Seurat v5	Hao et al. 2023	https://satijalab.org/seurat/
SingleCellExperiment	Amezquita et al. 2020	https://www.bioconductor.org/packages/release/bioc/html/SingleCellExperiment.html

Table 6: List of software and algorithms

4. Mouse Experiments

4.1. Mouse Strains

The following mouse strains were used for experiments:

IL-17AF$^{-/-}$ mice, herein referred to as IL-17$^{-/-}$, were provided by the lab of I. Prinz.[244] Control mice were IL-17$^{+/-}$ and were housed among IL-17$^{-/-}$ littermates (termed IL-17^{Cohoused}). Half of all knockout mice were housed only among other IL-17$^{-/-}$ mice directly after weaning from day 21 after birth (termed IL-17^{Separate}).

2D2 TCR (TCR^{MOG}) mice, described by Bettelli et al. 2003, were purchased from Jackson Laboratory and used at 50 weeks of age for *in vivo* T cell priming experiments.[55]

IL-17RA$^{fl/fl}$ mice[245] were created in our lab and bred to PDGFRβ-Cre^{ERT2} mice[246] purchased from Jackson Laboratory. These mice are herein referred to as IL-17RA$^{\Delta PER}$.

Both males and females above eight weeks of age were used for experiments. All mice used were on the C57BL/6 background and housed under specific pathogen-free conditions at the Translational Animal Research Center (TARC) of the University Medical Center Mainz. All animal experiments were approved by the local administration (Landesuntersuchungsamt Koblenz; G23-1-023) and were performed in accordance with the guidelines from the TARC Mainz.

4.2. Tamoxifen Treatment

All experimental IL-17RA$^{\Delta PER}$ mice received tamoxifen treatment at the age of 6-7 weeks old. A 20 mg/mL tamoxifen solution was prepared by dissolving 0.4 g tamoxifen powder (Merck) in 1 mL 99% ethanol and 19 mL olive oil pre-warmed to 56°C. Tamoxifen was dissolved by rotation overnight at 4°C. Each mouse received 100 µL (0.2 mg tamoxifen) intraperitoneally (i.p.) for five consecutive days.

4.3. Active EAE Induction

An emulsion of MOG_{35-55} in CFA was prepared by homogenization of 1 mg/mL MOG_{35-55} in PBS with CFA supplemented with *mycobacterium tuberculosis* H37RA. Solution was homogenized by sonification throughout the solution until completely emulsified. 100 µL of this solution containing 50 µg MOG_{35-55} were injected subcutaneously (s.c.) into the tail base. At the day of immunization and two days later, 150 ng PTx in PBS was additionally administered

intraperitoneally (i.p.) to promote the innate immune response to the peptide. From day 6 post immunization (p.i.), mice were weighed daily and the clinical scores were documented according to table 6. Upon reaching a score of 4.25, mice were sacrificed according to animal welfare regulations.

Symptoms and Behavior	Score
No symptoms, normal behavior	0
Decreased tone in the tail tip	0.25
Decreased tail tone	0.5
Tail partially paralyzed	0.75
Tail completely paralyzed	1.0
Mouse can be turned to the dorsal side but turns back immediately	1.25
Mouse can be turned to the dorsal side but turns back rather easily	1.5
Mouse can be turned to the dorsal side but needs more effort to turn back	1.75
Mouse can be turned to the dorsal side and stays at least 1 s in this position	2.0
Mouse walks with lowered buttocks	2.25
Mouse walks with lowered buttocks and shows wadding gait	2.5
Gait sorely afflicted, but walking movements are still recognizable	2.75
No clear walking movement but limbs not yet paralyzed	3.0
Paralysis of one of the hind legs	3.25
Paralysis of both hind legs but mouse still moves forward rather effortless	3.5
Paralysis of both hind legs; forward movement slowed down	3.75
Mouse stays in position and only moves forward with supreme effort	4.0
Mouse does not move forward and bends to one side	4.25
Mouse lies on one side even if turned to the other side	4.5
Mouse lies apathetically on the belly or side, breathing slowly, eyes (almost) closed	5.0
Mouse is dead	6.0

Table 7: Scoring system for the clinical signs of EAE

4.4. Adoptive Transfer (AT) EAE

4.4.1. Standard Th17 adoptive transfer EAE

Rag1$^{-/-}$ mice (C57BL/6J-Rag1em10Lutzy/J) carrying a knock-out allele of the recombination activation gene 1 locus were used as recipient mice for standard adoptive transfer EAE. Because these mice lack the ability to form mature B and T lymphocytes, this mouse line is useful in investigating the effector function of transferred T cells and allowing the researcher to easily relocate transferred cells in tissues of interest without additional congenic markers.

IL-17$^{-/-}$ mice and controls were immunized with MOG/CFA and PTx as described for active EAE immunization. Ten days after immunization, spleen, inguinal, and paraaortic lymph nodes were harvested and single cell suspensions were generated by passing the organs through a 40 µm cell strainer. Under sterile conditions, erythrocytes were lysed by incubating the cells with ACK for 3 minutes at room temperature. The reaction was stopped by adding FACS buffer and cells were pelleted by centrifugation at 400 x g for 10 min at 4°C. Cell pellets were resuspended in T cell medium and live cell numbers were determined. Cells were seeded at a concentration of 5 x 10^6 cells/mL in T cell medium supplemented with Th17-favoring conditions: 20 µg/mL MOG_{35-55}, 15 ng/mL IL-23, and 10 µg/mL α-IFN-γ. Cells were cultured for 4 days at 37°C and 5% CO_2. After 4 days, cells were harvested and live cell number was determined. Blasting cells as a percentage of live, single cells was determined by flow cytometric analysis of the cell size by gating forward scatter (FSC) against side scatter (SSC). 5 x 10^6 blasting cells were then transferred intravenously (i.v.) in sterile PBS into the recipient Rag1$^{-/-}$ animals. Recipient mice were furthermore treated with 150 ng PTx at the day of cell transfer and two days later. From day 6 post transfer (p.t.), recipient mice were weighed daily and the clinical scores were documented according to table 7.

4.4.2. "Criss-cross" adoptive transfer EAE

The "criss-cross" adoptive transfer EAE was used to compare the genotype effects of both transferred cells and the recipient environment within a single experiment. Active EAE was induced in donor IL-17$^{-/-}$ mice and controls and spleens and lymph nodes were harvested at day 10. Single cell suspensions were cultured according to the standard AT-EAE protocol (2.4.4.1). One day before cell transfer, IL-17$^{-/-}$ and control recipient mice were sub-lethally

irradiated with 4 Gray radiation to create a niche for the transferred cells to proliferate. After the four-day Th17 culture, 5 x 10^6 blasting cells from IL-$17^{-/-}$ or control donors were then transferred intravenously (i.v.) in sterile PBS into irradiated recipient IL-$17^{-/-}$ or control animals. Recipient mice were furthermore treated with 150 ng PTx at the day of cell transfer and two days later. From day 6 post transfer (p.t.), recipient mice were weighed daily and the clinical scores were documented according to table 7.

4.4.3. Lymph node & spleen adoptive transfer EAE

To compare the efficiency of transfer EAE from lymphocytes isolated from the spleen and lymph nodes, active EAE was induced in donor IL-$17^{-/-}$ mice and controls. Spleens and lymph nodes were harvested at day 10 and processed separately. Single cell suspensions were cultured separately by organ according to the standard AT-EAE protocol (2.4.4.1). After the four-day Th17 culture, lymphocyte-deficient $Rag^{-/-}$ recipient mice received an i.v. injection 5 x 10^6 blasting cells in sterile PBS from either the spleen or lymph nodes or either IL-$17^{-/-}$ or control donor mice. Recipient mice were furthermore treated with 150 ng PTx at the day of cell transfer and two days later. From day 6 post transfer (p.t.), recipient mice were weighed daily and the clinical scores were documented according to table 7.

4.4.4. CD4+ MACS adoptive transfer EAE

To investigate the independent effect of CD4+ T cells upon adoptive transfer, IL-$17^{-/-}$ mice and controls were immunized with MOG_{35-55}, spleens and lymph nodes were harvested at DPI 10 and single cell suspensions were cultured according to the conditions of the standard AT-EAE protocol (2.4.4.1). Ly5.1 mice (B6.SJL-PtprcaPepcb/BoyCrl) carrying the allelic variant Ptprca encoding for the congenic marker CD45.1, were used as recipient mice, since transferred cells can be easily identified with antibody staining against the C57BL/6 allelic variant Ptprcb (CD45.2). One day before cell transfer, Ly5.1 mice were sub-lethally irradiated with 4 Gray radiation to create a niche for the transferred cells to proliferate. After the four-day Th17 culture, cultured cells were collected and CD4+ cells were purified using magnetic sorting with $CD4^+$ microbeads (Miltenyi) following the manufacturer's protocol. Briefly, cultured cells were incubated with $CD4^+$ microbeads and the magnetically-labeled $CD4^+$ cells were collected and counted. 2x10^6 $CD4^+$ T cells were injected i.v. in sterile PBS into the tail vein of irradiated Ly5.1 wild-type recipient mice. Recipients were furthermore treated with 150 ng PTx at the day of

cell transfer and two days later. From day 6 post transfer (DPT), recipient mice were weighed daily and the clinical scores were documented according to table 7. Recipient mice were sacrificed at DPT 15 and the combined spinal cord and brain (CNS) and serum were analyzed.

4.5. *In vivo* Priming: Transfer of 2D2-TCR^{MOG} T cells

Priming of 2D2-TCR^{MOG} cells was performed according to an unpublished protocol recommended from the lab of Prof. Dr. Steffen Jung. Spleens were harvested from naïve 2D2 mice, mechanically dissociated in FACS Buffer and filtered through a 40 µm cell strainer. Erythrocytes were removed by ACK lysis for 3 minutes at room temperature. CD4$^+$ T cells were purified from single cell suspensions using the CD4$^+$ T cell isolation kit (Miltenyi) according to the manufacturer's protocol. Briefly, cells were incubated with a cocktail of biotin-conjugated antibodies targeting non-T cells. Cells were then incubated with anti-biotin microbeads and magnetically-labeled non-target cells were depleted from solutions to obtain a CD4$^+$ T cell purity of > 95%. Cell suspensions were counted and washed twice in pure PBS to remove any excess BSA. 1 x 10^4 2D2-TCR^{MOG} CD4$^+$ T cells in PBS were injected i.v. into the tail vein of IL-17$^{-/-}$ mice and controls 24 hours before active EAE induction. Active EAE was induced according to the protocol listed above and inguinal draining lymph nodes and spleens were harvested for flow cytometric analysis on day 5 of active EAE. Transferred cells were identified in donor mice by their expression of the congenic marker CD90.1.

4.6. *In vitro* "criss-cross" Th17 culture

The "criss-cross" *in vitro* Th17 culture was performed to observe the effects of IL-17$^{-/-}$ CD4$^+$ cells versus CD4$^-$ cells on cell blasting in culture. Single cell suspensions were obtained from the combined spleen and lymph nodes of IL-17$^{-/-}$ mice and controls at EAE DPI 10. CD4$^+$ T cells were purified using magnetic sorting with CD4$^+$ microbeads (Miltenyi) following the manufacturer's protocol. Briefly, cell suspensions were incubated with CD4$^+$ microbeads and both CD4$^-$ (unlabeled) cells and CD4$^+$ (labeled) cells were collected and counted. CD4$^+$ T cells from knockouts and controls were combined with CD4$^-$ cells of either knockouts or controls at a 1:4 ratio. Cells were seeded in 96-well U-bottom plates in triplicates at a concentration of 5 x 10^6 cells/mL in T cell medium supplemented with 20 µg/mL MOG_{35-55}, 15 ng/mL IL-23, and 10 µg/mL α-IFN-γ, and cultured for 4 days at 37°C and 5% CO_2. Blasting cells as a percentage

of live, single cells was determined by flow cytometric analysis of the cell size by gating forward scatter (FSC) versus side scatter (SSC).

4.7. $CD4^+$ Reconstitution of Lymphopenic Mice

$Rag1^{-/-}$ mice (B6.129S7-Rag1tm1Mom/J) that lack recombination activating genes (RAG), and therefore mature B and T lymphocytes, were used as recipient mice to investigate the functionality of transferred genetically modified T cells during EAE. $CD4^+$ T cells from naïve IL-$17^{-/-}$ mice and controls were purified from single splenocytes using the $CD4^+$ T cell isolation kit (Miltenyi) according to the manufacturer's protocol. Briefly, cells were incubated with a cocktail of biotin-conjugated antibodies targeting non-T cells. Cells were then incubated with anti-biotin microbeads and magnetically-labeled non-target cells were depleted from solutions to obtain a $CD4^+$ T cell purity of > 95%. Cell suspensions were counted and washed twice in pure PBS to remove any excess BSA. 5 x 10^6 $CD4^+$ T cells in PBS were injected i.v. into the tail vein of $Rag1^{-/-}$ mice 7 days before active EAE induction. Active EAE was induced according to the protocol listed above (2.4.3). Recipient mice were weighed daily from DPI 8 and the clinical scores were documented according to table 7. Inguinal draining lymph nodes, spleens, colons, and lungs were harvested for flow cytometric analysis on day 26 of active EAE.

5. Molecular Biology

5.1. Genotyping: DNA Isolation and Polymerase Chain Reaction

Ear or tail biopsies were taken at the recommended ages and lysed overnight at 56°C in TENS buffer supplemented with 400 mg/mL proteinase K. DNA was extracted by adding an equal volume of isopropyl alcohol to precipitate the DNA. DNA was pelleted by centrifugation at full speed for 10 min at room temperature. Supernatant was discarded and DNA was washed with 70% ethanol. After centrifugation at full speed for 10 min at room temperature, supernatant was again discarded and the pellet was dried at 37°C for 30 minutes and DNA was reconstituted in 200 µL distilled water and used for polymerase chain reaction (PCR).

PCR was performed in a total volume of 20 µL, composed of 1 µL DNA and 19 µL of a polymerase and primer containing master mix. To prepare the master mix, 500 µL REDTaq® ReadyMix™ were supplemented with 5 µL of each primer (stock concentration: 100 µM) and

filled with water to a total volume of 1 mL PCR reactions were performed at the primer-specific annealing temperature (table 8).

Amplified DNA fragments were distinguished by size by agarose gel electrophoreses. Agarose gels were prepared at 2.5% in 1x TAE buffer (total volume 400 mL) and supplemented with 12 µL Midori green DNA stain. Gels were run at a constant voltage of 120-130 V for 30-45 minutes. DNA bands were visualized under UV light using the Gel Doc XR+ gel documentation system (Bio-Rad) and band sizes were determined by comparing with the GeneRuler 100 bp plus DNA ladder (Thermo Fisher Scientific).

Primer Name	Primer Sequence	$T_{Annealing}$ [°C]	Direction
β-Actin	TGTTACCAACTGGGACGACA	58	Sense
β-Actin	GACATGCAAGGAGTGCAAGA		Anti-sense
IL17AF	ATCCAATCCCCCATCACCTT	55	Sense
IL17AF	GTTGGGACTTGCCATTCTGA		Anti-sense
IL17AF	TGCTTCCTCTACCAGCCATT		Anti-sense
IL17RA	GGCAGCCTTTGGGATCCCAAC	58	Sense
IL17RA	CTACTCTTCTCACCAGCGCGC		Anti-sense
IL17RA	GTGCCCACAGAGTGTCTTCTGT		Anti-sense
PDGFRb-Cre	CCACCTTGAATGAAGTCAACAC	60	Sense
PDGFRb-Cre	AGCTTGTGGCAGTGTAGCTG		Anti-sense
PDGFRb-Cre	ACATGTCCATCAGGTTCTTGC		Anti-sense
Universal-Cre	GCACTGATTTCGACCAGGTT	58	Sense
Universal-Cre	CCCGGCAAAACAGGTAGTTA		Anti-sense

Table 8: List of primers for PCR

5.2. RNA Isolation and Quantification

Tissues were snap-frozen in liquid nitrogen and stored at -80°C until further processing. RNA was extracted from frozen tissue (half brain or whole spleen) using the TRIzol™ reagent method. 800 µL TRIzol™ reagent was added to metal bead lysing matrix tubes (MP Biomedicals) followed by the addition of frozen tissue. After a 5-minute incubation at room temperature, the tissues were homogenized using the FastPrep-24 homogenizer (MP Biomedicals), then centrifuged at 12,000 x g for 10 minutes at 4°C. The supernatant was mixed

with 200 µL chloroform, incubated for 2-3 minutes at room temperature, and centrifuged again at 12,000 x g for 15 minutes at 4°C. RNA was precipitated by adding 400 µL isopropyl alcohol to the supernatant and centrifuging at full speed for 10 minutes at 4°C. The pellet was washed twice with 70% ethanol then resuspended in 100 µL nuclease-free water by incubation for 10 minutes at 56°C. RNA quality and concentration were determined by measuring absorbance at 260 nm and 280 nm using the NanoQuant Plate™ for the Infinite M200 pro plate reader (Tecan).

5.3. cDNA Reverse Transcription and Quantitative Real-Time PCR

1 µg of RNA was reverse transcribed into cDNA using the Quantitect® Reverse Transcription Kit (Qiagen). cDNA was diluted 1:4 in nuclease-free water and subsequently used for quantitative real-time PCR (RT-PCR) was performed with the StepOnePlus™ Real-Time PCR SYBR Green Kit (Life Technologies). Fold changes were calculated using the delta-delta CT method and normalized to controls. Hypoxanthin-Guanin-Phosphoribosyltransferase (*Hprt*) was used as a housekeeper gene for brain samples, while β-Actin (*Actb*) was used for spleen tissues. Primers for *Actb, Ccr7, Cxcl2, Hprt, Icam1, Icam2, Mmp2, Mmp9, Pecam1,* and *Vcam1* were ordered as QuantiTect Primer Assays (Qiagen). Primers for *Cxcl1* were designed with the primer-BLAST tool from the National Center for Biotechnology Information (NCBI). Primers for *Ccl19 and Ccl21* were taken from published sequences.[247] Sequences for these primers are given in the following table:

Primer Name	Primer Sequence (5' to 3')
Ccl19 fwd	TGTGTTCACCACACTAAGGGG
Ccl19 rev	CCTTTGTTCTTGGCAGAAGACT
Ccl21 fwd	ATCCAATCCCCCATCACCTT
Ccl21 rev	GTTGGGACTTGCCATTCTGA
Cxcl1 fwd	ACCATGGCTGGGATTCACCTC
Cxcl1 rev	CCAAGGGAGCTTCAGGGTCAA

Table 9: List of primers for RT-PCR

5.4. Enzyme-linked immunosorbent assay (ELISA)

Whole blood was stored at -80°C until assay could be performed. ELISA was performed using the anti-mouse IL-17 uncoated ELISA kit according to the manufacturer's protocol (Invitrogen).

Briefly, a 96-well flat-bottomed plate was coated overnight at 4°C with 100 µL of anti-mouse IL-17 capture antibody diluted in PBS. Coating solution was removed and washed three times with wash buffer (PBS + 0.05% Tween-20). Wells were blocked with 200 µL of ELISA/ELISPOT diluent for one hour at room temperature. Wells were washed once with wash buffer. Samples and standards were added to the wells and the plate was sealed and incubated overnight at 4°C. Wells were washed thrice with wash buffer, then 100 µL of detection antibody was added to each well and the plate was sealed and incubated at room temperature for 1 hour. Wells were washed thrice with wash buffer then 100 µL of Avidin-HRP was added to each well. Plate was sealed and incubated at room temperature for 30 minutes. Plate was washed five times with wash buffer then 100 µL of tetramethylbenzidine (TMB) substrate solution was added to each well and incubated at room temperature for 15 minutes. Stop solution (1M H_3PO_4) was added at 100 µL per well and absorbance was measured at 450 nm on an Infinite M200 pro TECAN plate reader (Tecan Trading AG, Switzerland). Concentrations of IL-17A were determined by referencing absorbance measurements from the standard curve.

5.5. Sphingosine-1-phosphate quantification

Sphingosine-1-phosphate (S1P) concentrations in the spleen and serum were measured according to Post et al. 2022.[248] Spleen tissue of equal masses were snap-frozen in liquid nitrogen until further processing. Serum was isolated from approximately 500 µL whole blood acquired by cardiac puncture using serum collection tubes. Serum volumes were equilibrated between samples before S1P quantification. Sphingolipids were extracted using methyl-tert-butyl ether (MTBE)-based liquid–liquid extraction method (LLE). Cells were pelleted in Precellys tubes (Peqlab) to which steel balls were manually added. 1000 µL of MTBE/methanol (10:3, v/v), which served as an extraction solvent, were added to the tubes and then 250 µL of ice-cold 0.1% formic acid containing 5 µM tetrahydrolipstatin/3'-(aminocarbonyl) [1,1'-biphenyl]3-yl)-cyclohexylcarbamate and 10 µg/mL butyl hydroxytoluene as homogenization solvent. A 10 µL methanolic solution of internal standard S1P d17:1 was then added to the tubes. The concentration of internal standards in the spike solution was set so as to result in a target concentration in the 100 µL final extracts of 200 ng/mL S1P d17:1. Samples were then homogenized for 20 s at 6000 rpm. Homogenates were transferred into 1.5 mL Eppendorf tubes, vortexed for 30 s at 4°C and centrifuged for 10 min at 13,000 rpm. Upper organic phase was recovered in new 1.5 mL tubes, evaporated to dryness under a gentle stream of nitrogen,

reconstituted in 90 µL methanol and stored at -20°C until further analysis. Lower aqueous phase was used for protein content determination using the BCA assay. Lipids were analyzed by liquid chromatography/multiple reaction monitoring (LC/MRM) using QTRAP 5500 (AB Sciex) operating in positive/ negative ion mode switching. Lipid species were quantified using the Multiquant software version 3.0.3. The determined lipid concentrations were normalized to protein content of the samples.

5.6. Well-based Single-cell RNA-Sequencing

For RNA sequencing of single $CD19^-$ splenocytes, four spleens per condition (12 total) were harvested using the standard protocol and $CD19^+$ cells were magnetically depleted using CD19 microbeads (Miltenyi). Samples were concentrated to 1000 cells/µL and stained with calcein, AM solution (Invitrogen) and viability was measured using the BD Rhapsody system (BD Biosciences). Samples were incubated with sample tags from the BD single-cell multiplexing kit (BD Biosciences) allowing for six samples to be simultaneously analyzed per cartridge (two samples per condition per cartridge). 30,000 cells were loaded onto each cartridge from the pooled samples (5,000 cells/sample). Magnetic beads were added, cells were lysed, and mRNA was extracted and captured using the BD Rhapsody Enhanced Cartridge Reagent Kit (BD Biosciences). cDNA was synthesized using the BD cDNA Kit (BD Biosciences), concentrations were determined with the Qubit Flex fluorometer (Thermo Fisher Scientific), and quality was assessed using the Agilent TapeStation 4150 (Agilent). Libraries were prepared with the BD Rhapsody System and 4 nM concentrated libraries were used for RNA sequencing (based on an average size of 675 bp). Cells were sequenced on the NovaSeq X Plus (Illumina) from 40,000 total cells with an average depth of 50,000 reads per cell.

6. Cell Biology

6.1. Cell Isolations

6.1.1. Leukocyte isolation from lymphoid tissues

For leukocyte isolation from lymphoid tissues (spleen and lymph nodes), tissues were digested with 2 mg/mL collagenase II and 50 µg/mL DNase I in PBS containing Mg^{2+} and Ca^{2+} for 30 minutes at 37°C shaking with 500 rpm. Erythrocytes from the spleen were lysed by incubation

with ACK for 3 minutes at room temperature. The reaction was stopped with FACS buffer and the cells were pelleted by centrifugation at 300 x g for 10 minutes at 4°C.

6.1.2. Leukocyte isolation from CNS tissues

For leukocyte isolation from the CNS parenchyma, brains and/or spinal cords were isolated from 0.9% NaCl perfused mice, finely minced in PBS with a razor blade, pelleted, then digested with 2 mg/mL collagenase II and 50 μg/mL DNase I in PBS containing Mg^{2+} and Ca^{2+} for 30 minutes in a 37°C water bath. The digestion reaction was stopped with 8 mL of FACS buffer. Tissue suspension was homogenized using an 18-gauge needle and centrifuged at 300 x g for 10 minutes at 4°C. Supernatant was discarded and the homogenate was mixed with 70% Percoll in PBS. A gradient of 30%, 37%, and 70% Percoll was generated by underlying the corresponding Percoll phases. Samples were centrifuged at 500 x g for 40 minutes at 20°C without acceleration or brake. The cell fraction between the 37% and 70% Percoll layers were collected and washed with FACS buffer.

Leukocyte isolation from the dural meninges was carried out according to Rustenhoven et al. 2021.[249] The top of the skull was removed from 0.9% NaCl perfused mice and placed into cold PBS. Meninges were peeled from the skull under a dissection microscope (Leica) using fine forceps and placed back into PBS until all samples were harvested. Samples were digested for 15 minutes at 37°C with 500 rpm constant agitation in 1 mL of pre-warmed digestion media (DMEM + 2% FBS + 1 mg/mL collagenase VIII + 0.5 mg/mL DNase I). Samples were filtered through a 70 μm strainer, washed with FACS buffer, and cells were stained for flow cytometry.

6.1.3. Leukocyte isolation from colon

Intestinal leukocytes were harvested from colon according to Shanmugavadivu et al. 2024.[250] Organs were removed from the mouse and the cecum was discarded from the colon. Fat was removed, the tissue was opened by cutting longitudinally and rinsed in 3% media to clear it of feces and debris. The epithelial layer was removed by incubating the tissue with 3% media containing 20 mM EDTA and 1 mM DTT for 20 minutes at 37°C on a horizontal roller. Samples were vortexed and shaken vigorously, rinsed with 3% media, then transferred to 0% media containing 5 mg/mL Liberase TL (Roche) and 100 μg/mL DNase I (Sigma-Aldrich) for cellular digestion. It was then cut into small pieces and incubated at 37°C for 30 minutes on a horizontal

roller. After digestion, the resulting cell suspension was filtered serially through 100 μm then 70 μm filters. Cells were washed and resuspended with 3% media, counted, and stained for flow cytometry.

6.1.4. Leukocyte isolation from liver

Livers were removed from 0.9% NaCl perfused mice and placed into PBS until all tissues were collected. Liver was minced into small pieces and forced gently through a 100 μm filter on a 50 mL conical tube using a syringe plunger. Tubes were filled up to 50 mL with RPMI containing 10% FCS and 1.25 mM HEPES. Samples were centrifuged at 100 x g for one minute at room temperature without brake or acceleration. Supernatant was transferred to a new tube and suspension was centrifuged at 500 x g for 8 minutes at room temperature. Supernatant was removed and the pellet was resuspended with 10 mL of 37.5% Percoll in Hank's Balanced Salt Solution without magnesium or calcium and containing 100 U/mL of heparin. Samples were centrifuged at 900 x g for 30 minutes at room temperature without brake or acceleration. Erythrocytes were lysed in 2 mL of ACK buffer for 5 minutes at room temperature. Reaction was stopped with 8 mL of FACS buffer then centrifuged at 500 x g for 8 minutes at 8°C. Cells were resuspended in FACS buffer, counted, and stained for flow cytometry.

6.1.5. Leukocyte isolation from lung

Lungs were removed from 0.9% NaCl perfused mice and placed into PBS until all lungs were collected. Lungs were then transferred to 1 mL of digestion buffer (100 U/mL collagenase IV in RPMI) in 2 mL tubes, cut into small pieces, and incubated for 30 minutes at 37°C with 500 rpm rotation. Samples were removed and resuspended with 1 mL pipette. Another 1 mL of digestion buffer was added and samples were incubated again for 30 minutes at 37°C with 500 rpm rotation. To stop the digestion reaction, samples were put on ice for 5 minutes, then 40 μL of 0.5M EDTA was added before vortexing and another 5-minute incubation at room temperature. Samples were filtered through a 100 μm cell strainer on a 50 mL conical tube and mechanically dissociated with the flat end of a syringe plunger. Filters were washed with 20 mL of 10 mM EDTA in PBS, centrifuged at 300 x g for 6 minutes at 4°C. Erythrocytes from the spleen were lysed by incubation with 1 x ACK for 3 minutes at room temperature. The reaction was stopped with FACS buffer and the cells were pelleted by centrifugation at 300 x g for 10 minutes at 4°C.

6.1.6. Leukocyte isolation from blood

Mice were euthanized with an overdose of CO_2 and 3-4 drops of blood were collected via cardiac puncture using a syringe with a 26G needle. The blood was placed into 1 mL of cold PBS on ice until all samples were collected. Samples were centrifuged at 200 x g for 10 minutes at 4°C and the pellets were resuspended in anti-Fc receptor block in FACS buffer and incubated for 15 minutes at 4°C. After another centrifugation at 200 x g for 10 minutes at 4°C the pellets were resuspended in 100 µL of FACS buffer containing surface antibodies and incubated at 4°C in the dark for 30 minutes. After the staining period, 1 mL of BD FACS lysing solution (BD Biosciences) was added directly to the samples and incubated for 5-10 minutes in the dark at room temperature. Samples were washed twice with FACS buffer and resuspended in 300 µL of FACS buffer. Samples were acquired within 48 hours using a FACSymphony A3 flow cytometer (BD Biosciences).

6.2. Flow Cytometry

Single cell suspensions were seeded at 2 x 10^6 cells per well in a 96-well plate (or 5 x 10^6 cells per well for restimulation; conditions stated below). Cells were pelleted by centrifugation at 300 x g for 5 minutes at 4°C. Fc receptors were blocked by resuspension in 100 µL of anti-mouse CD16/32 Fc blocking solution and incubated for 20 minutes at 4°C. Cells were washed then subsequently incubated for 30 minutes at 4°C in the dark in 50 µL of a cocktail containing surface-binding antibodies and a viability dye in FACS buffer. Cells were then washed and pelleted. Samples were either acquired directly on a FACSCantoII (BD Biosciences), FACSymphony A3 (BD Biosciences) for multidimensional myeloid analysis, or fixed overnight with 2% formaldehyde and acquired within one week. For intranuclear staining of the transcription factor Foxp3 as a marker for regulatory T cells, cells were stained for surface antibodies, then fixed and permeabilized with the Foxp3 kit (eBioscience™) according to kit instructions. Cells were then stained overnight for transcription factors. For intracytoplasmic stainings of cytokines and CD40L, cells were restimulated for 6h in the presence of 20 µg/mL MOG_{35-55} peptide and 1 ng/mL Brefeldin A at 37°C in T cell medium. After surface staining, cells were fixed and permeabilized with the Cytofix/Cytoperm kit (BD Biosciences) according to kit instructions, and stained for intracellular cytokines overnight. Analyses were performed with FlowJo™ v10 software (BD Biosciences).

6.3. Immunohistochemistry

Immunohistochemistry of the meninges was performed according to the protocol of Louveau et al. 2018.[251] Briefly, mice were transcardinally perfused with 0.9% NaCl and skull caps were removed and placed into 4% PFA overnight. Using fine forceps, dural meninges were carefully removed from the skull cap under a dissection microscope and placed into PBS in a 12-well plate (Leica). Meninges were washed twice for 5 minutes in PBS to remove any leftover PFA and blocked for one hour at room temperature in IHC blocking buffer (listed in table 3). Samples were incubated with CD3 primary antibody diluted in IHC blocking buffer overnight at 4°C. Samples were washed thrice for 5 minutes in PBS then stained with secondary antibodies in 0.05% Triton X-100 in PBS for one hour at room temperature. DAPI was added for the last five minutes (1:1000), samples were washed thrice, then placed onto microscope slides under a dissection microscope. Slides were covered and embedded in Shandon Immu-Mount (Fisher Scientific). Images were acquired with a TCS Sp8 DIVE confocal microscope (Leica).

7. Data Analysis

7.1. t-distributed Stochaistic Neighbor Embedding (t-SNE) of FACSymphony data

Dimensionality reduction analysis was performed using FlowJo software. Cells were pre-gated to exclude doublets, dead cells, and lymphocytes ($CD19^+$ B cells and $CD3^+$ T cells). $CD11b^+$ events were randomly downsampled using the Downsample plugin and samples from each condition were concatenated into one FCS file. Dimensionality reduction was performed using the t-SNE plugin. The FlowSOM plugin was used to cluster cells and ClusterExplorer plugin was used to investigate marker expression for manual cluster annotation.

7.2. Single Cell RNA Sequencing Analysis

7.2.1. Quality control and integration

RNA-Seq data in the form of FASTQ files were demultiplexed and aligned to the mm10 genome using Cell Ranger software (10x Genomics). The returned filtered cell barcode and feature matrices were then used for further analyses in R v4.1.0. Single-cell reads were mapped to the ens.mm.v102 Ensembl database for gene level annotation. Cells with high mitochondrial genes (> 20%) were removed and doublets were detected and removed using the scDblFinder

package. Batch correction and MNN-based data integration were performed using the batchelor and fastMNN packages. Data was normalized using the logNormCounts function of the scater package. Gene variation and highly variable genes were identified using scran to construct a single nearest neighbor (SNN) graph with k = 25. Dimensionality reduction was performed using principal component analysis (PCA) to identify principal components that capture the most significant variance in the gene expression data.

7.2.2. Cell annotation

Initial cell-type annotation was performed with reference to the official Immgen mouse dataset. Stromal cells and endothelial cells were removed from all samples. T cells were subclustered into either $CD4^+$ T cells or $CD8^+$ T cells based on their dual expression of *Cd3* and unique expression of *Cd4* or *Cd8*, respectively. Erythroid progenitors were identified by unique *Car2* expression, as described by Paul et al. 2015.[252] Stem-like progenitors were identified by expression of *Top2a* and further subclassified according to neutrophil or monocyte lineage markers. Monocytes were defined by *Ccr2* expression and subdivided into four subsets: two classical subsets expressing *Hspa1b* ("C1") or *Cd83* ("C2"), *Top2a*-expressing progenitors, and *Spn*-expressing non-classical monocytes. Neutrophils were defined by expression of the degranulation genes *S100a8, S100a9,* and *S100a11* and were further subdivided into subsets based on data from Evrard et al. 2018[191]: *Top2a*-expressing progenitors, *Mki67*-expressing proliferating neutrophils, *Cybb*^{hi} immature neutrophils, and *Il1b* and *Cxcr2*-expressing mature neutrophils. Dendritic cells nearly unanimously expressed *Itgax* and were subdivided into four subclusters: two classical DC subsets expressing *Xcr1* ("cDC1s") or *Sirpα* ("cDC2s"), *Zeb2*-expressing *Ccr2*-negative plasmacytoid DCs ("pDCs"), and high *Ccr7* and *Relb*-expressing migratory DCs ("migDCs"). Monocyte-derived macrophages were identified by dual *Ccr2* and *Zeb2* expression (termed "MoMacs").

7.2.3. Differential abundance and differential gene expression Analysis

Lowly expressed genes (< 10 reads) were removed and raw counts were used for differential abundance (DA) and differential gene expression (DEG) analysis using muscat, magrittr, and edgeR. Sample-level DEG analysis was performed in a "pseudo-bulk" manner using pbDS comparing IL-$17^{Cohoused}$ versus controls and IL-$17^{Separate}$ versus IL-$17^{Cohoused}$. An FDR < 0.05 and

$log_2FC > 0.5$ were used to identify DEGs for generation of volcano plots. Gene ontology (GO) enrichment (GO Biological Process 2015) of DEGs was performed using Enrichr.

7.2.4. Calculation of gene signatures with UCell

Cell signatures for MDSC were visualized on a UMAP using the UCell package. The following genes were included in the MDSC gene signature: *Cd84, Ctsd, Arg2, Pla2g7, Il1b, Clec4e, Junb, Wfdc17, Clec4d.*

3 Results

1. An IL-17-dependent microbiome promotes the progression of EAE

During steady-state, IL-17 plays an essential role in microbiome homeostasis of the host.[117] Through the use of separate and co-housing conditions of mice, previous research from our group suggests that the role played by IL-17 in microbiome homeostasis may also determine the outcome of autoimmune disease in the EAE model.[152] To determine whether IL-17 deletion or the housing conditions affected the development of EAE, IL-17 knockout mice (IL-17$^{-/-}$) were generated by the breeding of IL-17 homozygous knockout females (IL-17$^{-/-}$) to heterozygous knockout males (IL-17$^{+/-}$), resulting in 50% heterozygous and 50% homozygous IL-17 knockout offspring (Fig 6A). From the homozygous IL-17 knockout offspring, housing groups were created at weaning (21 days old) by housing half of the IL-17$^{-/-}$ mice among IL-17 heterozygous control littermates (to create the cohoused IL-17 knockout group, termed hereafter as IL-17^{Cohoused}) and housing the other half among only IL-17-deficient littermates (termed hereafter as IL-17^{Separate}). Since IL-17 is only expressed during inflammation and to confirm the deletion of IL-17, active EAE was induced in both groups of IL-17$^{-/-}$ mice (cohoused and separately housed) and controls according to the protocol shown in Fig. 6B. Leukocytes were isolated from the spinal cord and MOG-specific T cells were analyzed by flow cytometry (Fig. 6C) for expression of IL-17. The deletion of IL-17 was confirmed in IL-17$^{-/-}$ animals (Fig 6D).

IL-17 deficiency resulted in a reduced EAE score compared to controls (Fig 7A). An additional reduction in EAE score was observed between the IL-17^{Separate} group compared to the IL-17^{Cohoused} group. This implicates not only an effect of IL-17-deficiency, but also an effect of the IL-17-dependent microbiome on the outcome of EAE. This phenotype was largely observed as a result of EAE incidence, with IL-17^{Separate} mice having the lowest incidence of disease (45% of immunized animals) and IL-17^{Cohoused} mice having an intermediate disease incidence (54% of immunized animals) between IL-17^{Separate} mice and controls (92% of immunized animals) (Fig 7B). No significant differences were seen in the day of disease onset; both groups presented with clinical symptoms starting, on average, between day 13 to 15 after immunization (Fig 7C).

Pooled maximum clinical scores of all immunized mice showed a significant decrease in the peak disease score of IL-17^{Separate} compared to controls (Fig. 7D). Since significantly less

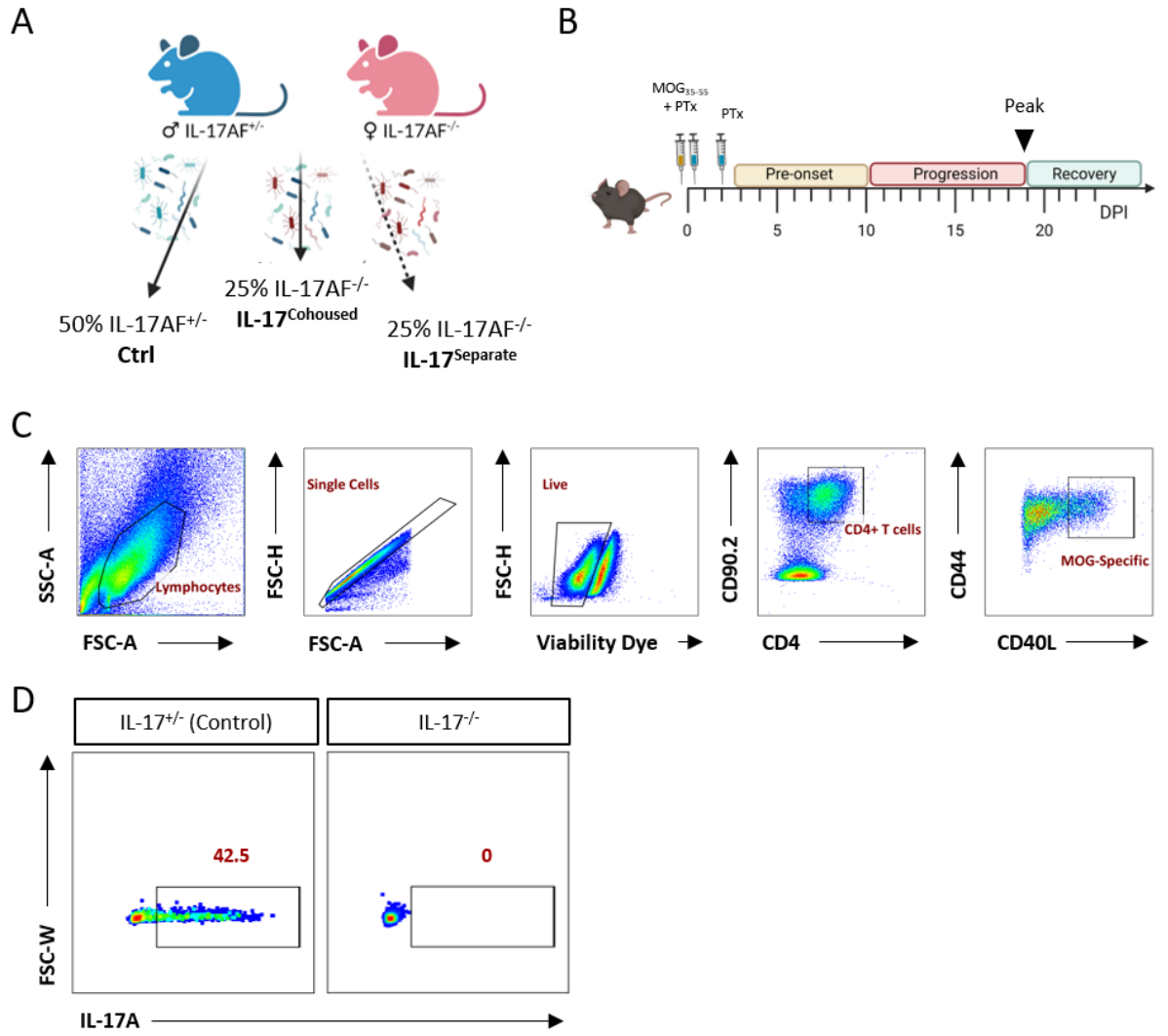

Figure 6: Generation of IL-17-deficient mice under separate and co-housing conditions. (**A**) Schematic overview of breeding strategy used to generate IL-17 knockout (IL-17$^{-/-}$) mice under separate (IL-17^{Separate}) and co-housed (IL-17^{Cohoused}) conditions. (**B**) Diagram illustrating protocol for active EAE induction by immunization with MOG_{35-55}/CFA and pertussis toxin (PTx). (**C**) Representative flow cytometry gating strategy used to identify live single cells, $CD4^+$ T cells ($CD90.2^+$ $CD4^+$), and MOG-specific ($CD44^+$ $CD40L^{hi}$) T cells isolated from the inflamed spinal cords of mice at peak EAE (DPI 19). (**D**) Representative flow cytometry dot plots showing IL-17A expression by MOG-specific T cells from the spinal cords of control and IL-17$^{-/-}$ mice at the peak of EAE.

IL-17^{Separate} mice exhibited symptoms, the significance in the peak score might be confounded by the decreased disease incidence of IL-17^{Separate} mice. To compare disease severity of sick mice between groups, data was pooled from only mice that became sick with a clinical score (Fig. 7E). Among sick mice, there was no significant difference in the maximum disease score

between the three groups. This implicates the role of IL-17 and its related microbiome as altering a so-called "tipping point" of disease; though IL-17-deficient mice have reduced EAE incidence, IL-17 plays no role in the disease severity until mice surpass an inflammatory threshold that leads to development of a clinical score.

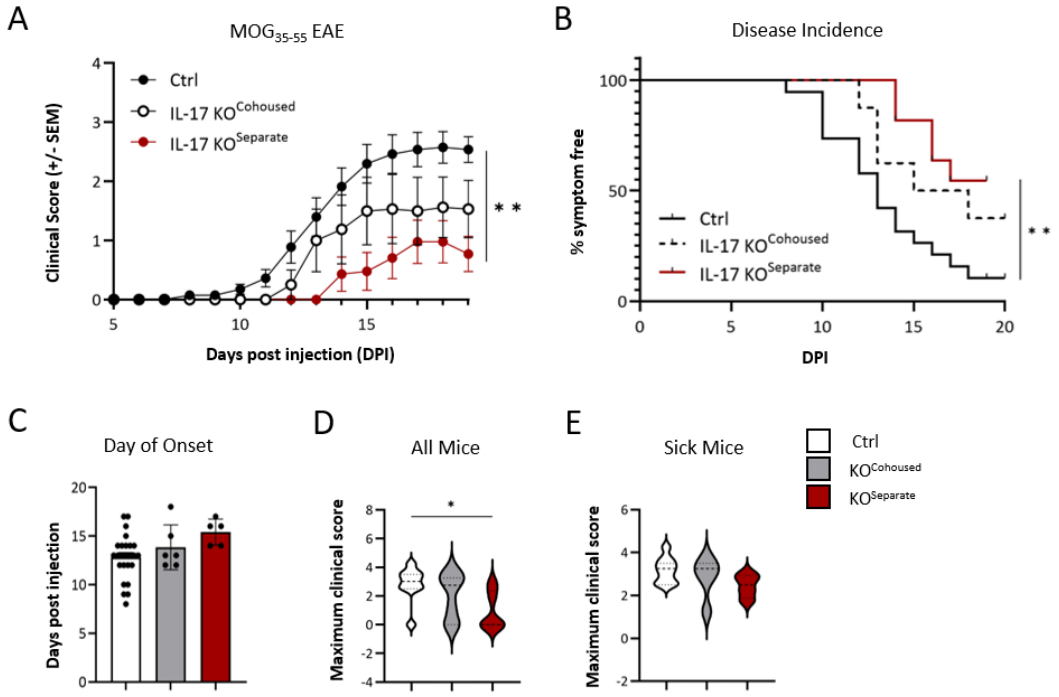

Figure 7: IL-17 and its dependent microbiome increase the incidence of MOG$_{35-55}$-EAE. (**A**) Active EAE clinical scores of IL-17-deficient mice either separately housed (red line; IL-17^{Separate}) or cohoused (black dashed line; IL-17^{Cohoused}) among controls (black line). Significance calculated from area under the curve (AUC). (**B**) Symptom-free survival curve, (**C**) day of disease onset, and peak scores of (**D**) all mice or (**E**) only sick mice from data shown in (A). Data combined from three independent experiments with n = 8-20 mice per group. Data is shown as either (A) mean +/- SEM or (C-E) mean +/- SD. P values calculated using one-way ANOVA of either (A) AUC or (D) individual data points. Kaplan-Meier survival analysis was performed on (B) with Wilcoxon rank test. * $p < 0.05$; ** $p < 0.01$.

2. IL-17-deficient mice have decreased numbers of leukocytes in the CNS parenchyma at the peak of EAE

Active EAE progression in the CNS requires the infiltration of mononuclear leukocytes that promote neuronal demyelination and the development of inflammatory lesions.[40,97] To investigate whether leukocyte infiltration into the CNS parenchymal tissue was affected by loss of IL-17, spinal cords were harvested from MOG$_{35-55}$-immunized IL-17$^{-/-}$ and control mice at the peak of disease (DPI 19) and T cell and myeloid cells were analyzed via flow cytometry. CD4^{+} T

cells were stained for common antigens and analyzed according to the gating strategy in figure 6C. Significantly fewer $CD4^+$ T cells were found in the spinal cords of immunized IL-$17^{Separate}$ mice compared to controls (Fig 8A, B). The percentage of MOG-specific T cells among total $CD4^+$ T cells was unchanged between groups, as represented by the flow cytometry dot plots in Fig. 8C. However, significantly fewer MOG-specific $CD4^+$ T cells were found in the spinal cords of IL-$17^{Separate}$ mice compared to controls (Fig. 8D). Surprisingly, IL-$17^{Cohoused}$ mice had the highest number of $CD4^+$ and MOG-specific T cells of any group (Figure 8B, D). This data, however, was obtained from a single experiment where IL-$17^{Cohoused}$ mice had an equal incidence to controls and did not reflect the general trend of decreased disease incidence seen in other experiments. Production of the EAE-related pro-inflammatory cytokines GM-CSF and IFNγ, quantified as cytokine-positive staining cells as a percentage of total MOG-specific T cells, was increased in both IL-$17^{-/-}$ groups (Fig. 8E). Increased cytokine production from the IL-$17^{-/-}$ MOG-specific T cells in the CNS suggests that the decrease in EAE incidence is largely due to number of MOG-specific T cells infiltrating the CNS, and not due to a lack of functionality.

Myeloid cells are the main drivers of neuronal demyelination during EAE and are recruited into the CNS by T cell-derived signals such as G-CSF and CXC chemokines.[39,97] We hypothesized that due to a decreased number of T cells in the CNS, fewer myeloid-recruiting signals would be released, and IL-$17^{Separate}$ mice would also have the least number of myeloid cells present in the CNS parenchyma. To quantify myeloid cells (characterized as $CD45^+$ $CD11b^{hi}$), $CD11b^-$ leukocytes and $CD45^{int}$ microglia were excluded, as seen in the flow cytometry gating strategy in Fig. 8F. As expected, myeloid cells were significantly reduced in IL-$17^{Separate}$ mice. A slight reduction in myeloid cell number in IL-$17^{Cohoused}$ mice compared to controls was also observed, though this did not reach statistical significance (Fig. 8G).

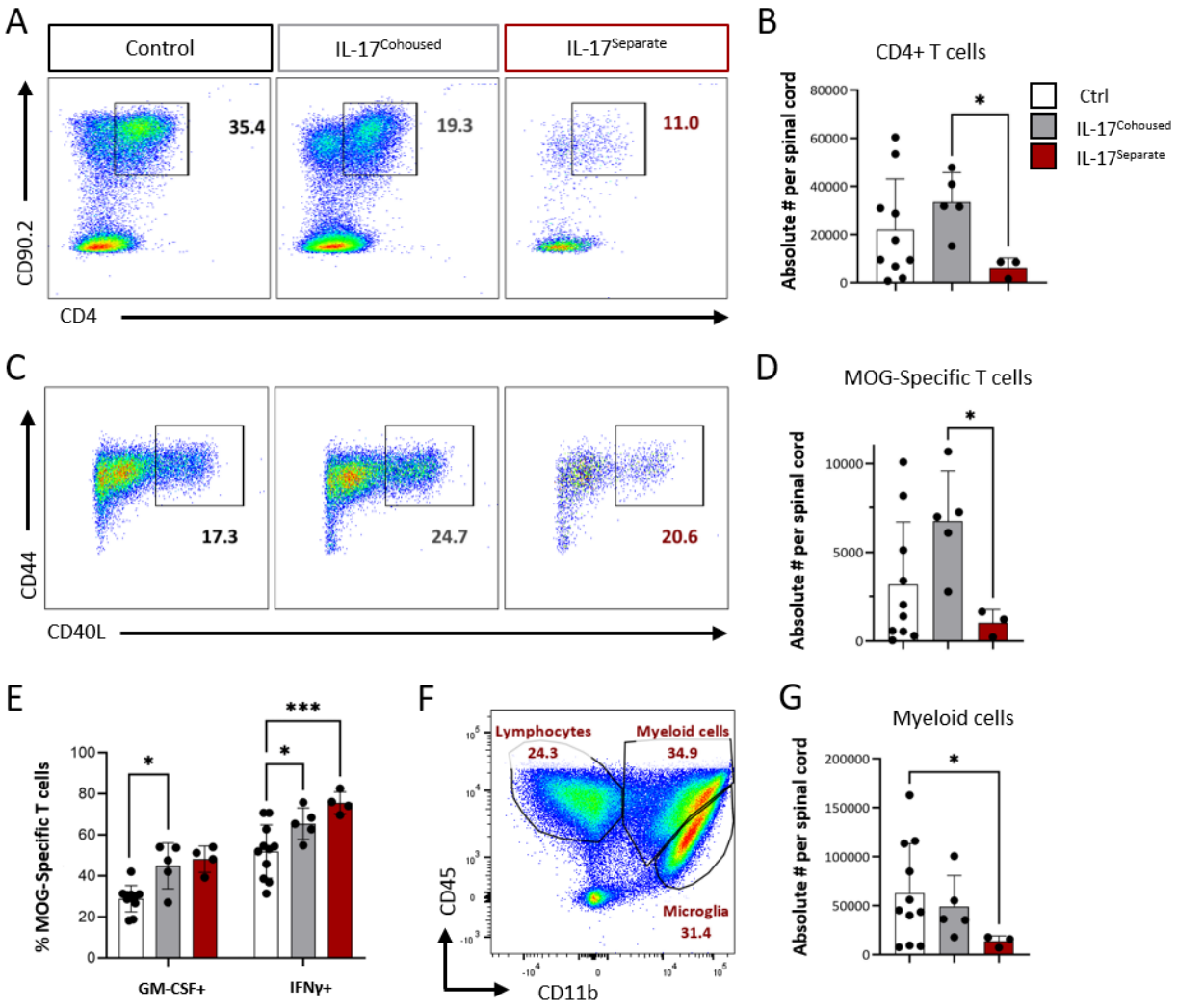

Figure 8: IL-17-deficient mice have reduced leukocytes in the spinal cord parenchyma at peak of EAE. The spinal cords of MOG_{35-55}-immunized mice were analyzed at peak (DPI 19) of EAE. (**A**) Dot plots of flow cytometry data showing the percentage of $CD4^+$ T cells among live single cells. (**B**) Quantification of absolute numbers of data shown in (A). (**C**) Dot plots of flow cytometry data showing the percentage of MOG-specific T cells, defined by high CD40L expression, among total $CD4^+$ cells. (**D**) Quantification of absolute numbers of data shown in (C). (**E**) Cytokine expression as a percentage of total MOG-specific T cells. (**F**) Representative gating strategy to identify total lymphocytes ($CD45^+CD11b^-$), myeloid cells ($CD45^+CD11b^+$), and microglia ($CD45^{int}$, $CD11b^+$). (**G**) Quantification of myeloid cells as absolute number per spinal cord of individual mice. Data is shown as mean +/- SD. Data from (B, D, E) is representative of two independent experiments. Data in (G) is from one independent experiment with one $IL\text{-}17^{Separate}$ data point excluded by statistical outlier analysis (Ctrl, n = 11; $IL\text{-}17^{Cohoused}$, n = 5; $IL\text{-}17^{Separate}$, n = 3). Analysis was performed using (B, D, G) Brown Forsynthe and Welch ANOVA for normally distributed data with unequal SDs or (E) ordinary one-way ANOVA. * $p < 0.05$; ** $p < 0.01$.

3. IL-17 is redundant for pathogenic T cell priming during EAE

Because IL-17-deficient mice had a reduced number of leukocytes in the CNS parenchyma, we hypothesized that IL-17 plays a role at earlier time points in the periphery to decrease the later disease incidence. One of the earliest stages in the EAE immune cascade is T cell priming with self-antigen by antigen presenting cells (APCs) in the skin draining lymph nodes (LNs) surrounding the site of immunization. Upon immunization with myelin oligodendrocyte glycoprotein peptide (MOG_{35-55}), the number of antigen-specific T cells that recognize the MOG_{35-55} peptide increase in number in the LNs until three to seven days after immunization. To amplify the quantifiable effect of T cell priming in IL-$17^{-/-}$ mice, a transgenic mouse line with a MOG_{35-55}-specific T cell receptor (TCR) was used (2D2-TCR^{MOG} mouse line first described in Bettelli et al. 2003).[55] To investigate whether IL-17 plays a role in the antigenic priming of T cells, mice were injected intravenously with 1 x 10^4 2D2-TCR^{MOG} $CD4^+$ T cells one day before immunization with MOG_{35-55} peptide (active EAE induction) and spleen and inguinal draining LNs were harvested five days after immunization for flow cytometry analysis, following the timeline of a previous study (Fig. 9A).[133] Upon recognition of self-antigen, antigen-specific T cells proliferate in number. Therefore, the number of transferred 2D2-TCR^{MOG} cells, identifiable by the congenic marker CD90.1 (Thy1.1), were quantified between IL-$17^{-/-}$ mice and controls as a readout for the strength of antigen-presentation (Fig. 9B). In the draining LNs, absolute number of transferred 2D2-TCR^{MOG} cells were non-significantly increased in IL-$17^{-/-}$ mice (Fig. 9C). IL-$17^{-/-}$ mice on average had nearly twice as many (2 x 10^4 per mouse) 2D2-TCR^{MOG} cells in the draining LNs as controls (1 x 10^4 per mouse). Percentage of cytokine producing transferred cells in the LNs was comparable between IL-$17^{-/-}$ mice and controls (Fig. 9D). In the spleen, the number of transferred cells was comparable between IL-$17^{-/-}$ mice and controls, with all mice having on average 5 x 10^4 transferred cells per spleen (Fig. 9E). Cytokine production by transferred cells in the spleen was also comparable between groups (Fig. 9F). From these data, it can be concluded that IL-17 plays no role in the antigenic priming of MOG-specific T cells by APCs, nor in the initial clonal expansion that occurs by these T cells in the earliest stages of EAE.

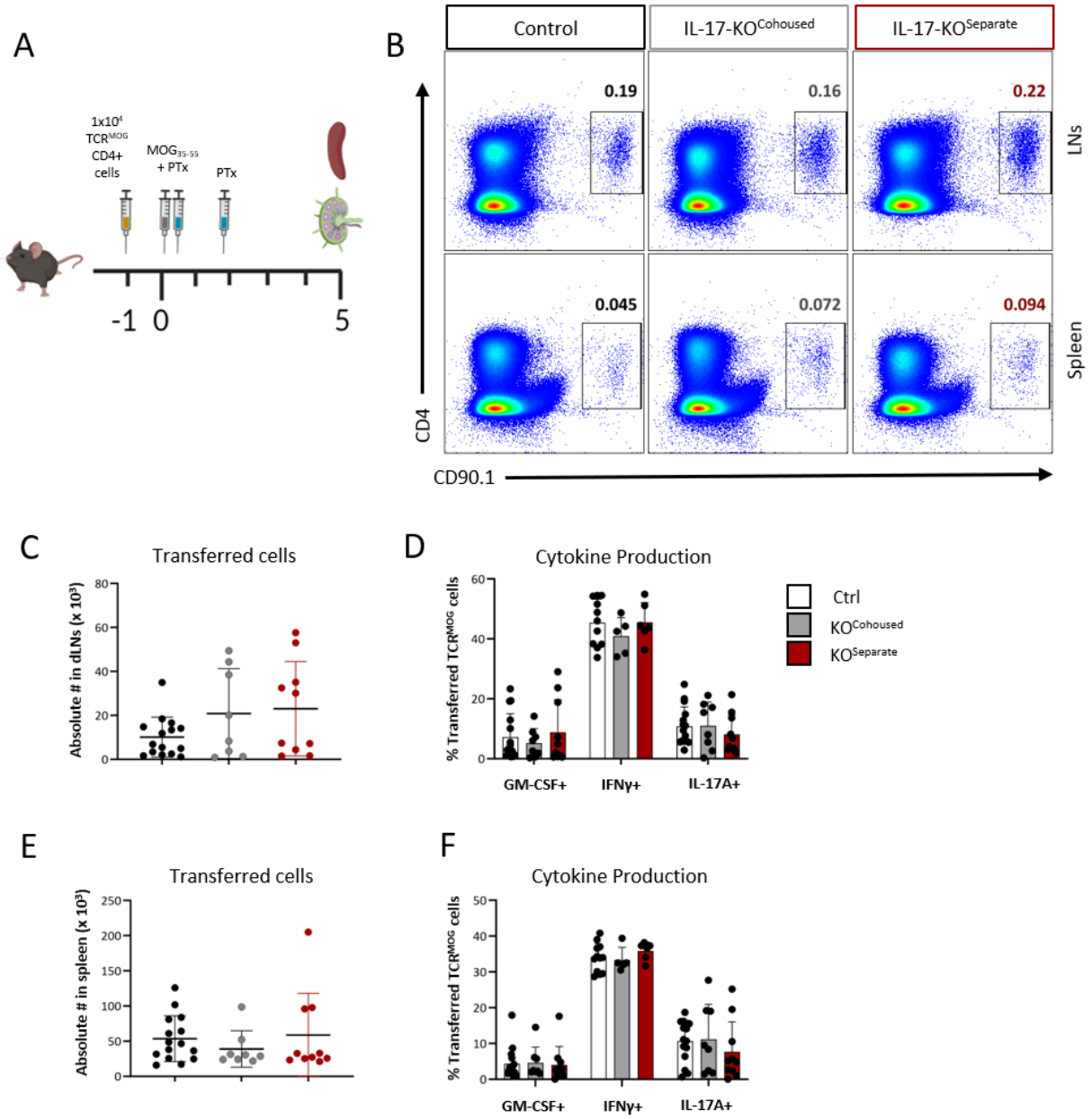

Figure 9: IL-17 is redundant for T cell priming in the secondary lymphoid organs during EAE. (**A**) Experimental overview. 10,000 MOG-specific (2D2-TCR^{MOG}) CD4-T cells were transferred into mice one day before immunization with MOG_{35-55} peptide in CFA. Inguinal draining (d)LNs and spleen were harvested 5 days after EAE induction to quantify cell number and cytokine production of transferred TCR^{MOG} cells. (**B**) Exemplary flow cytometry strategy from the LNs and spleen for gating of transferred TCR^{MOG} cells. Quantification of number of transferred cells and percentage of cytokine expression was quantified for the dLNs (**C**, **D**) and spleen (**E**, **F**). Data is shown as mean +/- SD and combined from two independent experiments (Ctrl, n = 15; IL-17^{Cohoused}, n = 8; IL-17^{Separate}, n = 10).

4. IL-17 is redundant for the expansion of peripheral pathogenic T cells

Since no differences in antigenic T-cell priming were observed at day 5 of EAE, a later time point was chosen to determine whether peripheral autoimmunity was progressing in the absence of IL-17. Day 10, referred to in this text as disease "pre-onset", is a critical time point in EAE. At pre-onset, antigen-specific lymphocytes are clonally expanding in the periphery and taking on phenotypes allowing their migration towards and infiltration of the CNS, where they initiate immune processes ultimately leading to demyelination.[80]

To investigate whether clonal expansion is inhibited by loss of IL-17 or the specific housing conditions, lymphocytes were isolated from the spleen at day 10 of EAE and analyzed via flow cytometry. $CD4^+$ T cells were defined by flow cytometric gating as $CD90.2^+$ and $CD4^+$ (Fig. 10A). As a percentage of total live cells, increased $CD4^+$ T cells are observed in both IL-$17^{-/-}$ groups, with IL-$17^{Separate}$ mice having a significantly increased percentage of $CD4^+$ T cells compared to controls (Fig. 10B). IL-$17^{Cohoused}$ mice additionally had a trend towards increased absolute numbers of $CD4^+$ T cells (Fig. 10C). MOG-specific T cells were gated from $CD4^+$ T cells based on the positive expression of CD44 and CD40L (Fig. 10D). CD44 is a general activation marker, while CD40L is rapidly expressed after antigen-specific activation. As it can be assumed that most T cells recently activated with self-antigen in the EAE model are MOG-specific, CD40L was used as a surrogate marker for MOG-specificity. MOG-specific T cells, both as a percentage of total $CD4^+$ T cells and in absolute number, were unchanged between all groups (Fig. 10E, F). Among these MOG-specific T cells, percentage of pro-inflammatory cytokine-producing cells remained the same among conditions (Fig. 10G). However, absolute numbers of $GM\text{-}CSF^+$ and $IFN\gamma^+$ T cells were increased in both IL-$17^{-/-}$ groups compared to controls, and significantly higher in IL-$17^{Cohoused}$ mice (Fig. 10H). While this may solely reflect the trend towards increased number of total $CD4^+$ and MOG-specific T cells, it shouldn't be discounted that increased number of GM-CSF and IFNγ producing cells may play a role in the peripheral disease pathogenesis.

Taken together, this data suggests that the absence of IL-17 does not prevent clonal expansion and pathogenicity of MOG-specific T cells in the periphery. To confirm whether IL-$17^{-/-}$ T cells maintain their pathogenic potential, a functional approach was taken. T cells with and without IL-17 were polarized *in vitro* under Th17-skewing conditions and adoptively transferred i.v. into

lymphopenic Rag1$^{-/-}$ host mice. IL-17$^{-/-}$ T cells successfully induced adoptive transfer EAE at a near similar severity to control T cells (Fig 10I). This data indicates that IL-17 signaling from T cells is not required to induce CNS neuroautoimmune inflammation and that rather other peripheral mechanisms are present that hinder the development of active EAE in IL-17$^{-/-}$ mice.

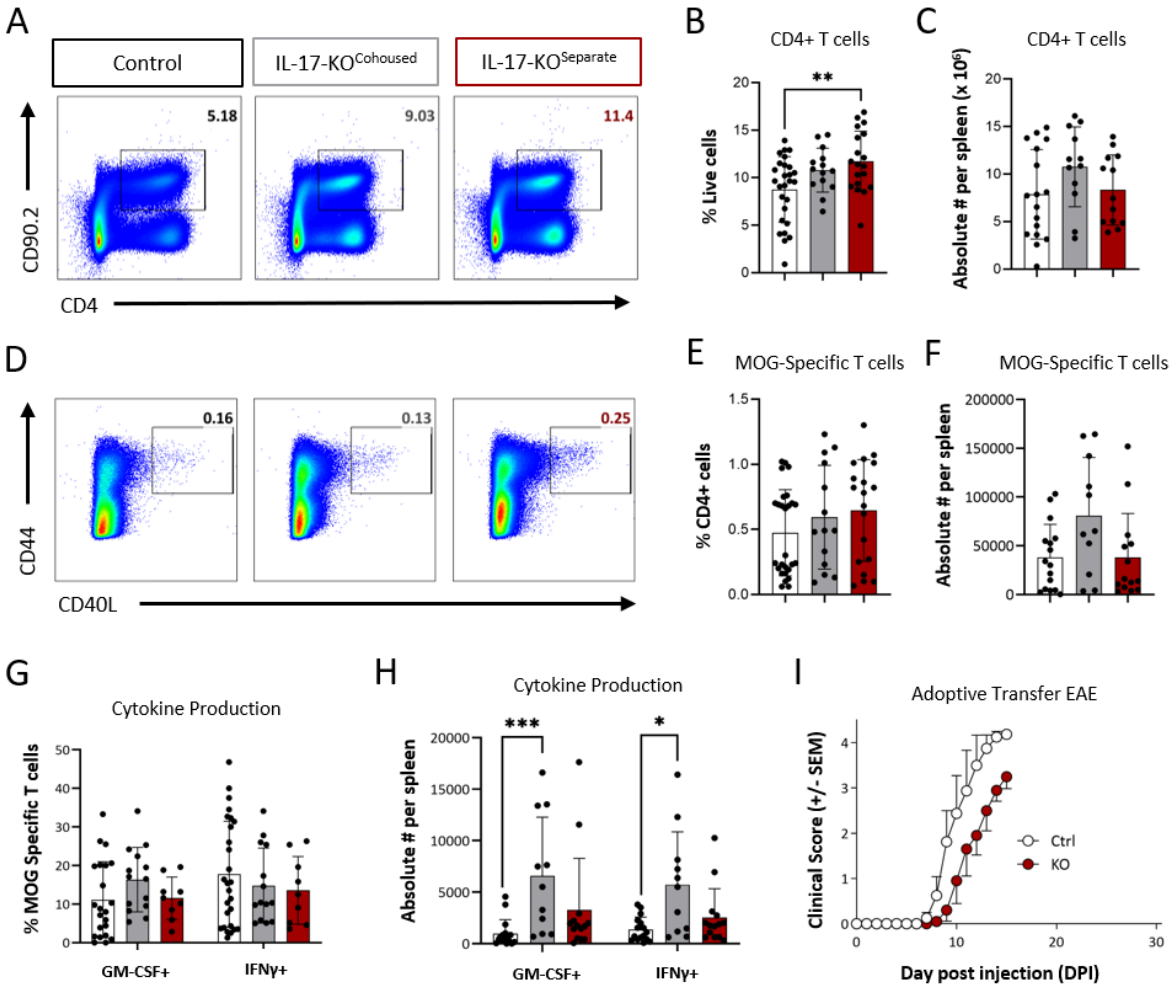

Figure 10: IL-17 is redundant for the clonal expansion and pathogenicity of splenic MOG-specific CD4$^+$ T cells. (**A**) Representative gating strategy of CD4$^+$ T cells in the spleen, pre-gated from single live cells. Quantification of CD4$^+$ T cells as (**B**) percentage of live cells and (**C**) absolute number. (**D**) Representative gating strategy of MOG-specific T cells (CD44$^+$ CD40L^{hi}) in the spleen, pre-gated from single live CD4$^+$ T cells. Quantification of MOG-specific T cells as (**E**) percentage of CD4$^+$ T cells and (**F**) absolute number. Quantification of cytokine expressing cells as (**G**) percentage of total MOG-specific T cells and (**H**) absolute number. (**I**) Clinical scores after adoptive transfer of encephalitogenic T cells from IL-17$^{-/-}$ mice (red dots) or controls (white dots). Data from (B-C, E-F, G-H) pooled from 3-4 independent experiments with at least n = 4 per experiment and shows mean +/- SD. Data in (I) from one experiment and shows mean +/- SEM with 7-8 per group. Analysis was performed using either (B) ordinary one-way ANOVA or (H) Kruskal-Wallis ANOVA for non-normal data. * $p < 0.05$; ** $p < 0.01$; *** $p < 0.001$.

5. IL-17 is essential for promotion of cell blasting by myeloid cells

In the IL-17-deficient environment, $CD4^+$ T cells are sufficiently primed with antigen, clonally expand, and produce inflammatory cytokines when restimulated with antigen *ex vivo*. This effect is seen independently of the housing conditions. It was suspected that other cell types present may actively suppress $CD4^+$ T cell responses in the periphery. Regulatory T cells (Tregs) are the paradigm suppressors of adaptive immune responses, mediating their suppressive effects on $CD4^+$ and $CD8^+$ T cell responses via the production of cytokines such as IL-10 and TGFβ.[28] Since an increase in overall $CD4^+$ T cell number was previously observed, it was hypothesized that an increased number of Tregs may inhibit other $CD4^+$ T cells in their peripheral functions. Flow cytometric analysis revealed no differences in Treg numbers between conditions (Fig. 11A). This suggested no imbalance in the suppressive to effector T cell ratio in IL-$17^{-/-}$ mice that might impede pathogenic T cell functions.

A more functional approach was then taken to investigate whether the IL-17-deficient environment suppresses pathogenic T cells. The adoptive transfer EAE model was adapted in a so-called "criss-cross" approach. Blasting cells (further described in the next paragraph) cultured from MOG_{35-55}-immunized IL-$17^{-/-}$ mice and controls were transferred into sub-lethally irradiated wild-type and IL-$17^{-/-}$ recipient hosts. This created four groups of recipients: controls receiving control or IL-$17^{-/-}$ cells, and knockouts receiving control or IL-$17^{-/-}$ cells. It was hypothesized that if a suppressive environment in IL-17-deficient hosts exists, these mice would be less susceptible to adoptive transfer EAE. Surprisingly, results showed that disease curves diverged based on genotype of transferred cells, with control cells inducing more severe disease with earlier day of onset than IL-$17^{-/-}$ cells, irrespective of the genotype of the hosts (Fig. 11B). This data was not only counterintuitive to the hypothesis of the experiment, but contradicted previous results showing minimal effect of IL-17 expression on severity of adoptive transfer EAE (Fig. 10I).

An observation made during this experiment was that after *ex vivo* Th17 culture, IL-$17^{-/-}$ cultures had fewer blasting cells than controls (Fig. 11C). Blasting cells can be visualized both under a microscope as a swelling of the cytoplasm and in flow cytometry as an increase in forward scatter properties. Blasting cells in Th17 cultures are not only an indication of pathogenicity of the culture, but the percentage of blasting cells as a percentage of total live

cells is used to calculate the number of injected cells in our lab's adoptive transfer EAE protocol (ref. section 2.4.4.1). Relative to controls, IL-17$^{-/-}$ mice had significantly fewer blasting cells after Th17 culture, with IL-17^{Cohoused} mice having the lowest percentage of approximately half the percentage of blasting cells as controls (Fig 11D).

The adoptive transfer EAE protocol used by our lab combines cells from the spleen and lymph nodes of immunized donor mice into one 4-day culture. To determine whether the decrease in blasting cell percentages differed between organs, spleen and lymph nodes from immunized mice were cultured separately and blasting cell percentage was determined by flow cytometry. Cultured IL-17$^{-/-}$ cells from the spleen showed a similar decrease in blasting cells compared to controls as observed for the combined cultures (Fig. 11E). This was unsurprising, as a greater proportion of cultured cells come from the spleen due to larger cell number overall. Lymph node cultures, however, showed an increased percentage of blasting cells in IL-17$^{-/-}$ mice (Fig. 11F). To determine whether these differences in blasting percentage had functional differences upon adoptive transfer, lymphopenic Rag1$^{-/-}$ mice received 5 x 10^6 blasting cells i.v. from either the spleen or lymph node cultures of controls and IL-17$^{-/-}$ mice. Surprisingly, decreased blasting cells from the IL-17$^{-/-}$ splenocytes did not correlate to a decreased EAE severity upon adoptive transfer as seen previously, with both control and IL-17$^{-/-}$ cultures resulting in a rapid and severe disease course leading to early termination of the experiment for these groups (Fig. 11G). The disease curves of lymph node recipients correlated to the blasting phenotype: IL-17$^{-/-}$ cultures resulted in an earlier day of onset compared to control cultures, though peak scores were unchanged (Fig. 11G).

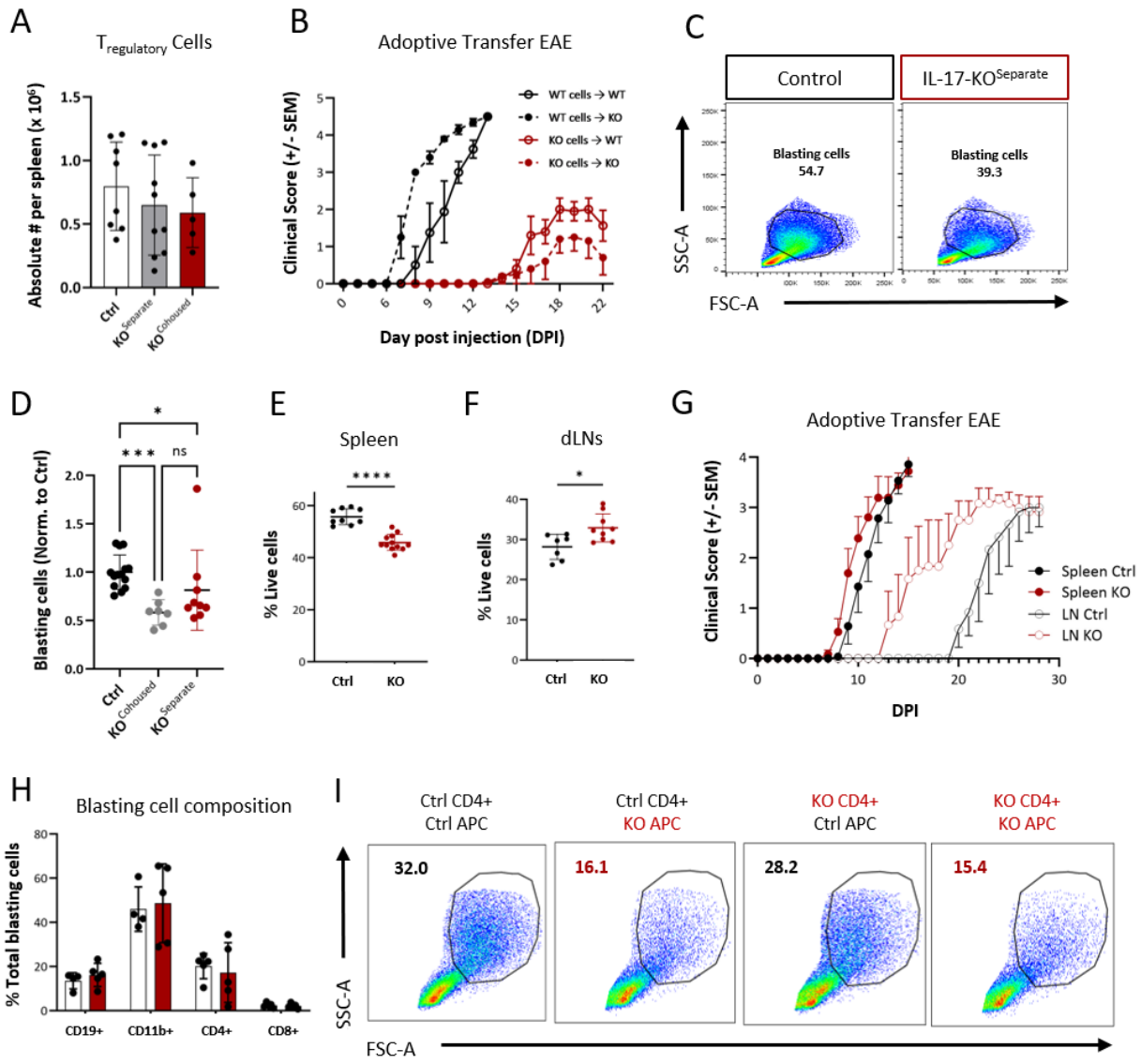

Figure 11: Investigation of a suppressive splenic environment in IL-17$^{-/-}$ mice. (**A**) Absolute numbers of Foxp3^{+} Tregs from the spleens of MOG$_{35-55}$-immunized mice at active EAE DPI 10. (**B**) Clinical scores after adoptive transfer of Th17-polarized WT cells (black) or IL-17$^{-/-}$ cells (red) into WT (solid lines) or KO (dashed lines) recipient mice. (**C**) Flow cytometry dot plot of blasting cells as a percentage of live cells from Th17 cultured donor cells as used for (B). (**D**) Quantification of blasting cells of cohoused and separately housed knockout mice normalized to controls. Data is pooled from 3 experiments and normalized within each experiment to average control blasting percentage. (**E**, **F**) Blasting cells quantified from the (E) spleen and (F) dLNs after 4 days of in vitro Th17 culture. (**G**) Clinical scores after adoptive transfer of cells from spleen (closed dots) or dLNs (open dots) of control mice (black) or KO mice (red). (**H**) Quantification of the composition of blasting cells from positive flow cytometric staining of B cell (CD19^{+}), myeloid (CD11b^{+}), or T cell markers (CD4^{+} or CD8^{+}). Data from one experiment. (**I**) CD4^{+} cells from IL-17$^{-/-}$ mice and controls were sorted from the spleen and dLNs of MOG$_{35-55}$-immunized mice at DPI 10 and cultured with the remaining CD4^{-} (APC) fraction of both groups for 4 days under Th17-skewing conditions. Flow cytometry dot plots show percentage of blasting cells as percentage of live cells. Adoptive transfer EAE clinical score data (B, G) is shown as mean +/- SEM. Other quantifications (A, D-F, H) show mean +/- SD. P-values calculated using either (D) one-way ANOVA or (F, G) student's t-test. * $p < 0.05$; *** $p < 0.001$; **** $p < 0.0001$.

Flow cytometry was used to analyze the composition of blasting cells for differences between control and IL-17$^{-/-}$ mice. While the composition of cell subsets was the same between groups, surprisingly, only 20% of blasting cells were CD4^{+} T cells (Fig. 11H). The majority of the blasting cells were composed of cells with antigen presenting capacity, including CD11b^{+} myeloid cells (50% of blasting) and CD19^{+} B cells (20% of blasting). It was hypothesized that IL-17$^{-/-}$ APCs may be the cause for decreased blasting cells in the IL-17$^{-/-}$ Th17 cultures. To investigate this, another criss-cross experiment was performed *in vitro*. CD4^{+} T cells were magnetically sorted by positive selection from MOG$_{35-55}$-immunized IL-17$^{-/-}$ mice and controls at EAE DPI 10 and co-cultured with the remaining CD4- fraction, termed the "APC" fraction, from both IL-17$^{-/-}$ and control mice. Co-culture of control CD4^{+} T cells with IL-17$^{-/-}$ APCs resulted in a blasting percentage that mirrored the full IL-17$^{-/-}$ culture (Fig. 11I). This indicated that *in vitro*, IL-17 is required for APCs to promote blasting of the entire culture. IL-17$^{-/-}$ APCs *in vitro* likely have changed functionality which regulates blasting function of themselves and their surrounding cells. This was a first indication of a potential suppressive function of IL-17$^{-/-}$ APCs, which may also exert suppressive or other regulatory functions *in vivo*.

6. Pathogenicity of IL-17-deficient T cells is retained in a CD4^{+} T cell adoptive transfer model of EAE

To exclude potential *in vivo* inhibitory effects of APCs in the adoptive transfer model of EAE, CD4^{+} T cells were magnetically sorted after four days of Th17 culture and 2x10^{6} CD4^{+} T cells were adoptively transferred i.v. into irradiated wild-type hosts. Though IL-17$^{-/-}$ CD4^{+} T cells were able to induce adoptive transfer (AT)-EAE, the disease scores of IL-17$^{-/-}$ recipients were lower than control CD4^{+} recipients (Fig. 12A). In line with the decrease in disease severity, fewer IL-17$^{-/-}$ CD4^{+} T cells were found in the CNS (combined brain and spinal cord) of recipient mice (Fig. 12B). CCR6 is a chemokine receptor that is essential for migration of pathogenic Th17 cells to the CNS during EAE.[71] Although fewer numbers of CD4^{+} T cells were observed in the CNS of IL-17$^{-/-}$ recipients, there was no observed difference in T cell CCR6 expression to suggest a deficiency in the CCR6 migratory axis (Fig. 12C). To determine whether the decrease in EAE severity correlated to a decreased concentration of circulating IL-17 levels, IL-17 concentrations were measured in the serum of host mice at day of analysis (peak of disease; day 15). IL-17 concentrations were comparable between IL-17$^{-/-}$ and control T cell recipients (Fig. 12D). This

suggests that the lack of IL-17 signaling from transferred $CD4^+$ T cells does not affect the ability of the host mice to produce IL-17 from other sources and that concentrations of circulating IL-17 were not responsible for the decrease in EAE severity observed upon $CD4^+$ T cell adoptive transfer EAE.

Inflammatory cytokine expression was quantified from transferred ($CD90.2^+$ $CD4^+$) MOG-specific ($CD44^+$ $CD40L^{hi}$) T cells (Fig. 12E). Approximately 70% and 60% of transferred MOG-specific T cells expressed GM-CSF and IFNγ, respectively, and this percentage was unchanged between genotypes (Fig. 12F). 30% of the transferred MOG-specific control T cells expressed IL-17A, while IL-$17^{-/-}$ transferred cells were confirmed to be negative for IL-17A expression. Numbers of both $GM\text{-}CSF^+$ and $IFN\gamma^+$ cells were reduced by about half in the CNS of hosts receiving IL-$17^{-/-}$ donor cells, mirroring the decrease seen in total $CD4^+$ T cells in the host CNS (Fig. 12G).

Analysis was also performed on ($CD90.1^+$ $CD4^+$) MOG-specific ($CD44^+$ $CD40L^{hi}$) host T cells (Fig. 12H). No differences were observed among MOG-specific T cells producing the inflammatory cytokines GM-CSF, IFNγ, or IL-17A as a percentage of total $CD4^+$ T cells (Fig. 12I). Notably, no host cells produced IL-17A, suggesting this cytokine may only be produced by the "first wave" of infiltrating T cells, represented in this model by the transferred cells. Transferred cytokine-producing cells also greatly outnumbered host cells, which were observed at only a tenth of transferred cell numbers in the spinal cords (Fig. 12G, J). Numbers of both $GM\text{-}CSF^+$ and $IFN\gamma^+$ host T cells were also reduced by approximately half in recipients of IL-$17^{-/-}$ T cells, though this did not reach statistical significance (Fig. 12J).

Taken together, this data suggests that while the IL-17-deficient cells retain the ability to induce disease, reduced numbers of $CD4^+$ T cells in the host CNS may contribute to an improved disease outcome. However, the question of *why* $CD4^+$ T cells are reduced in the CNS upon adoptive transfer is unclear.

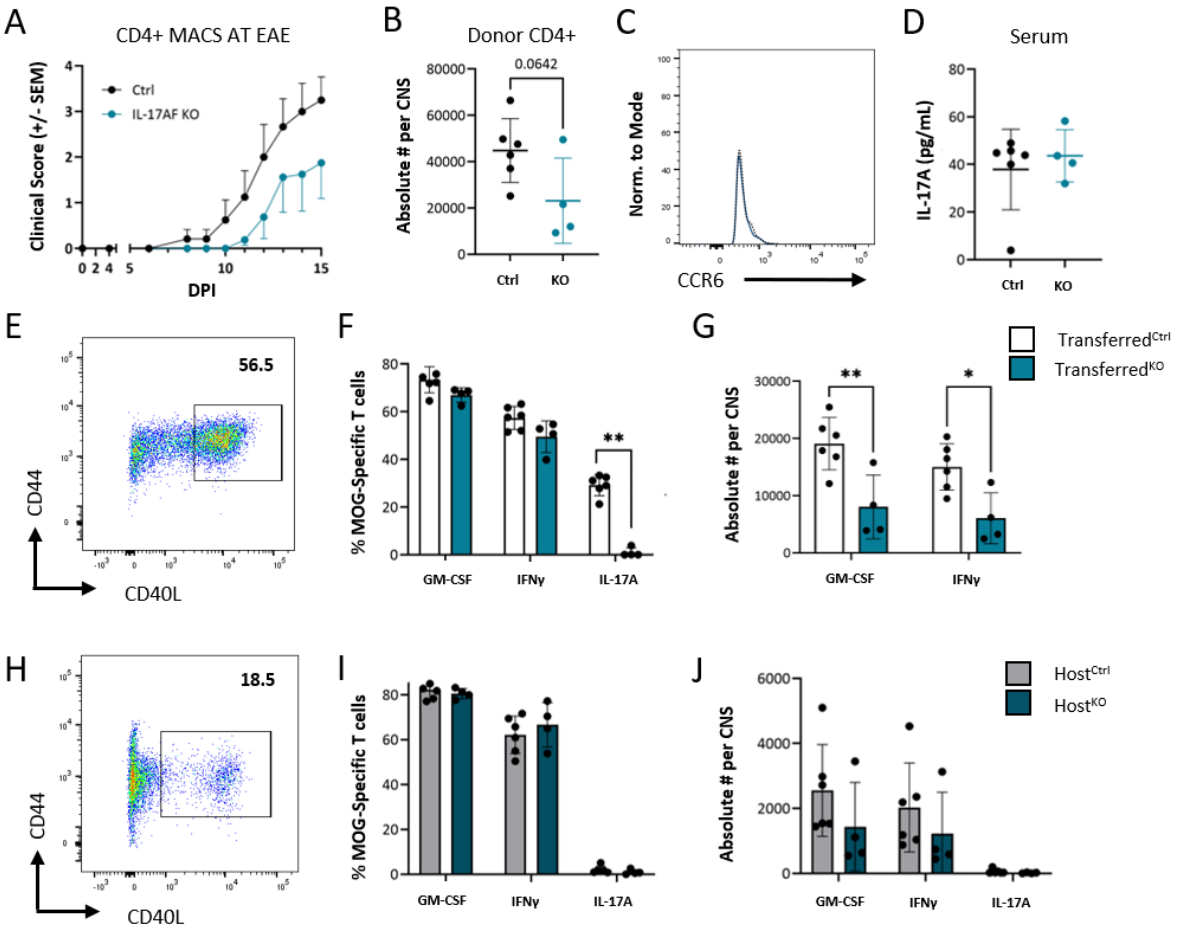

Figure 12: Reduced numbers of IL-17$^{-/-}$ CD4^{+} T cells are present in the CNS after adoptive transfer. Magnetically sorted CD4^{+} T cells from MOG$_{35-55}$-immunized IL-17$^{-/-}$ mice and controls were adoptively transferred into irradiated control mice and the CNS (combined brain and spinal cord) and serum of recipient mice were analyzed at day post transfer (DPT) 15. (**A**) Clinical scores after adoptive transfer of CD4^{+} T cells from immunized IL-17$^{-/-}$ mice (blue line) versus controls (black line). (**B**) Absolute number of transferred CD4^{+} T cells in the CNS. (**C**) Histogram of CCR6 expression on donor CD4^{+} T cells in the CNS. (**D**) Concentrations of IL-17A in the serum measured by ELISA. MOG-specific (CD44^{+} CD40L^{Hi}) transferred T cells in the CNS were analyzed via (**E**) flow cytometry. Pre-gated on single live CD45.2^{+} CD4^{+} CD90.2^{+} T cells. Cytokine production from transferred cells is shown as both (**F**) percentage and (**G**) number. MOG-specific (CD44^{+} CD40L^{Hi}) host T cells in the CNS were analyzed via (**H**) flow cytometry. Pre-gated on single live CD45.1^{+} CD4^{+} CD90.2^{+} T cells. Cytokine production from transferred cells is shown as both (**I**) percentage and (**J**) number. Data shown is from one experiment with n = 4-6 per group. Data from (B, D, F, G, I, J) is shown as mean +/- SD. Analysis of (B, G) was performed using student's t-test. * $p < 0.05$; ** $p < 0.01$.

7. IL-17 production from T cells is redundant for their migration

As previously discussed, several mechanisms simultaneously regulate the final outcome of T cell migration towards the CNS during EAE. Due to the observation of decreased number of T cells in the CNS but increased T cells in the spleens of actively immunized IL-17$^{-/-}$ mice, it was hypothesized that IL-17 deficiency may decrease the prevalence of EAE by regulating T cell migration towards the CNS, either in the periphery or in the CNS itself.

S1P is found in low concentrations in tissues and higher concentrations in blood and lymphatic circulation in a so-called "S1P gradient" that regulates lymphocyte egress or retention in peripheral tissues.[83] Expression and localization of the S1P receptor on T cells are additionally regulated to dictate whether T cells respond to S1P in the environment.[253] We hypothesized that IL-17$^{-/-}$ mice may have altered S1P concentrations or expression levels of S1PR that prevent T cell migration from the spleen. Concentrations of S1P were measured in both the serum and spleen of MOG_{35-55}-immunized mice on DPI 10 of active EAE. No differences were observed in the blood circulating or splenic S1P concentrations between IL-17$^{-/-}$ mice and controls (Fig. 13A, B). Cellular localization of S1PR1 was determined by flow cytometric staining to compare the intracellular versus extracellular location of S1PR1 on T cells. No differences were observed between IL-17$^{-/-}$ mice and controls (Fig. 13C). The vast majority of T cells in both groups expressed almost exclusively intracellular S1PR1 with no differences in expression level between genotypes, indicating a T cell readiness for migration out of the spleen (data not shown).

CCR7 and its ligands CCL19 and CCL21 are critically involved in the migration of T cells and dendritic cells (DCs) towards SLOs.[254] CCR7-deficient T cells have been shown to accumulate in the splenic red pulp with reduced ability to recirculate out of peripheral tissues.[255] Inside of the splenic tissue, extracellular matrix remodeling signals, such as matrix metalloproteinases (MMPs), are released by neutrophils to remodel tissue at sites of lymphocyte egress.[256] MMPs 2 and 9 have specifically been implicated in EAE to drive T cell migration and BBB breakdown. To gain insight into whether IL-17$^{-/-}$ mice exhibit changes in leukocyte-derived migration signals, quantitative real time PCR (RT-PCR) was performed on RNA isolated from whole splenic tissue at active EAE DPI 10. mRNA expression of CCR7, CCL19, and CCL21 was increased in IL-17^{Cohoused} mice and even further increased in IL-17^{Separate} mice compared to controls,

indicating that no deficiencies in CCR7-dependent signaling existed that might prevent T cells migration out of the spleen (Fig. 13D). On the contrary, increased CCR7 signaling suggests even heightened migratory signaling in IL-17$^{-/-}$ mice. While mRNA expression levels of MMP2 were unchanged (data not shown), MMP9 expression was significantly downregulated in the spleens of IL-17^{Cohoused} mice and even further downregulated in IL-17^{Separate} mice compared to controls (Fig. 13D).

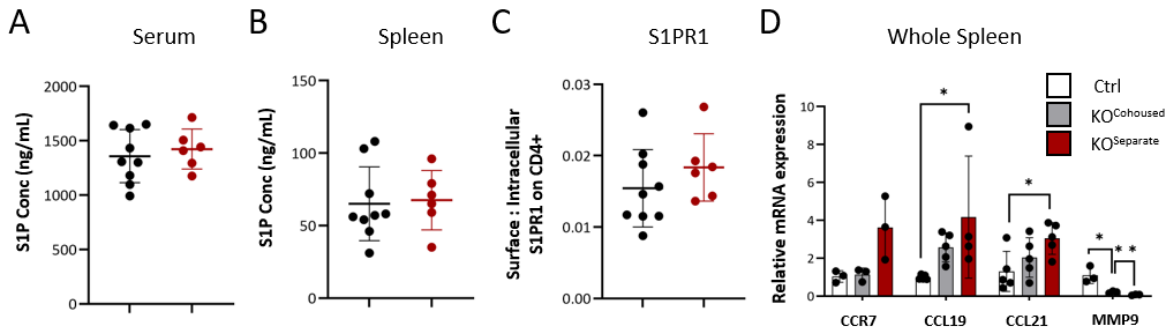

Figure 13: Analysis of peripheral migratory mediators in MOG$_{35-55}$-EAE mice at pre-onset DPI 10. Sphingosine-1-phosphate (S1P) concentrations were measured in (**A**) serum and (**B**) whole spleen. (**C**) Ratio of cellular location (surface to intracellular) of S1PR1 on splenic CD4$^+$ T cells quantified by flow cytometry. (**D**) Relative mRNA expression of migration-related genes in the spleen (relative values normalized to β-actin). Data from one independent experiment with n = 3-8 per group. Data is shown as mean +/- SD. Statistical analysis of (D) was performed using one-way ANOVA. * $p < 0.05$; ** $p < 0.01$.

Leukocytes in the spleen not only respond to intra-splenic migration signals, but are also recruited towards the CNS by chemokine gradients and infiltrate the parenchyma upon interaction with adhesion molecules. CXCL1 and CXCL2 are upregulated in the CNS during both MS and EAE and are well-established in recruitment of leukocytes towards the CNS during CNS autoimmunity.[209,257] Adhesion molecules, such as ICAM1, ICAM2, VCAM, and PECAM (CD31) are critical for the attachment of T cells to endothelial cells and transmigration into the CNS parenchyma.[88,90] A study by Wojkowska et al. found that IL-17A may play a role in both of these processes by promoting adhesion molecule expression and CXCL1 release from brain endothelial cells *in vitro*.[149] Other studies have implicated IL-17 as involved in the adhesion and tight junction molecule reorganization occurring at the BBB.[147,148] To determine whether these effects were observable *in vivo*, RT-PCR was performed on mRNA isolated from whole brain tissue. While expression levels of the chemokines CXCL1 and CXCL2 were unchanged in IL-17$^{-/-}$ mice, decreased gene expression was seen in nearly all adhesion molecules analyzed (Fig. 14A). While ICAM1, ICAM2, and VCAM had decreases in gene expression that were affected by both

IL-17 deletion and separate housing conditions, PECAM expression was significantly decreased in IL-17$^{-/-}$ mice irrespective of housing conditions. Contrary to what is seen in the spleen, MMP9 expression in the brain was unchanged among groups, while expression of MMP2 was significantly decreased in IL-17$^{-/-}$ mice. This suggests that changes in extracellular remodeling processes are not only occurring in the spleen of IL-17-deficient mice, but in the CNS as well. Though not significantly changed, decreases in the mRNA expression of tight junction molecules claudin-5 and occludin were observed as well in IL-17$^{-/-}$ mice. Importantly, none of these changes were linked with housing conditions, though trends were observed in ICAM-1, ICAM-2, and Claudin-5 expression.

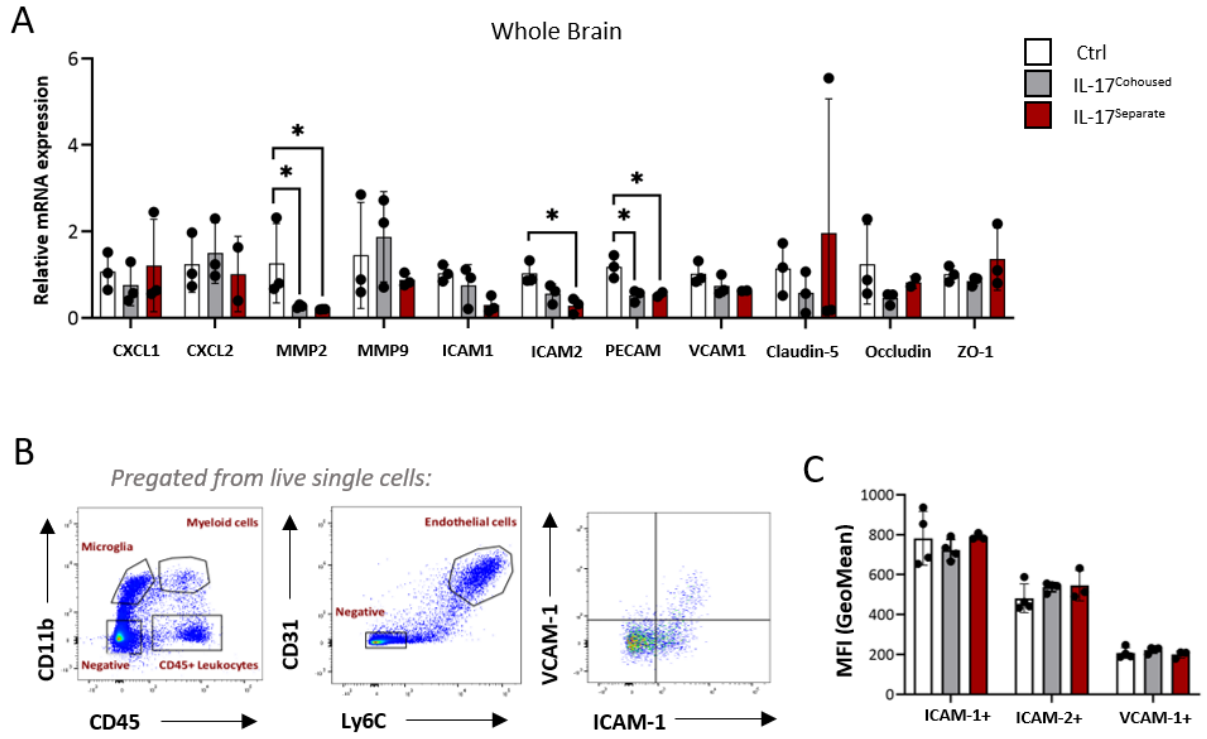

Figure 14: Analysis of pro-inflammatory molecules in the brain at EAE pre-onset. Mice were immunized for active EAE and brains were harvested at DPI 10. (**A**) Relative mRNA expression of inflammatory gene markers from total brain tissue (relative values normalized to HPRT). (**B**) Representative flow cytometry gating strategy to identify expression of adhesion molecules on BBB endothelial cells. (**C**) Mean fluorescence intensity (MFI) of adhesion molecule expression on endothelial cells. Bar graph data shown as mean +/- SD. Data each from one independent experiment with n = 3-5 per group. Statistical analysis performed using one-way ANOVA. * $p < 0.05$; ** $p < 0.01$.

To observe whether reduced mRNA expression translated into reduced protein expression of adhesion molecules, $CD31^+$ $Ly6C^+$ endothelial cells were analyzed via flow cytometry for their expression of ICAM-1, ICAM-2, and VCAM-1 (Fig. 14B). However, IL-$17^{-/-}$ mice had equal numbers (not shown) and expression levels of adhesion molecules on endothelial cells (Fig. 14C). Whether the decreased mRNA expression of MMPs and TJs translates into decreased protein expression in EAE-immunized IL-$17^{-/-}$ mice, should be determined for a better understanding of the molecular mediators of migration and inflammation that are altered in these mice. Further, the analysis of whole brain tissue cannot be used to judge expression levels of molecular mediators on specific cell types, which may be better analyzed using flow cytometry.

Finally, to determine *in vivo* whether lack of IL-17 expression inhibits peripheral $CD4^+$ T cells in their migration towards the CNS, Rag$1^{-/-}$ mice, which lack functional T and B cells, were reconstituted with $CD4^+$ T cells purified from the spleens of IL-$17^{-/-}$ mice and controls (Fig. 15A). After allowing for the settlement and homeostatic expansion of the transferred $CD4^+$ T cells in peripheral tissues for 7 days, active EAE was induced in reconstituted Rag$1^{-/-}$ mice and the disease development was monitored. Clinical scores of reconstituted mice were similar between groups, indicating no deficiency in the migratory capabilities of IL-$17^{-/-}$ T cells (Fig. 15B). Due to the close association of IL-17^+ $CD4^+$ T cells with mucosal tissues, we were also curious whether there existed a preferential settlement of the reconstituted cells in mucosal organs. No differences were seen between genotypes in the settlement of reconstituted $CD4^+$ T cells in either the dLNs, spleen, colon, or lung (Fig. 15C).

In summary, although IL-17-expressing $CD4^+$ T cells are critical drivers of EAE, our findings show that $CD4^+$ T cells lacking IL-17 expression remain pathogenic. $CD4^+$ T cells from MOG_{35-55}-immunized IL-$17^{-/-}$ mice are primed with self-antigen, expand in the periphery, produce inflammatory cytokines upon restimulation, and are able to induce EAE when adoptively transferred to wild-type recipients. Additionally, T cell-deficient mice reconstituted with IL-$17^{-/-}$ T cells develop EAE with a severity similar to controls. This suggests that IL-$17^{-/-}$ T cells exhibit no migratory defects and implicates other cells types in modulating disease progression in mice globally deficient in IL-17. To explore this possibility, we shifted our focus to other leukocyte subsets contributing to EAE development.

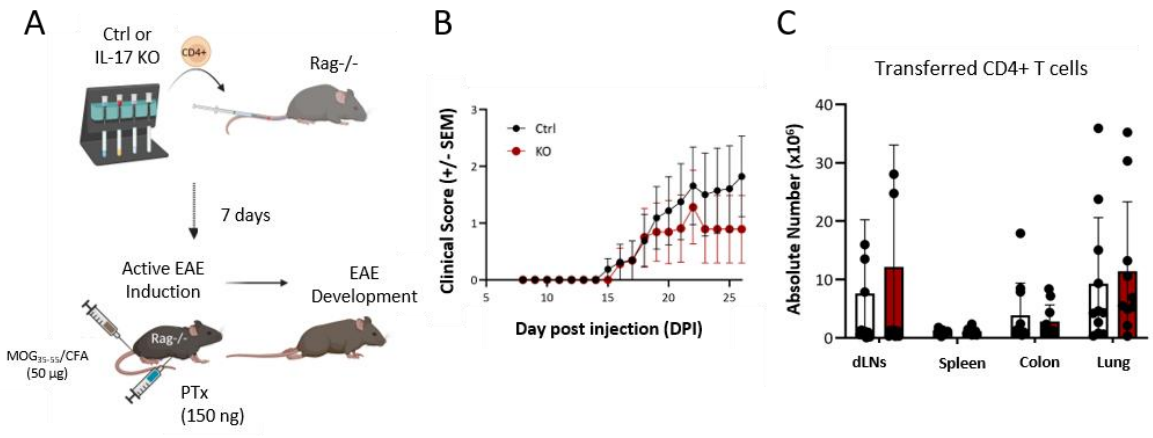

Figure 15: IL-17 from CD4⁺ T cells is redundant for their migration during EAE in an IL-17-sufficient environment. (**A**) Schematic overview of CD4⁺ reconstitution EAE for evaluation of in-vivo T-cell migration. CD4⁺ T cells were isolated by magnetic sorting from IL-17^{Separate} and control mice and 5 x 10^6 sorted cells were transferred into lymphocyte-deficient recipient mice (Rag1$^{-/-}$). Active EAE was induced in recipient mice 7 days after cell transfer and EAE disease progression was monitored. (**B**) EAE disease scores of Rag1$^{-/-}$ host mice from experimental setup described in (A). Graph is representative of two independent experiments with n = 8 per group. (**C**) Quantification of absolute numbers of CD4⁺ donor T cells recovered from respective organs of EAE-immunized host mice at EAE DPI 26. Data pooled from 2 independent experiments with n = 12 per group. Data is shown as either (B) mean +/- SEM or (C) mean +/- SD.

8. IL-17-deficiency alters the meningeal leukocyte composition during EAE

In the IL-17-deficient brain during active EAE, mRNA levels of T cell recruiting chemokines are unchanged, while mRNA levels of adhesion molecules are decreased. Additionally, CD4⁺ T cell numbers in the spleens of IL-17$^{-/-}$ mice and controls are similar, while IL-17$^{-/-}$ mice have nearly no T cells in the CNS parenchyma. It was therefore hypothesized that lymphocytes may be recruited to the CNS, yet unable to penetrate the BBB in the absence of IL-17. Several studies have implicated IL-17 in the destruction of the BBB by decreasing expression of tight junctional proteins, though these conclusions have been made from *in vitro* experiments alone.[147,148]

The meninges and subarachnoid space (SAS) are recognized as immunoregulatory hubs for autoreactive T cells trafficking to the CNS during EAE.[57,73,249] To determine whether T cells are present at the BBB of immunized IL-17$^{-/-}$ mice, dural meninges of IL-17$^{-/-}$ mice and controls were isolated just after the development of disease symptoms. This post-onset time point was chosen to ensure a sufficient number of actively migrating lymphocytes at the level of the meninges. Immunohistochemical stainings revealed that compared to controls, fewer CD3⁺ T

cells were present in the dural meninges of IL-17^{Cohoused} mice (Fig. 16A). Aligning with the EAE phenotype, even fewer T cells were present in IL-17^{Separate} mice compared to IL-17^{Cohoused}, indicating not only a genotype-dependent but also a housing-dependent decrease in T cells reaching the dural meninges.

To quantify these observations of T cells and to explore what changes may exist in other immune cell subsets, dural meninges were isolated at post-onset of EAE and multidimensional flow cytometry analysis was performed via qualitative 2D t-distributed stochastic neighbor embedding (t-SNE). Clusters were created using the ClusterExplorer plugin for FlowJo software and were manually annotated according to surface marker expression (Fig. 16B). t-SNE comparison showed changes in multiple immune subsets upon IL-17 deletion, none of which were housing-dependent (Fig. 16C). IL-17$^{-/-}$ mice irrespective of housing conditions displayed increased percentage of B cells, a loss of a specific subset of macrophages, and increased non-classical monocytes. Further, the distribution of neutrophils shifted on the tSNE plot, indicative of the existence of phenotypical differences between genotypes. With reference to a heatmap of marker expression (Fig. 16D), IL-17$^{-/-}$ neutrophils in the dural meninges express less Ly6G and less CD11b compared to controls (Fig. 16C). Previous studies indicate expression of Ly6G and CD11b as a marker of neutrophil maturity, suggesting that more immature neutrophils are present in the IL-17$^{-/-}$ meninges.[200] Furthermore, a small subpopulation of SiglecF^{+} neutrophils are lacking in IL-17$^{-/-}$ mice. Numerical quantification of immune cell subsets between conditions shows a step-wise decrease in CD45^{+} immune cells in the dura, with controls having an average of 22,900 cells per dura, IL-17^{Cohoused} mice having 18,500 per dura, and IL-17^{Separate} mice having the significantly lowest number of all groups, with 9,300 cells per dura on average (Fig. 16E). T and B cells combined consisted of only about 20% of all dural infiltrates. Both groups of IL-17$^{-/-}$ mice had decreases in T cell numbers of about half the numbers of control cells, and this effect was independent of housing conditions (Fig. 16F). B cell numbers in the IL-17^{Cohoused} mice were approximately four times the average of controls, with minimal increases observed in B cell number in the IL-17^{Separate} mice compared to controls (Fig. 16G). The vast majority of immune cells in the dural meninges were of myeloid origin, expressing either CD11b and/or CD11c. Quantification of CD11b^{+} myeloid cells showed a numerical trend that resembled the entire CD45^{+} immune cell compartment: controls had the highest number of myeloid cells with 17,200 cells per dura, IL-17^{Cohoused} mice had only 11,200 myeloid cells per

dura, and IL-17^{Separate} mice had significantly fewest myeloid cells, with only 5,500 myeloid cells per dura on average (Fig. 16H). The majority of myeloid cells were Ly6G^{+} neutrophils, of which again a step-wise decrease in number was seen: controls on average had 11,700 neutrophils per dura, IL-17^{Cohoused} mice had 7,750 neutrophils per dura, and IL-17^{Separate} had significantly fewest neutrophils, with only 3,200 neutrophils per dura on average (Fig. 16I).

In summary, IL-17$^{-/-}$ mice had a genotype and housing-dependent reduction in immune cells infiltrates in the dural meninges. This was largely due to a reduction of myeloid cells, which compose the majority of immune cells in the inflamed meninges. Neutrophils comprised the majority of myeloid cells and a genotype and housing-dependent reduction in neutrophil number was similarly observed. Neutrophils are critically involved in pro-inflammatory processes at sites of inflammation. The reduction of neutrophil numbers in the meninges, together with previous data showing decreased expression of MMP2 in the CNS parenchyma, suggests that neutrophils may play a role in the progression of EAE at multiple layers of the CNS, engaging in functions such as extracellular matrix remodeling or immunoregulation of other cell subsets. These results were obtained from one experiment only and must be confirmed for validity, yet this data suggests that T cells have a decreased ability to reach the CNS in IL-17-deficient mice and are not simply “stuck” at the BBB.

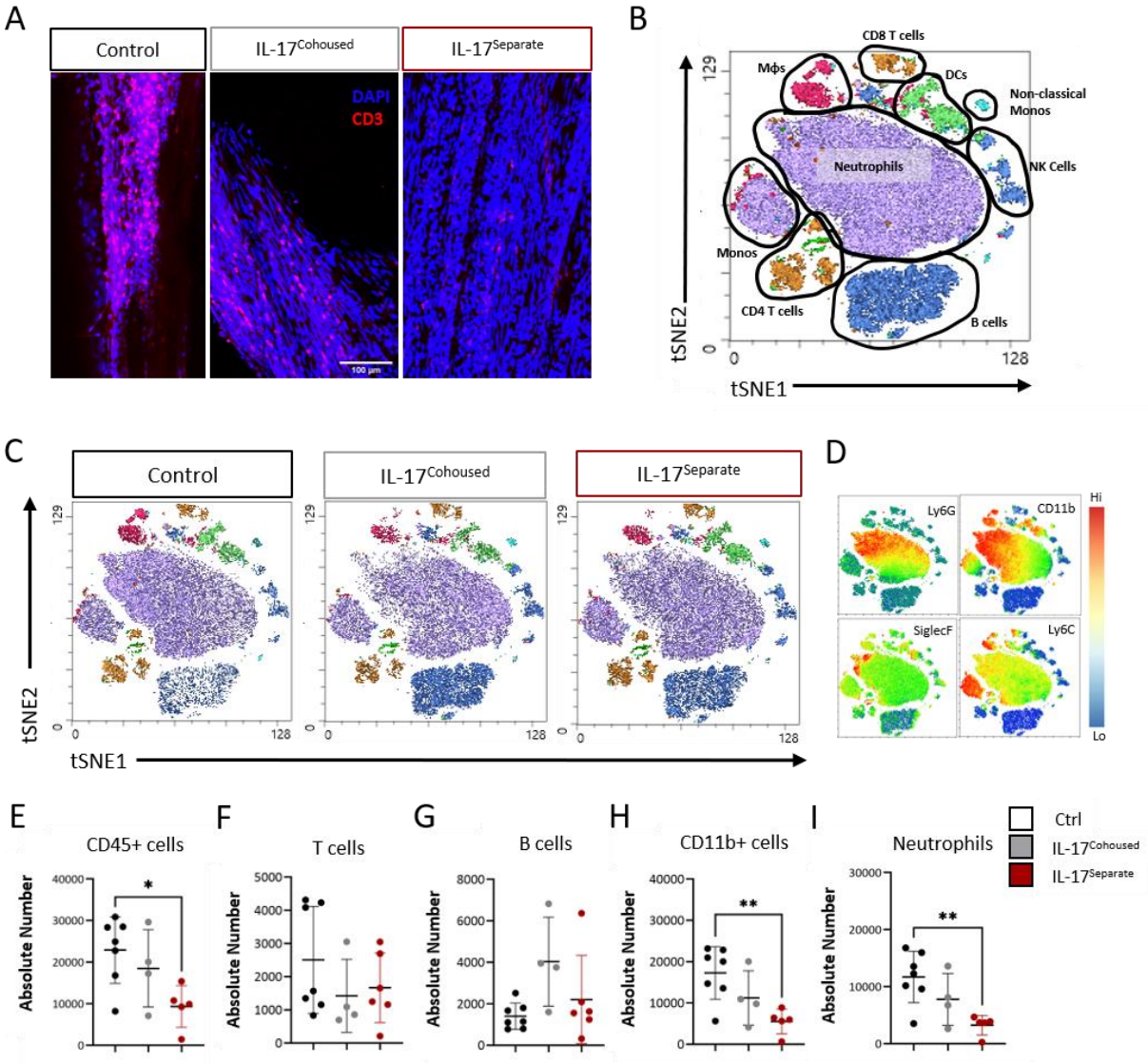

Figure 16: IL-17-deficient mice have reduced leukocytes in the dural meninges at EAE post-onset. (**A**) Confocal images of immunohistochemical staining of the dural sagittal meninges at post-onset of active EAE (DPI 16) with fluorescently labeled secondary antibodies to visualize T cells (CD3, red). Nuclear staining was performed with DAPI (blue). Images are representative of n = 2-4 per group. Scale bar = 100 µm. (**B**) Multidimensional flow cytometry analysis of the dural meninges at post-onset of active EAE (DPI 17). Exemplary annotation of data presented as a 2D t-SNE graph manually annotated according to expression of lineage markers. Live leukocytes ($CD45^+$) were randomly sampled with 6,655 cells taken per sample and n = 4 per condition. (**C**) Comparison of t-SNE plots between conditions. (**D**) Heatmap of relative marker expression of selected markers on combined t-SNE from (B). Quantification of absolute numbers of (**E**) immune cells ($CD45^+$), (**F**) T cells ($CD3^+$), (**G**) B cells ($CD19^+$), (**H**) $CD11b^+$ myeloid cells, and (**I**) neutrophils ($CD11b^+$ $Ly6G^+$) per dura. All data from one experiment. Data from (E-I) shown as mean +/- SD. Analysis was performed using one-way ANOVA. * $p < 0.05$; ** $p < 0.01$.

9. IL-17-deficiency alters the splenic myeloid cell composition during EAE

Until this point, *in vivo* experiments ruled out T cells as a driver of EAE suppression in IL-17-deficient mice and changes in myeloid cells were observed in the dural meninges during the peak of EAE. As B cells are acknowledged to play a minimal role in the pathogenesis of MOG_{35-55}-induced EAE, focus was then placed on the analysis of myeloid subsets in the periphery to observe whether the phenotype seen in the meninges was a local or global phenomenon.[60] Priority was first given to analysis of the spleen, due to its recognition in recent years as the major peripheral immunoregulatory hub during EAE.[75] Myeloid cells in the spleen were qualitatively analyzed by multidimensional flow cytometry by random sampling of non-lymphocytes ($CD19^-$ $CD3^-$) at active EAE DPI 10 and creation of 2D t-SNE graphs (Fig. 17A). Clusters were manually annotated according to surface marker expression (Fig. 17B). Comparison of t-SNE graphs between conditions revealed differences in many myeloid subsets, including increases in macrophages, non-classical monocytes, DCs, and NK cells (Fig. 17C). Strikingly, splenic neutrophils populations were also shifted in their t-SNE location in IL-$17^{-/-}$ mice similar to the observations made from the dura. In contrast to the dura, however, neutrophils in the IL-$17^{-/-}$ spleen appeared to be of a more mature phenotype than controls, with higher Ly6G, CD88, and CD11b expression. Numeric quantification of myeloid cells in the spleen showed that IL-$17^{-/-}$ mice had significantly fewer myeloid cells, with approximately half the number of $CD11b^+$ cells of the controls (Fig. 17D). This phenotype was independent of housing conditions. Manual gating of individual subsets revealed that IL-$17^{-/-}$ mice had significantly fewer neutrophil numbers in the spleen compared to controls, and that this was also independent of housing conditions (Fig. 17E). To verify that the changes in the splenic myeloid compartment of IL-$17^{-/-}$ mice was an EAE-specific phenotype and not a result of increased inflammation during steady-state, flow cytometry was used to analyze the splenic immune compartment of naïve IL-$17^{-/-}$ mice (Fig. 18A). No differences were seen in lymphocyte (Fig. 18B) or myeloid populations (Fig. 18C) in the spleen at steady-state, confirming that the altered myeloid compartment is an inflammation-driven phenomenon. This data from EAE pre-onset suggests that IL-17 already plays a role earlier in EAE progression in myeloid cell recruitment in the spleen. However, at this time point, no differences are observed due to

housing conditions unlike the results of the dural meninges, suggesting that the effect of the microbiome may play a role in the EAE model that is CNS-specific.

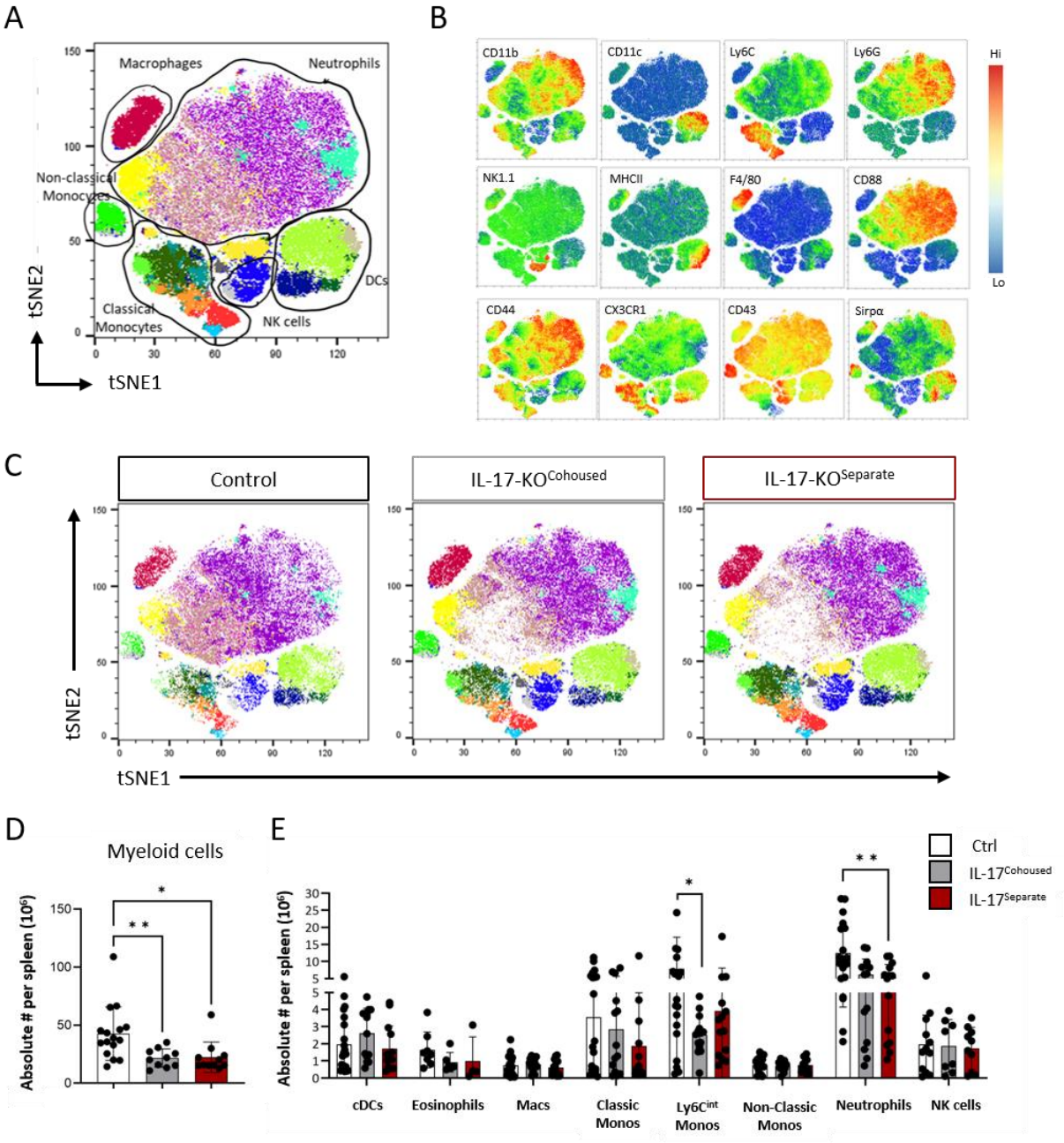

Figure 17: IL-17 deletion alters the composition of the splenic myeloid compartment. Splenocytes from IL-17$^{-/-}$ mice and controls at active EAE DPI 10 were analyzed by multidimensional flow cytometry. Exemplary annotation of data presented as a (**A**) 2D tSNE graph manually annotated according to relative marker expression shown in (**B**). Living non-lymphocytes (CD19^{-} CD3^{-}) were randomly sampled with 30,000 cells taken per sample and n = 4 per group. (**C**) Comparison of tSNE plots between conditions. Quantification of absolute numbers of (**D**) total myeloid cells (CD11b^{+}) and (**E**) individual myeloid subsets from manually gated flow cytometry data. Data shown in (A-C) is representative of 3 independent experiments. Data from (D, E) is shown as mean +/- SD and pooled from 3 independent experiments with n = 11-15 per group. Analysis was performed using one-way ANOVA on each cell subset. * $p < 0.05$; ** $p < 0.01$.

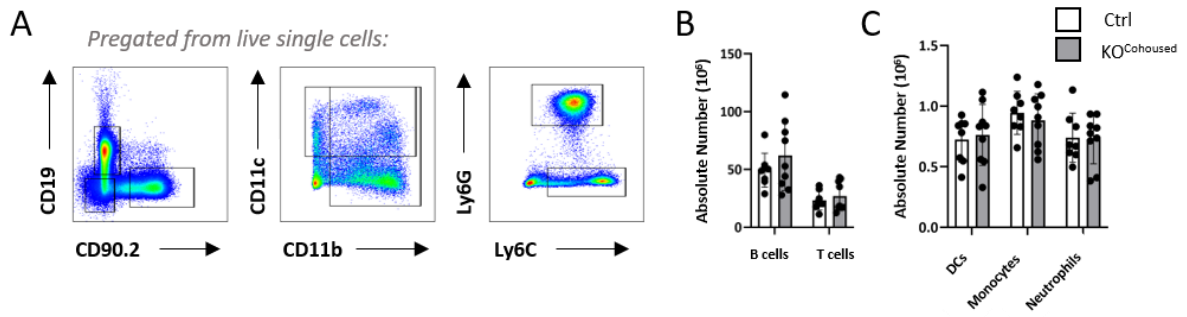

Figure 18: IL-17$^{-/-}$ mice show no differences in the splenic myeloid compartment at steady-state. Splenocytes from naïve IL-17$^{-/-}$ mice and controls were analyzed by flow cytometry. (**A**) Representative gating strategy to identify B cells (CD19^{+}), T cells (CD90.2^{+}), DCs (CD11c^{+}; gated from CD19^{-} CD90.2^{-}), monocytes (Ly6C^{+}; gated from CD11b^{+}) and neutrophils (Ly6G^{+}; gated from CD11b^{+}). Quantification of absolute numbers of (**B**) lymphocytes and (**C**) myeloid subsets from data shown in A. Data shown in (A-C) is from one experiment with n = 8-9 per group.

10. Neutrophil compartment is altered throughout the IL-17$^{-/-}$ peripheral environment during EAE

To determine whether the altered myeloid composition in the spleen and meninges was a tissue-specific or broader peripheral phenotype, multidimensional flow cytometry was performed on other peripheral organs. We hypothesized that 1) the splenic phenotype would be reflected in the blood, indicating reduced myeloid emigration from the bone marrow, and 2) gut-neighboring lymphoid tissues (mesenteric lymph nodes (mLNs), colon, and liver) may provide evidence for housing/microbiome-specific changes to myeloid cell composition. t-SNE analysis of the blood revealed a similar composition to the spleen, with Ly6G^{+} neutrophils and Ly6C^{+} monocytes comprising the largest percentage of myeloid cells (Fig. 19A). Blood myeloid cells of IL-17$^{-/-}$ mice showed similar differences to those in the spleen; macrophages and DCs were increased in percentage, while monocytes remained largely unchanged by IL-17 deficiency (Fig. 19B). Neutrophils also shifted towards a more mature Ly6G^{hi} phenotype, with fewer immature Ly6G^{lo} neutrophils. The myeloid composition of the liver was predominantly composed of mononuclear phagocytes, including Kupffer cells, monocytes, and monocyte-derived macrophages (Fig. 19C). Neutrophils were only subtly changed in the liver of IL-17$^{-/-}$ mice, though these differences mirrored the phenotype seen in the spleen and blood: IL-17$^{-/-}$ neutrophils were composed of more "mature" Ly6G^{hi} and CD11b^{hi} neutrophils (Fig. 19D).

The colon and mLNs are sites of high microbial settlement which is managed innately by cells with phagocytotic and antigen presenting function. Unsurprisingly, the myeloid compartment of the colon and mLNs were predominantly composed of classical antigen presenting cells, such as $CD11c^+$ DCs (Fig. 19E, G). While most colonic myeloid subsets were comparable between IL-$17^{-/-}$ mice and controls, neutrophils were decreased in the IL-$17^{Cohoused}$ mice and nearly absent in the IL-$17^{Separate}$ mice (Fig. 19F). In the mLNs, reductions were observed only among non-classical monocytes and neutrophils of IL-$17^{-/-}$ mice, with the strongest decrease observed in the IL-$17^{Cohoused}$ mice where these cell types were nearly absent (Fig. 19H).

To complement the t-SNE analysis, manual gating was performed on total $CD11b^+$ myeloid cells in each organ. Myeloid cells as a percentage of total $CD45^+$ immune cells were only reduced in the blood and liver (Fig. 20A). Absolute myeloid cell counts in the blood were not measured due to the technical challenges of normalizing cell count per volume. However, myeloid cells were reduced in count in all other organs excluding the colon (Fig. 20B). A non-significant, step-wise reduction in myeloid numbers was observed in the liver. On average, controls had the highest myeloid cell count (~2 x 10^6 per liver), followed by IL-$17^{Cohoused}$ mice (~1 x 10^6 cells per liver), and IL-$17^{Separate}$ mice (~0.5 x 10^6 myeloid cells per liver).

Neutrophils reflected the patterns observed with total $CD11b^+$ myeloid cells. Neutrophils, both as a percentage of total myeloid cells and absolute number, were reduced across nearly all organs and conditions (Fig. 20C, D). Both t-SNE and quantitative analysis produced data showing a consistent decrease in neutrophils across peripheral organs of IL-$17^{-/-}$ mice, confirming a broad role in neutrophil recruitment during inflammation. However, due to the limited number of mice used in the liver and blood analyses, more mice should be used to determine whether the microbiome has an effect on the IL-17-dependent neutrophil recruitment, maturation and/or maintenance in peripheral tissues.

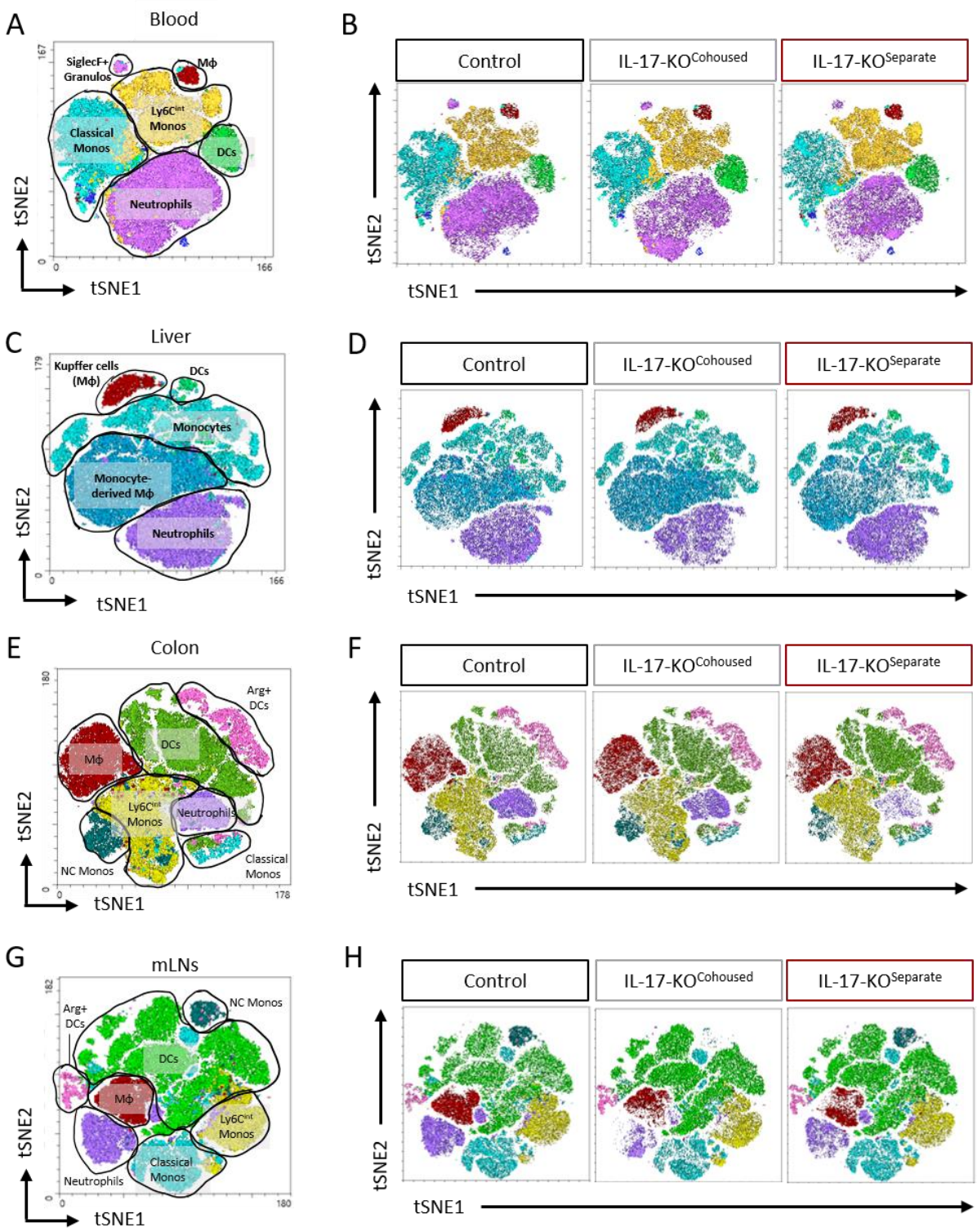

Figure 19: Cross-organ analysis of the peripheral myeloid compartment of IL-17$^{-/-}$ mice. Myeloid cells (CD3^{-} CD19^{-} CD11b^{+}) from IL-17$^{-/-}$ mice at active EAE DPI 10 were analyzed by multidimensional flow cytometry. Exemplary annotation of data from the (**A**) blood, (**C**) liver, (**E**) colon, and (**G**) mLNs presented as a 2D tSNE graph manually annotated according to expression of lineage-specific markers. 2D tSNE plot comparison between conditions for the (**B**) blood, (**D**) liver, (**F**) colon, and (**H**) mLNs. Data shown is from one experiment with n = 3 per group.

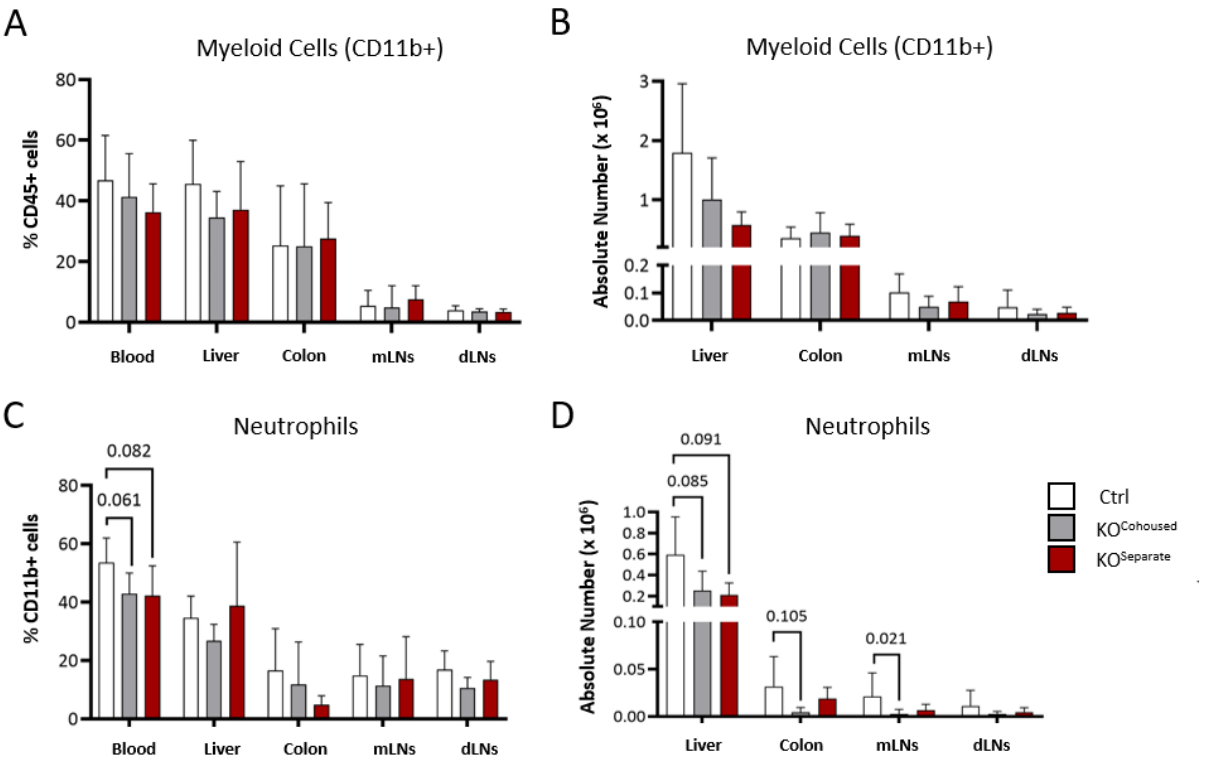

Figure 20: Quantification of myeloid cells across peripheral organs of IL-17-deficient mice. Myeloid cells ($CD3^-$ $CD19^-$ $CD11b^+$) from respective organs at active EAE DPI 10 were analyzed via flow cytometry for (**A**) percentage of total $CD45^+$ immune cells and (**B**) absolute number. Neutrophils ($Ly6G^+$) were gated from $CD11b^+$ myeloid cells and analyzed as (**C**) percentage of total myeloid cells ($CD11b^+$) and (**D**) absolute number. Data from 1 (liver, blood), or 2 (dLNs, colon) independent experiments with n = 4-20 per group. Data is shown as mean +/- SD. Analysis of (C, D) was performed using one-way ANOVA. Graph shows resulting p-values of this analysis.

11. Single-cell transcriptomic analysis of splenocytes at pre-onset of EAE

While quantitative flow cytometry provides valuable insights into cellular mechanisms, it is limited in its number of fluorometric parameters, making it challenging to assess molecular-level functional changes. To investigate molecular changes resulting from IL-17 deletion or separate housing conditions, single-cell RNA sequencing was performed on B cell-depleted splenocytes of mice at the pre-onset stage of active EAE (DPI 10) (Fig. 21A). Since B cells constitute a large portion of splenocytes and are published to play an inconsequential role in MOG_{35-55}-EAE[60], magnetic depletion of B cells was performed to increase sequencing depth for other splenocyte subsets. The remaining splenocytes were multiplexed with sample tags (BD Biosciences), mRNA was extracted and captured, and cDNA was synthesized. Libraries were prepared (BD Rhapsody system) and cells were sequenced on the NovaSeq X Plus (Illumina)

platform from 40,000 total cells with an average depth of 50,000 reads per cell. The resulting analysis yielded 25 clusters of immune cells, encompassing both lymphocyte and myeloid lineages (Fig. 21B).

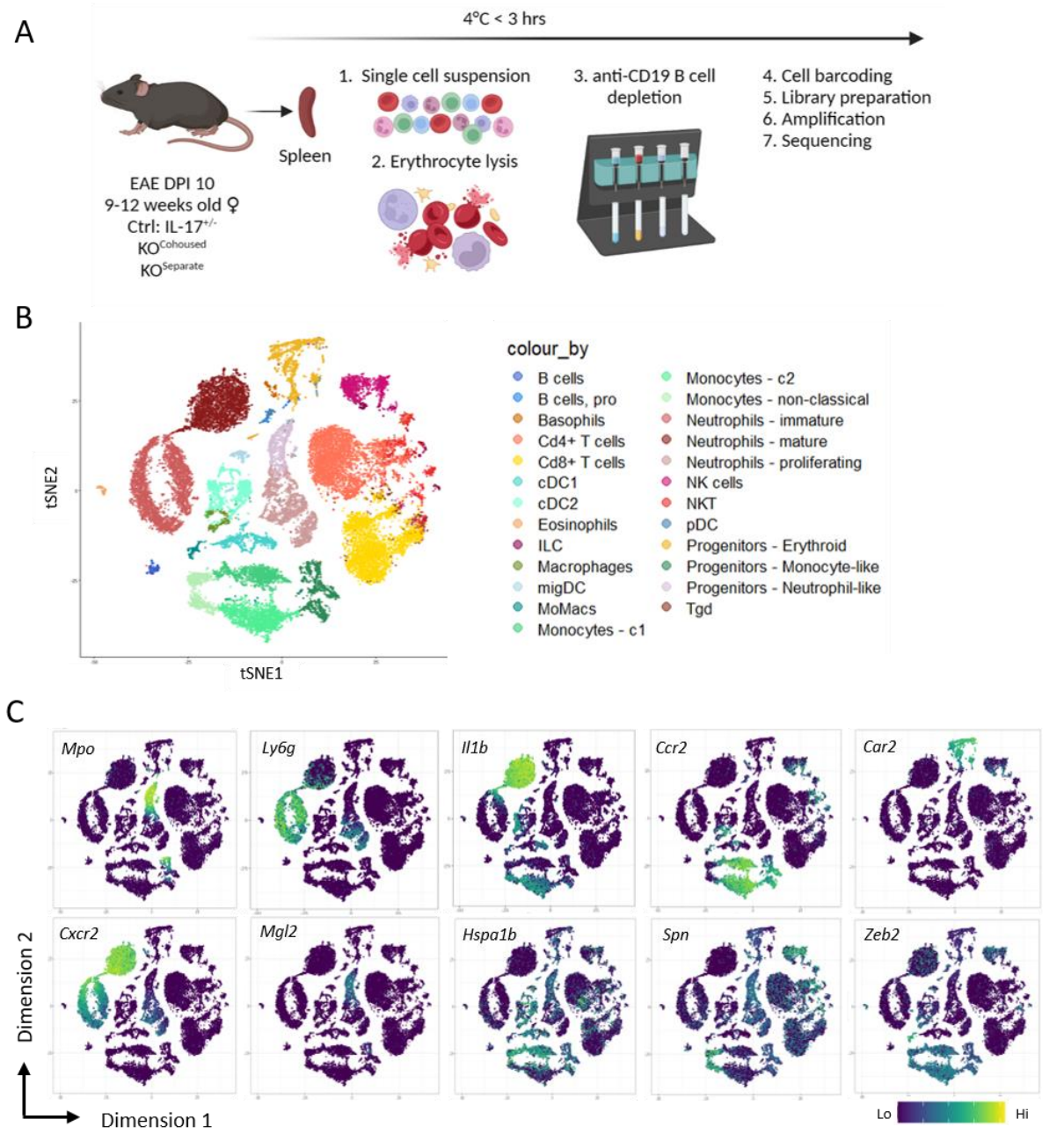

Figure 21: Single cell RNA sequencing strategy and cell cluster annotation of B cell-depleted splenocytes. (**A**) Experimental overview. Cells were isolated from MOG_{35-55}-immunized mice at active EAE DPI 10 for microwell-based single cell RNA sequencing (scRNA-seq) using the BD Rhapsody platform. Four mice were taken per condition, totaling n = 29,705 cells that were combined for analysis. (**B**) t-SNE map of CD45-barcoded splenocytes reveals 25 unique clusters. (**C**) t-SNE plots showing relative gene expression of cluster-specific markers used for manual cluster annotation. Green indicates high expression while purple indicates low expression of respective genes.

After unsupervised clustering, stromal and endothelial cells were removed and T cells were further subclustered into $CD4^+$ and $CD8^+$ subsets. Stem cell-like progenitors and differentiated myeloid subpopulations were manually classified according to the expression of lineage-specific markers (Fig. 21C). Erythroid progenitors were identified by unique *Car2* expression, as described by Paul et al. 2015.[252] Neutrophil and monocyte precursors both expressed *Mpo* and *Elane*, with neutrophil-like progenitors additionally expressing *Mgl2* and monocyte-like progenitors expressing the monocyte-lineage marker *Ccr2*. The entire neutrophil compartment expressed neutrophil-associated genes such as *Cebpe* and degranulation genes *S100a8*, *S100a9*, and *S100a11*. Neutrophils were further subdivided into subsets based on data from Evrard et al. 2018[191]: proliferating neutrophils expressed the proliferation genes *Top2a* and *Mki67,* immature neutrophils highly expressed *Ly6g* and the oxidative stress marker *Cybb*, and mature neutrophils highly expressed *Il1b* and *Cxcr2*.

Ccr2-expressing monocytes were further subclassified into three groups: two classical subsets, "C1" monocytes (expressing *Hspa1b*) and "C2" monocytes (expressing *Cd83* and *Il1b*) and one non-classical subset defined by *Spn* expression. *Zeb2* was used to identify Ccr2-expressing monocyte-derived macrophages ("MoMacs") or Ccr2-negative plasmacytoid dendritic cells (pDCs), as previously described.[258] Classical dendritic cells (cDCs) were subdivided into *Xcr1*/*Irf8*-expressing cDC1s and *Sirpα*-expressing cDC2s, while migratory DCs (migDCs) were identified by high *Ccr7* and *Relb* expression.

12. Gene expression of $CD4^+$ T cells is unaffected by loss of IL-17

Previous conclusions about peripheral IL-$17^{-/-}$ T cells were made after manipulation *ex vivo*; either after six-hour *in vitro* restimulation for cytokine production or after four-day Th17 culture for adoptive transfer experiments. While IL-$17^{-/-}$ $CD4^+$ T cells produced cytokines after antigen restimulation (Fig. 10G, H) and induced disease in adoptive transfer EAE (Fig. 10I), we wanted to rule out whether these findings were biased by the *in vitro* conditions. In particular, before adoptive transfer, $CD4^+$ T cells are cultured closely among APCs in the absence of stromal support and in media containing high levels of IL-23 and anti-IFNγ, which may not reflect *in vivo* conditions. To determine whether IL-$17^{-/-}$ T cells undergo molecular changes in the

peripheral environment without external manipulation, single cell sequencing analysis of T cells was performed.

T cells were automatically annotated according to the ImmGen mouse reference dataset, with $CD4^+$ T cells further manually classified based on CD3 and CD4 co-expression (Fig. 22A). Differential gene expression (DEG) analysis was performed on the entire $CD4^+$ T cell subset in a pseudobulk manner using edgeR. Surprisingly, only two genes were upregulated in IL-$17^{Cohoused}$ $CD4^+$ T cells compared to controls: the blood coagulation factor *F13a1* and a glycosyltransferase linked to pro-tumor activity, *St8sia6* (Fig. 22B). No gene expression differences were observed based on housing conditions comparing the IL-$17^{Separate}$ to IL-$17^{Cohoused}$ mice (Fig. 22C). Taking together the results of RNA sequencing and the multitude of previously performed functional analyses, we can state firmly and conclusively that IL-17 has no impact on $CD4^+$ T cell gene expression or functionality during pre-onset of EAE.

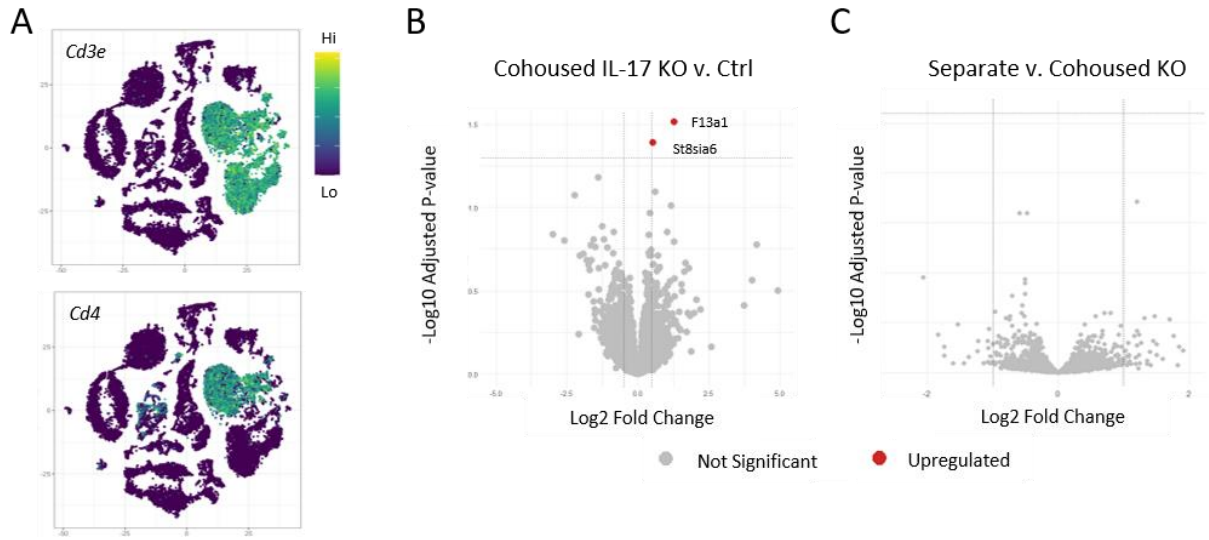

Figure 22: Splenic IL-$17^{-/-}$ $CD4^+$ T cells have no differences in gene expression. T cells from the spleens of MOG_{35-55}-immunized mice were harvested at active EAE day 10 for scRNA-seq analysis. (**A**) t-SNE map depicting gene expression of *Cd3e* and *Cd4* for the classification of $CD4^+$ T cells among total $CD45^+$ immune cells. (**B**) Log_2fold changes of differentially expressed genes in IL-$17^{Cohoused}$ (n = 1571 cells) compared to control (n = 790 cells) $CD4^+$ T cells. Upregulated genes (log2FC > 0.5, p-value < 0.05) are shown in red while insignificant genes are shown in grey. (**C**) Log_2fold changes of differentially expressed genes in IL-$17^{Separate}$ (n = 1702 cells) compared to IL-$17^{Cohoused}$ (n = 1571 cells). Non-significant genes are shown in grey.

13. IL-17 deletion is inconsequential for *Il17*-expressing splenocytes

The IL-17$^{-/-}$ mouse line retains exons 1, while exons 2 and 3 of the *Il17a* and *Il17f* genes are deleted. Consequently, *Il17a* and *Il17f* were not detected as DEGs in our dataset, and IL-17$^{-/-}$ mice expressed about one third of the number of mRNA transcripts compared to controls, as expected from the genetic system which lacks two of three exons (data not shown). Notably, CD4^{+} T cells were not the primary mRNA producers of either cytokine. The highest levels of *Il17a* and *Il17f* mRNA were found in ILCs and NKT cells (Fig. 23A, B). Since studies suggest the role of *Il17f* during EAE is largely redundant, DEG analysis was performed on lymphoid subsets expressing *Il17a*.[114] DEG analysis of ILCs and NKT cells, showed only one and two differentially expressed genes due to IL-17 deletion, respectively (Fig. 23C, D). Expression of *Il17a* by other previously reported cell subsets, such as γδ-T and NK cells, was also observed in our dataset (Fig. 23A). Again, no differences in gene expression were observed among these cell subsets and no DEGs were detected between the housing conditions for any lymphocyte subsets (data not shown). Previous reports have suggested that neutrophils polarized by IL-23 can upregulate STAT3-dependent RORγt to consequently express *Il17a* under inflammatory conditions.[259] The only non-lymphoid splenocytes shown to express *Il17a* during EAE in our dataset were erythrocyte progenitors and eosinophils, neither of which had differences in gene expression among IL-17 deletion (data not shown). *Il17f* mRNA expression was more universal and equally distributed, with most cell subsets expressing *Il17f* to some degree (Fig. 23B). Further investigation is needed to determine whether IL-17A or IL-17F mRNA translates into protein in these various cell types and to understand the functionality of IL-17 production from these cells. This data further confirms that IL-17 deletion has no effect on IL-17-expressing cells of the spleen during the pre-onset stage of the EAE model.

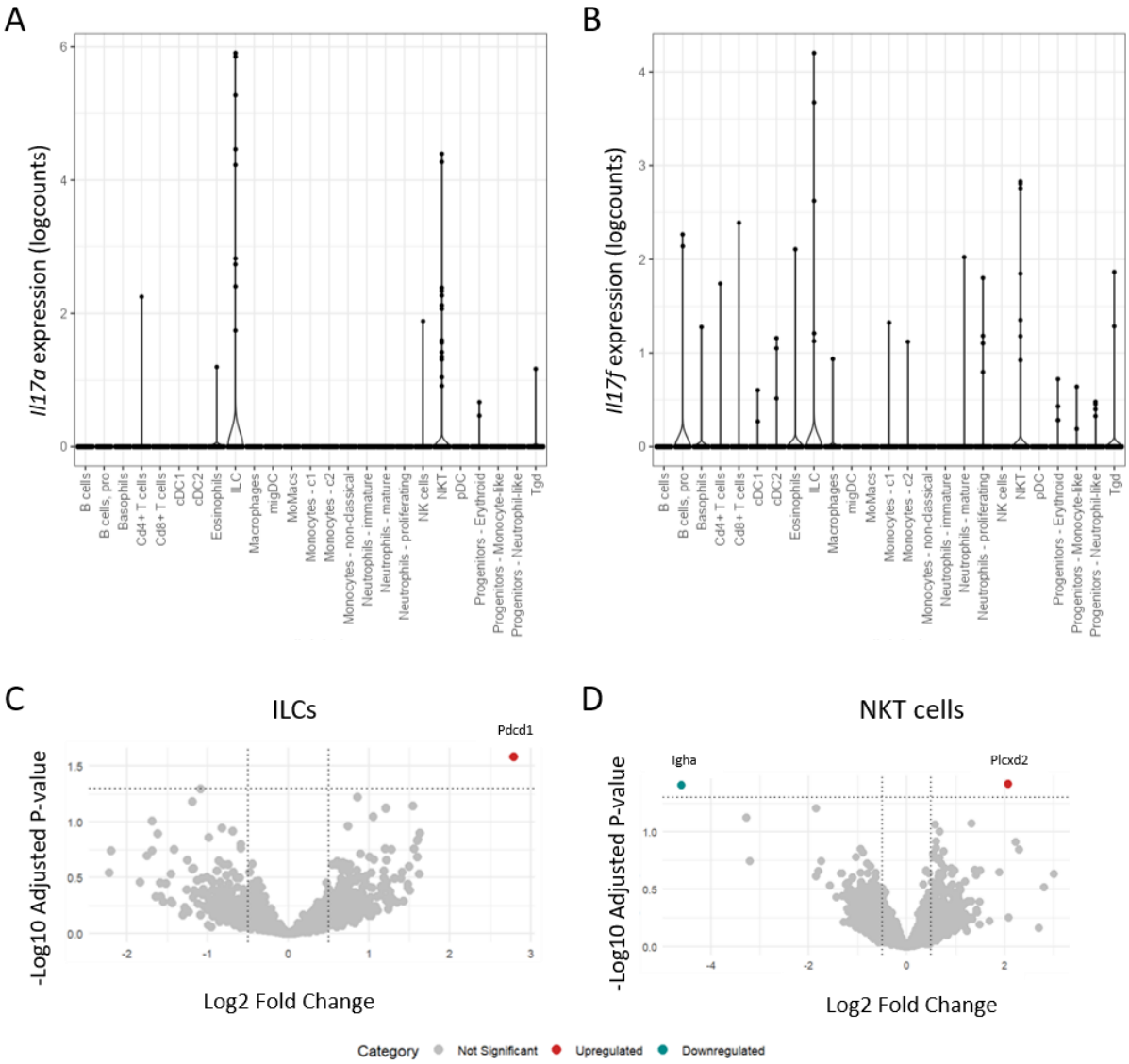

Figure 23: mRNA expression of IL-17A and IL-17F by splenic leukocytes during EAE pre-onset. mRNA levels of (**A**) Il17a and (**B**) Il17f among splenic immune cells of control mice at EAE DPI 10. Data is shown as log counts of mRNA expressing cells. Log_2fold changes of differentially expressed genes in IL-17^{Cohoused} compared to control (**C**) ILCs and (**D**) NKT cells. Upregulated genes ($log_2FC > 0.5$, p-value < 0.05) are shown in red, downregulated genes ($log_2FC < -0.5$, p-value < 0.05) are shown in blue, and insignificant genes are shown in grey.

14. Single cell transcriptomic analysis of IL-17 deficient neutrophils

Previous flow cytometry analysis showed that neutrophils are reduced in nearly all peripheral organs of IL-17$^{-/-}$ mice during the pre-onset stage of EAE. In the spleen specifically, neutrophils were observed to have a more "mature" phenotype according to previous research, with higher protein expression of Ly6G, CD88, and CD11b.[200] Single cell sequencing was used as a tool to answer several key questions: What are the exact identifies of the various neutrophil clusters in

the spleen and what might their functions be during pre-onset of EAE? Does IL-17 absence or presence affect functioning of these neutrophils? And relatedly, do IL-17$^{-/-}$ mice have more suppressive neutrophils which may reduce EAE severity starting in the periphery?

To characterize neutrophil populations in the spleen at DPI 10 of active EAE, neutrophils were subsetted and separately analyzed to gain greater depth of analysis (Fig. 24A). Four subsets were identified based on gene expression profiles: progenitor-like, proliferating, immature, and mature neutrophils. Progenitor-like neutrophils were the least abundant (928 detected cells), while proliferating (2,142 cells), immature (3,400 cells) and mature neutrophils (2,771 cells) were present in similar numbers. Quantification by condition showed that consistent with flow cytometry results, IL-17$^{-/-}$ mice had significantly fewer progenitor-like, proliferating, and immature neutrophils while mature neutrophil numbers remained unchanged (Fig. 24B). The top 15 gene signatures for each subset were determined using the Seurat FindAllMarkers function (Fig. 24C) and referenced to developmental signatures of neutrophils in so-called "neutrotime".[199] Progenitor-like neutrophils uniquely expressed genes involved in primary granule production such as *Mpo, Ctsg,* and *Elane*. Proliferating neutrophils were characterized by cell cycle-related genes, including *Ccna2, Top2a, Prc1,* and *Pimreg*. Immature neutrophils expressed markers associated with early-to-intermediate stage neutrotime signatures, such as *Ifitm6,* and *Capg*. Mature neutrophils expressed late-stage neutrophil signatures, including *Sirpb1b, Il1b,* and *Ccl6*, as well as ROS-related genes like *Ptgs2* and the transcription factor *Atf3*. Notably, mature neutrophils also expressed *Il1b* and *Wfdc17,* genes previously described as markers for myeloid-derived suppressor cells (MDSCs).[224]

To understand the functionality of these clusters, GO-term enrichment analysis was performed on the top 200 gene signatures for each cluster (Fig. 24D). Progenitor-like neutrophils showed enrichment in RNA processing genes, while proliferating neutrophils were enriched in gene signatures related to mitosis and chromosome dynamics, reflecting their proliferative state (Fig. 24D). Immature and mature neutrophils were associated with a broad range of immunoregulatory functions. Specifically, immature neutrophils expressed genes related to neutrophil activation and degranulation, angiogenesis, and ROS production (Fig. 24D). Mature neutrophils, on the other hand, expressed genes related to cell-cell adhesion, regulation of T cell activation, and leukocyte migration (Fig. 24D). These findings suggest that immature and

mature neutrophils are the relevant immunoregulatory cell types in the spleen during the pre-onset stage of EAE. Further, the imbalance of immature and mature neutrophil numbers in IL-17$^{-/-}$ mice points towards a disruption in the related immune functions of these subsets.

To identify potential target genes of IL-17 and the microbiome, DEG analysis was performed on all four subsets of neutrophils to compare the effects of gene deletion (IL-17^{Cohoused} vs. controls) and housing conditions (IL-17^{Separate} vs. IL-17^{Cohoused}). Genes were considered significant if $p < 0.05$ and $\log_2FC > 0.5$ (upregulated) or $\log_2FC < -0.5$ (downregulated). All subsets showed substantial changes in gene expression due to IL-17 deletion.

Progenitor-like neutrophils had 55 DEGs (47 upregulated, 8 downregulated) while proliferating neutrophils had 81 DEGs (59 upregulated, 22 downregulated) (Fig. 25A, B). The most highly upregulated gene in progenitor-like neutrophils was the adhesion molecule *Vcam1*, while *Thbs1,* an extracellular matrix remodeling protein, was most upregulated in proliferating neutrophils. Both subsets shared downregulation of *Lipg*, *Csf2rb*, *Lrg1*, and interferon-induced genes (*Ifitm1*, *Ifitm2*, and *Ifitm3*), and upregulation of *Trib1*, *Fosl2*, *B2m*, *Cd93*, and MHC class-Ib related genes (*H2-Q4*, *H2-Q6*, and *H2-Q7*). GO-term analysis indicated that DEGs of these early-stage neutrophils were involved in pathways related to neutrophil effector functioning, including regulation of cell activation state, leukocyte proliferation, and cytokine production (Fig. 25C, D). No significant gene expression changes were observed due to differences in housing conditions (Fig. 25E, F).

Late-stage neutrophils also exhibited vast changes in gene expression due to IL-17 deletion. Immature neutrophils had 64 DEGs (29 upregulated, 35 downregulated) while mature neutrophils had 34 DEGs (17 upregulated, 17 downregulated) (Fig. 26A, B). The most highly upregulated genes were *Ear2* and *Dubr* in immature neutrophils, and *Jaml* and *H2-Q6* in mature neutrophils. Both later-stage subsets downregulated similar genes to each other and to earlier-stage neutrophils, including *Prok2, Csf2rb, Lrg1, Emilin2, Lipg,* and interferon-induced *Ifitm* genes. GO-term analysis indicated that DEGs of IL-17$^{-/-}$ immature neutrophils were involved in pathways related to cytokine signaling, leukocyte activation, chemotaxis, apoptosis, and MHC class I signaling (Fig. 26C). DEGs of IL-17$^{-/-}$ mature neutrophils were involved in pathways related to cell activation, immunoglobulin and TNF production, and antigen processing and

presentation (Fig. 26D). No significant gene expression changes were observed due to differences in housing conditions (Fig. 26E, F).

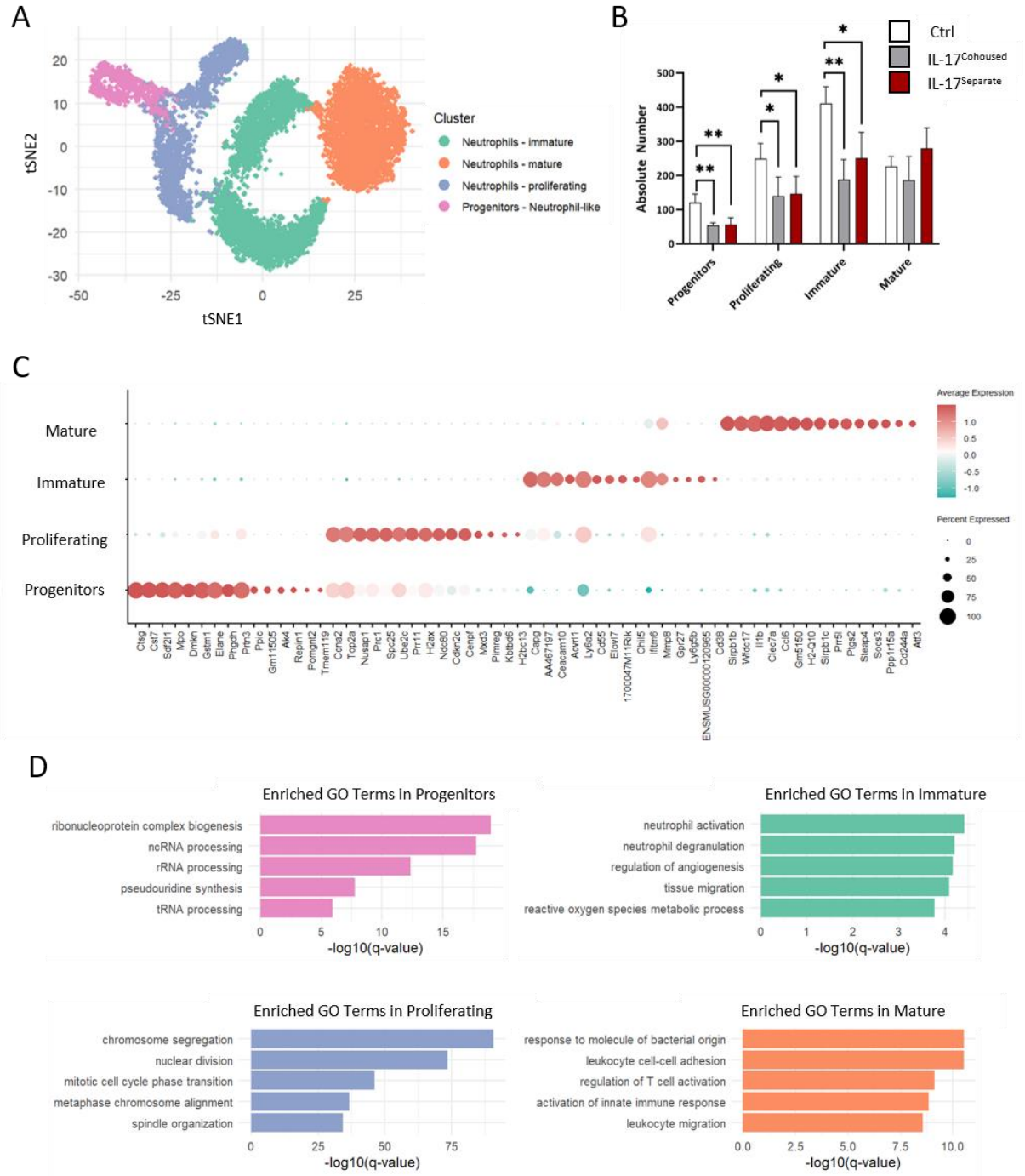

Figure 24: scRNA sequencing of IL-17-deficient splenic neutrophils at EAE pre-onset. (**A**) tSNE plot of neutrophil subsets defined by top 2,000 highly variable genes per cluster. Neutrophil-progenitors n = 928 cells, proliferating neutrophils n = 2142 cells, immature neutrophils n = 3400 cells, mature neutrophils n = 2771 cells. (**B**) Absolute number of cells per cluster for each condition. (**C**) Dot plot displaying the top 15 highly expressed marker genes of each cluster. Dot size represents the percentage of cells expressing the marker. Color represents the relative expression level of each marker. (**D**) Gene ontology (GO) enrichment analysis showing the top GO terms of each cluster using enrichR. Data in (B) shows mean +/- SD and was analyzed using one-way ANOVA. * $p < 0.05$; ** $p < 0.01$.

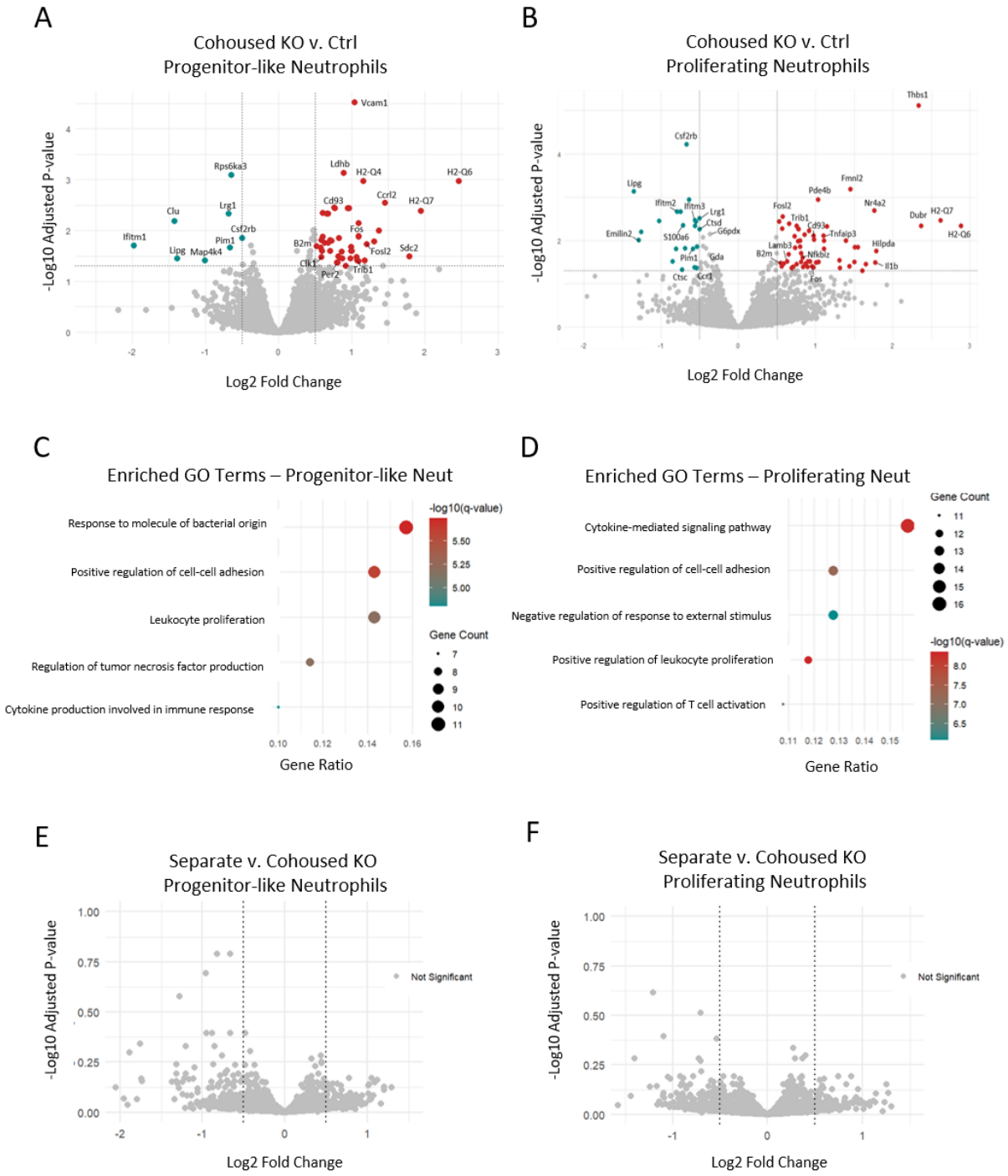

Figure 25: Differential gene expression analysis of splenic early-stage neutrophils at EAE pre-onset. Volcano plots showing log_2fold changes of differentially expressed genes (DEGs) in IL-17^{Cohoused} mice versus controls of (**A**) progenitor-like and (**B**) proliferating neutrophil subsets. DEGs are shown in red with a log_2fold change > 0.5 and differentially downregulated genes with a log_2fold change < -0.5 are shown in blue. Dot plots of enriched GO Terms of DEGs of (**C**) progenitor-like and (**D**) proliferating neutrophil subsets. Dot size represents the number of genes differentially regulated per GO term. Color represents the –log10(q-value) for each GO Term. Volcano plots showing log_2fold changes of DEGs of IL-17^{Separate} compared to IL-17^{Cohoused} mice for (**E**) progenitor-like and (**F**) proliferating neutrophil subsets.

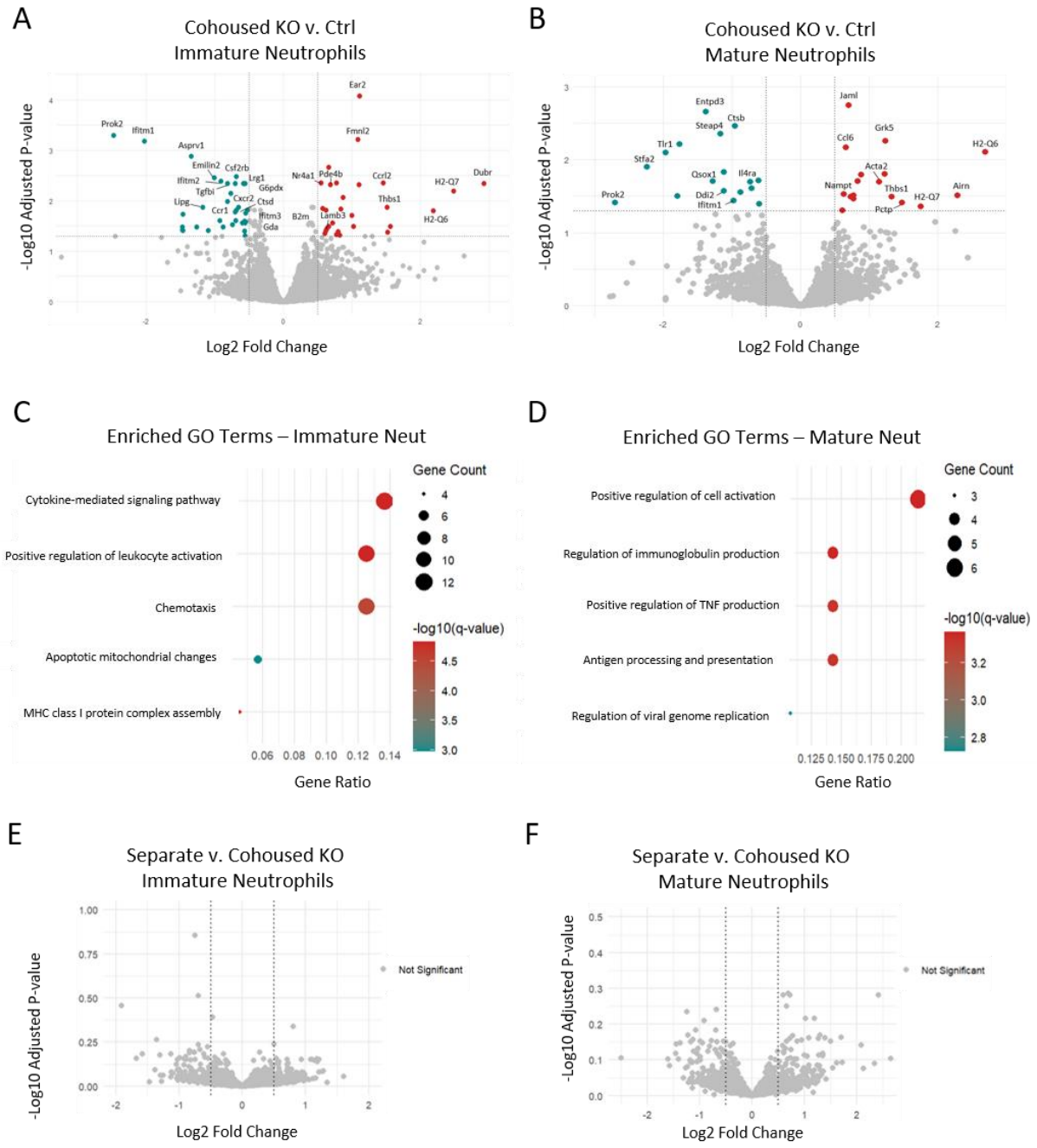

Figure 26: Differential gene expression analysis of late-stage splenic neutrophils at EAE pre-onset. Volcano plots showing log_2fold changes of differentially expressed genes (DEGs) in IL-17^{Cohoused} mice versus controls of (**A**) immature and (**B**) mature neutrophils at active EAE DPI 10. Upregulated genes are shown in red with a log_2fold change > 0.5 and downregulated genes with a log_2fold change < -0.5 are shown in blue. Dot plots of enriched GO Terms of DEGs of (**C**) immature and (**D**) mature neutrophil subsets. Dot size represents the number of genes differentially regulated per GO term. Color represents the –log10(q-value) for each GO Term. Volcano plots showing log_2fold changes of DEGs of IL-17^{Separate} compared to IL-17^{Cohoused} mice for (**E**) immature and (**F**) mature neutrophil subsets.

15. IL-17$^{-/-}$ mice have a greater proportion of myeloid cells with MDSC signatures

Myeloid-derived suppressor cells (MDSCs) are increasingly recognized for their regulatory roles in autoimmunity and cancer.[217] MDSCs can be divided into granulocytic (G-MDSCs) or monocytic (M-MDSCs), characterized by neutrophil or monocyte morphology, respectively.[218] Our *in vitro* results suggested that IL-17 was essential for cell blasting, a parameter indicative of the cell activation within a culture and that this effect was dependent on CD4^{-} (non-T cell) splenocytes (Fig. 11). We hypothesized that the myeloid cells of IL-17$^{-/-}$ mice may present with a suppressive phenotype, characteristic of MDSCs. Further, we hypothesized that the mature neutrophils retained in IL-17$^{-/-}$ mice may exhibit G-MDSC properties that suppress inflammation in the periphery during EAE. To explore this, neutrophils subsetted from scRNA-seq data were visualized by Uniform Manifold Approximation Projection (UMAP) and scored for expression levels of MDSC gene signatures using UCell (Fig. 27A). Mature neutrophils indeed had the highest MDSC gene signature scores of all neutrophil subsets (Fig. 27B). Immature neutrophils had low MDSC scores, while progenitor-like and proliferating neutrophils had near-zero MDSC gene signatures. The preservation of mature neutrophils and reduction in other neutrophil subsets suggest a shift of the neutrophil compartment towards G-MDSC functionality in IL-17$^{-/-}$ mice.

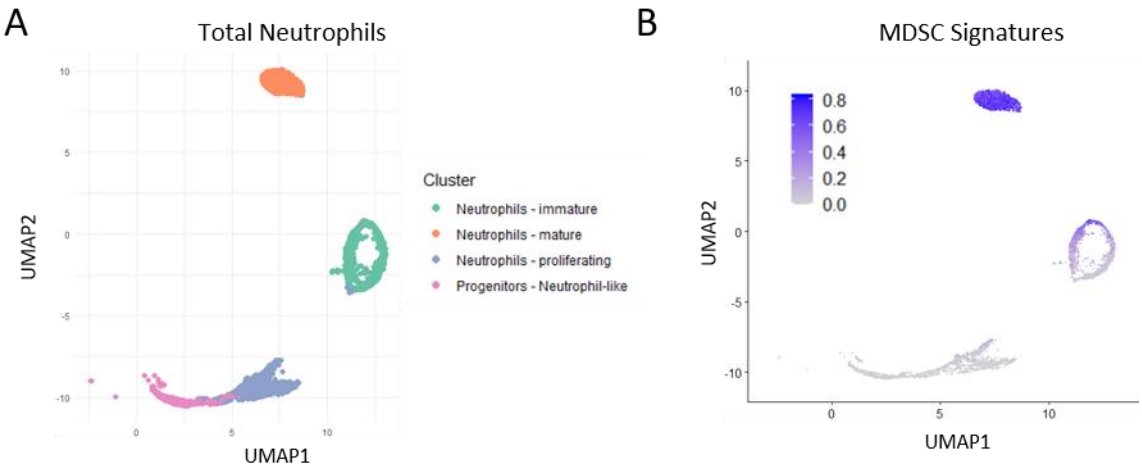

Figure 27: MDSC signature genes are predominantly expressed by mature neutrophils. (**A**) UMAP plot depicting neutrophil subsets. (**B**) Score of MDSC signature genes projected on UMAP from (A) calculated with UCell.

Both G-MDSCs and M-MDSCs are described for their involvement in the EAE context. To determine whether the shift towards an MDSC phenotype in IL-17$^{-/-}$ mice was a unique phenomenon of G-MDSCs or also M-MDSCs, monocyte subsets were similarly quantified and scored for expression of MDSC marker genes. Four monocyte subsets were identified based on gene expression profiles: progenitor-like, non-classical (NC), and two classical subsets, named C1 and C2, respectively (Fig. 28A). NC monocytes comprised the smallest fraction (795 detected cells), while progenitor-like (1,185 cells), C1 (1,211 cells) and C2 monocytes (1,753 cells) were found at higher and similar numbers. Quantification by condition showed a significant decrease in progenitor-like monocytes in IL-17$^{-/-}$ mice, whereas NC and classical C2 monocyte subsets were significantly increased in number (Fig. 28B). Classical C1 monocytes remained unchanged.

The top 15 gene signatures for each subset were calculated using the Seurat FindAllMarkers function, revealing unique gene expression signatures between monocytes (Fig. 28C). Similar to neutrophil progenitors, progenitor-like monocytes expressed granulocyte monocyte progenitor (GMP) gene signatures such as *Mpo, Ctsg,* and *Elane*. Classical C1 monocytes uniquely expressed cell-stress and microbial-sensing genes *Txnip* and *Tirap*, while C2 monocytes displayed high expression of genes related to effector processes such as vascular smooth muscle cell contraction (*Junb*), extracellular matrix remodeling (*Thbs1*), and pattern recognition responses (*Cd14*). NC monocytes expressed gene signatures confirmed in previous studies, such as the metabolic genes *Eno3* and *Pparg* and glycoprotein *Cd300e*.[260]

We hypothesized that, similar to neutrophils, the expanded monocyte subsets in IL-17$^{-/-}$ mice—C2 and NC monocytes—also had higher MDSC signatures. To test this, MDSC gene signatures were again analyzed using UCell (Fig. 28D). Indeed, C2 monocytes had the highest MDSC scores of all monocyte subsets, followed by NC monocytes (Fig. 28E). The remaining monocyte subsets had lower MDSC scores, with progenitor-like monocytes showing the lowest MDSC score (Fig. 28E). In summary, IL-17$^{-/-}$ mice have increased MDSCs of both G-MDSC and M-MDSC phenotype, which potentially leads to disease suppression in the periphery. This data suggests that IL-17 plays a critical role in the maturation process of both G- and M-MDSCs towards suppressive phenotypes.

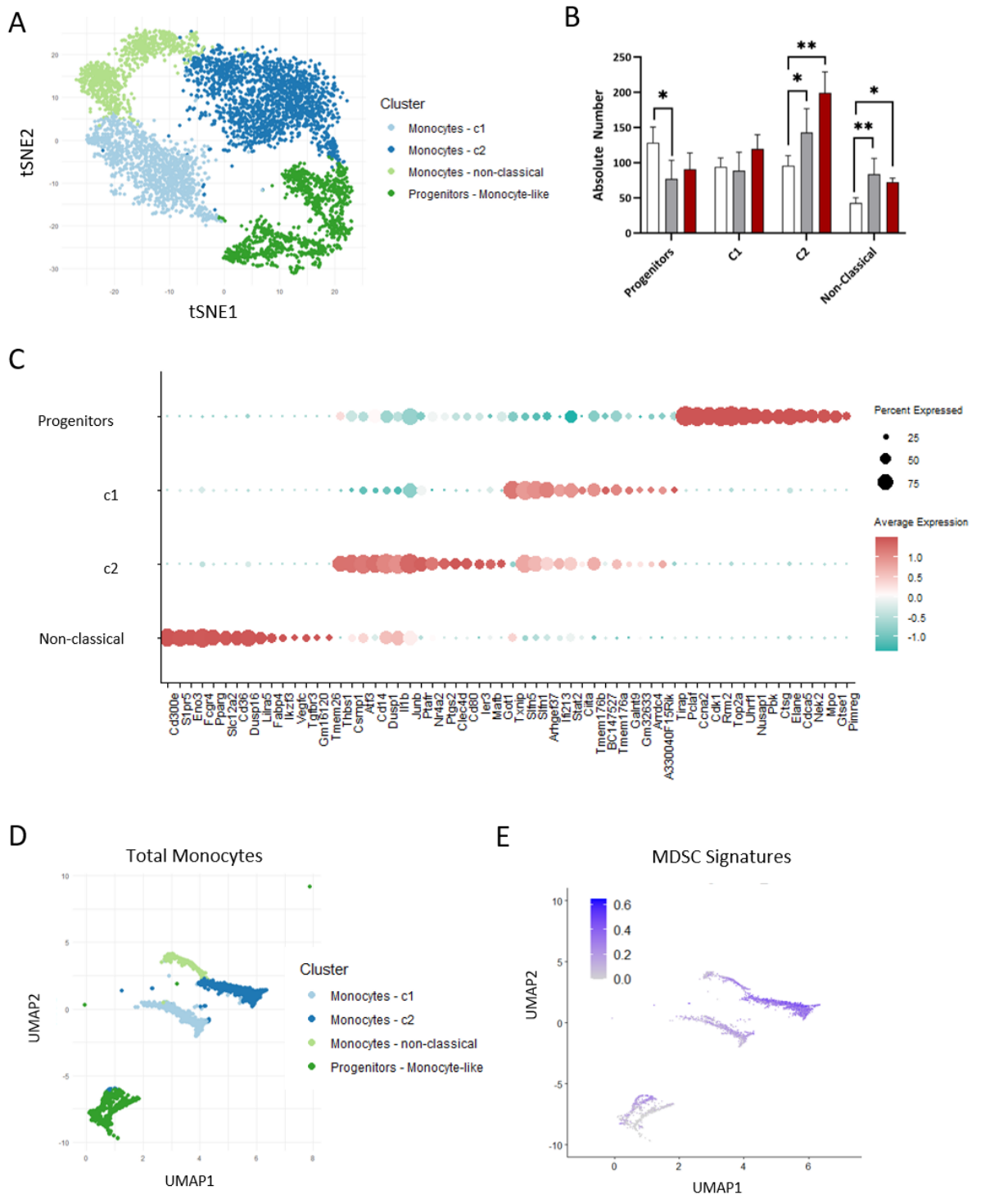

Figure 28: IL-17-deficient mice have increased monocyte subsets with MDSC signatures. (**A**) tSNE plot of monocyte subsets defined by top 2,000 highly variable genes per cluster. Monocyte-like progenitors: n = 1185, monocytes c1: n = 1211, monocytes c2: n = 1753, Non-classical monocytes: n = 795. (**B**) Absolute number of cells of each cluster for each condition. (**C**) Dot plot displaying the top 15 highly expressed marker genes of each cluster. Dot size represents the percentage of cells expressing the marker. Color represents the relative expression level of each marker. (**D**) UMAP plot depicting monocyte subsets. (**E**) Score of MDSC signature genes projected on UMAP from (D) calculated with UCell.

16. IL-17 signals to perivascular stromal cells (PvCs) to promote EAE pathogenesis

The target cells of IL-17 signaling during EAE have long been debated. Two key *in vitro* studies suggested that IL-17 signals to BBB endothelial cells, leading to barrier breakdown due to tight junction dysregulation.[147,148] However, these results may be confounded by the use of primary brain endothelial cells which often contain other cells of the glia limitans, including pericytes and astrocytes. Additionally, none of these findings have since been confirmed *in vivo*. Other studies investigating conditional deletion of IL-17RA *in vivo* on myeloid cells, mesenchymal stem cells, and reticular fibroblasts produced no effect on EAE outcomes.[119,133,261] Deletion of IL-17RA on intestinal epithelial cells worsened EAE severity, indicating that IL-17 signaling in the gut may even play a protective role.[151] This research does not explain, however, the work showing that EAE incidence is reduced in mice with complete IL-17RA deletion.[119] A study from Liu et al. showed *in vitro* that IL-17 signals to pericytes to induce neutrophil-recruiting chemokines like GM-CSF, CXCL1, and CXCL8.[262] Pericytes, the cells that ensheath vascular endothelial cells, were a promising candidate for IL-17RA deletion, due to their additional roles in immunomodulation.[263,264] Despite evidence pointing to IL-17's role at endothelial barriers, a specific target cell type had not been confirmed *in vivo*. We hypothesized that in the EAE context, IL-17 signals to pericytes to promote neutrophil recruitment and neuroinflammation.

To investigate this hypothesis, we developed a mouse line with pericyte-specific IL-17RA deletion. PDGFRβ is highly expressed on pericytes, and, to a lesser extent, on other perivascular cells (PvCs) such as smooth muscle cells and certain fibroblast subsets.[249] Therefore, IL-17RA floxed mice were crossed to the PDGFRb-Cre^{ERT2} strain to generate mice lacking IL-17RA signaling on pericytes (hereafter termed IL-17RA$^{\Delta PER}$ mice). Pericyte-specific deletion of IL-17RA led to significantly reduced clinical EAE scores (Fig. 28A). Like the global cytokine knockout model (IL-17$^{-/-}$ mice), this reduction was largely reflected by a significantly decreased EAE incidence (Fig. 28B). IL-17RA$^{\Delta PER}$ mice that developed EAE had similar disease severity as controls, as shown by peak scores (Fig. 28C). Unlike IL-17$^{-/-}$ mice, IL-17RA$^{\Delta PER}$ mice showed a trend towards delayed day of onset (Fig. 28D). Since the adoptive transfer EAE model develops independently of secondary lymphoid organs, we used this model to determine whether the ameliorated active EAE in IL-17RA$^{\Delta PER}$ mice was due to peripheral or CNS-mediated disease

mechanisms. Wild-type pathogenic Th17 cells were adoptively transferred into IL-17RA$^{\Delta PER}$ mice and controls using the standard protocol. No difference in severity in adoptive transfer EAE was observed, hinting towards a role of peripheral mechanisms mediating the reduction in active MOG_{35-55} EAE severity in IL-17RA$^{\Delta PER}$ mice (Fig. 28E).

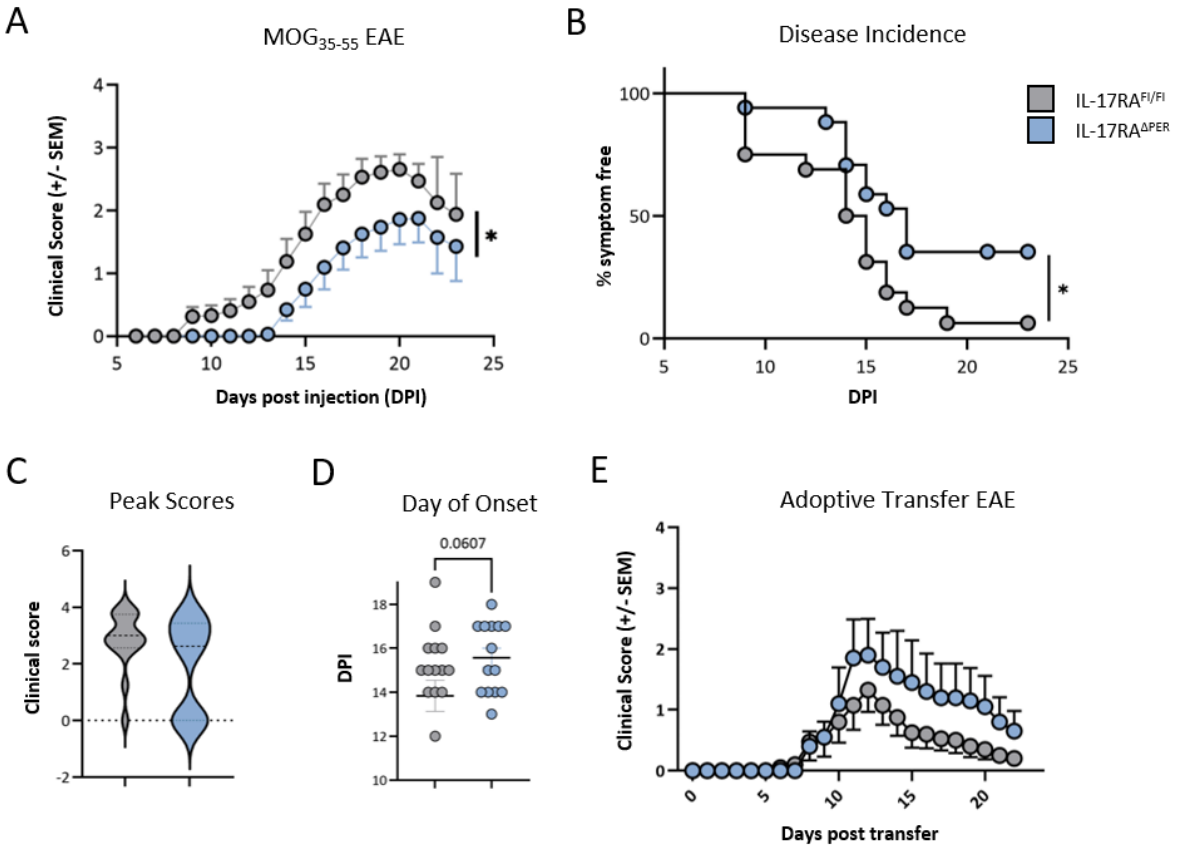

Figure 29: IL-17RA signals to pericytes to increase the incidence of MOG_{35-55}-EAE. (**A**) Clinical scores of MOG_{35-55}-immunized mice with conditional deletion of IL-17RA on PDGFRb^{+} cells (IL-17RA$^{\Delta PER}$) versus controls (IL-17RA$^{FI/FI}$). Significance calculated from area under the curve (AUC). (**B**) Symptom-free survival curve, (**C**) peak clinical scores, and (**D**) day of disease onset from data shown in (A). (**E**) Clinical scores after i.v. adoptive transfer of Th17 cells into IL-17RA$^{\Delta PER}$ (blue; n = 5) or control mice (grey; n = 10). Data in A-D combined from two independent experiments with n = 16 mice per group. Data from E is from one independent experiment. Data is shown as either (A, E) mean +/- SEM or mean +/- SD (C, D). P-values calculated using (A) t-test of AUC, (C, D) t-test of individual data points, or (B) Kaplan-Meier survival analysis with Wilcoxon rank test. * $p < 0.05$.

17. Loss of IL-17RA signaling on pericytes is redundant for T cell priming and expansion

Focus was next placed on determining which peripheral mechanisms are affected by loss of IL-17RA signaling on pericytes. To investigate this, T cell dynamics were analyzed at two key time points: priming (DPI 5) and pre-onset (DPI 10). Inguinal draining LNs were harvested for flow cytometry analysis to compare the number and percentage of $CD4^+$ T cells and cytokine production between conditions (Fig. 30A). Absolute number and percentage of $CD4^+$ T cells and $CD40L^{hi}$ MOG-specific T cells were unchanged in the dLNs from IL-17RA deletion at DPI 5 (Fig. 30B, C). Additionally, pro-inflammatory cytokine production from MOG-specific T cells was unchanged (Fig. 30D). This provides evidence for a redundancy of IL-17RA signaling in pericytes for antigenic priming of T cells in the dLNs. The same analysis was performed from spleens harvested at DPI 10 (Fig. 30E). Similarly, no differences were observed in the percentage and total number of $CD4^+$ or MOG-specific T cells (Fig. 30F, G). Production of pro-inflammatory cytokines was also unchanged at this time point (Fig. 30H). This data confirms previous results of global IL-17 cytokine deletion; IL-17 receptor deletion on pericytes plays no role in the T cell dynamics at priming or pre-onset stages of EAE.

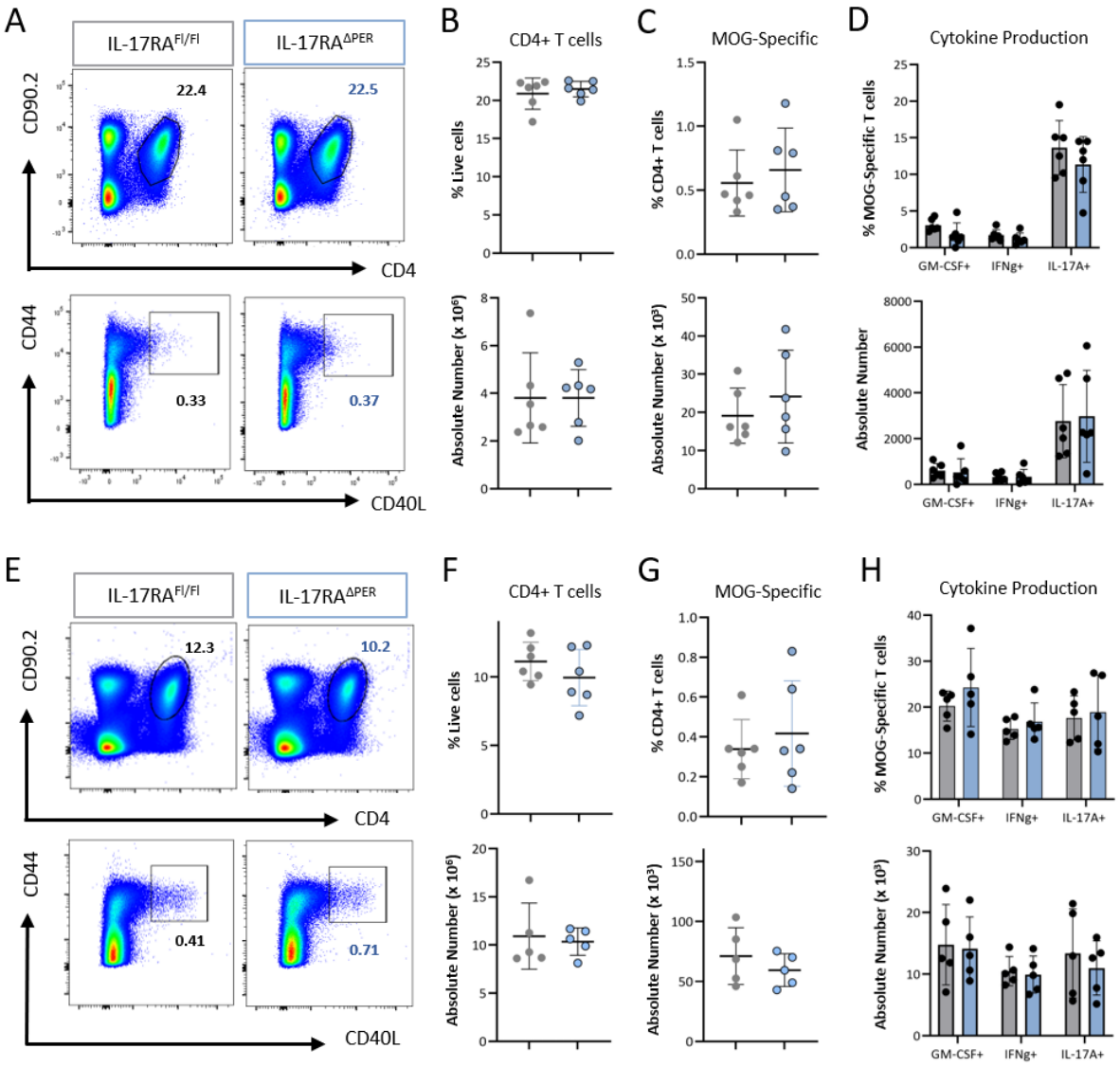

Figure 30: IL-17RA signaling to pericytes is redundant for T cell priming and expansion. **A-D**, Draining inguinal lymph nodes from MOG_{35-55}-immunized mice at active EAE day 5 were analyzed via flow cytometry. (**A**) Representative dot plots showing $CD4^+$ (above; % live cells) and MOG-specific T cells (below; % $CD4^+$ cells) as percentage of respective parent populations. Quantification of percentage of parent population and absolute cell number of (**B**) $CD4^+$ T cells and (**C**) MOG-specific T cells from data shown in (A). (**D**) Cytokine production from MOG-specific $CD4^+$ T cells shown as percentage of MOG-specific T cells and absolute number. **E-H**, Spleens from MOG_{35-55}-immunized mice at EAE day 10 were analyzed via flow cytometry. (**E**) Representative dot plots showing $CD4^+$ (above; % live cells) and MOG-specific T cells (below; % $CD4^+$ cells) as percentage of respective parent populations. Quantification of percentage of parent population and absolute number of (**F**) $CD4^+$ T cells and (**G**) MOG-specific T cells from data shown in (E). (**H**) Cytokine production from MOG-specific $CD4^+$ T cells shown as percentage of MOG-specific T cells and absolute cell number. All data produced from one experiment with n = 5-6 per group. All graphs show mean +/- SD.

18. Neutrophils are reduced upon loss of IL-17RA signaling on PvCs

During pre-onset of EAE, loss of IL-17 cytokine affected the peripheral myeloid compartment, particularly altering the number and composition of neutrophils. To investigate whether IL-17 signals to pericytes mediate these effects, multidimensional flow cytometry was used to analyze the splenic myeloid compartment at pre-onset (DPI 10) of active EAE (Fig. 31A). Major myeloid subsets, including neutrophils, monocytes, and DCs were identified based on expression of lineage markers (Fig. 31B). Unlike what was seen with global IL-17 cytokine deletion, no qualitative shifts in the myeloid cell compartment were observed in IL-17RA$^{\Delta PER}$ mice, indicating no phenotypic differences (Fig. 31C). However, quantitative analysis revealed a trend towards reduced percentage and number of myeloid cells in IL-17RA$^{\Delta PER}$ mice (Fig. 31D, E). Neutrophils, which comprised approximately 35-50% of all myeloid cells, were also found reduced in number in the spleens of IL-17RA$^{\Delta PER}$ mice (Fig. 31F). Although this data is based on a single experiment with few mice per condition, the trend of the data suggests a promising conclusion: IL-17 may signal to pericytes to recruit neutrophils during EAE, but this signaling may not be essential for the phenotypic maturation of neutrophils seen with total IL-17 cytokine deletion.

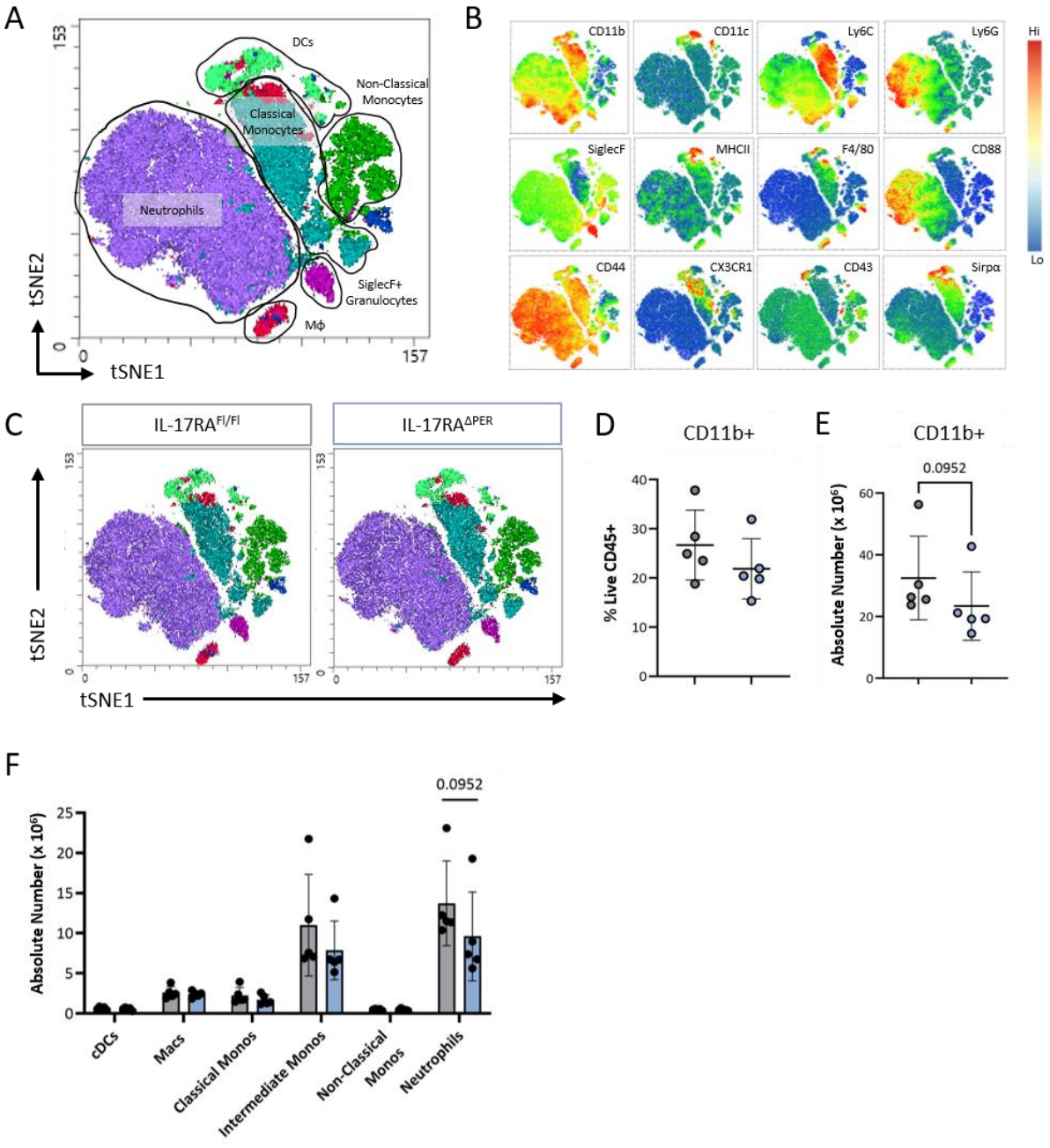

Figure 31: Pericyte IL-17RA signaling recruits neutrophils to the spleen during EAE. Analysis of the splenic myeloid compartment from MOG_{35-55}-immunized mice at active EAE day 10 was performed using multi-dimensional flow cytometry. Living non-lymphocytes ($CD19^-$ $CD3^-$) were randomly sampled with 13,500 cells taken per sample. (**A**) Exemplary annotation of data presented as a 2D t-SNE graph manually annotated according to relative marker expression shown in (**B**). (**C**) Comparison of t-SNE plots between conditions. Myeloid cells were quantified as (**D**) percentage of live $CD45^+$ leukocytes and (**E**) absolute numbers per spleen. (**F**) Absolute numbers of individual myeloid subsets were quantified by manually gating according to surface marker expression (cDCs: $CD11c^+MHCII^+$; Macs: $F4/80^+MHCII^+$; classical monocytes: $Ly6C^{hi}CD43^-$; intermediate monocytes: $Ly6C^{int}CD43^{int}$; non-classical monocytes: $Ly6C^{lo}CD43^{hi}$; neutrophils: $Ly6G^+$. All data from one experiment with n = 5 per group. Data shown in (D-F) is shown as mean +/- SD. P-values shown from analysis performed using student's t-test comparing knockouts and controls.

4 Discussion

The cytokine IL-17 is strongly associated to disease progression in human MS and its animal model, EAE.[112,239,240] *In vitro* research suggests that IL-17 contributes to BBB permeability by weakening tight junction molecules.[147,148] *In vivo* studies implicate IL-17's involvement across all disease stages, both in the CNS and peripheral tissues. Proposed functions range from the priming of pathogenic T cells, to proliferation of splenic fibroblasts, as well as late-stage cognitive defects in the hippocampus.[119,133,150] Our lab previously demonstrated that IL-17 influences EAE development by modulating intestinal microbiome homeostasis.[152] The aim of this project was to conduct temporal and organ-specific analyses to elucidate the cellular dynamics during EAE in the absence of IL-17 and its microbiome-mediated regulation.

Most previous studies on IL-17's role during EAE have used animals with genetic deletion of IL-17A alone. To limit potential compensatory effects of IL-17F, mice lacking both IL-17A and IL-17F were used in this project to abrogate all cytokine signaling to the IL-17RA-IL-17RC receptor complex during EAE. Deletion of IL-17 decreased the incidence of EAE to about half and CNS inflammatory infiltrates were significantly reduced. In the periphery, the absence of IL-17 was redundant for the priming and pathogenicity of $CD4^+$ T cells during EAE. Not only were IL-$17^{-/-}$ T cells identical to controls in number, activation status, and cytokine production, but these cells also retained the potential to adoptively transfer EAE to wild-type recipients. However, peripheral myeloid subsets, particularly neutrophils and monocytes, showed an altered abundance and phenotype in IL-$17^{-/-}$ mice. Decreased splenic myeloid abundance was also observed upon pericyte-specific deletion of IL-17RA.

Together, the data suggests that IL-17 provides critical signals to pericytes to recruit myeloid cells. Additionally, IL-17 may regulate myeloid maturity and pathogenicity, as the absence of IL-17 correlated with an increased proportion of phenotypically suppressive myeloid cells. Finally, the IL-17-regulated microbiome, was observed to have only modest synergistic effects with IL-17-deletion. The housing conditions of IL-$17^{-/-}$ mice, while influencing disease incidence, produced few differences at the level of gene and protein expression and abundance

of leukocytes, hinting at the microbiome's involvement in other organs or through alternative mechanisms.

1. IL-17 is redundant for CD4$^+$ T cell pathogenicity during EAE

The necessity of IL-17 from CD4$^+$ T cells for the induction of EAE is contested, and the research in some cases, contradictory. In some adoptive transfer studies, IL-17$^{-/-}$ CD4$^+$ T cells have been shown to effectively transfer disease,[112] while in others they do not.[152,265] Other research suggests that IL-17 expression may actually mark a stem-like CD4$^+$ T cell that has not yet developed pathogenic characteristics.[75] Yet in MS and during EAE, CD4$^+$ Th17 cells are the largest producers of IL-17 in the inflamed CNS and LNs.[112,239,266]

In this project, we observed a reduced number of MOG-specific T cells in the spinal cords of IL-17$^{-/-}$ mice after active MOG$_{35-55}$-EAE immunization. Among these T cells, there was an increased proportion of cytokine-producing cells, possibly attributed to IL-17's observed role in negative regulation of CD4$^+$ T cells via autocrine IL-17RA signaling.[267,268] This data suggests that the lower incidence of EAE in IL-17$^{-/-}$ mice may result from fewer T cells, rather than a lack in functionality of those cells. We hypothesized that IL-17 plays an earlier role in the periphery to promote the development of CNS-infiltrating pathogenic T cells. Analysis of MOG-specific CD4$^+$ T cells in SLOs was performed at priming (day 5) and pre-onset (day 10) stages of EAE. At both time points, IL-17$^{-/-}$ T cells were found in similar numbers to controls and produced comparable levels of the pro-inflammatory cytokines GM-CSF and IFNγ in the LNs, and even increased levels in the spleen. This data contradicts a previous finding showing that IL-17A is required for the priming of pathogenic T cells in the lymph nodes during active EAE development.[133] Single-cell RNA sequencing analysis of splenic CD4$^+$ T cells at pre-onset showed only two differentially expressed genes in IL-17^{Cohoused} CD4$^+$ T cells compared to controls: the blood coagulation factor *F13a1* and a glycosyltransferase linked to pro-tumor activity, *St8sia6*, neither of which might explain a decrease in EAE incidence among IL-17-deficient mice.[269] This data supports the hypothesis that during early stages of active EAE, IL-17 is redundant for the priming and expansion of peripheral CD4$^+$ T cells. Further, IL-17-deficient T cells are not transcriptionally different from controls, indicating a redundancy of IL-17 for their pathogenicity in the periphery.

Various adoptive transfer (AT) experiments were additionally performed to test whether IL-17 from T cells is required for their pathogenic functionality. IL-17$^{-/-}$ CD4^{+} T cells induced EAE in recipient mice whether transferred among other splenocytes or as a purified CD4^{+} suspension, though disease severity varied between experiments. Several reasons may exist for the inhibition of active EAE in IL-17$^{-/-}$ mice and promotion of AT-EAE by IL-17$^{-/-}$ T cells. First, AT-EAE is shown to occur independently of SLOs, such as the spleen and LNs, and is dependent largely on the reactivation of transferred cells in the CNS by MHCII^{+} APCs.[57] During active EAE, IL-17$^{-/-}$ T cells may have a reduced ability to exit SLOs and migrate towards the CNS—a factor irrelevant in AT-EAE. This hypothesis is supported by the unchanged CD4^{+} T cell count in the IL-17$^{-/-}$ spleen and their reduced presence in the dural meninges at EAE onset. Additionally, increased suppressive myeloid cells in the periphery may inhibit IL-17$^{-/-}$ T cells during active EAE, but not necessarily at the CNS during AT-EAE. Suppressive myeloid cells have been shown to accumulate in the spleen, an organ largely redundant in AT-EAE.[224]

Despite the ability of IL-17$^{-/-}$ transferred cells to induce disease in wild-type hosts in the AT-EAE model, disease severity was lower compared to control T cell transfers. Increased IL-17 from circulating CD4^{+} T cells is positively associated with MS severity.[266] Serum IL-17 levels were comparable between recipients of IL-17$^{-/-}$ and control CD4^{+} T cells, ruling out circulating IL-17 as a factor affecting AT-EAE severity. Comparable levels of circulating IL-17 also indicate that adoptive transfer of IL-17$^{-/-}$ T cells does not limit recipient mice from producing IL-17 from other sources, such as ILCs, iNKT, or γδ-T cells.[132,270]

Decreased AT-EAE disease severity may occur due to two reasons: suppression of the transferred cells *in vitro* by MDSCs present in the culture prior to transfer or decreased strength of reactivation. Our data supports the hypothesis that IL-17$^{-/-}$ mice have an increased presence of peripheral suppressive myeloid cells upon active EAE immunization, which could inhibit CD4^{+} T cell activity prior to adoptive transfer during the four-day Th17 culture. CD4^{+} splenocyte cultures taken from active EAE-immunized mice, regardless of genotype, showed reduced blasting cells after 4-day Th17 culture when co-cultured with IL-17$^{-/-}$ APCs. During AT-EAE, IL-17$^{-/-}$ mice receiving control Th17 cells developed disease similarly to control mice, suggesting that the rapid, CNS-specific disease progression of AT-EAE may make peripheral

MDSCs irrelevant in this model. To eliminate a potential effect of suppressive IL-17$^{-/-}$ APCs, future experiments might use an adoptive transfer protocol in which CD4^{+} T cells are directly isolated, purified, and cultured without the presence of myeloid cells.

T cell reactivation by CNS-resident APCs is a critical determinant of later disease severity, as strongly reactivated T cells produce higher levels of chemokines, leading to increased leukocyte migration to the CNS.[73,271] Weaker reactivation may result from either a reduced T cell presence at the CNS or diminished interactions between T cells and APCs. Earlier research documents the highest numbers of IL-17^{+} CD4^{+} T cells are observed just before active EAE onset in the CNS, adding evidence to support a possible role for IL-17 in reactivation.[76] Our data shows that less than half of the number of IL-17$^{-/-}$ CD4^{+} T cells enter the CNS than controls after adoptive transfer, supporting the hypothesis that fewer T cells reach the CNS without IL-17 expression. Additionally, IL-17 production was limited to transferred T cells, with about a third of transferred control T cells producing IL-17 at the peak of analysis. Host CD4^{+} T cells, recruited to the CNS in the so-called "second wave", produced no IL-17 in our model. Unfortunately, no myeloid analysis of the CNS was performed to investigate whether fewer myeloid cells were recruited to the CNS, which would provide additional evidence for weakened reactivation by IL-17$^{-/-}$ T cells. It is important to note that this experiment was performed once and results must be confirmed. If reproduced, future experiments such as flow cytometry and imaging of the SAS at time points of reactivation (i.e. 1-2 days after adoptive transfer) could clarify both the number of transferred cells reaching the CNS and how many of them engage directly with MHCII^{+} APCs.[70,272] Additionally, the target cells of IL-17 signaling during reactivation signaling should be clarified. Preliminary, unpublished data from our lab suggests that IL-17RA deletion on microglia, astrocytes, endothelial cells, and myeloid cells does not affect the outcome of active EAE, though adoptive transfer experiments were never performed in these mice. Additionally, IL-17 signaling to pericytes does not appear to play a detrimental role at the reactivation stage, as data from this thesis shows that IL-17RA deletion on pericytes produces a slightly more severe EAE.

In summary, this data supports the hypothesis that IL-17$^{-/-}$ T cells retain their pathogenicity in both active and adoptive transfer models of EAE, although reduced CD4^{+} T cell numbers in the CNS improves disease outcomes in the latter. Further investigation is needed to understand

why $CD4^+$ T cells are reduced in the CNS post-adoptive transfer, potentially owing to weakened reactivation within the CNS or suppression prior to transfer in the Th17 culture conditions.

2. The role of IL-17 in lymphocyte migration

Inhibition of lymphocyte migration to the CNS prevents the development of neuroinflammation, as seen by the efficacy of DMTs such as fingolimod and natalizumab.[48,91] Compared to controls, IL-$17^{-/-}$ $CD4^+$ T cells were similar in number in the spleen, but reduced in the dural meninges and CNS parenchyma during active EAE. No differences in mRNA expression nor protein expression of the CNS-homing chemokine receptor CCR6 was observed to suggest a migratory deficit in IL-$17^{-/-}$ T cells.[72,85,86] We hypothesized that IL-17 may be involved in CNS-directed T cell migration through regulation of other peripheral mechanisms.

To test whether IL-17 from $CD4^+$ T cells is necessary for their migration from SLOs, lymphopenic $Rag^{-/-}$ mice were reconstituted with $CD4^+$ T cells, allowing for lymphocyte settlement and expansion in peripheral tissues and SLOs. Active EAE immunization resulted in similar clinical scores between groups, indicating that IL-17 signaling from $CD4^+$ T cells is not required for their exit from SLOs and migration into the CNS during EAE. This does not rule out, however, the presence of IL-17 from other innate sources in $Rag^{-/-}$ mice, such as ILCs or γδ-T cells.[132,133] Single-cell sequencing results from lympho-competent mice revealed higher IL-17 mRNA levels in other spleen cell subsets, including iNKT cells and ILC3s, which, if also true in $Rag1^{-/-}$ mice, could compensate for the absence of CD4-derived IL-17.

As IL-17 from $CD4^+$ T cells was redundant for their migration, we hypothesized that other molecules involved in T cell migration may be altered by IL-17 deletion, such as S1P levels or expression of chemokines or adhesion molecules. S1P levels in the blood and CCR7 expression in the spleen were comparable between all groups during active EAE, indicating no changes in leukocyte egress versus retention signals. Protein expression of the adhesion molecules ICAM-1, ICAM-2, PECAM, and VCAM-1 were unchanged on IL-$17^{-/-}$ brain endothelial cells during EAE. This contradicts a previous study implicating IL-17 in the breakdown of the BBB via ICAM-1 upregulation.[147] It is important to note that prior studies implicating IL-17's involvement in BBB disruption were conducted *in vitro* with IL-17 protein concentrations

200-2000 times higher than the biological levels at the peak of EAE, potentially limiting their *in vivo* relevance.[147,148] More comprehensive analyses, such as single-cell RNA sequencing or proteomics of IL-17-deficient endothelial, perivascular, and glial cells, may provide a better understanding of the cell-type specific molecular changes occurring at the BBB.

Whole tissue RT-PCR analysis revealed reduced mRNA expression of neutrophil-derived MMP9 in the spleen and MMP2 in the brain. MMP2 and MMP9 regulate neuroinflammation through ECM reorganization, degradation of BBB tight junctions, and synergize to potentiate the effects of cytokine-induced chemokine expression, including CXCL8 and CXCL6.[273,274] Mice deficient for MMP2 and MMP9 are fully resistant against EAE development.[275] Decreases of MMPs should be confirmed with protein expression analysis, however, the reduction of MMP mRNA levels, along with globally reduced neutrophil numbers in IL-17$^{-/-}$ mice, suggests that neutrophil-mediated extracellular remodeling processes that facilitate leukocyte migration out of the splenic veins in the red pulp may be altered in the CNS and periphery of IL-17$^{-/-}$ mice.

3. IL-17-deficiency correlates with altered neutrophil maturity in immunoregulatory hubs

During steady-state, IL-17 maintains mucosal homeostasis and responses to pathogens by signaling to epithelial and stromal cells to induce the production of neutrophil-recruiting chemokines, such as CXCL-1 and CXCL-8.[242] IL-17's role in neutrophil recruitment during infection, cancer, and tissue injury is researched extensively, yet whether the same mechanisms are employed to exacerbate autoimmune neuroinflammation is a novel field.[119] In experimental autoimmune prostatitis, IL-17 was shown to recruit neutrophils in a CXCL-1/CXCL-2-dependent manner to promote autoimmunity in this model.[276] To our knowledge, the only study to link IL-17's pathogenicity during EAE to a neutrophil recruiting role emphasized a critical time window during the priming stage until DPI 5, which is inconsistent with our findings showing that IL-17 deficiency does not affect T cell priming in the periphery.[133] Our results indicate that neutrophils are globally reduced in number in IL-17$^{-/-}$ mice, including spleen, blood, liver, colon, and lymph nodes during pre-onset of EAE, and the meninges and CNS parenchyma at peak of EAE. In the pre-onset stage of EAE, Th17 cells expand in all peripheral organs before

chemokine-dependent migration towards the CNS.[76,174,277] Global IL-17-deficiency likely results in a full-body phenomenon of reduced neutrophil-recruiting abilities of T cells.

Additionally, neutrophils are phenotypically altered in peripheral organs of IL-17$^{-/-}$ mice. Initial flow cytometry results revealed that neutrophils (gated as the total Ly6G^{+} population) in the IL-17$^{-/-}$ spleen expressed higher Ly6G, CD88, and CD11b. A study investigating neutrophils in the spleen during *S. pneumoniae* infection observed that expression of Ly6G and CD11b positively correlated to neutrophil maturity and effector functioning.[200] It was unclear whether similar phenotypical and functional conclusions could be drawn between disease models. To investigate this, single-cell transcriptomics was performed to phenotype neutrophils in the splenic IL-17$^{-/-}$ environment. Unsupervised clustering of single-cell sequencing data revealed four subsets of neutrophils in the spleen during pre-onset of EAE with gene expression related to increasing stages of maturity. Both the number of neutrophil subsets and their core gene expression signatures aligned with results of previous publications investigating neutrophil signatures in the bone marrow, blood, and spleen.[191,199,224] Single-cell sequencing results confirmed the observations from flow cytometry. IL-17$^{-/-}$ mice had significant decreases in the three most immature neutrophil subsets, including progenitor-like, proliferating, and immature neutrophils. Mature neutrophils were unchanged in IL-17$^{-/-}$ mice, suggesting a role for IL-17 in either the recruitment of developing neutrophil subsets from the bone marrow or their peripheral maturation during inflammation-induced emergency granulopoiesis. Why mature neutrophils were unaffected in number in IL-17$^{-/-}$ is unclear. Mature neutrophils may be more resistant to apoptosis or represent a "marginated" pool that maintain residency, mature locally rather than in the bone marrow, or have a longer lifespan than immature subsets, though this would need to be investigated with fate mapping and kinetics experiments.

Flow cytometry analysis revealed that shifts in neutrophil surface marker expression varied between the periphery and CNS. While splenic neutrophils were observed to have a shift towards higher Ly6G, CD88, and CD11b expression to suggest maturity, neutrophils in the dura at peak of EAE expressed less Ly6G, CD88, and CD11b. This may suggest that more immature neutrophils are present in the IL-17$^{-/-}$ dural meninges. Preliminary RT-PCR data showed that IL-17$^{-/-}$ mice have a significant reduction of MMP9 transcripts in the spleen, but reduced MMP2 transcripts in the brain, also providing evidence for differences in neutrophil functioning

between the CNS and periphery. While these observations must be confirmed, our data suggests that phenotypic, and likely, functional differences exist between splenic and meningeal neutrophils in IL-17$^{-/-}$ mice during EAE.

4. Transcriptomic analysis of IL-17$^{-/-}$ neutrophils

Upon reaching maturity, neutrophils acquire various effector functions such as granule and NET release, production of ROS and ECM remodeling proteins, phagocytosis, and antigen-presentation.[40,259] Correspondingly, in our dataset, later-stage neutrophils, defined as immature and mature, have the highest gene expression related to these effector functions. Immature neutrophils expressed genes related to degranulation, angiogenesis, tissue migration, and ROS production, while mature neutrophils had expression patterns related to innate immune signaling, cell adhesion, chemotaxis, and T cell activation. Reduced immature neutrophils in IL-17$^{-/-}$ spleens provides evidence for a shift in the effector functions of neutrophils at the pre-onset of EAE.

Contrast comparison of splenic neutrophils from IL-17^{Cohoused} versus controls shows that all neutrophil subsets, irrespective of maturity, have differential transcriptomes related to neutrophil effector functions. Both IL-17$^{-/-}$ immature and mature neutrophils have decreased gene expression related to cell activation, such as *Il4ra* in mature neutrophils and *Tnfsf13b*, *Ctsc*, *Cd38*, and *Csf2rb* in immature neutrophils.[259] As neutrophil activation is a prerequisite for effector function, decreased activation signatures in immature and mature neutrophils implicates deficiencies in their effector functions. This hypothesis is supported by the downregulation of genes involved in NETosis and angiogenesis in our data. Immature neutrophils from IL-17^{Cohoused} mice showed downregulation of genes encoding cathepsins (*Ctsb, Ctsc,* and *Ctsd*), which engage in proteolytic cleavage of histone modifying proteins that critically regulate NETosis.[278] Furthermore, across maturation states, IL-17$^{-/-}$ neutrophils show several DEGs related to regulation of angiogenesis and vascular tone (*Jaml*, *Lipg*, *Lrg1*, *Prok2*, *Thbs1, Vcam1*).[278–280] The protokineticin *Prok2*, downregulated in both immature and mature neutrophils, is documented to regulate biological functions such as neurogenesis, angiogenesis, and neutrophil migration in response to G-CSF.[281] The co-dysregulation of NETosis and angiogenesis is noteworthy, as these processes often occur hand-in-hand during

inflammation. NETs signal to endothelial cells to regulate angiogenesis, tissue damage, and vascular tone and, when dysregulated, contribute to conditions such as thrombosis, fibrosis, atherosclerosis, stroke, and hypertension.[204,208] In a mouse model of Alzheimer's disease, neutrophils were observed to release both NETs and IL-17 in meningeal vessels.[282] Vascular tone is a critical regulator of leukocyte migration into and out of tissues and alterations in the vasculature could both explain lymphocyte accumulation in the spleen, decreased leukocytes in the CNS, and the resulting decreased EAE incidence in IL-17$^{-/-}$ mice.

In summary, IL-17$^{-/-}$ neutrophils exhibit DEG patterns related to effector functioning across stages of maturity. The expression of genes related to NET production is particularly noteworthy, as NETs play roles in tissue remodeling, angiogenesis, and leukocyte recruitment. Investigating ROS production may be predictive of altered effector functioning, since ROS is essential for NET production.[203] Immunocytochemical staining for NET markers, such as NE or citrullinated histones, could provide further evidence for dysregulated NETosis. Additionally, stimulating endothelial cells *in vitro* with supernatants or NETs from IL-17$^{-/-}$ neutrophil cultures could yield insights into the potential impact of IL-17$^{-/-}$ NET production on vascular remodeling.

5. IL-17 limits the development of MDSCs during EAE

Myeloid-derived suppressor cells (MDSCs) potently suppress T cell activity to reduce T cell-mediated autoimmune inflammation.[187,219] These cells have been previously described as having decreased phagocytotic ability and increased resistance to apoptosis.[283] Preliminary data from this thesis supports the hypothesis that IL-17$^{-/-}$ mice have more peripheral MDSCs that reduce EAE incidence. Cell blasting, a marker of activation, was reduced upon *ex vivo* culture of IL-17$^{-/-}$ splenocytes under Th17 conditions. This effect was dependent on IL-17$^{-/-}$ myeloid cells, as IL-17$^{-/-}$ CD4^{+} T cells did not affect the blasting composition of cells when cultured with IL-17-sufficient myeloid cells, despite increased IFNγ production that is shown to enhance MDSC functions.[284]

Flow cytometry analysis of IL-17$^{-/-}$ myeloid cells revealed reduced neutrophil numbers and increased expression of maturity markers, such as Ly6G, CD11b, and CD88. Single-cell RNA sequencing analysis of neutrophils identified four clusters ranging in maturity from early to

late-stages based off of gene transcription signatures.[191] While IL-17$^{-/-}$ mice showed decreased numbers of progenitor, proliferating, and immature neutrophils, mature neutrophils remained unaffected, confirming the shift in maturation observed via flow cytometry. Notably, mature neutrophils expressed the highest levels of previously reported MDSC marker genes, such as *Il1b*, *Wfdc17*, *Clec4d*, *Ctsd*, and *Jaml*.[224] Our dataset indicated that mature neutrophils also highly expressed *Sirb1b, Sirpb1c, Clec7a, and Ccr6* transcripts, suggesting their potential as novel biomarkers of MDSCs during EAE.

Comparative analysis of DEGs between IL-17$^{-/-}$ mice and controls revealed that mature IL-17$^{-/-}$ neutrophils express higher levels of *Thbs1*, a glycoprotein linked to suppressive functioning and vasodilation by perivascular neutrophils in hepatocellular carcinoma.[279,285] The polarization of IL-17$^{-/-}$ neutrophils towards a MDSC phenotype may begin during early maturation. Proliferating and immature IL-17$^{-/-}$ neutrophils showed reduced expression of *Emilin2*, an angiogenic factor inversely correlated with MDSC presence in a colorectal cancer model.[286] Why neutrophils with mature signatures persist in IL-17$^{-/-}$ mice despite decreased progenitors and immature cells remains unclear. MDSCs are known to be anti-proliferative and resistant to apoptosis, which likely contribute to an extended lifespan.[283] Additionally, MDSCs may represent a "marginated" pool of neutrophils that do not reenter circulation, are long-lived, and unaffected by IL-17 deletion.[197] Mature IL-17$^{-/-}$ neutrophils may adopt gene expression patterns promoting longevity, as seen by upregulation of *Airn*, an inhibitor of the insulin-like growth factor receptor 2 (*Igf2r*), linked to neutrophil accumulation and persistence in allergic inflammation.[287]

In conclusion, the preservation of mature neutrophils with MDSC signatures and reduction of immature effector subsets in IL-17$^{-/-}$ mice indicate a shift towards a more suppressive neutrophil profile and ameliorated disease. It remains to be determined whether MDSCs represent a fully mature population. While MDSCs have been previously classified an "immature" population, other studies indicate overlaps in gene expression between MDSCs and mature neutrophils, including *Il1b* and *Wfdc17*.[191,218,224] Single-cell trajectory analysis using algorithms like Monocle could provide insights into the development of neutrophil subsets during EAE, clarify whether MDSCs are truly mature cells, and identify defining markers and transcription factors for MDSC development. Further exploration of the kinetics and

functionality of mature neutrophils could include fate-mapping experiments and assessments of NETosis, ROS and T cell suppression. Additionally, metabolomics could reveal IL-17-dependent changes toward a MDSC metabolic profile, seen by increased glycolysis, fatty acid oxidation, and lipid metabolism.[288]

6. Role of the IL-17-dependent microbiome

Recent research has highlighted the role played by the host microbiome and its metabolic products in the development and homeostasis of the innate and adaptive immune systems.[159–161] During autoimmune neuroinflammation, the microbiome has been shown to influence T cell reprogramming, microglial function, and modulate the immune response through afferent ENS signaling.[163,180,185] This thesis is an extension of our lab's previously published work, which showed that the microbiome of IL-17$^{-/-}$ mice under different housing conditions translates to different EAE outcomes.[152] In Regen et al. 2021, the fecal microbiome of IL-17$^{-/-}$ mice was shown to contain higher levels of gram-positive LPS-producing bacteria, such as *Firmicutes*, *Erysipelotrichaceae*, *Clostridiales* and *Ruminococcus*, as well as segmented filamentous bacteria (SFB) that permeate the intestinal barrier.[152] In this study, IL-17$^{-/-}$ mice cohoused with controls (IL-17^{Cohoused}) displayed an "intermediate" microbiome profile between controls and IL-17$^{-/-}$ mice housed separately (IL-17^{Separate}) from controls. To delineate the distinct effects of IL-17 deletion and the microbiome, these three groups were used as a comparison in this study.

Fewer IL-17$^{-/-}$ mice developed disease than controls, but this effect was strongest when IL-17$^{-/-}$ mice were housed separately from controls after weaning, aligning with the previous findings.[152] However, no statistical significance was reached between housing conditions and the incidence reduction between groups was modest (approximately 10% difference). Consistent with disease incidence, IL-17^{Separate} mice had fewer CD4^{+} T cells and myeloid cells within the CNS compared to IL-17^{Cohoused} mice. However, no differences were observed in the spleen, where CD4^{+} MOG-specific T cells and myeloid cell numbers were similar between housing conditions. Additionally, Treg numbers did not vary by housing condition to suggest a polarization towards more suppressive T cells. Finally, transcriptomic analysis of CD4^{+} T cells revealed minimal differences in gene expression, implying that the microbiome plays no role in splenic T cell reprogramming within our model.

No effects on neutrophil numbers were observed between housing conditions to suggest that the microbiome synergizes with IL-17 functions. This indicates a unique function of the microbiome, which may be difficult to pinpoint. In the original publication, IL-17^{Cohoused} mice have an intermediate microbiome between IL-17^{Separate} and controls.[152] While the microbiomes between IL-17^{Cohoused} mice and controls were significantly different, no statistical significance was observed between separate and cohoused knockout microbiomes in the original publication.[152] It is likely that the microbiome-dependent effect observed in IL-17^{Separate} mice is also present in IL-17^{Cohoused} mice, making the effect of the microbiome and cytokine deletion difficult to quantify and even more difficult to separate from each other.

The modest changes to the microbiome between housing conditions may be reflected by CNS-resident cell homeostasis, a topic not addressed in this thesis. This may occur indirectly through signaling of microbial products to bile acid receptors on astrocytes and microglia in the white matter or directly by stimulating intestinal sympathetic nerve fibers.[157,182] Studies have indicated that the microbiome can affect microglial homeostasis and inflammatory responses by polarizing microglia toward a type-I immune response, effectively weakening their response to type-II inflammation in the EAE model.[179,180] Microglia are crucial producers of chemokines after T cell reactivation and play a key role in demyelination of neurons. RNA sequencing analysis of microglia during pre- and post-clinical EAE stages may reveal whether similar effects are present in our model. The microbiome also signals directly to vagal nerve fibers and indirectly by promoting acetylcholine-synthesizing T cells in the gut.[185] Both vagotomy and vagus nerve stimulation has been shown to reduce EAE severity.[183,184] Although the field of ENS-driven autoimmune research is still emerging and the regulatory signals for pro- versus anti-inflammatory effects are unknown, an analysis of intestinal metabolites—particularly neuropeptides and neurotransmitters—could provide initial clues about changes in ENS-signaling mediators between housing conditions. While splenic T cells remain unchanged across housing conditions, the possibility that intestinal T cells signaling to the ENS are altered cannot be dismissed. Sequencing analysis of intestinal T cells during pre-onset stages of EAE could provide insights into whether microbiome-dependent T cell regulation is gut-specific.

7. IL-17 signals to pericytes to recruit neutrophils and promote EAE development

Pericytes are cells of mesodermal origin that critically regulate the stability and integrity of blood vessels in both the CNS and periphery.[289] In this context, pericytes not only provide structural support for endothelial cells, but also regulate blood vessel permeability and contractility, participate in the local immune response by acting as antigen-presenting cells (APCs), secrete cytokines and other inflammatory mediators, and regulate leukocyte migration by modulating the expression of tight junctions and adhesion molecules.[263] In the periphery, pericytes may also have additional functions in tissue repair, fibrogenesis, and angiogenesis.[290] Th17 cells have long been considered to act on the BBB via the production of IL-17, but evidence supporting the action of endothelial cells is weak and often primary cell isolation methods do not discriminate between endothelial and perivascular cells.[147,148] A study comparing human endothelial cells to pericytes demonstrated that not only do pericytes express higher levels of IL-17RA, but that IL-17 acts on pericytes, rather than endothelial cells, to produce inflammatory cytokines such as IL-6, TNF, and IL-1β, and CXCL-8.[262] To date, no data have been published showing whether IL-17 signaling in pericytes plays a role during EAE.

To investigate whether IL-17 signaling to pericytes plays a role during EAE, the pericyte-specific PDGFRβ-Cre^{ERT2} mouse line was used. PDGFRβ is expressed on perivascular cells, including primarily pericytes and some subsets of fibroblasts and smooth muscle cells lining the abluminal side of capillaries and postcapillary venules.[249,264] This thesis has shown that IL-17 signals to its receptor on PDGFRβ^{+} pericytes to promote autoimmune neuroinflammation in the MOG_{35-55}-EAE model, potentially through the recruitment of neutrophils. Similar to IL-17$^{-/-}$ mice, reduced neutrophils were most strongly observed in the spleen. Within the spleen, PDGFRβ-expressing cells are mainly located in the red pulp. The splenic red pulp supports hematological functions such as the filtration of red blood cells and platelets, fetal erythropoiesis, and extravasation of leukocytes into the blood stream via the splenic vein.[291] Neutrophils critically regulate leukocyte migration through the production of NETs and ECM-remodeling factors including metalloproteinases (MMPs), fibronectins, collagenases, and the gelatinases MMP2 and MMP9.[208,256]

IL-17 signaling to PDGFRβ-expressing perivascular cells may regulate EAE development through the recruitment of neutrophils with tissue remodeling or angiogenic properties that restructure tissues to accommodate the efflux and influx of migrating leukocytes. Some data from this thesis already support this hypothesis, including decreased mRNA levels of the gelatinases MMP2 and MMP9 in the spleen and brain of IL-17$^{-/-}$ mice, respectively. However, the expression of NETs and other remodeling factors should also be investigated to determine the precise involvement of these factors. To our knowledge, no *in vivo* cellular target of IL-17 has been discovered thus far to explain the cytokine's disease promotion in the EAE context. Further studies are needed to confirm pericytes as a cellular target of IL-17 during neuroinflammation. Identification of a cellular target of IL-17 could lead to more precision therapies for MS treatment if confirmed in human tissues.

5 Summary

Interleukin-17 (IL-17) is a pro-inflammatory cytokine that signals in tissues throughout the body to coordinate microbial homeostasis, host pathogen responses, and tissue repair. Increased IL-17 is associated with several autoimmune diseases, including multiple sclerosis (MS) and its animal model experimental autoimmune encephalomyelitis (EAE). We found that global deletion of IL-17 leads to a reduction in EAE incidence and reduced leukocyte infiltration into the central nervous system (CNS). This effect was partially mediated by the microbiome, with knockout mice housed separately from controls having an even greater EAE resistance and lower CNS leukocyte infiltration. While the priming, expansion, and pathogenicity of CD4+ T cells were unaffected, peripheral myeloid cells, particularly neutrophils, were decreased in IL-17-deficient mice but unaffected by housing conditions. In the spleen, neutrophils also exhibited differences in maturation state, with IL-17-deficient mice having less immature neutrophils but unaffected numbers of mature neutrophils with gene expression patterns resembling myeloid-derived suppressor cells (MDSCs). Variation in the maturation state of neutrophils was additionally observed in the dural meninges of IL-17-deficient mice. The recruitment of neutrophils, but not the maturation, were mediated through IL-17RA signaling on perivascular cells. Mice lacking IL-17RA on perivascular cells (IL-17RA$^{\Delta PER}$) had decreased splenic neutrophils, but no differences in expression of surface markers to indicate changes in neutrophil phenotypes. Outside of the CNS, no differences in any leukocyte populations were observed upon separate housing conditions. Our findings indicate that IL-17 signaling plays a critical role in the recruitment and maturation of neutrophils with inflammatory and suppressive phenotypes during EAE.

6 Zusammenfassung

Interleukin-17 (IL-17) ist ein proinflammatorisches Zytokin, das in Geweben im ganzen Körper als Botenstoff dient, um die mikrobielle Homöostase, die Reaktion des Wirts auf Krankheitserreger und die Gewebereparatur zu koordinieren. Eine erhöhte IL-17-Konzentration wird mit mehreren Autoimmunkrankheiten in Verbindung gebracht, darunter die Multiple Sklerose (MS) und ihr Tiermodell, die Experimentelle Autoimmune-Enzephalomyelitis (EAE). Wir haben gezeigt, dass die globale Deletion von IL-17 zu einer Verringerung der EAE-Inzidenz und einer geringeren Leukozyten-Infiltration in das zentrale Nervensystem (ZNS) führt. Dieser Effekt wurde teilweise durch das Mikrobiom vermittelt, denn IL-17-Knockout-Mäuse, die getrennt von Kontrolltieren aufwuchsen, wiesen eine noch höhere EAE-Resistenz und eine geringere Leukozyten-Infiltration in das ZNS auf. Das Priming, die Expansion und die Pathogenität von $CD4^+$ T-Zellen waren nicht beeinträchtigt. Hingegen wurde die Anzahl peripherer myeloider Zellen, insbesondere neutrophiler Granulozyten, durch die IL-17-Deletion verringert, aber nicht durch die Haltungsbedingungen beeinflusst. In der Milz wiesen die Neutrophilen auch Unterschiede in ihrem Reifestadium auf, mit weniger unreifen Neutrophilen, aber einer unveränderten Anzahl reifer Neutrophiler, in IL-17-defizienten Mäusen. Die reifen Neutrophilen zeigten Genexpressionsmuster, die myeloiden Suppressorzellen (MDSCs) ähneln. Variationen im Reifestadium der Neutrophilen wurden zusätzlich in der Dura mater von $IL\text{-}17^{-/-}$ Mäusen beobachtet. Es wurde zudem gezeigt, dass die Rekrutierung, nicht aber die Reifung, von Neutrophilen durch IL-17RA-Signalgebung auf perivaskulären Zellen vermittelt wird. Mäusen, denen IL-17RA auf perivaskulären Zellen fehlte ($IL\text{-}17RA^{\Delta PER}$), hatten verringerte Zahlen Neutrophiler in der Milz, aber die Neutrophilen zeigten keine Unterschiede in der Expression von Oberflächenmarkern, die auf Veränderungen des Phänotyps hingewiesen hätten. Außerhalb des ZNS wurden zwischen den verschiedenen Haltungsbedingungen keine Unterschiede in Leukozyten-Populationen festgestellt. Unsere Ergebnisse deuten darauf hin, dass der IL-17-Signalweg eine entscheidende Rolle in der Rekrutierung und möglicherweise auch der Reifung neutrophiler Granulozyten mit entzündlichen und suppressiven Phänotypen während der EAE spielt.

7 References

1. King, R. (2020). Atlas of MS 3rd Edition. https://www.msif.org/wp-content/uploads/2020/12/Atlas-3rd-Edition-Epidemiology-report-EN-updated-30-9-20.pdf

2. Baecher-Allan, C., Kaskow, B. J., & Weiner, H. L. (2018). Multiple sclerosis: Mechanisms and immunotherapy. *Neuron*, *97*(4), 742–768. https://doi.org/10.1016/j.neuron.2018.01.021

3. Charcot, J. M. (1880). Leçons Sur Les Maladies Du Système Nerveux : Faites à La Salpêtrière. vol. 1A.

4. Kuhlmann, T., Lassmann, H., & Brück, W. (2008). Diagnosis of inflammatory demyelination in biopsy specimens: a practical approach. *Acta Neuropathologica*, *115*(3), 275–287. https://doi.org/10.1007/s00401-007-0320-8

5. Lassmann, H. (2018). Multiple sclerosis pathology. *Cold Spring Harbor Perspectives in Medicine*, *8*(3), a028936. https://doi.org/10.1101/cshperspect.a028936

6. Fisniku, L. K., Chard, D. T., Jackson, J. S., Anderson, V. M., Altmann, D. R., Miszkiel, K. A., Thompson, A. J., & Miller, D. H. (2008). Gray matter atrophy is related to long-term disability in multiple sclerosis. *Annals of Neurology*, *64*(3), 247–254. https://doi.org/10.1002/ana.21423

7. Lublin, F. D., Reingold, S. C., Cohen, J. A., Cutter, G. R., Sørensen, P. S., Thompson, A. J., Wolinsky, J. S., Balcer, L. J., Banwell, B., Barkhof, F., Bebo, B., Calabresi, P. A., Clanet, M., Comi, G., Fox, R. J., Freedman, M. S., Goodman, A. D., Inglese, M., Kappos, L., … Polman, C. H. (2014). Defining the clinical course of multiple sclerosis. *Neurology*, *83*(3), 278–286. https://doi.org/10.1212/wnl.0000000000000560

8. Cree, B. A., Arnold, D. L., Chataway, J., Chitnis, T., Fox, R. J., Ramajo, A. P., Murphy, N., & Lassmann, H. (2021). Secondary progressive multiple sclerosis. *Neurology*, *97*(8), 378–388. https://doi.org/10.1212/wnl.0000000000012323.

9. Dendrou, C. A., Fugger, L., & Friese, M. A. (2015). Immunopathology of multiple sclerosis. *Nature Reviews. Immunology*, *15*(9), 545–558. https://doi.org/10.1038/nri3871

10. Filippi, M., Bar-Or, A., Piehl, F., Preziosa, P., Solari, A., Vukusic, S., & Rocca, M. A. (2018). Multiple sclerosis. *Nature Reviews Disease Primers*, *4*(1). https://doi.org/10.1038/s41572-018-0041-4

11. Moutsianas, L., Jostins, L., Beecham, A. H., Dilthey, A. T., Xifara, D. K., Ban, M., Shah, T. S., Patsopoulos, N. A., Alfredsson, L., Anderson, C. A., Attfield, K. E., Baranzini, S. E.,

Barrett, J., Binder, T. M. C., Booth, D., Buck, D., Celius, E. G., Cotsapas, C., D'Alfonso, S., … McVean, G. (2015). Class II HLA interactions modulate genetic risk for multiple sclerosis. *Nature Genetics*, *47*(10), 1107–1113. https://doi.org/10.1038/ng.3395

12. Sawcer, S., Hellenthal, G., Pirinen, M., Spencer, C. C. A., Patsopoulos, N. A., Moutsianas, L., Dilthey, A., Su, Z., Freeman, C., Hunt, S. E., Edkins, S., Gray, E., Booth, D. R., Potter, S. C., Goris, A., Band, G., Oturai, A. B., Strange, A., Saarela, J., … Compston, A. (2011). Genetic risk and a primary role for cell-mediated immune mechanisms in multiple sclerosis. *Nature*, *476*(7359), 214–219. https://doi.org/10.1038/nature10251

13. Ascherio, A., & Munger, K. L. (2007). Environmental risk factors for multiple sclerosis. Part I: The role of infection. *Annals of Neurology*, *61*(4), 288–299. https://doi.org/10.1002/ana.21117

14. Munger, K., Levin, L., O'Reilly, E., Falk, K., & Ascherio, A. (2011). Anti-Epstein–Barr virus antibodies as serological markers of multiple sclerosis: a prospective study among United States military personnel. *Multiple Sclerosis Journal*, *17*(10), 1185–1193. https://doi.org/10.1177/1352458511408991

15. Bjornevik, K., Cortese, M., Healy, B. C., Kuhle, J., Mina, M. J., Leng, Y., Elledge, S. J., Niebuhr, D. W., Scher, A. I., Munger, K. L., & Ascherio, A. (2022). Longitudinal analysis reveals high prevalence of Epstein-Barr virus associated with multiple sclerosis. *Science*, *375*(6578), 296–301. https://doi.org/10.1126/science.abj8222

16. Levin, L. I., Munger, K. L., O'Reilly, E. J., Falk, K. I., & Ascherio, A. (2010). Primary infection with the Epstein-Barr virus and risk of multiple sclerosis. *Annals of Neurology*, *67*(6), 824–830. https://doi.org/10.1002/ana.21978

17. Lünemann, J. D., Jelčić, I., Roberts, S., Lutterotti, A., Tackenberg, B., Martin, R., & Münz, C. (2008). EBNA1-specific T cells from patients with multiple sclerosis cross react with myelin antigens and co-produce IFN-γ and IL-2. *The Journal of Experimental Medicine*, *205*(8), 1763–1773. https://doi.org/10.1084/jem.20072397

18. Lanz, T. V., Brewer, R. C., Ho, P. P., Moon, J., Jude, K. M., Fernandez, D., Fernandes, R. A., Gomez, A. M., Nadj, G., Bartley, C. M., Schubert, R. D., Hawes, I. A., Vazquez, S. E., Iyer, M., Zuchero, J. B., Teegen, B., Dunn, J. E., Lock, C. B., Kipp, L. B., . . . Robinson, W. H. (2022). Clonally expanded B cells in multiple sclerosis bind EBV EBNA1 and GlialCAM. *Nature*, *603*(7900), 321–327. https://doi.org/10.1038/s41586-022-04432-7

19. Munger, K. L., Levin, L. I., Hollis, B. W., Howard, N. S., & Ascherio, A. (2006). Serum 25-Hydroxyvitamin D levels and risk of multiple sclerosis. *JAMA*, *296*(23), 2832. https://doi.org/10.1001/jama.296.23.2832

20. Bove, R., & Chitnis, T. (2013). Sexual disparities in the incidence and course of MS. *Clinical Immunology*, *149*(2), 201–210. https://doi.org/10.1016/j.clim.2013.03.005

21. Maté, G., & Maté, D. (2022). *The myth of normal: Trauma, Illness & Healing in a Toxic Culture.* Random House.

22. Morgan, B. P., Gommerman, J. L., & Ramaglia, V. (2021). An "Outside-In" and "Inside-Out" Consideration of Complement in the Multiple Sclerosis Brain: Lessons From Development and Neurodegenerative Diseases. *Frontiers in Cellular Neuroscience*, *14*. https://doi.org/10.3389/fncel.2020.600656

23. Engelhardt, B., Carare, R. O., Bechmann, I., Flügel, A., Laman, J. D., & Weller, R. O. (2016). Vascular, glial, and lymphatic immune gateways of the central nervous system. *Acta Neuropathologica*, 132(3), 317–338. https://doi.org/10.1007/s00401-016-1606-5

24. Luchicchi, A., Preziosa, P., & Hart, B. (2021). Editorial: "Inside-Out" vs "Outside-In" Paradigms in Multiple Sclerosis Etiopathogenesis. *Frontiers in Cellular Neuroscience*, *15*. https://doi.org/10.3389/fncel.2021.666529

25. Astier, A. L., Meiffren, G., Freeman, S., & Hafler, D. A. (2006). Alterations in CD46-mediated Tr1 regulatory T cells in patients with multiple sclerosis. *Journal of Clinical Investigation*, *116*(12), 3252–3257. https://doi.org/10.1172/jci29251

26. Venken, K., Hellings, N., Thewissen, M., Somers, V., Hensen, K., Rummens, J., Medaer, R., Hupperts, R., & Stinissen, P. (2007). Compromised CD4+ CD25high regulatory T-cell function in patients with relapsing-remitting multiple sclerosis is correlated with a reduced frequency of FOXP3-positive cells and reduced FOXP3 expression at the single-cell level. *Immunology*, *123*(1), 79–89. https://doi.org/10.1111/j.1365-2567.2007.02690.x

27. Viglietta, V., Baecher-Allan, C., Weiner, H. L., & Hafler, D. A. (2004). Loss of Functional Suppression by CD4+CD25+ Regulatory T Cells in Patients with Multiple Sclerosis. *The Journal of Experimental Medicine*, *199*(7), 971–979. https://doi.org/10.1084/jem.20031579

28. Fletcher, J. M., Lalor, S. J., Sweeney, C. M., Tubridy, N., & Mills, K. H. G. (2010). T cells in multiple sclerosis and experimental autoimmune encephalomyelitis. *Clinical & Experimental Immunology*, *162*(1), 1–11. https://doi.org/10.1111/j.1365-2249.2010.04143.x

29. Babbe, H., Roers, A., Waisman, A., Lassmann, H., Goebels, N., Hohlfeld, R., Friese, M., Schröder, R., Deckert, M., Schmidt, S., Ravid, R., & Rajewsky, K. (2000). Clonal expansions of CD8+ T cells dominate the T cell infiltrate in active multiple sclerosis lesions as shown by micromanipulation and single cell polymerase chain reaction. *The Journal of Experimental Medicine*, *192*(3), 393–404. https://doi.org/10.1084/jem.192.3.393

30. Mars, L. T., Saikali, P., Liblau, R. S., & Arbour, N. (2010). Contribution of CD8 T lymphocytes to the immuno-pathogenesis of multiple sclerosis and its animal models. *Biochimica Et Biophysica Acta (BBA) - Molecular Basis of Disease, 1812*(2), 151–161. https://doi.org/10.1016/j.bbadis.2010.07.006

31. Margoni, M., Preziosa, P., Filippi, M., & Rocca, M. A. (2021). Anti-CD20 therapies for multiple sclerosis: current status and future perspectives. *Journal of Neurology, 269*(3), 1316–1334. https://doi.org/10.1007/s00415-021-10744-x

32. Cencioni, M. T., Mattoscio, M., Magliozzi, R., Bar-Or, A., & Muraro, P. A. (2021). B cells in multiple sclerosis — from targeted depletion to immune reconstitution therapies. *Nature Reviews Neurology, 17*(7), 399–414. https://doi.org/10.1038/s41582-021-00498-5

33. Jelcic, I., Nimer, F. A., Wang, J., Lentsch, V., Planas, R., Jelcic, I., Madjovski, A., Ruhrmann, S., Faigle, W., Frauenknecht, K., Pinilla, C., Santos, R., Hammer, C., Ortiz, Y., Opitz, L., Grönlund, H., Rogler, G., Boyman, O., Reynolds, R., … Martin, R. (2018). Memory B cells activate Brain-Homing, autoreactive CD4+ T cells in multiple sclerosis. *Cell, 175*(1), 85-100.e23. https://doi.org/10.1016/j.cell.2018.08.011

34. Duddy, M., Niino, M., Adatia, F., Hebert, S., Freedman, M., Atkins, H., Kim, H. J., & Bar-Or, A. (2007). Distinct effector cytokine profiles of memory and naive human B cell subsets and implication in multiple sclerosis. *The Journal of Immunology, 178*(10), 6092–6099. https://doi.org/10.4049/jimmunol.178.10.6092

35. Bar-Or, A., Fawaz, L., Fan, B., Darlington, P. J., Rieger, A., Ghorayeb, C., Calabresi, P. A., Waubant, E., Hauser, S. L., Zhang, J., & Smith, C. H. (2009). Abnormal B-cell cytokine responses a trigger of T-cell–mediated disease in MS? *Annals of Neurology, 67*(4), 452–461. https://doi.org/10.1002/ana.21939

36. Li, R., Rezk, A., Miyazaki, Y., Hilgenberg, E., Touil, H., Shen, P., Moore, C. S., Michel, L., Althekair, F., Rajasekharan, S., Gommerman, J. L., Prat, A., Fillatreau, S., & Bar-Or, A. (2015). Proinflammatory GM-CSF–producing B cells in multiple sclerosis and B cell depletion therapy. *Science Translational Medicine, 7*(310). https://doi.org/10.1126/scitranslmed.aab4176

37. Magliozzi, R., Howell, O. W., Nicholas, R., Cruciani, C., Castellaro, M., Romualdi, C., Rossi, S., Pitteri, M., Benedetti, M. D., Gajofatto, A., Pizzini, F. B., Montemezzi, S., Rasia, S., Capra, R., Bertoldo, A., Facchiano, F., Monaco, S., Reynolds, R., & Calabrese, M. (2018). Inflammatory intrathecal profiles and cortical damage in multiple sclerosis. *Annals of Neurology, 83*(4), 739–755. https://doi.org/10.1002/ana.25197

38. Bogie, J. F. J., Stinissen, P., & Hendriks, J. J. A. (2014). Macrophage subsets and microglia in multiple sclerosis. *Acta Neuropathologica, 128*(2), 191–213. https://doi.org/10.1007/s00401-014-1310-2

39. Rumble, J. M., Huber, A. K., Krishnamoorthy, G., Srinivasan, A., Giles, D. A., Zhang, X., Wang, L., & Segal, B. M. (2015). Neutrophil-related factors as biomarkers in EAE and MS. *The Journal of Experimental Medicine, 212*(1), 23–35. https://doi.org/10.1084/jem.20141015

40. De Bondt, M., Hellings, N., Opdenakker, G., & Struyf, S. (2020). Neutrophils: underestimated players in the pathogenesis of multiple sclerosis (MS). *International Journal of Molecular Sciences, 21*(12), 4558. https://doi.org/10.3390/ijms21124558

41. Lassmann, H. (2018b). Multiple sclerosis pathology. *Cold Spring Harbor Perspectives in Medicine, 8*(3), a028936. https://doi.org/10.1101/cshperspect.a028936

42. Lublin, F. D., & Reingold, S. C. (1996). Defining the clinical course of multiple sclerosis. *Neurology, 46*(4), 907–911. https://doi.org/10.1212/wnl.46.4.907

43. Bierhansl, L., Hartung, H., Aktas, O., Ruck, T., Roden, M., & Meuth, S. G. (2022). Thinking outside the box: non-canonical targets in multiple sclerosis. *Nature Reviews Drug Discovery, 21*(8), 578–600. https://doi.org/10.1038/s41573-022-00477-5

44. Montalban, X., Hauser, S. L., Kappos, L., Arnold, D. L., Bar-Or, A., Comi, G., De Seze, J., Giovannoni, G., Hartung, H., Hemmer, B., Lublin, F., Rammohan, K. W., Selmaj, K., Traboulsee, A., Sauter, A., Masterman, D., Fontoura, P., Belachew, S., Garren, H., … Wolinsky, J. S. (2016). Ocrelizumab versus Placebo in Primary Progressive Multiple Sclerosis. *New England Journal of Medicine, 376*(3), 209–220. https://doi.org/10.1056/nejmoa1606468

45. Ruck, T., Bittner, S., Wiendl, H., & Meuth, S. (2015). Alemtuzumab in multiple sclerosis: mechanism of action and beyond. *International Journal of Molecular Sciences, 16*(7), 16414–16439. https://doi.org/10.3390/ijms160716414

46. Jakimovski, D., Kolb, C., Ramanathan, M., Zivadinov, R., & Weinstock-Guttman, B. (2018). Interferon β for Multiple Sclerosis. *Cold Spring Harbor Perspectives in Medicine, 8*(11), a032003. https://doi.org/10.1101/cshperspect.a032003

47. Prod'homme, T., & Zamvil, S. S. (2018). The evolving mechanisms of action of glatiramer acetate. *Cold Spring Harbor Perspectives in Medicine, 9*(2), a029249. https://doi.org/10.1101/cshperspect.a029249

48. Kappos, L., Radue, E., O'Connor, P., Polman, C., Hohlfeld, R., Calabresi, P., Selmaj, K., Agoropoulou, C., Leyk, M., Zhang-Auberson, L., & Burtin, P. (2010). A Placebo-Controlled trial of oral fingolimod in relapsing multiple sclerosis. *New England Journal of Medicine, 362*(5), 387–401. https://doi.org/10.1056/nejmoa0909494

49. Subei, A. M., & Cohen, J. A. (2015). Sphingosine 1-Phosphate receptor modulators in multiple sclerosis. *CNS Drugs, 29*(7), 565–575. https://doi.org/10.1007/s40263-015-0261-z

50. Kremer, D., Göttle, P., Hartung, H., & Küry, P. (2016). Pushing forward: Remyelination as the new frontier in CNS diseases. *Trends in Neurosciences, 39*(4), 246–263. https://doi.org/10.1016/j.tins.2016.02.004

51. Najm, F. J., Madhavan, M., Zaremba, A., Shick, E., Karl, R. T., Factor, D. C., Miller, T. E., Nevin, Z. S., Kantor, C., Sargent, A., Quick, K. L., Schlatzer, D. M., Tang, H., Papoian, R.,

Brimacombe, K. R., Shen, M., Boxer, M. B., Jadhav, A., Robinson, A. P., ... Tesar, P. J. (2015). Drug-based modulation of endogenous stem cells promotes functional remyelination in vivo. *Nature, 522*(7555), 216–220. https://doi.org/10.1038/nature14335

52. Rivers, T. M., Sprunt, D. H., & Berry, G. P. (1933). OBSERVATIONS ON ATTEMPTS TO PRODUCE ACUTE DISSEMINATED ENCEPHALOMYELITIS IN MONKEYS. *The Journal of Experimental Medicine, 58*(1), 39–53. https://doi.org/10.1084/jem.58.1.39

53. Procaccini, C., De Rosa, V., Pucino, V., Formisano, L., & Matarese, G. (2015). Animal models of Multiple Sclerosis. *European Journal of Pharmacology, 759*, 182–191. https://doi.org/10.1016/j.ejphar.2015.03.042

54. Litzenburger, T., Fässler, R., Bauer, J., Lassmann, H., Linington, C., Wekerle, H., & Iglesias, A. (1998). B lymphocytes producing demyelinating autoantibodies: Development and function in gene-targeted transgenic mice. *The Journal of Experimental Medicine, 188*(1), 169–180. https://doi.org/10.1084/jem.188.1.169

55. Bettelli, E., Pagany, M., Weiner, H. L., Linington, C., Sobel, R. A., & Kuchroo, V. K. (2003). Myelin oligodendrocyte glycoprotein–specific T cell receptor transgenic mice develop spontaneous autoimmune optic neuritis. *The Journal of Experimental Medicine, 197*(9), 1073–1081. https://doi.org/10.1084/jem.20021603

56. Mendel, I., De Rosbo, N. K., & Ben-Nun, A. (1995). A myelin oligodendrocyte glycoprotein peptide induces typical chronic experimental autoimmune encephalomyelitis in H-2b mice: Fine specificity and T cell receptor Vβ expression of encephalitogenic T cells. *European Journal of Immunology, 25*(7), 1951–1959. https://doi.org/10.1002/eji.1830250723

57. Greter, M., Heppner, F. L., Lemos, M. P., Odermatt, B. M., Goebels, N., Laufer, T., Noelle, R. J., & Becher, B. (2005). Dendritic cells permit immune invasion of the CNS in an animal model of multiple sclerosis. *Nature Medicine, 11*(3), 328–334. https://doi.org/10.1038/nm1197

58. Acs, P., & Kalman, B. (2012). Pathogenesis of Multiple Sclerosis: What Can We Learn from the Cuprizone Model. *Methods in Molecular Biology*, 403–431. https://doi.org/10.1007/978-1-60761-720-4_20

59. Goverman, J. (2009). Autoimmune T cell responses in the central nervous system. *Nature Reviews. Immunology, 9*(6), 393–407. https://doi.org/10.1038/nri2550

60. Hjelmström, P., Juedes, A. E., Fjell, J., & Ruddle, N. H. (1998). Cutting Edge: B Cell-Deficient Mice Develop Experimental Allergic Encephalomyelitis with Demyelination After Myelin Oligodendrocyte Glycoprotein Sensitization. *The Journal of Immunology, 161*(9), 4480–4483. https://doi.org/10.4049/jimmunol.161.9.4480

61. Jensen, P. E. (2007). Recent advances in antigen processing and presentation. *Nature Immunology, 8*(10), 1041–1048. https://doi.org/10.1038/ni1516

62. Chitnis, T. & Khoury, S. J. (2003). Role of costimulatory pathways in the pathogenesis of multiple sclerosis and experimental autoimmune encephalomyelitis. *Journal of Allergy and Clinical Immunology, 112*(5), 850. https://doi.org/10.1016/j.jaci.2003.08.026

63. Aarts, S. A., Seijkens, T. T., Kusters, P. J., Van Tiel, C. M., Reiche, M. E., Toom, M. D., Beckers, L., Van Roomen, C. P., De Winther, M. P., Kooij, G., & Lutgens, E. (2018). Macrophage CD40 signaling drives experimental autoimmune encephalomyelitis. *The Journal of Pathology, 247*(4), 471–480. https://doi.org/10.1002/path.5205

64. Becher, B., Durell, B. G., Miga, A. V., Hickey, W. F., & Noelle, R. J. (2001). The Clinical Course of Experimental Autoimmune Encephalomyelitis and Inflammation Is Controlled by the Expression of Cd40 within the Central Nervous System. *The Journal of Experimental Medicine, 193*(8), 967–974. https://doi.org/10.1084/jem.193.8.967

65. Louveau, A., Smirnov, I., Keyes, T. J., Eccles, J. D., Rouhani, S. J., Peske, J. D., Derecki, N. C., Castle, D., Mandell, J. W., Lee, K. S., Harris, T. H., & Kipnis, J. (2015). Structural and functional features of central nervous system lymphatic vessels. Nature, 523(7560), 337–341. https://doi.org/10.1038/nature14432

66. Xu, H., Lotfy, P., Gelb, S., Pragana, A., Hehnly, C., Byer, L. I., Shipley, F. B., Zawadzki, M. E., Cui, J., Deng, L., Taylor, M., Webb, M., Lidov, H. G., Andermann, M. L., Chiu, I. M., Ordovas-Montanes, J., & Lehtinen, M. K. (2024). The choroid plexus synergizes with immune cells during neuroinflammation. Cell, 187(18), 4946-4963.e17. https://doi.org/10.1016/j.cell.2024.07.002

67. Quintana, F. J. (2017). Astrocytes to the rescue! Glia limitans astrocytic endfeet control CNS inflammation. Journal of Clinical Investigation, 127(8), 2897–2899. https://doi.org/10.1172/jci95769

68. Louveau, A., Harris, T. H., & Kipnis, J. (2015). Revisiting the mechanisms of CNS immune privilege. Trends in Immunology, 36(10), 569–577. https://doi.org/10.1016/j.it.2015.08.006

69. Marchetti, L., & Engelhardt, B. (2020). Immune cell trafficking across the blood-brain barrier in the absence and presence of neuroinflammation. Vascular Biology, 2(1), H1–H18. https://doi.org/10.1530/vb-19-0033

70. Rossi, B., & Constantin, G. (2016). Live imaging of immune responses in experimental models of multiple sclerosis. *Frontiers in Immunology, 7*. https://doi.org/10.3389/fimmu.2016.00506

71. Heng, A. H. S., Han, C. W., Abbott, C., McColl, S. R., & Comerford, I. (2022b). Chemokine-Driven migration of Pro-Inflammatory CD4+ T cells in CNS autoimmune disease. Frontiers in Immunology, 13. https://doi.org/10.3389/fimmu.2022.817473

72. Reboldi, A., Coisne, C., Baumjohann, D., Benvenuto, F., Bottinelli, D., Lira, S., Uccelli, A., Lanzavecchia, A., Engelhardt, B., & Sallusto, F. (2009b). C-C chemokine receptor 6–

regulated entry of TH-17 cells into the CNS through the choroid plexus is required for the initiation of EAE. Nature Immunology, 10(5), 514–523. https://doi.org/10.1038/ni.1716

73. Kivisäkk, P., Imitola, J., Rasmussen, S., Elyaman, W., Zhu, B., Ransohoff, R. M., & Khoury, S. J. (2008b). Localizing central nervous system immune surveillance: Meningeal antigen-presenting cells activate T cells during experimental autoimmune encephalomyelitis. Annals of Neurology, 65(4), 457–469. https://doi.org/10.1002/ana.21379

74. Berer, K., Boziki, M., & Krishnamoorthy, G. (2014). Selective accumulation of Pro-Inflammatory T cells in the intestine contributes to the resistance to autoimmune demyelinating disease. *PLoS ONE, 9*(2), e87876. https://doi.org/10.1371/journal.pone.0087876

75. Schnell, A., Huang, L., Singer, M., Singaraju, A., Barilla, R. M., Regan, B. M., Bollhagen, A., Thakore, P. I., Dionne, D., Delorey, T. M., Pawlak, M., Horste, G. M. Z., Rozenblatt-Rosen, O., Irizarry, R. A., Regev, A., & Kuchroo, V. K. (2021). Stem-like intestinal Th17 cells give rise to pathogenic effector T cells during autoimmunity. *Cell, 184*(26), 6281-6298.e23. https://doi.org/10.1016/j.cell.2021.11.018

76. Korn, T., Reddy, J., Gao, W., Bettelli, E., Awasthi, A., Petersen, T. R., Bäckström, B. T., Sobel, R. A., Wucherpfennig, K. W., Strom, T. B., Oukka, M., & Kuchroo, V. K. (2007). Myelin-specific regulatory T cells accumulate in the CNS but fail to control autoimmune inflammation. *Nature Medicine, 13*(4), 423–431. https://doi.org/10.1038/nm1564

77. Odoardi, F., Sie, C., Streyl, K., Ulaganathan, V. K., Schläger, C., Lodygin, D., Heckelsmiller, K., Nietfeld, W., Ellwart, J., Klinkert, W. E. F., Lottaz, C., Nosov, M., Brinkmann, V., Spang, R., Lehrach, H., Vingron, M., Wekerle, H., Flügel-Koch, C., & Flügel, A. (2012). T cells become licensed in the lung to enter the central nervous system. *Nature, 488*(7413), 675–679. https://doi.org/10.1038/nature11337

78. Hiltensperger, M., Beltrán, E., Kant, R., Tyystjärvi, S., Lepennetier, G., Moreno, H. D., Bauer, I. J., Grassmann, S., Jarosch, S., Schober, K., Buchholz, V. R., Kenet, S., Gasperi, C., Öllinger, R., Rad, R., Muschaweckh, A., Sie, C., Aly, L., Knier, B., … Korn, T. (2021). Skin and gut imprinted helper T cell subsets exhibit distinct functional phenotypes in central nervous system autoimmunity. *Nature Immunology, 22*(7), 880–892. https://doi.org/10.1038/s41590-021-00948-8

79. Kroenke, M. A., Carlson, T. J., Andjelkovic, A. V., & Segal, B. M. (2008). IL-12– and IL-23–modulated T cells induce distinct types of EAE based on histology, CNS chemokine profile, and response to cytokine inhibition. *The Journal of Experimental Medicine, 205*(7), 1535–1541. https://doi.org/10.1084/jem.20080159

80. Flügel, A., Berkowicz, T., Ritter, T., Labeur, M., Jenne, D. E., Li, Z., Ellwart, J. W., Willem, M., Lassmann, H., & Wekerle, H. (2001b). Migratory Activity and Functional Changes of Green Fluorescent Effector Cells before and during Experimental Autoimmune

Encephalomyelitis. Immunity, 14(5), 547–560. https://doi.org/10.1016/s1074-7613(01)00143-1

81. Tiper, I. V., East, J. E., Subrahmanyam, P. B., & Webb, T. J. (2016). Sphingosine 1-phosphate signaling impacts lymphocyte migration, inflammation and infection. *Pathogens and Disease, 74*(6), ftw063. https://doi.org/10.1093/femspd/ftw063

82. Thangada, S., Khanna, K. M., Blaho, V. A., Oo, M. L., Im, D., Guo, C., Lefrancois, L., & Hla, T. (2010). Cell-surface residence of sphingosine 1-phosphate receptor 1 on lymphocytes determines lymphocyte egress kinetics. *The Journal of Experimental Medicine, 207*(7), 1475–1483. https://doi.org/10.1084/jem.20091343

83. Matloubian, Matloubian, M., Lo, C. G., Cinamon, G., Lesneski, M. J., Xu, Y., Brinkmann, V., Allende, M. L., Proia, R. L., & Cyster, J. G. (2004). Lymphocyte egress from thymus and peripheral lymphoid organs is dependent on S1P receptor 1. *Nature, 427*(6972), 355–360. https://doi.org/10.1038/nature02284

84. Eken, A., Duhen, R., Singh, A. K., Fry, M., Buckner, J. H., Kita, M., Bettelli, E., & Oukka, M. (2017). S1P1 deletion differentially affects TH17 and Regulatory T cells. *Scientific Reports, 7*(1). https://doi.org/10.1038/s41598-017-13376-2

85. Annunziato, F., Cosmi, L., Santarlasci, V., Maggi, L., Liotta, F., Mazzinghi, B., Parente, E., Fili, L., Ferri, S., Frosali, F., Giudici, F., Romagnani, P., Parronchi, P., Tonelli, F., Maggi, E., & Romagnani, S. (2007). Phenotypic and functional features of human Th17 cells. *The Journal of Experimental Medicine, 204*(8), 1849–1861. https://doi.org/10.1084/jem.20070663

86. Singh, S. P., Zhang, H. H., Foley, J. F., Hedrick, M. N., & Farber, J. M. (2008). Human T cells that are able to produce IL-17 express the chemokine receptor CCR6. *The Journal of Immunology, 180*(1), 214–221. https://doi.org/10.4049/jimmunol.180.1.214

87. Kara, E. E., McKenzie, D. R., Bastow, C. R., Gregor, C. E., Fenix, K. A., Ogunniyi, A. D., Paton, J. C., Mack, M., Pombal, D. R., Seillet, C., Dubois, B., Liston, A., MacDonald, K. P. A., Belz, G. T., Smyth, M. J., Hill, G. R., Comerford, I., & McColl, S. R. (2015). CCR2 defines in vivo development and homing of IL-23-driven GM-CSF-producing Th17 cells. *Nature Communications, 6*(1). https://doi.org/10.1038/ncomms9644

88. Jahromi, N. H., Marchetti, L., Moalli, F., Duc, D., Basso, C., Tardent, H., Kaba, E., Deutsch, U., Pot, C., Sallusto, F., Stein, J. V., & Engelhardt, B. (2020). Intercellular adhesion molecule-1 (ICAM-1) and ICAM-2 differentially contribute to peripheral activation and CNS entry of autoaggressive TH1 and TH17 cells in experimental autoimmune encephalomyelitis. *Frontiers in Immunology, 10*. https://doi.org/10.3389/fimmu.2019.03056

89. Baron, J. L., Madri, J. A., Ruddle, N. H., Hashim, G., & Janeway, C. A. (1993). Surface expression of alpha 4 integrin by CD4 T cells is required for their entry into brain parenchyma. *The Journal of Experimental Medicine, 177*(1), 57–68. https://doi.org/10.1084/jem.177.1.57

90. Steiner, O., Coisne, C., Cecchelli, R., Boscacci, R., Deutsch, U., Engelhardt, B., & Lyck, R. (2010). Differential roles for endothelial ICAM-1, ICAM-2, and VCAM-1 in Shear-Resistant T cell arrest, polarization, and directed crawling on Blood–Brain barrier endothelium. *The Journal of Immunology, 185*(8), 4846–4855. https://doi.org/10.4049/jimmunol.0903732

91. Polman, C. H., O'Connor, P. W., Havrdova, E., Hutchinson, M., Kappos, L., Miller, D. H., Phillips, J. T., Lublin, F. D., Giovannoni, G., Wajgt, A., Toal, M., Lynn, F., Panzara, M. A., & Sandrock, A. W. (2006). A randomized, Placebo-Controlled trial of natalizumab for relapsing multiple sclerosis. *New England Journal of Medicine, 354*(9), 899–910. https://doi.org/10.1056/nejmoa044397

92. Bauer, J., Sminia, T., Wouterlood, F. G., & Dijkstra, C. D. (1994). Phagocytic activity of macrophages and microglial cells during the course of acute and chronic relapsing experimental autoimmune encephalomyelitis. *Journal of Neuroscience Research, 38*(4), 365–375. https://doi.org/10.1002/jnr.490380402

93. Komuczki, J., Tuzlak, S., Friebel, E., Hartwig, T., Spath, S., Rosenstiel, P., Waisman, A., Opitz, L., Oukka, M., Schreiner, B., Pelczar, P., & Becher, B. (2019). Fate-Mapping of GM-CSF expression identifies a discrete subset of Inflammation-Driving T helper cells regulated by cytokines IL-23 and IL-1β. *Immunity, 50*(5), 1289-1304.e6. https://doi.org/10.1016/j.immuni.2019.04.006

94. Benveniste, E. N. (1997). Role of macrophages/microglia in multiple sclerosis and experimental allergic encephalomyelitis. *Journal of Molecular Medicine, 75*, 165–173.

95. Goldmann, T., Wieghofer, P., Müller, P. F., Wolf, Y., Varol, D., Yona, S., Brendecke, S. M., Kierdorf, K., Staszewski, O., Datta, M., Luedde, T., Heikenwalder, M., Jung, S., & Prinz, M. (2013). A new type of microglia gene targeting shows TAK1 to be pivotal in CNS autoimmune inflammation. *Nature Neuroscience, 16*(11), 1618–1626. https://doi.org/10.1038/nn.3531

96. Diebold, M., Fehrenbacher, L., Frosch, M., & Prinz, M. (2023). How myeloid cells shape experimental autoimmune encephalomyelitis: At the crossroads of outside-in immunity. *European Journal of Immunology, 53*(10). https://doi.org/10.1002/eji.202250234

97. Shi, K., Li, H., Chang, T., He, W., Kong, Y., Qi, C., Li, R., Huang, H., Zhu, Z., Zheng, P., Ruan, Z., Zhou, J., Shi, F., & Liu, Q. (2022). Bone marrow hematopoiesis drives multiple sclerosis progression. *Cell, 185*(13), 2234-2247.e17. https://doi.org/10.1016/j.cell.2022.05.020

98. Locatelli, G., Theodorou, D., Kendirli, A., Jordão, M. J. C., Staszewski, O., Phulphagar, K., Cantuti-Castelvetri, L., Dagkalis, A., Bessis, A., Simons, M., Meissner, F., Prinz, M., & Kerschensteiner, M. (2018). Mononuclear phagocytes locally specify and adapt their phenotype in a multiple sclerosis model. *Nature Neuroscience, 21*(9), 1196–1208. https://doi.org/10.1038/s41593-018-0212-3

99. Mendiola, A. S., Ryu, J. K., Bardehle, S., Meyer-Franke, A., Ang, K. K., Wilson, C., Baeten, K. M., Hanspers, K., Merlini, M., Thomas, S., Petersen, M. A., Williams, A., Thomas, R., Rafalski, V. A., Meza-Acevedo, R., Tognatta, R., Yan, Z., Pfaff, S. J., Machado, M. R., . . . Akassoglou, K. (2020). Transcriptional profiling and therapeutic targeting of oxidative stress in neuroinflammation. *Nature Immunology, 21*(5), 513–524. https://doi.org/10.1038/s41590-020-0654-0

100. Liu, L., Belkadi, A., Darnall, L., Hu, T., Drescher, C., Cotleur, A. C., Padovani-Claudio, D., He, T., Choi, K., Lane, T. E., Miller, R. H., & Ransohoff, R. M. (2010). CXCR2-positive neutrophils are essential for cuprizone-induced demyelination: relevance to multiple sclerosis. *Nature Neuroscience, 13*(3), 319–326. https://doi.org/10.1038/nn.2491

101. Byun, D. J., Lee, J., Ko, K., & Hyun, Y. (2024). NLRP3 exacerbates EAE severity through ROS-dependent NET formation in the mouse brain. *Cell Communication and Signaling, 22*(1). https://doi.org/10.1186/s12964-023-01447-z

102. Nowaczewska-Kuchta, A., Ksiazek-Winiarek, D., Szpakowski, P., & Glabinski, A. (2024). The role of neutrophils in multiple sclerosis and ischemic stroke. *Brain Sciences, 14*(5), 423. https://doi.org/10.3390/brainsci14050423

103. Trias, E., King, P. H., Si, Y., Kwon, Y., Varela, V., Ibarburu, S., Kovacs, M., Moura, I. C., Beckman, J. S., Hermine, O., & Barbeito, L. (2018). Mast cells and neutrophils mediate peripheral motor pathway degeneration in ALS. *JCI Insight, 3*(19). https://doi.org/10.1172/jci.insight.123249

104. Ajami, B., Bennett, J. L., Krieger, C., McNagny, K. M., & Rossi, F. M. V. (2011). Infiltrating monocytes trigger EAE progression, but do not contribute to the resident microglia pool. *Nature Neuroscience, 14*(9), 1142–1149. https://doi.org/10.1038/nn.2887

105. Aubé, B., Lévesque, S. A., Paré, A., Chamma, É., Kébir, H., Gorina, R., Lécuyer, M., Alvarez, J. I., De Koninck, Y., Engelhardt, B., Prat, A., Côté, D., & Lacroix, S. (2014). Neutrophils mediate Blood–Spinal cord barrier disruption in demyelinating neuroinflammatory diseases. *The Journal of Immunology, 193*(5), 2438–2454. https://doi.org/10.4049/jimmunol.1400401

106. Jiang, W., St-Pierre, S., Roy, P., Morley, B. J., Hao, J., & Simard, A. R. (2016). Infiltration of CCR2+Ly6Chigh Proinflammatory Monocytes and Neutrophils into the Central Nervous System Is Modulated by Nicotinic Acetylcholine Receptors in a Model of Multiple Sclerosis. *The Journal of Immunology, 196*(5), 2095–2108. https://doi.org/10.4049/jimmunol.1501613

107. Liu, Y., Hao, W., Letiembre, M., Walter, S., Kulanga, M., Neumann, H., & Fassbender, K. (2006). Suppression of microglial inflammatory activity by myelin phagocytosis: Role of P47-PHOX-Mediated Generation of Reactive Oxygen Species. *Journal of Neuroscience, 26*(50), 12904–12913. https://doi.org/10.1523/jneurosci.2531-06.2006

108. Miron, V. E., Boyd, A., Zhao, J., Yuen, T. J., Ruckh, J. M., Shadrach, J. L., Van Wijngaarden, P., Wagers, A. J., Williams, A., Franklin, R. J. M., & Ffrench-Constant, C.

(2013). M2 microglia and macrophages drive oligodendrocyte differentiation during CNS remyelination. *Nature Neuroscience, 16*(9), 1211–1218. https://doi.org/10.1038/nn.3469

109. Sosa, R. A., Murphey, C., Robinson, R. R., & Forsthuber, T. G. (2015). IFN-γ ameliorates autoimmune encephalomyelitis by limiting myelin lipid peroxidation. *Proceedings of the National Academy of Sciences, 112*(36). https://doi.org/10.1073/pnas.1505955112

110. Gaffen, S. L. (2009). Structure and signalling in the IL-17 receptor family. *Nature Reviews. Immunology, 9*(8), 556–567. https://doi.org/10.1038/nri2586

111. Iwakura, Y., Ishigame, H., Saijo, S., & Nakae, S. (2011). Functional specialization of interleukin-17 family members. *Immunity, 34*(2), 149–162. https://doi.org/10.1016/j.immuni.2011.02.012

112. Komiyama, Y., Nakae, S., Matsuki, T., Nambu, A., Ishigame, H., Kakuta, S., Sudo, K., & Iwakura, Y. (2006). IL-17 plays an important role in the development of experimental autoimmune encephalomyelitis. *The Journal of Immunology, 177*(1), 566–573. https://doi.org/10.4049/jimmunol.177.1.566

113. Yang, X. O., Chang, S. H., Park, H., Nurieva, R., Shah, B., Acero, L., Wang, Y., Schluns, K. S., Broaddus, R. R., Zhu, Z., & Dong, C. (2008). Regulation of inflammatory responses by IL-17F. *The Journal of Experimental Medicine, 205*(5), 1063–1075. https://doi.org/10.1084/jem.20071978

114. Wanke, F., Tang, Y., Gronke, K., Klebow, S., Moos, S., Hauptmann, J., Shanmugavadivu, A., Regen, T., Mufazalov, I. A., Gabriel, L. A., Reißig, S., Diefenbach, A., Kurschus, F. C., & Waisman, A. (2018). Expression of IL-17F is associated with non-pathogenic Th17 cells. *Journal of Molecular Medicine, 96*(8), 819–829. https://doi.org/10.1007/s00109-018-1662-5

115. Chang, S. H., Park, H., & Dong, C. (2006). ACT1 adaptor protein is an immediate and essential signaling component of interleukin-17 receptor. *Journal of Biological Chemistry, 281*(47), 35603–35607. https://doi.org/10.1074/jbc.c600256200

116. Dong, C. (2008). Regulation and pro-inflammatory function of interleukin-17 family cytokines. *Immunological Reviews, 226*(1), 80–86. https://doi.org/10.1111/j.1600-065x.2008.00709.x

117. Veldhoen, M. (2017). Interleukin 17 is a chief orchestrator of immunity. *Nature Immunology, 18*(6), 612–621. https://doi.org/10.1038/ni.3742

118. Monin, L., & Gaffen, S. L. (2017). Interleukin 17 Family cytokines: signaling mechanisms, biological activities, and therapeutic implications. *Cold Spring Harbor Perspectives in Biology, 10*(4), a028522. https://doi.org/10.1101/cshperspect.a028522

119. Majumder, S., & McGeachy, M. J. (2021). IL-17 in the Pathogenesis of Disease: Good intentions gone awry. *Annual Review of Immunology, 39*(1), 537–556. https://doi.org/10.1146/annurev-immunol-101819-092536

120. Dubin, P. J., & Kolls, J. K. (2008). Th17 cytokines and mucosal immunity. *Immunological Reviews, 226*(1), 160–171. https://doi.org/10.1111/j.1600-065x.2008.00703.x

121. Fossiez, F., Djossou, O., Chomarat, P., Flores-Romo, L., Ait-Yahia, S., Maat, C., Pin, J. J., Garrone, P., Garcia, E., Saeland, S., Blanchard, D., Gaillard, C., Mahapatra, B. D., Rouvier, E., Golstein, P., Banchereau, J., & Lebecque, S. (1996). T cell interleukin-17 induces stromal cells to produce proinflammatory and hematopoietic cytokines. *The Journal of Experimental Medicine, 183*(6), 2593–2603. https://doi.org/10.1084/jem.183.6.2593

122. Erbel, C., Akhavanpoor, M., Okuyucu, D., Wangler, S., Dietz, A., Zhao, L., Stellos, K., Little, K. M., Lasitschka, F., Doesch, A., Hakimi, M., Dengler, T. J., Giese, T., Blessing, E., Katus, H. A., & Gleissner, C. A. (2014). IL-17A influences essential functions of the Monocyte/Macrophage lineage and is involved in advanced murine and human atherosclerosis. *The Journal of Immunology, 193*(9), 4344–4355. https://doi.org/10.4049/jimmunol.1400181

123. Fujino, S. (2002). Increased expression of interleukin 17 in inflammatory bowel disease. *Gut, 52*(1), 65–70. https://doi.org/10.1136/gut.52.1.65

124. Wu, W., Chen, F., Liu, Z., & Cong, Y. (2016). Microbiota-specific TH17 cells. *Inflammatory Bowel Diseases, 22*(6), 1473–1482. https://doi.org/10.1097/mib.0000000000000775

125. Kim, E. K., Kwon, J., Lee, S., Lee, E., Kim, D. S., Moon, S., Lee, J., Kwok, S., Park, S., & Cho, M. (2017). IL-17-mediated mitochondrial dysfunction impairs apoptosis in rheumatoid arthritis synovial fibroblasts through activation of autophagy. *Cell Death and Disease, 8*(1), e2565. https://doi.org/10.1038/cddis.2016.490

126. Wei, L., Abraham, D., & Ong, V. (2022). The yin and yang of IL-17 in systemic sclerosis. *Frontiers in Immunology, 13*. https://doi.org/10.3389/fimmu.2022.885609

127. Ramakrishnan, R. K., Bajbouj, K., Heialy, S. A., Mahboub, B., Ansari, A. W., Hachim, I. Y., Rawat, S., Salameh, L., Hachim, M. Y., Olivenstein, R., Halwani, R., Hamoudi, R., & Hamid, Q. (2020). IL-17 induced autophagy regulates mitochondrial dysfunction and fibrosis in severe asthmatic bronchial fibroblasts. *Frontiers in Immunology, 11*. https://doi.org/10.3389/fimmu.2020.01002

128. Yim, Y. S., Park, A., Berrios, J., Lafourcade, M., Pascual, L. M., Soares, N., Kim, J. Y., Kim, S., Kim, H., Waisman, A., Littman, D. R., Wickersham, I. R., Harnett, M. T., Huh, J. R., & Choi, G. B. (2017). Reversing behavioural abnormalities in mice exposed to maternal inflammation. *Nature, 549*(7673), 482–487. https://doi.org/10.1038/nature23909

129. Andruszewski, D., Uhlfelder, D. C., Desiato, G., Regen, T., Schelmbauer, C., Blanfeld, M., Scherer, L., Radyushkin, K., Pozzi, D., Waisman, A., & Mufazalov, I. A. (2024). Embryo-restricted responses to maternal IL-17A promote neurodevelopmental disorders in mouse offspring. *Molecular Psychiatry*. https://doi.org/10.1038/s41380-024-02772-6

130. Cua, D. J., & Tato, C. M. (2010). Innate IL-17-producing cells: the sentinels of the immune system. *Nature Reviews. Immunology, 10*(7), 479–489. https://doi.org/10.1038/nri2800

131. Martin, B., Hirota, K., Cua, D. J., Stockinger, B., & Veldhoen, M. (2009). Interleukin-17-Producing γδ T Cells Selectively Expand in Response to Pathogen Products and Environmental Signals. *Immunity, 31*(2), 321–330. https://doi.org/10.1016/j.immuni.2009.06.020

132. Sutton, C. E., Lalor, S. J., Sweeney, C. M., Brereton, C. F., Lavelle, E. C., & Mills, K. H. (2009). Interleukin-1 and IL-23 Induce Innate IL-17 Production from γδ T Cells, Amplifying Th17 Responses and Autoimmunity. *Immunity, 31*(2), 331–341. https://doi.org/10.1016/j.immuni.2009.08.001

133. McGinley, A. M., Sutton, C. E., Edwards, S. C., Leane, C. M., DeCourcey, J., Teijeiro, A., Hamilton, J. A., Boon, L., Djouder, N., & Mills, K. H. (2020). Interleukin-17A Serves a Priming Role in Autoimmunity by Recruiting IL-1β-Producing Myeloid Cells that Promote Pathogenic T Cells. *Immunity, 52*(2), 342-356.e6. https://doi.org/10.1016/j.immuni.2020.01.002

134. Van De Pavert, S. A., & Mebius, R. E. (2010). New insights into the development of lymphoid tissues. *Nature Reviews. Immunology, 10*(9), 664–674. https://doi.org/10.1038/nri2832

135. Pikor, N. B., Astarita, J. L., Summers-Deluca, L., Galicia, G., Qu, J., Ward, L. A., Armstrong, S., Dominguez, C. X., Malhotra, D., Heiden, B., Kay, R., Castanov, V., Touil, H., Boon, L., O'Connor, P., Bar-Or, A., Prat, A., Ramaglia, V., Ludwin, S., … Gommerman, J. L. (2015). Integration of TH17- and Lymphotoxin-Derived signals initiates Meningeal-Resident stromal cell remodeling to propagate neuroinflammation. *Immunity, 43*(6), 1160–1173. https://doi.org/10.1016/j.immuni.2015.11.010

136. Lee, Y. K., Turner, H., Maynard, C. L., Oliver, J. R., Chen, D., Elson, C. O., & Weaver, C. T. (2009). Late developmental plasticity in the T Helper 17 lineage. *Immunity, 30*(1), 92–107. https://doi.org/10.1016/j.immuni.2008.11.005

137. Veldhoen, M., Hocking, R. J., Atkins, C. J., Locksley, R. M., & Stockinger, B. (2006). TGFB in the context of an inflammatory cytokine milieu supports de novo differentiation of IL-17-Producing T cells. *Immunity, 24*(2), 179–189. https://doi.org/10.1016/j.immuni.2006.01.001

138. Yang, X. O., Panopoulos, A. D., Nurieva, R., Chang, S. H., Wang, D., Watowich, S. S., & Dong, C. (2007). STAT3 regulates cytokine-mediated generation of inflammatory

helper T cells. *Journal of Biological Chemistry, 282*(13), 9358–9363. https://doi.org/10.1074/jbc.c600321200

139. Zhou, L., Ivanov, I. I., Spolski, R., Min, R., Shenderov, K., Egawa, T., Levy, D. E., Leonard, W. J., & Littman, D. R. (2007). IL-6 programs TH-17 cell differentiation by promoting sequential engagement of the IL-21 and IL-23 pathways. *Nature Immunology, 8*(9), 967–974. https://doi.org/10.1038/ni1488

140. Wu, B., & Wan, Y. (2020). Molecular control of pathogenic Th17 cells in autoimmune diseases. *International Immunopharmacology, 80*, 106187. https://doi.org/10.1016/j.intimp.2020.106187

141. Lee, J. S., Tato, C. M., Joyce-Shaikh, B., Gulen, M. F., Cayatte, C., Chen, Y., Blumenschein, W. M., Judo, M., Ayanoglu, G., McClanahan, T. K., Li, X., & Cua, D. J. (2015). Interleukin-23-Independent IL-17 Production Regulates Intestinal Epithelial Permeability. *Immunity, 43*(4), 727–738. https://doi.org/10.1016/j.immuni.2015.09.003

142. Belkaid, Y., Bouladoux, N., & Hand, T. W. (2013). Effector and memory T cell responses to commensal bacteria. *Trends in Immunology, 34*(6), 299–306. https://doi.org/10.1016/j.it.2013.03.003

143. Ivanov, I. I., Atarashi, K., Manel, N., Brodie, E. L., Shima, T., Karaoz, U., Wei, D., Goldfarb, K. C., Santee, C. A., Lynch, S. V., Tanoue, T., Imaoka, A., Itoh, K., Takeda, K., Umesaki, Y., Honda, K., & Littman, D. R. (2009). Induction of intestinal TH17 cells by segmented filamentous bacteria. *Cell, 139*(3), 485–498. https://doi.org/10.1016/j.cell.2009.09.033

144. Yamazaki, S., Inohara, N., Ohmuraya, M., Tsuneoka, Y., Yagita, H., Katagiri, T., Nishina, T., Mikami, T., Funato, H., Araki, K., & Nakano, H. (2022). IκBζ controls IL-17-triggered gene expression program in intestinal epithelial cells that restricts colonization of SFB and prevents Th17-associated pathologies. *Mucosal Immunology, 15*(6), 1321–1337. https://doi.org/10.1038/s41385-022-00554-3

145. Atarashi, K., Tanoue, T., & Honda, K. (2010). Induction of lamina propria Th17 cells by intestinal commensal bacteria. *Vaccine, 28*(50), 8036–8038. https://doi.org/10.1016/j.vaccine.2010.09.026

146. Omenetti, S., Bussi, C., Metidji, A., Iseppon, A., Lee, S., Tolaini, M., Li, Y., Kelly, G., Chakravarty, P., Shoaie, S., Gutierrez, M. G., & Stockinger, B. (2019). The intestine harbors functionally distinct homeostatic Tissue-Resident and inflammatory TH17 cells. *Immunity, 51*(1), 77-89.e6. https://doi.org/10.1016/j.immuni.2019.05.004

147. Huppert, J., Closhen, D., Croxford, A., White, R., Kulig, P., Pietrowski, E., Bechmann, I., Becher, B., Luhmann, H. J., Waisman, A., & Kuhlmann, C. R. W. (2009). Cellular mechanisms of IL-17-induced blood-brain barrier disruption. *The FASEB Journal, 24*(4), 1023–1034. https://doi.org/10.1096/fj.09-141978

148. Kebir, H., Kreymborg, K., Ifergan, I., Dodelet-Devillers, A., Cayrol, R., Bernard, M., Giuliani, F., Arbour, N., Becher, B., & Prat, A. (2007). Human TH17 lymphocytes

promote blood-brain barrier disruption and central nervous system inflammation. *Nature Medicine, 13*(10), 1173–1175. https://doi.org/10.1038/nm1651

149. Wojkowska, D., Szpakowski, P., & Glabinski, A. (2017). Interleukin 17A Promotes Lymphocytes Adhesion and Induces CCL2 and CXCL1 Release from Brain Endothelial Cells. *International Journal of Molecular Sciences, 18*(5), 1000. https://doi.org/10.3390/ijms18051000

150. Di Filippo, M., Mancini, A., Bellingacci, L., Gaetani, L., Mazzocchetti, P., Zelante, T., La Barbera, L., De Luca, A., Tantucci, M., Tozzi, A., Durante, V., Sciaccaluga, M., Megaro, A., Chiasserini, D., Salvadori, N., Lisetti, V., Portaccio, E., Costa, C., Sarchielli, P., . . . Calabresi, P. (2021). Interleukin-17 affects synaptic plasticity and cognition in an experimental model of multiple sclerosis. *Cell Reports, 37*(10), 110094. https://doi.org/10.1016/j.celrep.2021.110094

151. Kumar, P., Monin, L., Castillo, P., Elsegeiny, W., Horne, W., Eddens, T., Vikram, A., Good, M., Schoenborn, A. A., Bibby, K., Montelaro, R. C., Metzger, D. W., Gulati, A. S., & Kolls, J. K. (2016). Intestinal interleukin-17 receptor signaling mediates reciprocal control of the gut microbiota and autoimmune inflammation. *Immunity, 44*(3), 659–671. https://doi.org/10.1016/j.immuni.2016.02.007

152. Regen, T., Isaac, S., Amorim, A., Núñez, N. G., Hauptmann, J., Shanmugavadivu, A., Klein, M., Sankowski, R., Mufazalov, I. A., Yogev, N., Huppert, J., Wanke, F., Witting, M., Grill, A., Gálvez, E. J. C., Nikolaev, A., Blanfeld, M., Prinz, I., Schmitt-Kopplin, P., . . . Waisman, A. (2021). IL-17 controls central nervous system autoimmunity through the intestinal microbiome. *Science Immunology, 6*(56). https://doi.org/10.1126/sciimmunol.aaz6563

153. Amatya, N., Garg, A. V., & Gaffen, S. L. (2017). IL-17 Signaling: the yin and the yang. *Trends in Immunology, 38*(5), 310–322. https://doi.org/10.1016/j.it.2017.01.006

154. Havrdová, E., Belova, A., Goloborodko, A., Tisserant, A., Wright, A., Wallstroem, E., Garren, H., Maguire, R. P., & Johns, D. R. (2016). Activity of secukinumab, an anti-IL-17A antibody, on brain lesions in RRMS: results from a randomized, proof-of-concept study. *Journal of Neurology, 263*(7), 1287–1295. https://doi.org/10.1007/s00415-016-8128-x

155. Segal, B. M., Constantinescu, C. S., Raychaudhuri, A., Kim, L., Fidelus-Gort, R., & Kasper, L. H. (2008). Repeated subcutaneous injections of IL12/23 p40 neutralising antibody, ustekinumab, in patients with relapsing-remitting multiple sclerosis: a phase II, double-blind, placebo-controlled, randomised, dose-ranging study. *The Lancet Neurology, 7*(9), 796–804. https://doi.org/10.1016/s1474-4422(08)70173-x

156. Vollmer, T. L., Wynn, D. R., Alam, M. S., & Valdes, J. (2010). A phase 2, 24-week, randomized, placebo-controlled, double-blind study examining the efficacy and safety of an anti-interleukin-12 and -23 monoclonal antibody in patients with relapsing–remitting or secondary progressive multiple sclerosis. *Multiple Sclerosis Journal, 17*(2), 181–191. https://doi.org/10.1177/1352458510384496

157. Straub, R. H., Wiest, R., Strauch, U. G., Harle, P., & Scholmerich, J. (2006). The role of the sympathetic nervous system in intestinal inflammation. *Gut, 55*(11), 1640–1649. https://doi.org/10.1136/gut.2006.091322

158. Goverse, G., Stakenborg, M., & Matteoli, G. (2016). The intestinal cholinergic anti-inflammatory pathway. *The Journal of Physiology, 594*(20), 5771–5780. https://doi.org/10.1113/jp271537

159. Buga, A. M., Padureanu, V., Riza, A., Oancea, C. N., Albu, C. V., & Nica, A. D. (2023). The Gut–Brain axis as a therapeutic target in multiple sclerosis. *Cells, 12*(14), 1872. https://doi.org/10.3390/cells12141872

160. Parodi, B., & De Rosbo, N. K. (2021). The Gut-Brain axis in multiple sclerosis. Is its dysfunction a pathological trigger or a consequence of the disease? Frontiers in *Immunology, 12*. https://doi.org/10.3389/fimmu.2021.718220

161. Ley, R. E., Peterson, D. A., & Gordon, J. I. (2006). Ecological and evolutionary forces shaping microbial diversity in the human intestine. *Cell, 124*(4), 837–848. https://doi.org/10.1016/j.cell.2006.02.017

162. Miyake, S., Kim, S., Suda, W., Oshima, K., Nakamura, M., Matsuoka, T., Chihara, N., Tomita, A., Sato, W., Kim, S., Morita, H., Hattori, M., & Yamamura, T. (2015). Dysbiosis in the Gut Microbiota of Patients with Multiple Sclerosis, with a Striking Depletion of Species Belonging to Clostridia XIVa and IV Clusters. *PLoS ONE, 10*(9), e0137429. https://doi.org/10.1371/journal.pone.0137429

163. Berer, K., Gerdes, L. A., Cekanaviciute, E., Jia, X., Xiao, L., Xia, Z., Liu, C., Klotz, L., Stauffer, U., Baranzini, S. E., Kümpfel, T., Hohlfeld, R., Krishnamoorthy, G., & Wekerle, H. (2017). Gut microbiota from multiple sclerosis patients enables spontaneous autoimmune encephalomyelitis in mice. Proceedings of the National Academy of *Sciences, 114*(40), 10719–10724. https://doi.org/10.1073/pnas.1711233114

164. Chen, J., Chia, N., Kalari, K. R., Yao, J. Z., Novotna, M., Soldan, M. M. P., Luckey, D. H., Marietta, E. V., Jeraldo, P. R., Chen, X., Weinshenker, B. G., Rodriguez, M., Kantarci, O. H., Nelson, H., Murray, J. A., & Mangalam, A. K. (2016). Multiple sclerosis patients have a distinct gut microbiota compared to healthy controls. *Scientific Reports, 6*(1). https://doi.org/10.1038/srep28484

165. Jangi, S., Gandhi, R., Cox, L. M., Li, N., Von Glehn, F., Yan, R., Patel, B., Mazzola, M. A., Liu, S., Glanz, B. L., Cook, S., Tankou, S., Stuart, F., Melo, K., Nejad, P., Smith, K., Topçuolu, B. D., Holden, J., Kivisäkk, P., . . . Weiner, H. L. (2016). Alterations of the human gut microbiome in multiple sclerosis. *Nature Communications, 7*(1). https://doi.org/10.1038/ncomms12015

166. Cosorich, I., Dalla-Costa, G., Sorini, C., Ferrarese, R., Messina, M. J., Dolpady, J., Radice, E., Mariani, A., Testoni, P. A., Canducci, F., Comi, G., Martinelli, V., & Falcone, M. (2017). High frequency of intestinal TH17 cells correlates with microbiota alterations and

disease activity in multiple sclerosis. *Science Advances, 3*(7). https://doi.org/10.1126/sciadv.1700492

167. Sharifa, M., Ghosh, T., Daher, O. A., Bhusal, P., Alaameri, Y. A., Naz, J., Ekhator, C., Bellegarde, S. B., Bisharat, P., Vaghani, V., & Hussain, A. (2023). Unraveling the Gut-Brain axis in multiple sclerosis: exploring dysbiosis, oxidative stress, and therapeutic insights. *Cureus*. https://doi.org/10.7759/cureus.47058

168. Duarte-Silva, E., Meuth, S. G., & Peixoto, C. A. (2022). Microbial metabolites in multiple sclerosis: Implications for pathogenesis and treatment. *Frontiers in Neuroscience, 16*. https://doi.org/10.3389/fnins.2022.885031

169. Mangalam, A., Shahi, S. K., Luckey, D., Karau, M., Marietta, E., Luo, N., Choung, R. S., Ju, J., Sompallae, R., Gibson-Corley, K., Patel, R., Rodriguez, M., David, C., Taneja, V., & Murray, J. (2017). Human Gut-Derived commensal bacteria suppress CNS inflammatory and demyelinating disease. *Cell Reports, 20*(6), 1269–1277. https://doi.org/10.1016/j.celrep.2017.07.031

170. Vendrik, K. E. W., Ooijevaar, R. E., De Jong, P. R. C., Laman, J. D., Van Oosten, B. W., Van Hilten, J. J., Ducarmon, Q. R., Keller, J. J., Kuijper, E. J., & Contarino, M. F. (2020). Fecal microbiota transplantation in neurological disorders. *Frontiers in Cellular and Infection Microbiology, 10*. https://doi.org/10.3389/fcimb.2020.00098

171. Al, K. F., Craven, L. J., Gibbons, S., Parvathy, S. N., Wing, A. C., Graf, C., Parham, K. A., Kerfoot, S. M., Wilcox, H., Burton, J. P., Kremenchutzky, M., Morrow, S. A., Casserly, C., Meddings, J., Sharma, M., & Silverman, M. S. (2022). Fecal microbiota transplantation is safe and tolerable in patients with multiple sclerosis: A pilot randomized controlled trial. *Multiple Sclerosis Journal - Experimental Translational and Clinical, 8*(2). https://doi.org/10.1177/20552173221086662

172. Rahimlou, M., Nematollahi, S., Husain, D., Banaei-Jahromi, N., Majdinasab, N., & Hosseini, S. A. (2022). Probiotic supplementation and systemic inflammation in relapsing-remitting multiple sclerosis: A randomized, double-blind, placebo-controlled trial. *Frontiers in Neuroscience, 16*. https://doi.org/10.3389/fnins.2022.901846

173. Salami, M., Kouchaki, E., Asemi, Z., & Tamtaji, O. R. (2018). How probiotic bacteria influence the motor and mental behaviors as well as immunological and oxidative biomarkers in multiple sclerosis? A double blind clinical trial. *Journal of Functional Foods, 52*, 8–13. https://doi.org/10.1016/j.jff.2018.10.023

174. Berer, K., Boziki, M., & Krishnamoorthy, G. (2014b). Selective accumulation of Pro-Inflammatory T cells in the intestine contributes to the resistance to autoimmune demyelinating disease. *PLoS ONE, 9*(2), e87876. https://doi.org/10.1371/journal.pone.0087876

175. Lee, Y. K., Menezes, J. S., Umesaki, Y., & Mazmanian, S. K. (2010). Proinflammatory T-cell responses to gut microbiota promote experimental autoimmune

encephalomyelitis. *Proceedings of the National Academy of Sciences, 108*, 4615–4622. https://doi.org/10.1073/pnas.1000082107

176. Round, J. L., & Mazmanian, S. K. (2010). Inducible Foxp3 + regulatory T-cell development by a commensal bacterium of the intestinal microbiota. *Proceedings of the National Academy of Sciences, 107*(27), 12204–12209. https://doi.org/10.1073/pnas.0909122107

177. Ochoa-Repáraz, J., Mielcarz, D. W., Wang, Y., Begum-Haque, S., Dasgupta, S., Kasper, D. L., & Kasper, L. H. (2010). A polysaccharide from the human commensal Bacteroides fragilis protects against CNS demyelinating disease. *Mucosal Immunology, 3*(5), 487–495. https://doi.org/10.1038/mi.2010.29

178. Bhaumik, S., & Basu, R. (2017). Cellular and Molecular Dynamics of Th17 Differentiation and its Developmental Plasticity in the Intestinal Immune Response. *Frontiers in Immunology, 8*. https://doi.org/10.3389/fimmu.2017.00254

179. Erny, D., De Angelis, A. L. H., Jaitin, D., Wieghofer, P., Staszewski, O., David, E., Keren-Shaul, H., Mahlakoiv, T., Jakobshagen, K., Buch, T., Schwierzeck, V., Utermöhlen, O., Chun, E., Garrett, W. S., McCoy, K. D., Diefenbach, A., Staeheli, P., Stecher, B., Amit, I., & Prinz, M. (2015). Host microbiota constantly control maturation and function of microglia in the CNS. *Nature Neuroscience, 18*(7), 965–977. https://doi.org/10.1038/nn.4030

180. Hosang, L., Canals, R. C., Van Der Flier, F. J., Hollensteiner, J., Daniel, R., Flügel, A., & Odoardi, F. (2022). The lung microbiome regulates brain autoimmunity. *Nature, 603*(7899), 138–144. https://doi.org/10.1038/s41586-022-04427-4

181. Rothhammer, V., Mascanfroni, I. D., Bunse, L., Takenaka, M. C., Kenison, J. E., Mayo, L., Chao, C., Patel, B., Yan, R., Blain, M., Alvarez, J. I., Kébir, H., Anandasabapathy, N., Izquierdo, G., Jung, S., Obholzer, N., Pochet, N., Clish, C. B., Prinz, M., . . . Quintana, F. J. (2016). Type I interferons and microbial metabolites of tryptophan modulate astrocyte activity and central nervous system inflammation via the aryl hydrocarbon receptor. *Nature Medicine, 22*(6), 586–597. https://doi.org/10.1038/nm.4106

182. Bhargava, P., Smith, M. D., Mische, L., Harrington, E., Fitzgerald, K. C., Martin, K., Kim, S., Reyes, A. A., Gonzalez-Cardona, J., Volsko, C., Tripathi, A., Singh, S., Varanasi, K., Lord, H., Meyers, K., Taylor, M., Gharagozloo, M., Sotirchos, E. S., Nourbakhsh, B., . . . Calabresi, P. A. (2020). Bile acid metabolism is altered in multiple sclerosis and supplementation ameliorates neuroinflammation. *Journal of Clinical Investigation, 130*(7), 3467–3482. https://doi.org/10.1172/jci129401

183. Wang, X., Eguchi, A., Yang, Y., Chang, L., Wan, X., Shan, J., Qu, Y., Ma, L., Mori, C., Yang, J., & Hashimoto, K. (2022). Key role of the gut–microbiota–brain axis via the subdiaphragmatic vagus nerve in demyelination of the cuprizone-treated mouse brain. *Neurobiology of Disease, 176*, 105951. https://doi.org/10.1016/j.nbd.2022.105951

184. Natarajan, C., Le, L. H. D., Gunasekaran, M., Tracey, K. J., Chernoff, D., & Levine, Y. A. (2024). Electrical stimulation of the vagus nerve ameliorates inflammation and disease activity in a rat EAE model of multiple sclerosis. *Proceedings of the National Academy of Sciences, 121*(28). https://doi.org/10.1073/pnas.2322577121

185. Rosas-Ballina, M., Olofsson, P. S., Ochani, M., Valdés-Ferrer, S. I., Levine, Y. A., Reardon, C., Tusche, M. W., Pavlov, V. A., Andersson, U., Chavan, S., Mak, T. W., & Tracey, K. J. (2011). Acetylcholine-Synthesizing T cells relay neural signals in a vagus nerve circuit. *Science, 334*(6052), 98–101. https://doi.org/10.1126/science.1209985

186. Burn, G. L., Foti, A., Marsman, G., Patel, D. F. & Zychlinsky, A. The Neutrophil. Immunity vol. 54 1377–1391 Preprint at https://doi.org/10.1016/j.immuni.2021.06.006 (2021).

187. Furze, R. C., & Rankin, S. M. (2008). Neutrophil mobilization and clearance in the bone marrow. *Immunology, 125*(3), 281–288. https://doi.org/10.1111/j.1365-2567.2008.02950.x

188. Owens, T., Benmamar-Badel, A., Wlodarczyk, A., Marczynska, J., Mørch, M. T., Dubik, M., Arengoth, D. S., Asgari, N., Webster, G., & Khorooshi, R. (2020). Protective roles for myeloid cells in neuroinflammation. *Scandinavian Journal of Immunology, 92*(5). https://doi.org/10.1111/sji.12963

189. Giladi, A., Paul, F., Herzog, Y., Lubling, Y., Weiner, A., Yofe, I., Jaitin, D., Cabezas-Wallscheid, N., Dress, R., Ginhoux, F., Trumpp, A., Tanay, A., & Amit, I. (2018). Single-cell characterization of haematopoietic progenitors and their trajectories in homeostasis and perturbed haematopoiesis. *Nature Cell Biology, 20*(7), 836–846. https://doi.org/10.1038/s41556-018-0121-4

190. Naik, S. H., Perié, L., Swart, E., Gerlach, C., Van Rooij, N., De Boer, R. J., & Schumacher, T. N. (2013). Diverse and heritable lineage imprinting of early haematopoietic progenitors. *Nature, 496*(7444), 229–232. https://doi.org/10.1038/nature12013

191. Evrard, M., Kwok, I. W., Chong, S. Z., Teng, K. W., Becht, E., Chen, J., Sieow, J. L., Penny, H. L., Ching, G. C., Devi, S., Adrover, J. M., Li, J. L., Liong, K. H., Tan, L., Poon, Z., Foo, S., Chua, J. W., Su, I., Balabanian, K., . . . Ng, L. G. (2018). Developmental analysis of bone marrow neutrophils reveals populations specialized in expansion, trafficking, and effector functions. *Immunity, 48* (2), 364-379.e8. https://doi.org/10.1016/j.immuni.2018.02.002

192. Kim, M., Yang, D., Kim, M., Kim, S., Kim, D., & Kang, S. (2017). A late-lineage murine neutrophil precursor population exhibits dynamic changes during demand-adapted granulopoiesis. *Scientific Reports, 7* (1). https://doi.org/10.1038/srep39804

193. Kwok, I., Becht, E., Xia, Y., Ng, M., Teh, Y. C., Tan, L., Evrard, M., Li, J. L., Tran, H. T., Tan, Y., Liu, D., Mishra, A., Liong, K. H., Leong, K., Zhang, Y., Olsson, A., Mantri, C. K., Shyamsunder, P., Liu, Z., . . . Ng, L. G. (2020). Combinatorial Single-Cell analyses of Granulocyte-Monocyte progenitor heterogeneity reveals an early uni-potent

neutrophil progenitor. *Immunity, 53* (2), 303-318.e5. https://doi.org/10.1016/j.immuni.2020.06.005

194. Athens, J. W., Haab, O. P., Raab, S. O., Mauer, A. M., Ashenbrucker, H., Cartwright, G. E., & Wintrobe, M. M. (1961). LEUKOKINETIC STUDIES. IV. THE TOTAL BLOOD, CIRCULATING AND MARGINAL GRANULOCYTE POOLS AND THE GRANULOCYTE TURNOVER RATE IN NORMAL SUBJECTS. *Journal of Clinical Investigation, 40* (6), 989–995. https://doi.org/10.1172/jci104338

195. Lahoz-Beneytez, J., Elemans, M., Zhang, Y., Ahmed, R., Salam, A., Block, M., Niederalt, C., Asquith, B., & Macallan, D. (2016). Human neutrophil kinetics: modeling of stable isotope labeling data supports short blood neutrophil half-lives. *Blood, 127* (26), 3431–3438. https://doi.org/10.1182/blood-2016-03-700336

196. Palomino-Segura, M., Sicilia, J., Ballesteros, I., & Hidalgo, A. (2023). Strategies of neutrophil diversification. *Nature Immunology, 24* (4), 575–584. https://doi.org/10.1038/s41590-023-01452-x

197. Ussov, W. Y., Aktolun, C., Myers, M. J., Jamar, F., & Peters, A. M. (1995). Granulocyte margination in bone marrow: comparison with margination in the spleen and liver. *Scandinavian Journal of Clinical and Laboratory Investigation, 55*(1), 87–96. https://doi.org/10.3109/00365519509075382

198. Hidalgo, A., Chilvers, E. R., Summers, C., & Koenderman, L. (2019). The neutrophil life cycle. *Trends in Immunology, 40* (7), 584–597. https://doi.org/10.1016/j.it.2019.04.013

199. Grieshaber-Bouyer, R., Radtke, F. A., Cunin, P., Stifano, G., Levescot, A., Vijaykumar, B., Nelson-Maney, N., Blaustein, R. B., Monach, P. A., Nigrovic, P. A., Aguilar, O., Allan, R., Astarita, J., Austen, K. F., Barrett, N., Baysoy, A., Benoist, C., Brown, B. D., Buechler, M., . . . Yoshida, H. (2021). The neutrotime transcriptional signature defines a single continuum of neutrophils across biological compartments. *Nature Communications, 12* (1). https://doi.org/10.1038/s41467-021-22973-9

200. Deniset, J. F., Surewaard, B. G., Lee, W., & Kubes, P. (2017). Splenic Ly6Ghigh mature and Ly6Gint immature neutrophils contribute to eradication of S. pneumoniae. *The Journal of Experimental Medicine, 214* (5), 1333–1350. https://doi.org/10.1084/jem.20161621

201. Guilliams, M., Mildner, A., & Yona, S. (2018). Developmental and functional heterogeneity of monocytes. *Immunity, 49* (4), 595–613. https://doi.org/10.1016/j.immuni.2018.10.005

202. Adrover, J. M., Aroca-Crevillén, A., Crainiciuc, G., Ostos, F., Rojas-Vega, Y., Rubio-Ponce, A., Cilloniz, C., Bonzón-Kulichenko, E., Calvo, E., Rico, D., Moro, M. A., Weber, C., Lizasoaín, I., Torres, A., Ruiz-Cabello, J., Vázquez, J., & Hidalgo, A. (2020). Programmed 'disarming' of the neutrophil proteome reduces the magnitude of inflammation. *Nature Immunology, 21*(2), 135–144. https://doi.org/10.1038/s41590-019-0571-2

203. Papayannopoulos, V., Metzler, K. D., Hakkim, A., & Zychlinsky, A. (2010). Neutrophil elastase and myeloperoxidase regulate the formation of neutrophil extracellular traps. *The Journal of Cell Biology, 191*(3), 677–691. https://doi.org/10.1083/jcb.201006052

204. Papayannopoulos, V. (2017). Neutrophil extracellular traps in immunity and disease. Nature Reviews. *Immunology, 18*(2), 134–147. https://doi.org/10.1038/nri.2017.105

205. Allen, C., Thornton, P., Denes, A., McColl, B. W., Pierozynski, A., Monestier, M., Pinteaux, E., Rothwell, N. J., & Allan, S. M. (2012). Neutrophil Cerebrovascular Transmigration Triggers Rapid Neurotoxicity through Release of Proteases Associated with Decondensed DNA. *The Journal of Immunology, 189*(1), 381–392. https://doi.org/10.4049/jimmunol.1200409

206. Kang, L., Yu, H., Yang, X., Zhu, Y., Bai, X., Wang, R., Cao, Y., Xu, H., Luo, H., Lu, L., Shi, M., Tian, Y., Fan, W., & Zhao, B. (2020). Neutrophil extracellular traps released by neutrophils impair revascularization and vascular remodeling after stroke. *Nature Communications, 11*(1). https://doi.org/10.1038/s41467-020-16191-y

207. Wong, S. L., Demers, M., Martinod, K., Gallant, M., Wang, Y., Goldfine, A. B., Kahn, C. R., & Wagner, D. D. (2015). Diabetes primes neutrophils to undergo NETosis, which impairs wound healing. *Nature Medicine, 21* (7), 815–819. https://doi.org/10.1038/nm.3887

208. Aldabbous, L., Abdul-Salam, V., McKinnon, T., Duluc, L., Pepke-Zaba, J., Southwood, M., Ainscough, A. J., Hadinnapola, C., Wilkins, M. R., Toshner, M., & Wojciak-Stothard, B. (2016). Neutrophil extracellular traps promote angiogenesis. *Arteriosclerosis Thrombosis and Vascular Biology, 36* (10), 2078–2087. https://doi.org/10.1161/atvbaha.116.307634

209. Grist, J. J., Marro, B. S., Skinner, D. D., Syage, A. R., Worne, C., Doty, D. J., Fujinami, R. S., & Lane, T. E. (2018). Induced CNS expression of CXCL1 augments neurologic disease in a murine model of multiple sclerosis via enhanced neutrophil recruitment. *European Journal of Immunology, 48* (7), 1199–1210. https://doi.org/10.1002/eji.201747442

210. McColl, S. R., Staykova, M. A., Wozniak, A., Fordham, S., Bruce, J., & Willenborg, D. O. (1998). Treatment with Anti-Granulocyte Antibodies Inhibits the Effector Phase of Experimental Autoimmune Encephalomyelitis. *The Journal of Immunology, 161* (11), 6421–6426. https://doi.org/10.4049/jimmunol.161.11.6421

211. Määttä, J. A., Sjöholm, U. R., Nygårdas, P. T., Salmi, A. A., & Hinkkanen, A. E. (1998). Neutrophils secreting tumor necrosis factor alpha infiltrate the central nervous system of BALB/c mice with experimental autoimmune encephalomyelitis. *Journal of Neuroimmunology, 90*(2), 162–175. https://doi.org/10.1016/s0165-5728(98)00135-0

212. Minns, D., Smith, K. J., Alessandrini, V., Hardisty, G., Melrose, L., Jackson-Jones, L., MacDonald, A. S., Davidson, D. J., & Findlay, E. G. (2021). The neutrophil antimicrobial

peptide cathelicidin promotes Th17 differentiation. *Nature Communications, 12* (1). https://doi.org/10.1038/s41467-021-21533-5

213. Steinbach, K., Piedavent, M., Bauer, S., Neumann, J. T., & Friese, M. A. (2013). Neutrophils amplify autoimmune central nervous system infiltrates by maturing local APCs. *The Journal of Immunology, 191* (9), 4531–4539. https://doi.org/10.4049/jimmunol.1202613

214. Gabrilovich, D. I., Bronte, V., Chen, S., Colombo, M. P., Ochoa, A., Ostrand-Rosenberg, S., & Schreiber, H. (2007). The terminology issue for Myeloid-Derived suppressor cells. *Cancer Research, 67* (1), 425. https://doi.org/10.1158/0008-5472.can-06-3037

215. Marigo, I., Bosio, E., Solito, S., Mesa, C., Fernandez, A., Dolcetti, L., Ugel, S., Sonda, N., Bicciato, S., Falisi, E., Calabrese, F., Basso, G., Zanovello, P., Cozzi, E., Mandruzzato, S., & Bronte, V. (2010). Tumor-Induced tolerance and immune suppression depend on the C/EBPβ transcription factor. *Immunity, 32* (6), 790–802. https://doi.org/10.1016/j.immuni.2010.05.010

216. Poschke, I., Mougiakakos, D., Hansson, J., Masucci, G. V., & Kiessling, R. (2010). Immature Immunosuppressive CD14+HLA-DR−/low Cells in Melanoma Patients Are Stat3hi and Overexpress CD80, CD83, and DC-Sign. *Cancer Research, 70* (11), 4335–4345. https://doi.org/10.1158/0008-5472.can-09-3767

217. Gabrilovich, D. I. (2017). Myeloid-Derived suppressor cells. *Cancer Immunology Research, 5* (1), 3–8. https://doi.org/10.1158/2326-6066.cir-16-0297

218. Gabrilovich, D. I., & Nagaraj, S. (2009). Myeloid-derived suppressor cells as regulators of the immune system. *Nature Reviews. Immunology, 9* (3), 162–174. https://doi.org/10.1038/nri2506

219. Molon, B., Ugel, S., Del Pozzo, F., Soldani, C., Zilio, S., Avella, D., De Palma, A., Mauri, P., Monegal, A., Rescigno, M., Savino, B., Colombo, P., Jonjic, N., Pecanic, S., Lazzarato, L., Fruttero, R., Gasco, A., Bronte, V., & Viola, A. (2011). Chemokine nitration prevents intratumoral infiltration of antigen-specific T cells. *The Journal of Experimental Medicine, 208* (10), 1949–1962. https://doi.org/10.1084/jem.20101956

220. Jiang, Q., Duan, J., Van Kaer, L., & Yang, G. (2023). The role of Myeloid-Derived suppressor cells in multiple sclerosis and its animal model. *Aging and Disease, 0*. https://doi.org/10.14336/ad.2023.0323-1

221. Condamine, T., & Gabrilovich, D. I. (2010). Molecular mechanisms regulating myeloid-derived suppressor cell differentiation and function. *Trends in Immunology, 32* (1), 19–25. https://doi.org/10.1016/j.it.2010.10.002

222. Condamine, T., Mastio, J., & Gabrilovich, D. I. (2015). Transcriptional regulation of myeloid-derived suppressor cells. *Journal of Leukocyte Biology, 98* (6), 913–922. https://doi.org/10.1189/jlb.4ri0515-204r

223. Zhao, Z., Qin, J., Qian, Y., Huang, C., Liu, X., Wang, N., Li, L., Chao, Y., Tan, B., Zhang, N., Qian, M., Li, D., Liu, M., & Du, B. (2024). FFAR2 expressing myeloid-derived suppressor cells drive cancer immunoevasion. *Journal of Hematology & Oncology, 17* (1). https://doi.org/10.1186/s13045-024-01529-6

224. Alshetaiwi, H., Pervolarakis, N., McIntyre, L. L., Ma, D., Nguyen, Q., Rath, J. A., Nee, K., Hernandez, G., Evans, K., Torosian, L., Silva, A., Walsh, C., & Kessenbrock, K. (2020). Defining the emergence of myeloid-derived suppressor cells in breast cancer using single-cell transcriptomics. *Science Immunology, 5* (44). https://doi.org/10.1126/sciimmunol.aay6017

225. Casacuberta-Serra, S., Costa, C., Eixarch, H., Mansilla, M. J., López-Estévez, S., Martorell, L., Parés, M., Montalban, X., Espejo, C., & Barquinero, J. (2016). Myeloid-derived suppressor cells expressing a self-antigen ameliorate experimental autoimmune encephalomyelitis. *Experimental Neurology, 286*, 50–60. https://doi.org/10.1016/j.expneurol.2016.09.012

226. Parekh, V. V., Wu, L., Olivares-Villagómez, D., Wilson, K. T., & Van Kaer, L. (2013). Activated invariant NKT cells control central nervous system autoimmunity in a mechanism that involves Myeloid-Derived suppressor cells. *The Journal of Immunology, 190* (5), 1948–1960. https://doi.org/10.4049/jimmunol.1201718

227. Zhu, B., Bando, Y., Xiao, S., Yang, K., Anderson, A. C., Kuchroo, V. K., & Khoury, S. J. (2007). CD11B+LY-6CHI suppressive monocytes in experimental autoimmune encephalomyelitis. *The Journal of Immunology, 179* (8), 5228–5237. https://doi.org/10.4049/jimmunol.179.8.5228

228. Wegner, A., Verhagen, J., & Wraith, D. C. (2017). Myeloid-derived suppressor cells mediate tolerance induction in autoimmune disease. *Immunology, 151* (1), 26–42. https://doi.org/10.1111/imm.12718

229. Ioannou, M., Alissafi, T., Lazaridis, I., Deraos, G., Matsoukas, J., Gravanis, A., Mastorodemos, V., Plaitakis, A., Sharpe, A., Boumpas, D., & Verginis, P. (2011). Crucial role of granulocytic Myeloid-Derived suppressor cells in the regulation of central nervous system autoimmune disease. *The Journal of Immunology, 188* (3), 1136–1146. https://doi.org/10.4049/jimmunol.1101816

230. Khorooshi, R., Marczynska, J., Dieu, R. S., Wais, V., Hansen, C. R., Kavan, S., Thomassen, M., Burton, M., Kruse, T., Webster, G. A., & Owens, T. (2020). Innate signaling within the central nervous system recruits protective neutrophils. *Acta Neuropathologica Communications, 8* (1). https://doi.org/10.1186/s40478-019-0876-2

231. Melero-Jerez, C., Fernández-Gómez, B., Lebrón-Galán, R., Ortega, M. C., Lara, I. S., Ojalvo, A. C., Clemente, D., & De Castro, F. (2020). Myeloid-derived suppressor cells support remyelination in a murine model of multiple sclerosis by promoting oligodendrocyte precursor cell survival, proliferation, and differentiation. *Glia, 69* (4), 905–924. https://doi.org/10.1002/glia.23936

232. Glenn, J. D., Liu, C., & Whartenby, K. A. (2019). Frontline Science: Induction of experimental autoimmune encephalomyelitis mobilizes Th17-promoting myeloid derived suppressor cells to the lung. *Journal of Leukocyte Biology, 105* (5), 829–841. https://doi.org/10.1002/jlb.4hi0818-335r

233. Yi, H., Guo, C., Yu, X., Zuo, D., & Wang, X. (2012). Mouse CD11B+GR-1+ myeloid cells can promote TH17 cell differentiation and experimental autoimmune encephalomyelitis. *The Journal of Immunology, 189* (9), 4295–4304. https://doi.org/10.4049/jimmunol.1200086

234. Ortega, M. C., Lebrón-Galán, R., Machín-Díaz, I., Naughton, M., Pérez-Molina, I., García-Arocha, J., Garcia-Dominguez, J. M., Goicoechea-Briceño, H., Sol, V. V., Quintanero-Casero, V., García-Montero, R., Galán, V., Calahorra, L., Camacho-Toledano, C., Martínez-Ginés, M. L., Fitzgerald, D. C., & Clemente, D. (2023). Central and peripheral myeloid-derived suppressor cell-like cells are closely related to the clinical severity of multiple sclerosis. *Acta Neuropathologica, 146* (2), 263–282. https://doi.org/10.1007/s00401-023-02593-x

235. Wang, Z., Zheng, G., Li, G., Wang, M., Ma, Z., Li, H., Wang, X., & Yi, H. (2020). Methylprednisolone alleviates multiple sclerosis by expanding myeloid-derived suppressor cells via glucocorticoid receptor β and S100A8/9 up-regulation. *Journal of Cellular and Molecular Medicine, 24* (23), 13703–13714. https://doi.org/10.1111/jcmm.15928

236. Dopkins, N., Miranda, K., Wilson, K., Holloman, B. L., Nagarkatti, P., & Nagarkatti, M. (2021). Effects of orally administered cannabidiol on neuroinflammation and intestinal inflammation in the attenuation of experimental autoimmune encephalomyelitis. *Journal of Neuroimmune Pharmacology, 17* (1–2), 15–32. https://doi.org/10.1007/s11481-021-10023-6

237. Elliott, D. M., Singh, N., Nagarkatti, M., & Nagarkatti, P. S. (2018). Cannabidiol attenuates experimental autoimmune encephalomyelitis model of multiple sclerosis through induction of Myeloid-Derived suppressor cells. *Frontiers in Immunology, 9*. https://doi.org/10.3389/fimmu.2018.01782

238. Melero-Jerez, C., Suardíaz, M., Lebrón-Galán, R., Marín-Bañasco, C., Oliver-Martos, B., Machín-Díaz, I., Fernández, Ó., De Castro, F., & Clemente, D. (2019). The presence and suppressive activity of myeloid-derived suppressor cells are potentiated after interferon-β treatment in a murine model of multiple sclerosis. *Neurobiology of Disease, 127*, 13–31. https://doi.org/10.1016/j.nbd.2019.02.014

239. Tzartos, J. S., Friese, M. A., Craner, M. J., Palace, J., Newcombe, J., Esiri, M. M., & Fugger, L. (2007). Interleukin-17 Production in Central Nervous System-Infiltrating T Cells and Glial Cells Is Associated with Active Disease in Multiple Sclerosis. *American Journal of Pathology, 172* (1), 146–155. https://doi.org/10.2353/ajpath.2008.070690

240. Lock, C., Hermans, G., Pedotti, R., Brendolan, A., Schadt, E., Garren, H., Langer-Gould, A., Strober, S., Cannella, B., Allard, J., Klonowski, P., Austin, A., Lad, N., Kaminski, N.,

Galli, S. J., Oksenberg, J. R., Raine, C. S., Heller, R., & Steinman, L. (2002). Gene-microarray analysis of multiple sclerosis lesions yields new targets validated in autoimmune encephalomyelitis. *Nature Medicine, 8* (5), 500–508. https://doi.org/10.1038/nm0502-500

241. Eyerich, K., Dimartino, V., & Cavani, A. (2017). IL-17 and IL-22 in immunity: Driving protection and pathology. *European Journal of Immunology, 47* (4), 607–614. https://doi.org/10.1002/eji.201646723

242. Mills, K. H. G. (2022). IL-17 and IL-17-producing cells in protection versus pathology. *Nature Reviews. Immunology, 23* (1), 38–54. https://doi.org/10.1038/s41577-022-00746-9

243. Zimmermann, J., Nitsch, L., Krauthausen, M., & Müller, M. (2023). IL-17A Facilitates Entry of Autoreactive T-Cells and Granulocytes into the CNS During EAE. *NeuroMolecular Medicine, 25* (3), 350–359. https://doi.org/10.1007/s12017-023-08739-0

244. Haas, J. D., Ravens, S., Düber, S., Sandrock, I., Oberdörfer, L., Kashani, E., Chennupati, V., Föhse, L., Naumann, R., Weiss, S., Krueger, A., Förster, R., & Prinz, I. (2012). Development of Interleukin-17-Producing γδ T Cells Is Restricted to a Functional Embryonic Wave. *Immunity, 37* (1), 48–59. https://doi.org/10.1016/j.immuni.2012.06.003

245. Malki, K. E., Karbach, S. H., Huppert, J., Zayoud, M., Reißig, S., Schüler, R., Nikolaev, A., Karram, K., Münzel, T., Kuhlmann, C. R., Luhmann, H. J., Von Stebut, E., Wörtge, S., Kurschus, F. C., & Waisman, A. (2012). An alternative pathway of Imiquimod-Induced Psoriasis-Like skin inflammation in the absence of interleukin-17 receptor A signaling. *Journal of Investigative Dermatology, 133* (2), 441–451. https://doi.org/10.1038/jid.2012.318

246. Cuervo, H., Pereira, B., Nadeem, T., Lin, M., Lee, F., Kitajewski, J., & Lin, C. (2017). PDGFRβ-P2A-CreERT2 mice: a genetic tool to target pericytes in angiogenesis. *Angiogenesis, 20* (4), 655–662. https://doi.org/10.1007/s10456-017-9570-9

247. Akhavanpoor, M., Gleissner, C. A., Gorbatsch, S., Doesch, A., Akhavanpoor, H., Wangler, S., Jahn, F., Lasitschka, F., Katus, H., & Erbel, C. (2014). CCL19 and CCL21 modulate the inflammatory milieu in atherosclerotic lesions. *Drug Design Development and Therapy*, 2359. https://doi.org/10.2147/dddt.s72394

248. Post, J. M., Lerner, R., Schwitter, C., Lutz, B., Lomazzo, E., & Bindila, L. (2022). Lipidomics and transcriptomics in neurological diseases. *Journal of Visualized Experiments, 181*. https://doi.org/10.3791/59423

249. Rustenhoven, J., Drieu, A., Mamuladze, T., De Lima, K. A., Dykstra, T., Wall, M., Papadopoulos, Z., Kanamori, M., Salvador, A. F., Baker, W., Lemieux, M., Da Mesquita, S., Cugurra, A., Fitzpatrick, J., Sviben, S., Kossina, R., Bayguinov, P., Townsend, R. R., Zhang, Q., . . . Kipnis, J. (2021). Functional characterization of the dural sinuses as a

neuroimmune interface. *Cell, 184* (4), 1000-1016.e27. https://doi.org/10.1016/j.cell.2020.12.040

250. Shanmugavadivu, A., Carter, K., Zonouzi, A. P., Waisman, A., & Regen, T. (2024). Protocol for the collection and analysis of the different immune cell subsets in the murine intestinal lamina propria. *STAR Protocols, 5* (3), 103154. https://doi.org/10.1016/j.xpro.2024.103154

251. Louveau, A., Herz, J., Alme, M. N., Salvador, A. F., Dong, M. Q., Viar, K. E., Herod, S. G., Knopp, J., Setliff, J. C., Lupi, A. L., Da Mesquita, S., Frost, E. L., Gaultier, A., Harris, T. H., Cao, R., Hu, S., Lukens, J. R., Smirnov, I., Overall, C. C., . . . Kipnis, J. (2018). CNS lymphatic drainage and neuroinflammation are regulated by meningeal lymphatic vasculature. *Nature Neuroscience, 21*(10), 1380–1391. https://doi.org/10.1038/s41593-018-0227-9

252. Paul, F., Arkin, Y., Giladi, A., Jaitin, D. A., Kenigsberg, E., Keren-Shaul, H., Winter, D., Lara-Astiaso, D., Gury, M., Weiner, A., David, E., Cohen, N., Lauridsen, F. K. B., Haas, S., Schlitzer, A., Mildner, A., Ginhoux, F., Jung, S., Trumpp, A., . . . Amit, I. (2015). Transcriptional heterogeneity and lineage commitment in myeloid progenitors. *Cell, 163* (7), 1663–1677. https://doi.org/10.1016/j.cell.2015.11.013

253. Brinkmann, V., Davis, M. D., Heise, C. E., Albert, R., Cottens, S., Hof, R., Bruns, C., Prieschl, E., Baumruker, T., Hiestand, P., Foster, C. A., Zollinger, M., & Lynch, K. R. (2002). The immune modulator FTY720 targets sphingosine 1-Phosphate receptors. *Journal of Biological Chemistry, 277* (24), 21453–21457. https://doi.org/10.1074/jbc.c200176200

254. Förster, R., Davalos-Misslitz, A. C., & Rot, A. (2008). CCR7 and its ligands: balancing immunity and tolerance. *Nature Reviews. Immunology, 8* (5), 362–371. https://doi.org/10.1038/nri2297

255. Debes, G. F., Arnold, C. N., Young, A. J., Krautwald, S., Lipp, M., Hay, J. B., & Butcher, E. C. (2005). Chemokine receptor CCR7 required for T lymphocyte exit from peripheral tissues. *Nature Immunology, 6* (9), 889–894. https://doi.org/10.1038/ni1238

256. Korpos, E., Wu, C., Song, J., Hallmann, R., & Sorokin, L. (2009). Role of the extracellular matrix in lymphocyte migration. *Cell and Tissue Research, 339* (1), 47–57. https://doi.org/10.1007/s00441-009-0853-3

257. Tsutsui, M., Hirase, R., Miyamura, S., Nagayasu, K., Nakagawa, T., Mori, Y., Shirakawa, H., & Kaneko, S. (2018). TRPM2 exacerbates central nervous system inflammation in experimental autoimmune encephalomyelitis by increasing production of CXCL2 chemokines. *Journal of Neuroscience, 38* (39), 8484–8495. https://doi.org/10.1523/jneurosci.2203-17.2018

258. Wu, X., Briseño, C. G., Grajales-Reyes, G. E., Haldar, M., Iwata, A., Kretzer, N. M., Kc, W., Tussiwand, R., Higashi, Y., Murphy, T. L., & Murphy, K. M. (2016). Transcription factor Zeb2 regulates commitment to plasmacytoid dendritic cell and monocyte fate.

Proceedings of the National Academy of Sciences, 113 (51), 14775–14780. https://doi.org/10.1073/pnas.1611408114

259. Li, Y., Wang, W., Yang, F., Xu, Y., Feng, C., & Zhao, Y. (2019). The regulatory roles of neutrophils in adaptive immunity. *Cell Communication and Signaling, 17* (1). https://doi.org/10.1186/s12964-019-0471-y

260. Amorim, A., De Feo, D., Friebel, E., Ingelfinger, F., Anderfuhren, C. D., Krishnarajah, S., Andreadou, M., Welsh, C. A., Liu, Z., Ginhoux, F., Greter, M., & Becher, B. (2022). IFNγ and GM-CSF control complementary differentiation programs in the monocyte-to-phagocyte transition during neuroinflammation. *Nature Immunology, 23* (2), 217–228. https://doi.org/10.1038/s41590-021-01117-7

261. Kurte, M., Luz-Crawford, P., Vega-Letter, A. M., Contreras, R. A., Tejedor, G., Elizondo-Vega, R., Martinez-Viola, L., Fernández-O'Ryan, C., Figueroa, F. E., Jorgensen, C., Djouad, F., & Carrión, F. (2018). IL17/IL17RA as a novel signaling axis driving mesenchymal stem cell therapeutic function in experimental autoimmune encephalomyelitis. *Frontiers in Immunology, 9*. https://doi.org/10.3389/fimmu.2018.00802

262. Liu, R., Lauridsen, H. M., Amezquita, R. A., Pierce, R. W., Jane-Wit, D., Fang, C., Pellowe, A. S., Kirkiles-Smith, N. C., Gonzalez, A. L., & Pober, J. S. (2016). IL-17 promotes Neutrophil-Mediated immunity by activating microvascular pericytes and not endothelium. *The Journal of Immunology, 197* (6), 2400–2408. https://doi.org/10.4049/jimmunol.1600138

263. Hurtado-Alvarado, G., Cabañas-Morales, A. M., & Gómez-Gónzalez, B. (2014). Pericytes: brain-immune interface modulators. *Frontiers in Integrative Neuroscience, 7*. https://doi.org/10.3389/fnint.2013.00080

264. Török, O., Schreiner, B., Schaffenrath, J., Tsai, H., Maheshwari, U., Stifter, S. A., Welsh, C., Amorim, A., Sridhar, S., Utz, S. G., Mildenberger, W., Nassiri, S., Delorenzi, M., Aguzzi, A., Han, M. H., Greter, M., Becher, B., & Keller, A. (2021). Pericytes regulate vascular immune homeostasis in the CNS. *Proceedings of the National Academy of Sciences, 118* (10). https://doi.org/10.1073/pnas.2016587118

265. Langrish, C. L., Chen, Y., Blumenschein, W. M., Mattson, J., Basham, B., Sedgwick, J. D., McClanahan, T., Kastelein, R. A., & Cua, D. J. (2005). IL-23 drives a pathogenic T cell population that induces autoimmune inflammation. *The Journal of Experimental Medicine, 201* (2), 233–240. https://doi.org/10.1084/jem.20041257

266. Wing, A. C., Hygino, J., Ferreira, T. B., Kasahara, T. M., Barros, P. O., Sacramento, P. M., Andrade, R. M., Camargo, S., Rueda, F., Alves-Leon, S. V., Vasconcelos, C. C., Alvarenga, R., & Bento, C. a. M. (2015). Interleukin-17- and interleukin-22-secreting myelin-specific CD4+ T cells resistant to corticoids are related with active brain lesions in multiple sclerosis patients. *Immunology, 147* (2), 212–220. https://doi.org/10.1111/imm.12552

267. Nagata, T., Mckinley, L., Peschon, J. J., Alcorn, J. F., Aujla, S. J., & Kolls, J. K. (2008). Requirement of IL-17RA in CON A induced hepatitis and negative regulation of IL-17 production in mouse T cells. *The Journal of Immunology, 181* (11), 7473–7479. https://doi.org/10.4049/jimmunol.181.11.7473

268. Smith, E., Stark, M. A., Zarbock, A., Burcin, T. L., Bruce, A. C., Vaswani, D., Foley, P., & Ley, K. (2008). IL-17A Inhibits the Expansion of IL-17A-Producing T Cells in Mice through "Short-Loop" Inhibition via IL-17 Receptor. *The Journal of Immunology, 181* (2), 1357–1364. https://doi.org/10.4049/jimmunol.181.2.1357

269. Li, Z., Zhang, C., Zong, X., Wang, Z., Ren, R., Wang, L., Sun, P., Zhu, C., Guo, M., Guo, G., Hu, G., & Wu, Y. (2022). ST8SIA6-AS1 promotes the Epithelial-to-Mesenchymal transition and angiogenesis of pituitary adenoma. *Journal of Oncology, 2022*, 1–15. https://doi.org/10.1155/2022/7960261

270. Van Kaer, L., Wu, L., & Parekh, V. V. (2015). Natural killer T cells in multiple sclerosis and its animal model, experimental autoimmune encephalomyelitis. *Immunology, 146* (1), 1–10. https://doi.org/10.1111/imm.12485

271. Kawakami, N., Lassmann, S., Li, Z., Odoardi, F., Ritter, T., Ziemssen, T., Klinkert, W. E., Ellwart, J. W., Bradl, M., Krivacic, K., Lassmann, H., Ransohoff, R. M., Volk, H., Wekerle, H., Linington, C., & FlüGel, A. (2004). The activation status of neuroantigen-specific T cells in the target organ determines the clinical outcome of autoimmune encephalomyelitis. *The Journal of Experimental Medicine, 199*(2), 185–197. https://doi.org/10.1084/jem.20031064

272. Hannocks, M., Zhang, X., Gerwien, H., Chashchina, A., Burmeister, M., Korpos, E., Song, J., & Sorokin, L. (2017). The gelatinases, MMP-2 and MMP-9, as fine tuners of neuroinflammatory processes. *Matrix Biology, 75–76*, 102–113. https://doi.org/10.1016/j.matbio.2017.11.007

273. Van Den Steen, P. E., Proost, P., Wuyts, A., Van Damme, J., & Opdenakker, G. (2000). Neutrophil gelatinase B potentiates interleukin-8 tenfold by aminoterminal processing, whereas it degrades CTAP-III, PF-4, and GRO-α and leaves RANTES and MCP-2 intact. *Blood, 96* (8), 2673–2681. https://doi.org/10.1182/blood.v96.8.2673

274. Song, J., Wu, C., Korpos, E., Zhang, X., Agrawal, S. M., Wang, Y., Faber, C., Schäfers, M., Körner, H., Opdenakker, G., Hallmann, R., & Sorokin, L. (2015). Focal MMP-2 and MMP-9 activity at the Blood-Brain barrier promotes Chemokine-Induced leukocyte migration. *Cell Reports, 10* (7), 1040–1054. https://doi.org/10.1016/j.celrep.2015.01.037

275. Zhang, C., Chen, J., Wang, H., Chen, J., Zheng, M., Chen, X., Zhang, L., Liang, C., & Zhan, C. (2022). IL -17 exacerbates experimental autoimmune prostatitis via CXCL1 / CXCL2 - mediated neutrophil infiltration. *Andrologia, 54* (8). https://doi.org/10.1111/and.14455

276. Odoardi, F., Kawakami, N., Klinkert, W. E. F., Wekerle, H., & Flügel, A. (2007). Blood-borne soluble protein antigen intensifies T cell activation in autoimmune CNS lesions

and exacerbates clinical disease. *Proceedings of the National Academy of Sciences, 104*(47), 18625–18630. https://doi.org/10.1073/pnas.0705033104

277. Qu, Z., Han, Y., Zhu, Q., Ding, W., Wang, Y., Zhang, Y., Wei, W., Lei, Y., Li, M., Jiao, Y., Gu, K., & Zhang, Y. (2023). A novel neutrophil extracellular traps signature for overall survival prediction and tumor microenvironment identification in gastric cancer. *Journal of Inflammation Research, Volume 16*, 3419–3436. https://doi.org/10.2147/jir.s417182

278. Negri, L., & Ferrara, N. (2018). The prokineticins: neuromodulators and mediators of inflammation and myeloid Cell-Dependent angiogenesis. *Physiological Reviews, 98*(2), 1055–1082. https://doi.org/10.1152/physrev.00012.2017

279. Mack, E. A., Stein, S. J., Rome, K. S., Xu, L., Wertheim, G. B., Melo, R. C. N., & Pear, W. S. (2019). Trib1 regulates eosinophil lineage commitment and identity by restraining the neutrophil program. *Blood, 133* (22), 2413–2426. https://doi.org/10.1182/blood.2018872218

280. Grenier, C., Caillon, A., Munier, M., Grimaud, L., Champin, T., Toutain, B., Fassot, C., Blanc-Brude, O., & Loufrani, L. (2021). Dual role of thrombospondin-1 in Flow-Induced remodeling. *International Journal of Molecular Sciences, 22*(21), 12086. https://doi.org/10.3390/ijms222112086

281. Lu, Y., Nayer, B., Singh, S. K., Alshoubaki, Y. K., Yuan, E., Park, A. J., Maruyama, K., Akira, S., & Martino, M. M. (2024). CGRP sensory neurons promote tissue healing via neutrophils and macrophages. *Nature, 628*(8008), 604–611. https://doi.org/10.1038/s41586-024-07237-y

282. Zenaro, E., Pietronigro, E., Della Bianca, V., Piacentino, G., Marongiu, L., Budui, S., Turano, E., Rossi, B., Angiari, S., Dusi, S., Montresor, A., Carlucci, T., Nanì, S., Tosadori, G., Calciano, L., Catalucci, D., Berton, G., Bonetti, B., & Constantin, G. (2015). Neutrophils promote Alzheimer's disease–like pathology and cognitive decline via LFA-1 integrin. *Nature Medicine, 21* (8), 880–886. https://doi.org/10.1038/nm.3913

283. Chornoguz, O., Grmai, L., Sinha, P., Artemenko, K. A., Zubarev, R. A., & Ostrand-Rosenberg, S. (2010). Proteomic pathway analysis reveals inflammation increases Myeloid-Derived suppressor cell resistance to apoptosis. *Molecular & Cellular Proteomics, 10* (3), M110.002980. https://doi.org/10.1074/mcp.m110.002980

284. Zehntner, S. P., Brickman, C., BourbonnièRe, L., Remington, L., Caruso, M., & Owens, T. (2005). Neutrophils that infiltrate the central nervous system regulate T cell responses. *The Journal of Immunology, 174* (8), 5124–5131. https://doi.org/10.4049/jimmunol.174.8.5124

285. Giraud, J., Chalopin, D., Ramel, E., Boyer, T., Zouine, A., Derieppe, M., Larmonier, N., Adotevi, O., Bail, B. L., Blanc, J., Laurent, C., Chiche, L., Derive, M., Nikolski, M., & Saleh, M. (2024). THBS1+ myeloid cells expand in SLD hepatocellular carcinoma and

contribute to immunosuppression and unfavorable prognosis through TREM1. *Cell Reports, 43* (2), 113773. https://doi.org/10.1016/j.celrep.2024.113773

286. Andreuzzi, E., Fejza, A., Polano, M., Poletto, E., Camicia, L., Carobolante, G., Tarticchio, G., Todaro, F., Di Carlo, E., Scarpa, M., Scarpa, M., Paulitti, A., Capuano, A., Canzonieri, V., Maiero, S., Fornasarig, M., Cannizzaro, R., Doliana, R., Colombatti, A., . . . Mongiat, M. (2022). Colorectal cancer development is affected by the ECM molecule EMILIN-2 hinging on macrophage polarization via the TLR-4/MyD88 pathway. *Journal of Experimental & Clinical Cancer Research, 41*(1). https://doi.org/10.1186/s13046-022-02271-y

287. Zhang, L., Chun, Y., Arditi, Z., Grishina, G., Lo, T., Wisotzkey, K., Agashe, C., Grishin, A., Wang, J., Sampson, H. A., Sicherer, S., Berin, M. C., & Bunyavanich, S. (2024). Joint transcriptomic and cytometric study of children with peanut allergy reveals molecular and cellular cross talk in reaction thresholds. *Journal of Allergy and Clinical Immunology, 153*(6), 1721–1728. https://doi.org/10.1016/j.jaci.2023.12.028

288. Veglia, F., Sanseviero, E., & Gabrilovich, D. I. (2021). Myeloid-derived suppressor cells in the era of increasing myeloid cell diversity. *Nature Reviews. Immunology, 21*(8), 485–498. https://doi.org/10.1038/s41577-020-00490-y

289. Sims, D. E. (1986). The pericyte—A review. *Tissue and Cell, 18* (2), 153–174. https://doi.org/10.1016/0040-8166(86)90026-1

290. Nehls, V., & Drenckhahn, D. (1993). The versatility of microvascular pericytes: from mesenchyme to smooth muscle? *Histochemistry, 99*(1), 1–12. https://doi.org/10.1007/bf00268014

291. Mueller, S. N., & Germain, R. N. (2009). Stromal cell contributions to the homeostasis and functionality of the immune system. *Nature Reviews. Immunology, 9*(9), 618–629. https://doi.org/10.1038/nri2588

8 Acknowledgements

This thesis would not have been possible without the guidance, support, and encouragement of many. I am deeply grateful for the contributions of each person I have encountered on this path.

First and foremost, I would like to thank Dr. Tommy Regen, as this academic accomplishment would have been impossible without him. Tommy, thank you for granting me a position as a PhD student, for your guidance, support, many laughs, and for believing in me as a scientist and a human being. To our IMM Secretary of State, Susi Gahr, thank you for being the super glue holding an entire institute together. To our lab technicians, Michaela Blanfeld, Elena Zurkowski, and Bettina Kalt—You are the unspoken heroes of all of our experiments—thank you sincerely for your patience, your dedicated time and many efforts. I also want to extend thanks to the collaborators of this project, including Dr. Matthias Klein for help in generating the single cell dataset, Dr. Laura Bindila for the lipidomics analysis, and Dr. Federico Marini for the thorough analysis of single cell data and for making it oh-so *fun*.

The encouraging environment of the IMM was one of the highlights of my time here. Many people contributed to this in ways, large and small, not all of which I can mention here, but all of whom I am grateful to. To Dr. Nadine Hövelmeyer and Dr. Björn Clausen, you strengthened me and supported me in ways I do not have enough words to thank you for. Thank you for showing up for me, for believing me, and for your integrity and acknowledgement that the respect of human beings is the foundation for performing good science. To Dr. Arthi Shanmugavadivu, thank you for being a mentor and friend to me as a young scientist. Thanks to Theresa Schaller and Eva Schramm-Hermann for running this road with me from start to finish. I'm grateful for the way our friendship has evolved over the course of a PhD. Thanks as well to Dr. Lisa Johann, Dr. Nishada Ramphal, Dr. Jefferson Antonio Leite, and Dr. Ilgiz Mufazalov for the stimulating scientific discussions and honest inputs. To Rebecca Jasser, Zeynep Ergun, and Aysan Poursadegh-Zonouzi for being sources of friendship that are honest and true, that lift me when I'm low, and humble me when I'm soaring too high. And finally, to Hannah Münster for reading my thesis and for doing the work to continue this project.

Last but not least, I want to thank my support systems outside of science. To Philipp Latzke, thank you for the many hours of presentation practice at the start of my PhD, for giving me the honest feedback I didn't want, but needed to hear, for withstanding the arguments that resulted from it, and for being one of the dearest sources of friendship I've ever known. Cheers to Café George for the caffeine-fueled writing sessions at my little corner in the back. And finally, thanks to Sophie Terhedebrügge, Maximilian Kaltenborn, Sarah Loibl, and The Cozy Gang at home for being my chosen family and for providing safe spaces that always feel like home.

9 Eidesstattliche Versicherung

Hiermit versichere ich, dass ich die von mir vorgelegte Dissertation angefertigt, die benutzten Quellen und Hilfsmittel vollständig angegeben und die Stellen der Arbeit, einschließlich Tabellen und Abbildungen, die andere Werke im Wortlaut oder dem Sinn nach entnommen sind, in jedem Einzelfall als Entlehnung kenntlich gemacht habe; dass diese Dissertation noch keiner anderen Fakultät oder Universität zur Prüfung vorgelegen hat, dass sie noch nicht veröffentlicht worden ist, sowie dass ich eine solche Veröffentlichung vor Abschluss des Promotionsverfahrens nicht vornehmen werde. Die Bestimmungen dieser Promotionsordnung sind mir bekannt. Die von mir vorgelegte Dissertation ist von Herrn Dr. rer. nat. Tommy Regen betreut worden.

Mainz, Januar 2024 Katlynn Carter

10 Curriculum Vitae

Katlynn Carter

Address: Hindenburgstraße 17
55118 Mainz
Email: kacarter@uni-mainz.de
Telephone: +49 (0) 1577 3424006
Website: www.linkedin.com/in/katlynncarter

EDUCATION

Doctoral Candidate, Neuroimmunology (finalized approximately March 2025) 2019-2024
Johannes Gutenberg University, Mainz, Germany
Dissertation: Interleukin-17 signaling in autoimmunity

Master of Science, Neuroscience (1.6) 2016-2019
University of Bonn, Bonn, Germany
Thesis: Parkinson's Disease and the Gut-Brain Axis: Search for a Responsive Cellular Model to Bacterial Metabolites (grade 1.3)

Bachelor of Science, Biology with Chemistry Minor (1.2) 2012-2016
California State University Channel Islands, Camarillo, CA
Thesis: Cloning of Neuroglobin Regulatory Sequences in Balaenoptera
Magna Cum Laude Graduate

WORK EXPERIENCE

Research Assistant, University Clinic of Mainz 2021-2024
- Supervisor: Prof. Dr. Ari Waisman
- Tasks: Primary cell isolation from tissues, flow cytometry, qPCR, confocal microscopy

Research Assistant (Part-time), University Clinic of Bonn, Bonn, Germany 2019
- Supervisor: Dr. Bernd Evert
- Tasks: Isolation and sequencing of viral DNA (PCR, qPCR, pyrosequencing)

Parkinson's Disease and the Gut-Brain Axis—Search for a Responsive Cellular Model to Bacterial Metabolites, Master thesis, University of Bonn 2018-2019
- Supervisor: Prof. Dr. Ulrich Wüllner & Dr. Bernd Evert
- Tasks: Establishing *in vitro* models to investigate short chain fatty acid signaling (cell culture, flow cytometry, Western blotting, RT-PCR)

Student Research Assistant, University Clinic of Bonn 2017 – 2019
- Supervisor: Prof. Dr. Harald Neumann
- Tasks: Purification and quantification of polysialic acids (HPLC, SDS-PAGE)

RESEARCH EXPERIENCE / SCIENTIFIC ACHIEVEMENTS

Impact of Mitochondrial DNA Mutations on Neurodegenerative Diseases, University of Bonn — Spring 2018

- Task: Investigating regulation of various mitochondrial nucleases (RT-PCR, Southern blotting)

Epigenetic Changes to the Aging Brain, University of Bonn — Winter 2017

- Task: Analysis of histone modifications between cell types and brain regions in aging mice (Immunohistochemistry, microscopy, FIJI software)

Independent Research, Bachelor thesis, CSU Channel Islands, Camarillo, CA, USA — Spring 2016

- Task: Investigating differences in neuroglobin regulatory sequences between cetaceans (Cell culture, tissue digestion, PCR, molecular cloning)

Student Research Assistant, Biology Department at CSU Channel Islands, Camarillo, USA — 2014-2016

- Task: Culture of various human cancer cell lines (cell culture, ELISA)

PROFESSIONAL PRESENTATIONS

European Congress of Immunology, Dublin, Ireland — Sept. 2024
Oral presentation titled '*IL-17 alters neutrophils to promote susceptibility to MOG$_{35-55}$ EAE*'

Brain-Periphery Interplay and CNS Diseases, Leuven, Belgium — Nov. 2023
Poster titled '*An IL-17-dependent microbiome modulates resistance against MOG$_{35-55}$ EAE'*

Cell Symposia: Neuro-Immune Axis, Lisbon, Portugal — Sept. 2022
Poster titled '*IL-17 modulates peripheral immune cell dynamics in CNS autoimmunity*'

SAGE Research Forum**,** Camarillo, CA — May 2015
Poster of Bachelor thesis '*Cloning of neuroglobin regulatory sequences in Balaenoptera*'

California State University Research Competition, San Bernadino, CA — April 2015
Talk titled '*Analysis of properties of proposed anti-cancer agents against female cancer cell lines*'

American Society for Biotechnology and Molecular Biology, Boston, MA — March 2015
Poster titled '*Effect of anti-cancer agents on invasiveness of cancer cells*'

Southern California Conference for Undergraduate Research, Fullerton, CA — Nov. 2014
Poster titled '*Profiling of normal and cancer cell lines by phenotypic microarray*'

FURTHER TRAINING (SOCIAL & PROFESSIONAL)

Special Skills	Software	Languages
Animal handling (FELASA certified)	Microsoft Office	English (native)
Cell culture (primary cultures & cell lines)	Statistical software (SPSS, GraphPad Prism)	German (B2)
Immunohistochemistry	FACS Diva	
Multidimensional flow cytometry	FIJI	
Western blot	FlowJo	

11 Publications

2024 Liu, X., Demircik, F., Antipova, M., Stylianakis, E., Klein, M., Bejarano, D., Abdelrahman, E., Bering, A., Blanfeld, M., Carter, K., Johann, L., Uhlfelder, D., Blickberndt, E., … Lemmermann, N. (Under revision). B cells modulate the homeostasis of splenic marginal zone antigen-presenting cells to promote the anti-viral CD8+ T cell response. *Nature Immunology*.

2024 Shanmugavadivu, A., Carter, K., Poursadegh Zonouzi, A., Waisman, A., Regen, T. (2024). CELL-TIP: Tailored isolation protocol for isolating and analyzing the different immune cell subsets in the murine intestinal lamina propria. STAR Protocols. https://doi.org/10.1016/j.xpro.2024.103154

2018 Krauss, S., Nalavade, R., Weber, S., Carter, K., & Evert, B. O. (2018). Upregulation of miR-25 and miR-181 family members correlates with reduced expression of ATXN3 in lymphocytes from SCA3 Patients. MicroRNA, 07. doi:10.2174/2211536607666180821162403